Can a Pump-probe Experiment be Simulated Efficiently?

Thesis Submitted for the Degree
Doctor of Philosophy

by

Michael Khasin

Submitted to the Hebrew University Senate
in the year
2008

This work was carried out under the supervision of

Professor Ronnie Kosloff

Acknowledgments

I thank Ronnie Kosloff for his unlimited support and guidance.

I thank Lajos Diosi, Evgeniy Khain and Dani Steinitz for their interest in my work and numerous fruitful discussions.

Many thanks are given to Dorit Aharonov, Nir Barnea, Howard Barnum, Maurice Cohen, Bob Dorfman, Omri Gat, Salman Habib , Yuri Khodorkovsky, Ami Leviatan and Amichai Vardi for sharing their insights with me.

Thanks are given to Eva Guez and Daniel Harries for their advice and invaluable help in preparation of this manuscript.

Thanks to my parents for all their encouragement.

Thanks to Amira, George, Noam, Adi and Uri who never let me forget that there are other important things in the world.

Abstract

Measuring a quantum system disturbs its evolution. A pump-probe experiment is designed to monitor the autonomous dynamics of a quantum system between consecutive measurements. Modeling the evolution of observables in the pump-probe experiment is an essential ingredient of research in quantum dynamics.To be of practical importance the models should be amenable to efficient simulations on contemporary computers. This dissertation deals with the problem of efficient simulation of the pump-probe experiment.

The number of independent observables of a quantum system having the effective Hilbert space dimension N grows as N^2. In physically interesting applications that number of observables can be neither measured nor calculated. Therefore, a small subset of observables should be in the focus of an efficient dynamical simulation scheme.

Commonly, the distinguished subset of observables considered in the context of efficient simulations is the subalgebra of local observables with respect to a given partition. The main obstacle on the way of efficient simulation of local dynamics is quantum entanglement. An initial pure state of a composite quantum system generically develops entanglement in the course of its unitary evolution. We propose and analyze two possible routes for quantum dynamics without entanglement: i) the initial mixed state unitary evolution and ii) an open system evolution of the composite system coupled locally to dephasing environment.

Sufficient mixing of an initial state, measured by its temperature, is shown to result in the evolution with vanishing entanglement. Critical temperature for the crossover to the no-entanglement dynamical regime is calculated. An outline of the computation scheme for efficient simulation of the corresponding mixed state dynamics is presented.

Coupling to local environment is believed to be generally detrimental to quantum entanglement. We have found that this view is incorrect. Certain types of local system-bath interactions can have a negligible effect on entanglement on the characteristic time-scale of the composite system purity decay. This is typical to an evolution of open systems, subjected to the Poissonian noise. On the other hand, local Gaussian noise is shown to be destructive to quantum entanglement. A local Gaussian noise has effect equivalent to a weak measurement of local observables of the composite quantum system. The destructive effect of the weak measurement on quantum entanglement can be attributed to the large time-scale separation between the decoherence of the density operator in a local basis and the dephasing of the composite system. In this sense the states in the corresponding local basis can be termed robust states. The robust states are suggested to

be an appropriate computational basis for the simulation of the corresponding open system evolution.

We have developed a computational scheme incorporating the foregoing observations into a more general mathematical framework. This is the framework of the generalized coherent states, associated with a given Lie-algebra of observables. The primary focus in our work has been on compact semisimple subalgebras of observables which generalizes the local subalgebras case.

The relation of the theory of the generalized coherent state to the problem of efficient simulation of quantum dynamics can be established by two independent approaches.

The first one is a generalization of the concept of entanglement to a general Lie-algebraic setting. The passage to the generalized coherent states as a preferred computational basis for efficient simulation of quantum dynamics is obtained as a generalization of the common use of products states for simulation of local observables of quantum many-body systems.

The second approach follows a direct argument based on the following definition of an efficient simulation. The simulation of a Lie-algebra of observables is defined as efficient if the necessary computational resources do not depend on the Hilbert space representation of the algebra. In other words, the simulation is efficient if it can be performed group-theoretically. This definition leads to the choice of the spectrum-generating algebra (SGA) of observables as a distinguished set for efficient simulations and the associated generalized coherent states as a distinguished computational basis. More specifically, the following restrictions on the observables must be satisfied:

- The set consists of operators weakly nonlinear in the elements of the spectrum generating algebra (SGA) of the system
- The Hamiltonian is weakly nonlinear in the elements of the SGA of the system

Weakly nonlinear is defined as being a polynomial (in the elements of the SGA) of a fixed order, independent on the Hilbert space representation of the SGA. If the two restrictions are satisfied and

- The evolving state can be represented as superposition of a small number of the generalized coherent states (GCS), associated with the SGA

the evolution can be simulated efficiently. *Small number* is defined as a number independent on the Hilbert space representation of the SGA.

We propose a scheme for simulating dynamics of the SGA observables based on expansion of the evolving state in the generalized coherent states, associated

with the SGA. The computation of the expectation values of the observables can be performed efficiently, provided the number of terms in the expansion of the state is small.

A generic quantum dynamics leads to extensive growth of terms in the GCS expansion of the evolving state. As a consequence, solving the Schroedinger equation becomes inefficient. Nonetheless, we have found that if in addition to the restrictions defined above

- The SGA is a compact semisimple Lie-algebra of operators
- The SGA and its Hilbert space representation comply with the well-defined classicality condition
- The Hamiltonian complies with a certain condition, termed moderate nonlinearity with respect to the SGA
- The initial state of the system is canonical with respect to an operator moderately nonlinear in the elements of the SGA

a dramatic gain in efficiency can be obtained using the idea of dynamical coarse-graining of the unitary dynamics.

Our method employs simulation of the unitary dynamics of the restricted set of observables by a pertinent open-system dynamics. The open-system dynamics corresponds to a non unitary evolution of the original system under the weak measurement of the SGA elements. It is simulated using unraveling of the evolving density operator into pure-states stochastic trajectories. The pure-state evolution is governed by the stochastic Nonlinear Schroedinger equation which is solved numerically. The pure-state evolution can be simulated at low cost due to the measurement-induced localization of the states in the phase-space, associated with the SGA. On the level of the density operator, the measurement introduces a coarse-graining of the evolving state, destroying its fine-structure but leaving unaffected the dynamics of the smooth observables belonging to the restricted set. The latter property is a consequence of the wide separation of time-scales in the open dynamics of a quantum system satisfying the conditions cited above.

Adding weak measurement to the unitary dynamics serves as a computational tool in the proposed method. A by-product of the method is a tool of simulating an open-system dynamics. The open dynamics does not necessarily have the particular form assumed in our method. It is sufficient that the bath has strong localizing effect on the dynamics. On the other hand, it seems necessary that the open-system dynamics be Markovian. Otherwise, the reduced dynamics of the system will involve polynomials of arbitrary orders in the SGA of the system and the simulation cannot be performed efficiently.

The method has been implemented in an algorithm for simulation of many-body dynamics, driven by a $\mathfrak{su}(2)$-algebraic Hamiltonian. The algorithm has been applied to simulation of the dynamics of a bosonic gas in a double-well trap. The dynamics represents a competition between the hopping rate from well to well and a two-body repulsive interaction between the particles. The single-particle observables of a system of $2 * 10^4$ atoms in the strong interaction regime were simulated and the convergence of the computation was checked. A dramatic reduction of the computational complexity has been demonstrated.

Contents

Chapter 1

Introduction

1.1 Pump-probe experiment as a monitor of quantum dynamics

A measurement performed on a quantum system disturbs its evolution. Therefore, monitoring an evolution of a quantum system becomes both a theoretical and a practical problem. A pump-probe experiment is designed to monitor quantum dynamics. The *initial state* of the system is a stationary thermal state. A *pump* is an interaction with an external field aimed at moving the system away from the equilibrium. The response of the system to the pump is monitored. A *probe* is a copy of the pump applied to the disturbed system with a certain delay. The system's response to the probe depends on its instantaneous state. It is monitored and compared to the reference response to the pump. The system is left to relax to the initial thermal state and the sequence pump-probe is repeated with a larger delay. Each sequence can be interpreted as an independent experiment performed on a copy of the system of interest. The series of pump-probes obtained with increasing delays gives the picture of the evolving system.

The pump-probe experiment should be distinguished from experiments performing weak measurement of the evolving quantum system, where the same copy of the system is monitored along the evolution.

While the classical dynamics can be monitored in either one of the two modes with the same result, quantum system entangles with the measurement apparatus (Peres, 1998) and the back reaction of the measurement must be taken into account unless a fresh copy of the system is provided. Thus, the pump-probe experiment monitors what can be termed as a measurement-independent (autonomous) quantum evolution.

Modeling of a pump-probe experiment includes i) building an initial state of the system, ii) a theory of system-pump (probe) interaction, which predicts the

state of the system immediately after the application of the pump and relates the measured response to the state of the system (Gershgoren *et al.*, 2001) and iii)a theory of the autonomous evolution of the system between the pump and the probe.

The three steps: the preparation of the initial state, the time-dependent evolution under the action of the pump (probe) and the autonomous evolution of the system must be simulated on a computer in order to compare the model to the experiment. It is this latter task which is the topic of the present work.

1.2 Efficient simulation of quantum dynamics

1.2.1 The role of quantum and classical correlations in defining the computational complexity of quantum dynamics.

Quantum vs. classical correlations.

Let us assume that the system is partitioned into subsystems (degrees of freedom). The state of the system is said to be uncorrelated with respect to the partition if it obtains a form of a product of states of the subsystems. If a state can be represented as a statistical mixture of such product states it is said to be classically correlated, otherwise - it is said to be quantum correlated or entangled (R. F. Werner, 1989; Peres, 1998). A pure quantum correlated state is necessarily entangled.

Computational complexity of quantum dynamics I.

The definition of efficient simulation The computational complexity (Brassard & Bratley, 2000) of a problem is measured in the memory and CPU resources for its solution as a function of the size of the problem. The problem of simulation of quantum dynamics, governed by the Schroedinger or Liouville-von- Neumann equation, can be solved using resources, scaling polynomially with the Hilbert space dimension of the system (Kosloff, 1988). If the quantum system is represented as a composite system of subsystems, the Hilbert space dimension scales exponentially with the number of the subsystems. This makes one talk about the exponential wall [1] in front of a practical implementation of a simulation. In this context, the size of the problem is understood as the number of subsystems of the composite quantum system.

[1] Walter Kohn, Nobel Lecture, January 28, 1999

In the theory of the computational complexity efficient solution is provided to a problem if the necessary memory and CPU resources scale polynomially with the size of the problem. In the context of simulation of a composite-quantum-system dynamics, "efficient" means scaling polynomially with the number of subsystems (degrees of freedom).

The computational complexity of dynamics is related to the extent of correlations in the evolving state. The evolution of an uncorrelated state can be simulated efficiently. The number of independent parameters of an uncorrelated state grows linearly with the number of degrees of freedom and the variational equations of motion (Kramer & Saraceno, 1981) for the parameters can be solved efficiently. The paradigmatic example is solving quantum many-body dynamics with the Hartree-Fock ansatz (Beck *et al.*, 2000). Correlations are generically created in the course of the evolution of a composite system unless the subsystem do not interact. In the latter case the simulation of the composite system reduces to the simulation of the subsystem dynamics, which is efficient by the common definition.

Necessary and sufficient conditions for efficient simulation. Unentangled pure states are product states. Product states span the Hilbert space of the composite system. Therefore, an entangled pure state can be represented as a superposition of unentangled states. The number of terms in the superposition scales exponentially with the number of degrees of freedom. As a consequence, a generic entangled state of a many-body system cannot be represented efficiently in the given product states basis. It seems to imply that *restricted entanglement is a necessary condition for efficient representation and, therefore, for efficient simulation of quantum dynamics.*

Restricted entanglement does not automatically mean that the simulation can be performed efficiently. For the computational purposes it seems necessary to be able to represent the evolving states as (a mixture of) superpositions of a small number of product states. An unentangled mixed state is a statistical mixture of product states. Nonetheless, finding the local bases in which the unentangled state can be represented as a statistical mixture of product states cannot generally be done efficiently (Jozsa & Linden, 2003). *Finding an appropriate time-dependent basis of product-states efficiently seems to be a necessary ingredient of efficient simulation of quantum dynamics.*

In classical mechanics both conditions are satisfied. A state of a classical system is always classically correlated (Diosi, 2007). Moreover, the evolving state can be represented as a statistical mixture of trajectories in the many-body phase space. Each trajectory is a product of local bases of delta-localized states in the

phase-space and the evolution of this time dependent basis is governed by the Hamiltonian equations of motion.

Each trajectory can be simulated efficiently but a generic state is a mixture of a continuum of trajectories. Apparently the evolution of a state cannot be simulated in practice. But the state is never a physical observable. Observables are expectation values of certain phase-space function, and if the functions are sufficiently smooth their expectation values are practically insensitive to the fine details of the state. The robust, coarse-grained features of the state can be simulated using only a limited size sampling of the trajectories leading to convergence of the expectation values of the interesting observables (Hoover, 1999).

The example of classical mechanics implies that the two conditions, restricted entanglement plus an efficient algorithm for following the time dependent basis, are sufficient for simulation of the dynamics of a *subset of observables* of the system.

Algorithms for efficient simulation of weakly entangled quantum evolution have been developed in chemical physics (Beck *et al.*, 2000) and solid state physics (Vidal, 2003). The condition of restricted entanglement is satisfied in many molecular systems and in low-dimensional lattices in the solid state. The approach taken in the Ref.(Beck *et al.*, 2000) is based on solving variational equations of motion for the time dependent local basis, while the methods of simulating low-dimensional lattices dynamics in the solid states physics (Vidal, 2003) use a non variational procedure for updating the basis. The distinguished set of observables in both methods is the set of local observables. For successful implementation the initial state must be weakly entangled.

1.2.2 The role of generalized quantum and classical correlations in defining the computational complexity of quantum dynamics.

The generalized quantum and classical correlations

Entanglement is an observable-dependent concept (Filippo, 2000; Viola *et al.*, 2001; Zanardi, 2001). The same dynamics can generate extensive entanglement with respect to one partition and no entanglement at all with respect to another partition. The simplest example is the transformation to normal modes in a linear system. Linear dynamics generate no entanglement between the normal modes, while local modes get entangled in the same dynamics. *A choice of different partition may solve the problem of efficient simulation.* This is analogous to looking for coordinates in which the Hamiltonian separates. If such a transformation exists, the problem can be solved efficiently for appropriate initial states

of the system.

Still, a generic many-body system cannot be separated. Can the procedure of partitioning be generalized in such a way that non separable systems can be simulated efficiently?

To answer this problem we note that partition of a system is mathematically equivalent to expressing the Hamiltonian and other observables of the system in terms of the local observables, i.e., observables pertaining to the subsystems. Mathematically, an arbitrary operator of the system is represented as a tensor product of local observables. A partition is equivalent to singling out a set of local observables as the distinguished set of observables from an experimental or a theoretical standpoints. Dropping a word "local" we obtain a generalization of the notion of partition. The corresponding concepts of classical and quantum correlations can be generalized as well. This generalized framework has been developed in Refs.(Barnum *et al.*, 2003; Klyachko, quant-ph/0206012) for quantum systems in finite dimensional Hilbert spaces. These groups have coined the term *generalized entanglement*, referring to generalized quantum correlations with respect to a distinguished set of observables. Particularly rich mathematical structure and important physical implications are obtained if the distinguished set of observables is closed under the commutation relation, i.e., comprise a Lie-algebra (Section 4).

Computational complexity of quantum dynamics II.

When the effective Hilbert space dimension of a subsystem is fixed but the number of subsystems varies, scaling of the computational resources with the number of subsystems is an adequate measure of the efficiency of simulation. The paradigmatic example of such systems is a spin chain. Each spin is a two-level system and the Hilbert space dimension equals two to the power of the number of spins. Efficient simulations of the spin chain dynamics scale polynomially with the number of spins in the chain and logarithmically with the Hilbert space dimension.

In applications one often encounters the situation, where the number of degrees of freedom is fixed but the effective Hilbert space dimension of each degree of freedom varies. In that case, the total Hilbert space dimension scales polynomially with the variable parameter − the effective Hilbert space dimension of a single degree of freedom, which is a more appropriate measure of the size of the problem. The term efficient simulation must be redefined accordingly to suit this case.

Moreover, partitioning of a system into subsystems or degrees of freedom reflects the choice of local observables as a distinguished set of observables, which are at the focus of the simulation. The choice of the observables is generally not

restricted to local observables. If a different subset of observables is in the focus of the simulation, there is no advantage in partitioning the system and a reference to the number of subsystems in the definition of efficient simulation is irrelevant.

We adopt the following definition of efficient simulation.

Definition: *Let the subset of distinguished observables be a Lie-subalgebra of observables, represented irreducibly on the Hilbert space of the system. The simulation is defined as efficient if the memory and the CPU resources necessary to compute the evolution of the distinguished observables do not depend on the Hilbert space representation of the algebra.*

A paradigmatic example of a system that can be simulated efficiently is a system, driven by a Hamiltonian linear in the elements of the distinguished subalgebra of observables. The Heisenberg equations of motion for the elements of the subalgebra can be solved using resources independent of the Hilbert space representation of the algebra. A simple example of such systems is harmonic oscillator with respect to the oscillator algebra (Perelomov, 1985)) or a spin in magnetic field with respect to the angular momentum algebra (Cohen-Tannoudji *et al.*, 1977).

Mean field solutions (Kramer & Saraceno, 1981) of quantum many-body problems are examples of an approximate simulation of the quantum dynamics, which is efficient according to our definition.

The computational resources of an efficient simulation do not depend on the Hilbert space but scale polynomially with the dimension of the fixed subalgebra of observables. If the dimension of the subalgebra is not fixed like in the case of local observables of a spin chain with a variable number of spins, the Hilbert space dimension is an exponential function of the dimension of the local subalgebra. The conventional definition of efficient simulation demands scaling logarithmically with the Hilbert space dimension, i.e., polynomially in the dimension of the local subalgebra, which is consistent with our definition.

Heuristically, the simulation is efficient if the computational effort is proportional to the amount of desired information and not to the total amount of information contained in the system.

Efficiency of a simulation can be related to the extent of the generalized quantum (classical) correlations of the evolving system using an important concept of the generalized coherent states (GCS). This relation is established in Chapter (4).

1.2.3 The role of the initial state in defining the computational complexity of quantum dynamics

The generalized entanglement of an initial state of the simulated system with respect to the distinguished subalgebra of observables must be weak in order that efficient simulation be possible (Chapter 4). Accordingly, the initial state must be a mixture of weakly entangled pure states.

If the field of the pump couples to the system through an element of the distinguished subalgebra of observables, the generalized entanglement of the state does not change. This is due to the fact that the generalized entanglement with respect to a Lie-algebra of observables is invariant under unitary transformations, generated by the algebra (Barnum *et al.*, 2003). The linear coupling is an adequate model at low intensities of the field. Therefore, for efficient simulation it is necessary that the initial state of the system (before the pump) be (generalized) unentangled. Initial state of the system in a pump-probe experiment is typically a thermal state. Therefore, an important question is whether a thermal state of the system is generalized-entangled with respect to the distinguished subalgebra of observables.

The (conventional) entanglement of thermal states has been a field of intensive research in recent years, motivated by developments in the quantum-information and computation science (see Chapter 2 and the references therein). It can be shown that entanglement of thermal states tends to zero with temperature. Moreover, a thermal state can be viewed as a result of imaginary time propagation from the initial maximally mixed state (i.e., the state proportional to identity operator), which is an unentangled state. Therefore, at sufficiently large temperature it can be assumed without loss of generality that the initial state is pure unentangled state. This idea is further explored in Chapter 4.

Ground states of many-body systems are often generalized unentangled (Barnum *et al.*, 2003) with respect to the spectrum-generating algebra (SGA) (Dothan, 1970; Bohm *et al.*, 1988) of the system. The SGA is shown to be a distinguished algebra of observables from the computational perspective in Chapter 4.

Generic evolution of an initially unentangled thermal state generates quantum correlations. An important and interesting question is whether the extent of quantum correlations, generated in the course of the evolution depends on the temperature. This is a question addressed in Chapter 2.

1.2.4 The role of coupling to a bath in defining the computational complexity of quantum dynamics

Open systems are systems, coupled to an environment (bath). The role of the bath in defining the computational complexity of the open-system dynamics is rooted in the effect the bath has on the dynamics of quantum and classical (generalized) correlations. An external bath may create quantum correlations in the open system but may also destroy them (Chapter 3). Deterioration of entanglement, caused by interaction with environment, is a curse of the quantum information processing and quantum computation (M. A. Nielsen and I. L. Chuang, 2000).

One of the first rigorous results relating external noise to the computational complexity of quantum dynamics belongs to Dorit Aharonov and Michael Ben-Or (Aharonov & Ben-Or, quant-ph/9611029). They have shown that sufficiently strong external noise diminishes the computational complexity of a quantum computing with the result that the latter can be simulated efficiently. Since then the topic has been extensively investigated both in the quantum information processing and in a more physical settings (see Chapter 3 and the references therein). The conclusion can be summarized in four words: local noise destroys entanglement.

Local Gaussian noise can be shown to correspond to a weak measurement of a subset of local operators (Chapter 3). This observation can be used to generalize the notion of local noise to a noise, associated with an arbitrary set of observables. Particularly interesting is the noise, associated with the spectrum-generating algebra of observables (Chapter 4). This noise corresponds to a weak measurement of the elements of the SGA. Dynamics of a quantum system under the action of a weak measurement is investigated in a general Lie-algebraic setting in Section 4.3 of Chapter 4.

Dynamics of generalized quantum correlations, associated with the SGA, under the action of a weak measurement, has never been investigated in a general setting before. Nonetheless, weak measurements and other forms of the system-bath interactions were found to destroy quantum correlations, associated with subalgebras other than local algebra. An example is the localization of the phase-space representation of a state of quantum (nonlinear) oscillator under a weak measurement of position (momentum) operator (Diosi, 1988a; Gisin & Percival, 1993; Halliwell & Zoupas, 1995). This localization can be interpreted as deterioration of quantum correlations, associated with the Heisenberg-Weyl subalgebra of observables (Gilmore, 1974).

The effect of weak measurement of a subalgebra of operators on the compu-

tational complexity of simulating their dynamics is the central theme of Chapter 4.

Chapter 2

Generation of quantum entanglement at finite temperature

2.1 Introduction

Typically interacting systems develop correlations. Pure initial states, following a unitary evolution, become entangled, while mixed states or initial pure states of an open system develop both quantum and classical correlations. If no quantum correlations are generated in the course of the evolution the system can probably be simulated efficiently. Given a generic interaction, there are two possible routes for quantum dynamics without entanglement: i) the system is open to interaction with an environment; ii) the system follows a unitary evolution from an initial mixed state. The dynamics of quantum correlations in an open-system evolution is addresses in Chapter 3. The present Chapter investigates the case of vanishing mixed state entanglement in a generic unitary evolution of a bi- and tripartite composite system. The evolution of a pure state is found to generate quantum entanglement both in the case of direct interaction between the subsystems and in the case of indirect interaction, mediated by the third party.

2.1.1 Efficient simulation of a classically-correlated system

It is possible that an arbitrary pure state of a given composite quantum system develops entanglement in the course of the evolution, while particular mixed initial states remain classically correlated. Can this property be used for efficient simulation of the composite system dynamics? A necessary ingredient of simu-

lating a mixed state evolution seems to be an ability to represent the state as a mixture of pure states, following an evolution that can be simulated efficiently. The pertinent pure-state evolution cannot be the original dynamics, since by assumption an arbitrary initial state generates entanglement. Therefore, one may look for a modified dynamics of the pure states with a property, that the statistical average of the pure-states evolutions gives the correct mixed state evolution of the system. This scenario can be realized in the following way.

A mixed state dynamics is driven by the Liouville-von-Neumann equation for the density operator of the system. An equivalent representation of the dynamics is a phase-space representation. Given a subalgebra of observables, represented irreducibly on the Hilbert space of the quantum system, a (generalized) phase-space of the system can be constructed with an associated set of the generalized coherent states (GCS)(Perelomov, 1985; Zhang *et al.*, 1990), that span the Hilbert space (see Chapter 4 for details). (In the context of the present Chapter, the distinguished subalgebra is the algebra of local operators of the subsystems, and the GCS is the set of product (unentangled) states of the composite system.) A point in the phase space corresponds to a single GCS. A density operator of the system can be reproduced as a pseudo mixture of the GCS. The pseudo probability density of GCS in the mixture is called a P-representation of the density operator. A GCS has P-representation which is a δ-function on the phase-space.

The evolution of the P-representation is driven by the quantum Fokker-Planck equation of motion (Gardiner, 1983). Fokker-Plank equation is a partial differential equation of dimension of the underlying phase-space plus one (time). Classical Fokker-Planck equation for the probability density distribution can be solved by decomposing the distribution into a mixture of δ-like distributions. Each δ-like distribution follows a stochastic trajectory, driven by the classical Langevin equations (Gardiner, 1983). This decomposition is referred to as stochastic unraveling of the evolution. The Langevin equation is an ordinary first order differential equation for the phase-space variables and can be solved efficiently. Subsequent averaging recovers the evolution of the distribution to a desired accuracy. The unraveling of the classical Fokker-Planck equation into stochastic trajectories is possible due to its very important property: positive distributions evolve into positive distributions.

This property does not hold in quantum case. An initial positive P-representation of the state generically evolves into a P-representation which can be negative in parts of the phase-space. This property is often referred to as a sign problem (Miller, 2005). The development of the negative regions corresponds to production of the (generalized) quantum correlations. In fact, (generalized) classically

correlated states can be represented as proper mixtures of the generalized coherent states (GCS, see Chapter 4), associated with the phase-space. A single GCS has a nonnegative P-distribution (δ-function), therefore a mixture of the GCS is nonnegative as well.

If *no entanglement* is generated, the P-distribution remains nonnegative and unraveling of the quantum Fokker-Plank equation into quantum Langevin equations becomes possible. This procedure has been performed by Gardiner (Gardiner, 1983). Solution of the quantum Langevin equation can be performed efficiently, since its complexity depends only on the corresponding phase-space dimension, which is an algebraic property of the distinguished observables independent on the Hilbert space representation [1]

As an example consider a system of n spins. The dimension of the Hilbert space is 2^n. The phase space, associated with the subalgebra of local operators has dimension $2 * n$. Therefore, a (stochastic) trajectory in the phase space can be simulated efficiently.

In conclusion, if a particular mixed state evolves into a classically correlated state its evolution can in principle be simulated efficiently.

2.1.2 Hot states are disentangled

Sufficiently small neighborhood of the identity operator consists of classically correlated states (Gurvitz & Barnum, 2003). This neighborhood is finite for finite-dimensional systems and contracts as the Hilbert space dimension increases. Therefore, sufficiently hot (finite-dimensional) quantum system are classically correlated. Moreover, a short time dynamics generates no entanglement, unless the initial states lies on the boundary of the neighborhood. Therefore, it can be simulated efficiently.

What is "sufficiently hot" depends on the dynamics. This question is in the focus of Section 2.2.

2.2 Temperature Dependence of Interaction-Induced Entanglement

[1] A more accurate analysis (Zhang *et al.*, 1990) shows the dimension of the phase-space, associated with the subalgebra of observables depends on the representation, but is always bounded by the dimension of the subalgebra.

Temperature dependence of interaction-induced entanglement

Michael Khasin and Ronnie Kosloff
Fritz Haber Research Center for Molecular Dynamics, Hebrew University of Jerusalem, Jerusalem 91904, Israel
(Received 20 May 2005; published 3 November 2005)

Both direct and indirect weak nonresonant interactions are shown to produce entanglement between two initially disentangled systems prepared as a tensor product of thermal states, provided the initial temperature is sufficiently low. Entanglement is determined by the Peres-Horodecki criterion, which establishes that a composite state is entangled if its partial transpose is not positive. If the initial temperature of the thermal states is higher than an upper critical value T_{uc} the minimal eigenvalue of the partially transposed density matrix of the composite state remains positive in the course of the evolution. If the initial temperature of the thermal states is lower than a lower critical value $T_{lc} \leqslant T_{uc}$ the minimal eigenvalue of the partially transposed density matrix of the composite state becomes negative, which means that entanglement develops. We calculate the lower bound T_{lb} for T_{lc} and show that the negativity of the composite state is negligibly small in the interval $T_{lb} < T < T_{uc}$. Therefore the lower-bound temperature T_{lb} can be considered as *the* critical temperature for the generation of entanglement. It is conjectured that above this critical temperature a composite quantum system could be simulated using classical computers.

DOI: 10.1103/PhysRevA.72.052303 PACS number(s): 03.67.Mn, 03.65.Ud

I. INTRODUCTION

Efficient simulation of quantum dynamics on classical computers is hampered by the problem of scaling: the complexity of computation in quantum dynamics scales exponentially with the number of degrees of freedom [1]. The reason for this exponential growth is the entanglement of the degrees of freedom generated during the evolution. This problem is of a fundamental character: entanglement is viewed as one of the main peculiarities of the quantum dynamics as compared to its classical counterpart [2,3]. Asking under what conditions entanglement is generated along the evolution of the quantum system is closely associated with the question of the quantum-classical transition [4,5].

It is customary in quantum-dynamical simulations to assume that the initial state of the composite system is factorized in the relevant local basis [6]. An important question is whether the product form is conserved along the evolution [7,8]. The answer was generally found to be negative both for the pure- [8,9] and for the mixed-state [9] dynamics.

A pure composite state is entangled if and only if it is not factorized in the local basis. For mixed states the situation is more complex [10]. For a bipartite composite system separability [11] is defined as a decomposition of the density matrix of the composite system in the form

$$\hat{\boldsymbol{\rho}}_{12} = \sum p_i \hat{\boldsymbol{\rho}}_1^i \otimes \hat{\boldsymbol{\rho}}_2^i, \tag{1}$$

where $0 \leqslant p_i \leqslant 1$, $\Sigma_i p_i = 1$, and $\hat{\boldsymbol{\rho}}_1$ and $\hat{\boldsymbol{\rho}}_2$ are density matrices on Hilbert spaces of the first and the second subsystem, respectively. Separable states exhibit only classical correlations. States that cannot be represented in the form (1) exhibit correlations that cannot be explained within any classical theory and are said to be entangled. There are two qualitatively different kinds of the mixed-state entanglement [12]: free entanglement and bound entanglement. Free entanglement can be brought into a form useful for quantum-information processing and bound entanglement is "useless" in this sense.

Separable states are not of the product form generally. Thus the important question remains, under what conditions does the mixed state of the composite system evolving from the initial product (or generally separable) state develop entanglement along the evolution. If quantum correlations in the composite system do not develop during the evolution one may speculate that the dynamics of the composite system has classical character. A possible practical implication is that this "separable dynamics" could be simulated efficiently on classical computers.

The dynamics of entanglement was investigated recently in various systems: the quantum Brownian particle [13], harmonic chain [14], two-qubit system interacting with the common harmonic bath [15], Jaynes-Cummings model [16], NMR [17], various spin systems [18–20], Morse oscillator coupled to the spin bath [21], and bipartite Gaussian states in quantum optics [22] to mention just some cases. The purpose of the present paper is to explore the temperature dependence of entanglement generation in the course of evolution of a bipartite state in the limit of weak coupling and nonresonant interaction between the parts. Under these limitations nondegenerate perturbation theory was applied to the calculation of the bipartite entanglement in the evolving composite system. We have considered two cases of interaction: (1) direct interaction, when two initially disentangled systems are brought into contact (cf. Fig. 1), and (2) indirect interaction, when two noninteracting and initially disentangled systems are brought into contact with the third party (cf. Fig. 5). In each case the initial state of the composite system was taken to be the product of the thermal states of the parts.

To establish quantum entanglement the Peres-Horodecki criterion is employed [23,24]. The Peres-Horodecki criterion states that the bipartite system is entangled when the partially transposed density matrix of the system possesses a negative eigenvalue. The converse statement is generally not true: there exist inseparable states whose partial transposes are

positive [25]. It is proved in Ref. [12] that states whose partial transposes are positive (PPT states in what follows) do not exhibit free entanglement. Therefore PPT states are either separable or bound entangled and as a consequence are not useful in quantum-information processing. In the context of simulating a quantum composite system with classical computers, we are interested in the possibility of maintaining a separable [cf. Eq. (1)] or approximately separable form during the evolution. We conjecture on the basis of Ref. [26], where it is proved that PPT density matrices of a low rank are separable, that sufficiently cold (or, perhaps, sufficiently pure, in general) initial states that remain PPT during the evolution are at least approximately separable.

It is a well-known fact that in a sufficiently small neighborhood of a maximally mixed state, which can be viewed as a thermal state at infinite temperature, all states are separable [28–31]. Since the interactions studied in the present work are weak and nonresonant, the dynamics keeps the evolving state in the vicinity of the initial state. By assumption initial states are thermal product states. It is expected then that starting somewhere in the separable ball around the maximally mixed state, the evolving state will remain separable in the course of the evolution. Given that entanglement is generated at sufficiently low initial temperature, a finite crossover temperature, depending on the details of the interaction, should exist: below this temperature the interaction generates entanglement in the course of the evolution of the composite system and above it the evolving state remains separable. Since all separable states are PPT states the analogous critical temperature should exist for the PPT character of the evolution. In principle, there may exist several critical temperatures for the PPT quality for the given interaction. Therefore we define the lower and the upper critical temperatures T_{lc} and T_{uc} such that if the composite system evolves from the initial thermal state at temperature $T<T_{lc}$ the minimal eigenvalue of the partial transpose of the state becomes negative in the course of the evolution and if $T>T_{uc}$ the PPT character of the state is preserved. In the present work a lower bound T_{lb} of the T_{lc} is calculated in cases of both direct (1) and indirect (2) interactions between the parts.

Applying the Peres-Horodecki criterion to the case (1) of a direct interaction we show that for sufficiently low initial temperature of the subsystems the interaction does induce entanglement unless the ground state of either one of the subsystem is invariant under the interaction. The lower bound T_{lb} of the lower critical temperatures T_{lc} was calculated in the limit of weak intersystem coupling and shown to be tight: the negativity of the composite state [27], which is a quantitative counterpart of the Peres-Horodecki criterion and a measure of entanglement, is shown to be generally negligible for temperatures in the interval $T_{lb}<T<T_{uc}$.

In the case (2) of indirect coupling two scenarios with time-scale separation are studied: (a) two"slow" noninteracting systems coupled to a "fast" third party and (b) two "fast" noninteracting systems coupled to a "slow" third party. Under some technical assumptions about the form of the interaction we find in both cases that for sufficiently low initial temperature of the noninteracting systems entanglement is induced by the interaction with the third party. We calculate the lower-bound temperature T_{lb} in both cases of the time-scale separation.

In case that the directly or indirectly interacting subsystems are spins the lower-bound temperature coincides with the upper critical temperature, i.e., at $T>T_{lb}$ the spins stay disentangled. In the higher-dimensional cases it is found that the negativity of the evolving composite state is negligibly small at $T>T_{lb}$. Therefore the lower-bound temperature T_{lb} may be considered as an effective crossover temperature for the PPT character of the evolution. It may be suspected that T_{lb} corresponds to a critical purity of the evolving state below which the state remains separable according to the general result [28–31], cited above. To see that this is not the case we note that the radius of the largest separable ball [30] (and of the largest PPT ball [31], too) about the maximally mixed state is defined by the condition that the purity of the state is low enough, namely, that $\mathrm{Tr}\,\rho^2 \leqslant 1/(d-1)$, where d stands for the overall dimension of the composite state. Since, as will be shown, T_{lb} is a monotonically decreasing function of the coupling strength the (effective) crossover to the PPT evolution is found for initial states of arbitrarily high purity, provided the coupling strength is small enough. Therefore, the effective crossover at T_{lb} cannot be attributed to the "static" proximity of the evolving state to the maximally mixed state but rather T_{lb} is determined dynamically.

In both cases (1) and (2) the evolution starts from an uncorrelated initial state of the composite system represented by the tensor product of thermal states of the subsystems involved. As a consequence, initially the eigenstates of the partially transposed density matrix of the composite state are nonnegative. The evolution under the interaction perturbs the initial state. The new eigenvalues of the partially transposed density matrix are calculated by nondegenerate perturbation theory assuming the coupling is weak and the interaction is nonresonanant. The time dependence of the minimal eigenvalue is not analyzed in detail. As the time evolution of the density matrix is quasiperiodic the minimal eigenvalue of the partially transposed density matrix is also a quasiperiodic function of time. The interaction is said to induce entanglement if the minimal eigenvalue becomes negative in the course of the evolution.

II. ENTANGLEMENT BETWEEN TWO DIRECTLY INTERACTING SYSTEMS

A composite system $A \otimes B$ (see Fig. 1) evolves under the following Hamiltonian:

$$\hat{\mathbf{H}}_{total} = \hat{\mathbf{H}} + \gamma \hat{\mathbf{V}}, \tag{2}$$

where $\hat{\mathbf{H}} = \hat{\mathbf{H}}_a \otimes \hat{\mathbf{1}} + \hat{\mathbf{1}} \otimes \hat{\mathbf{H}}_b$, $\hat{\mathbf{V}} = \hat{\mathbf{V}}_a \otimes \hat{\mathbf{V}}_b$, and γ scales the magnitude of the interaction. Let the initial state be

$$\hat{\boldsymbol{\rho}}(0) = \hat{\boldsymbol{\rho}}_a \otimes \hat{\boldsymbol{\rho}}_b, \tag{3}$$

where both $\hat{\boldsymbol{\rho}}_a$ and $\hat{\boldsymbol{\rho}}_b$ are thermal states: $\hat{\boldsymbol{\rho}}_{a,b} = Z_{a,b}^{-1} \times \exp(-\hat{\mathbf{H}}_{a,b}/T)$, where $Z_{a,b}^{-1}$ is the normalization factor. The Boltzmann constant k_B is unity throughout the paper. The evolution is followed in the interaction picture. Then

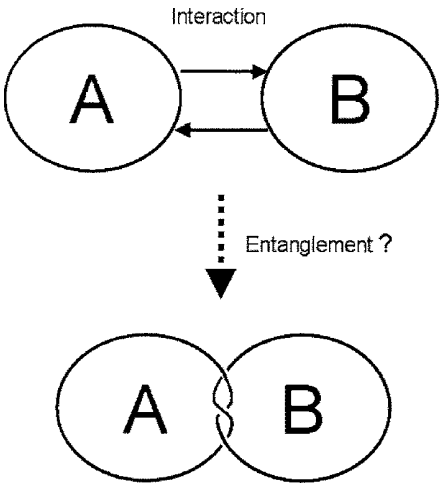

FIG. 1. The coupling scheme for two directly interacting systems.

$$\frac{\partial \hat{\boldsymbol{\rho}}'}{\partial t} = -i\gamma[\hat{\mathbf{V}}_a(t) \otimes \hat{\mathbf{V}}_b(t), \hat{\boldsymbol{\rho}}'], \tag{4}$$

where

$$\hat{\boldsymbol{\rho}}'(t) = e^{-i\hat{\mathbf{H}}t}\hat{\boldsymbol{\rho}}\, e^{i\hat{\mathbf{H}}t},$$

$$\hat{\mathbf{V}}_{a,b}(t) = e^{i\hat{\mathbf{H}}_{a,b}t}\hat{\mathbf{V}}e^{-i\hat{\mathbf{H}}_{a,b}t}. \tag{5}$$

Here and in the rest of the paper we take $\hbar = 1$. It is clear that the density matrix $\hat{\boldsymbol{\rho}}(t)$ is separable if and only if $\hat{\boldsymbol{\rho}}'(t)$ is separable. In what follows the prime on $\hat{\boldsymbol{\rho}}'(t)$ are omitted for simplicity. In the first order in the coupling γ the evolution of $\hat{\boldsymbol{\rho}}$ becomes

$$\hat{\boldsymbol{\rho}}(t) = \hat{\boldsymbol{\rho}}(0) - i\gamma\int_0^t [\hat{\mathbf{V}}_a(t') \otimes \hat{\mathbf{V}}_b(t'), \hat{\boldsymbol{\rho}}(0)]dt'. \tag{6}$$

Entanglement of $\hat{\boldsymbol{\rho}}(t)$ is established by the application of the Peres-Horodecki criterion. This is carried out by calculating the partial transpose of the state. The partial transposition T_a with respect to subsystem A of a bipartite state $\hat{\boldsymbol{\rho}}_{ab}$ expanded in a local orthonormal basis as $\hat{\boldsymbol{\rho}}_{ab} = \Sigma\rho_{ij,kl}|i\rangle\langle j| \otimes |k\rangle\langle l|$ is defined as

$$\rho_{ab}^{T_a} \equiv \sum \rho_{ij,kl}|j\rangle\langle i| \otimes |k\rangle\langle l|. \tag{7}$$

The spectrum of the partially transposed density matrix does not depend on the choice of local basis or on the choice of the subsystem with respect to which the partial transposition is performed. By the Peres-Horodecki criterion the eigenvalues of a partially transposed *separable* bipartite state are nonnegative.

The density operator (6) under the partial transposition (T^a) becomes:

$$\hat{\boldsymbol{\rho}}(t)^{T_a} = \hat{\boldsymbol{\rho}}(0)^{T_a} - i\gamma\int_0^t [\hat{\mathbf{V}}_a(t') \otimes \hat{\mathbf{V}}_b(t'), \hat{\boldsymbol{\rho}}(0)]^{T_a}dt'. \tag{8}$$

Let $|ik\rangle \equiv |i\rangle \otimes |k\rangle$ be the local orthonormal basis of the system $A \otimes B$ composed of the eigenvectors of the unperturbed Hamiltonian $\hat{\mathbf{H}} = \hat{\mathbf{H}}_a + \hat{\mathbf{H}}_b$:

$$\hat{\mathbf{H}}_{a,b}|i\rangle = E_{a,b}^i|i\rangle, \tag{9}$$

where $E_{a,b}^i$, $i = 1, 2, \ldots$, is the unperturbed energy spectrum of the Hamiltonian $\hat{\mathbf{H}}_{a,b}$. The initial state is of the tensor product form [see Eq. (3)]; therefore

$$\hat{\boldsymbol{\rho}}(0)^{T_a}|ik\rangle = \hat{\boldsymbol{\rho}}(0)|ik\rangle = \hat{\boldsymbol{\rho}}_a \otimes \hat{\boldsymbol{\rho}}_b|ik\rangle = P_{ik}|ik\rangle, \tag{10}$$

where $P_{ik} \equiv p_{a,i}p_{b,k}$ and $p_{a,i}, p_{b,k}$ are defined by $p_{a,i} = \langle i|\hat{\boldsymbol{\rho}}_a|i\rangle$ and $p_{b,k} = \langle k|\hat{\boldsymbol{\rho}}_b|k\rangle$. The matrix elements of $\hat{\boldsymbol{\rho}}(t)^{T_a}$ in the chosen basis are given by

$$\langle ik|\hat{\boldsymbol{\rho}}(t)^{T_a}|jl\rangle = P_{ik}\delta_{(ik),(jl)} + M_{ik,jl}, \tag{11}$$

where

$$\begin{aligned}
M_{ik,jl} &= i\gamma\int_0^t \langle ik|[\hat{\mathbf{V}}_a(t') \otimes \hat{\mathbf{V}}_b(t'), \hat{\boldsymbol{\rho}}_a \otimes \hat{\boldsymbol{\rho}}_b]^{T_a}|jl\rangle dt' \\
&= i\gamma\int_0^t [\langle ik|\hat{\boldsymbol{\rho}}_a\hat{\mathbf{V}}_a(t')^T \otimes \hat{\mathbf{V}}_b(t')\hat{\boldsymbol{\rho}}_b|jl\rangle \\
&\quad - \langle ik|\hat{\mathbf{V}}_a(t')^T\hat{\boldsymbol{\rho}}_a \otimes \hat{\boldsymbol{\rho}}_b\hat{\mathbf{V}}_b(t')|jl\rangle]dt' \\
&= i\gamma(P_{il} - P_{jk})\int_0^t \langle i|\hat{\mathbf{V}}_a(t')^T|j\rangle\langle k|\hat{\mathbf{V}}_b(t')|l\rangle dt' \\
&= i\gamma(P_{il} - P_{jk})\int_0^t \langle j|\hat{\mathbf{V}}_a|i\rangle\langle k|\hat{\mathbf{V}}_b|l\rangle e^{it'(E_a^i - E_a^j + E_b^l - E_b^k)}dt' \\
&= \gamma(P_{il} - P_{jk})\langle j|\hat{\mathbf{V}}_a|i\rangle\langle k|\hat{\mathbf{V}}_b|l\rangle\frac{e^{it(E_a^i - E_a^j + E_b^l - E_b^k)} - 1}{(E_a^i - E_a^j + E_b^l - E_b^k)},
\end{aligned} \tag{12}$$

where $\hat{\mathbf{X}}^T$ designates the transpose of the operator $\hat{\mathbf{X}}$.

When $T = 0$, the zero eigenvalue of the initial state $\hat{\boldsymbol{\rho}}(0)$ is degenerate. As a result the zero eigenvalue of the partially transposed initial density operator $\hat{\boldsymbol{\rho}}(0)^{T_a} = \hat{\boldsymbol{\rho}}(0)$ is also degenerate. The zero eigenvalues correspond to empty initially unoccupied states. By the standard secular perturbation theory the first-order correction to the degenerate eigenvalue $\lambda^{(0)} = 0$ of the matrix $\hat{\boldsymbol{\rho}}(0)^{T_a}$ is given by

$$|M_{nn'} - \lambda^{(1)}\delta_{nn'}| = 0, \tag{13}$$

where $|n\rangle$ and $|n'\rangle$ are eigenvectors of the matrix $\hat{\boldsymbol{\rho}}_a^T \otimes \hat{\boldsymbol{\rho}}_b$, corresponding to the degenerate $\lambda^{(0)} = 0$. Since $\hat{\boldsymbol{\rho}}(0)^{T_a} = \hat{\boldsymbol{\rho}}_a^T \otimes \hat{\boldsymbol{\rho}}_b = \hat{\boldsymbol{\rho}}_a \otimes \hat{\boldsymbol{\rho}}_b$ the eigenvectors of $\hat{\boldsymbol{\rho}}_a^T \otimes \hat{\boldsymbol{\rho}}_b$, corresponding to $\lambda^{(0)} = 0$ are $|n\rangle = \{|1\rangle \otimes |i\rangle, |i\rangle \otimes |1\rangle, |i\rangle \otimes |j\rangle, i, j = 2, 3, \ldots\}$.

Therefore at $T = 0$, $P_{ik} = \delta_{ik}\delta_{k1}$, and by inspection of Eq. (12), the only nonvanishing matrix elements in the degenerate subspace spanned by $|n\rangle$ and $|n'\rangle$ are $M_{1i,j1}$ and $M_{j1,1i}$ where either $i \neq 1$ or $j \neq 1$. Since the trace of the matrix M is zero, either all its eigenvalues vanish or some of them are negative. All the eigenvalues of M cannot vanish unless $M = 0$, which from Eq. (12) implies $[\hat{\mathbf{V}}_a, \hat{\boldsymbol{\rho}}_a] = 0$ or $[\hat{\mathbf{V}}_b, \hat{\boldsymbol{\rho}}_b] = 0$, i.e., the ground state of either one of the subsystems is invariant under the interaction. In this case the interaction acts

locally on the subsystems and cannot entangle them. Otherwise there are negative solutions to Eq. (13) and as a consequence the partial transpose of the density operator attains negative eigenvalues already in the first order in the coupling. Therefore, according to the Peres-Horodecki criterion, entanglement develops at zero temperature. We remark that this is a well-known result for the pure-state evolution but the present derivation will be employed also in the case of a finite temperature.

To simplify the study of the generation of entanglement at finite temperatures it is assumed that the only nonzero matrix elements of $\hat{\mathbf{V}}_{a,b}$ are those between neighboring states, i.e., $(\hat{\mathbf{V}}_{a,b})_{ij} \propto \delta_{i,j\pm1}$. Under this assumption the partially transposed density matrix $\hat{\boldsymbol{\rho}}(t)^{T_a}$ obtains the following structure:

$$\hat{\boldsymbol{\rho}}(t)^{T_a} = \begin{pmatrix} P_{11} & 0 & 0 & M_{11,22} & 0 & 0 & 0 & . & . \\ 0 & P_{12} & M_{12,21} & 0 & M_{12,23} & 0 & 0 & . & . \\ 0 & M^*_{12,21} & P_{21} & 0 & 0 & M_{21,32} & 0 & . & . \\ M^*_{11,22} & 0 & 0 & P_{22} & 0 & 0 & M_{22,33} & . & . \\ 0 & M^*_{12,23} & 0 & 0 & P_{23} & M_{23,32} & 0 & . & . \\ 0 & 0 & M^*_{21,32} & 0 & M^*_{23,32} & P_{32} & 0 & . & . \\ 0 & 0 & 0 & M^*_{22,33} & 0 & 0 & P_{33} & . & . \\ . & . & . & . & . & . & . & . & . \\ . & . & . & . & . & . & . & . & . \end{pmatrix}, \tag{14}$$

where P_{ij} are defined after Eq. (10) and $M_{ki,jl}$ by Eq. (12).

There are two kinds of matrix elements $M_{ki,jl}$: $M_{ki,(k+1)(i+1)}$ and $M_{ki,(k\pm1)(i\mp1)}$ (other elements are their counterparts under the transposition). Matrix elements $M_{ki,(k+1)(i+1)}$ couple the unperturbed eigenvalues P_{ki} and $P_{(k+1)(i+1)}$. For small coupling strength γ, $|M_{ki,(k+1)(i+1)}| \ll P_{ki}$ and the contribution of $M_{ki,(k+1)(i+1)}$ to the correction to P_{ki} is negligible and cannot make the eigenvalue negative. On the other hand, the ratio $|M_{ki,(k+1)(i+1)}|/P_{(k+1)(i+1)} \propto \gamma(P_{k(i+1)} - P_{(k+1)i})/P_{(k+1)(i+1)}$ can in general be arbitrarily large for low temperatures but for sufficiently high temperatures it tends to zero and as a consequence the contribution of the coupling element $M_{ki,(k+1)(i+1)}$ to the correction to $P_{(k+1)(i+1)}$ is negligible. It can be checked along the same lines that the ratio of the coupling matrix elements $M_{ki,(k\pm1)(i\mp1)}$ to the unperturbed eigenvalues P_{ki} and $P_{(k\pm1)(i\mp1)}$ of the partially transposed density matrix (14) vanish for sufficiently high temperature. Therefore, at least for composite systems with finite Hilbert space dimensions, there exists a finite upper critical temperature T_{uc}. Above T_{uc} the spectrum of the partially transposed density matrix remains positive. In close vicinity of T_{uc} from below the minimal eigenvalue becomes negative in the course of the evolution. These conclusions stay in accord with a general result that finite-dimensional composite states in sufficiently small neighborhood of the maximally mixed state (i.e., thermal states at infinite temperature) are separable [28–31].

At sufficiently low initial temperature the minimal eigenvalue of the partially transposed density matrix becomes negative in the course of the evolution. This means that there exists a finite lower critical temperature T_{lc}. Below T_{lc} the composite system $A \otimes B$ develops entanglement. In a sufficiently close vicinity of T_{lc} from above the state remains PPT in the course of evolution. It is possible that $T_{lc} = T_{uc}$. This equality is confirmed in all numerical tests. A lower bound T_{lb} for the lower critical temperature T_{lc} can be calculated using perturbation analysis. It is shown that this bound is tight since the free entanglement in the interval $T_{lb} < T < T_{uc}$ is negligibly small under the weak-coupling assumption. Therefore, from the practical point of view the lower bound T_{lb} for T_{lc} can be considered as *the* critical temperature for entanglement. For simplicity the lower bound for the lower critical temperature is termed "the lower-bound temperature" throughout the paper.

At low temperatures the leading-order contribution to the negative eigenvalue of the partially transposed density matrix comes from the matrix elements $M_{11,22}, M_{12,21}$ (and their complex conjugates) that do not vanish at $T=0$. Therefore, to the leading order in γ, the nonvanishing eigenvalues of the partially transposed density matrix Eq. (14) are the eigenvalues of the following effective partially transposed density matrix $\hat{\boldsymbol{\rho}}(t)^{T_a}_{eff}$:

$$\hat{\boldsymbol{\rho}}(t)^{T_a}_{eff} = \begin{pmatrix} P_{11} & 0 & 0 & M_{11,22} \\ 0 & P_{12} & M_{12,21} & 0 \\ 0 & M^*_{12,21} & P_{21} & 0 \\ M^*_{11,22} & 0 & 0 & P_{22} \end{pmatrix}. \tag{15}$$

The critical temperature, calculated for the effective 4×4 matrix (15), is a lower bound for the lower critical temperature T_{lc} of the bipartite system $A \otimes B$. The eigenvalues of Eq. (15) are eigenvalues of two 2×2 matrices:

$$\begin{pmatrix} P_{12} & M_{12,21} \\ M^*_{12,21} & P_{21} \end{pmatrix} \tag{16}$$

and

$$\begin{pmatrix} P_{11} & M_{11,22} \\ M^*_{11,22} & P_{22} \end{pmatrix}. \tag{17}$$

The eigenvalues of the matrix (16) are

$$\lambda_{\pm} = \frac{P_{12}+P_{21} \pm \sqrt{(P_{12}+P_{21})^2 - 4(P_{12}P_{21} - |M_{12,21}|^2)}}{2}, \tag{18}$$

where from Eq. (12)

$$M_{12,21} = \gamma \langle 2|\hat{\mathbf{V}}_a|1\rangle\langle 2|\hat{\mathbf{V}}_b|1\rangle \frac{e^{it\Delta E_{11}}-1}{\Delta E_{11}}(P_{11}-P_{22}), \tag{19}$$

where we define $\Delta E_{11}=E^2_a-E^1_a+E^2_b-E^1_b$, which is the lowest joint excitation energy of the composite system.

From Eq. (18), λ_- will be negative whenever $P_{12}P_{21} < |M_{12,21}|^2$ and positive if $P_{12}P_{21} > |M_{12,21}|^2$. The lower-bound temperature T_{lb} is evaluated from the condition $P_{12}P_{21}=|M_{12,21}|^2$. Since $|M_{12,21}|$ is an oscillating function of time [see Eq. (19)] the amplitude of $|M_{12,21}|$ is taken to be equal to $\sqrt{P_{12}P_{21}}$:

$$\frac{2\gamma}{\Delta E_{11}}|\langle 2|\hat{\mathbf{V}}_a|1\rangle\langle 2|\hat{\mathbf{V}}_b|1\rangle|(P_{11}-P_{22}) = \sqrt{P_{12}P_{21}}. \tag{20}$$

Assuming that T_{lb} is low $P_{11}-P_{22}\approx P_{11}$ and then

$$\frac{2\gamma}{\Delta E_{11}}|\langle 2|\hat{\mathbf{V}}_a|1\rangle\langle 2|\hat{\mathbf{V}}_b|1\rangle| = \sqrt{\frac{P_2P_3}{P_1^2}} = e^{-\Delta E_{11}/2T_{lb}}. \tag{21}$$

Since $e^{-\Delta E_{11}/2T}$ is a monotonic function of the temperature, at $T>T_{lb}\lambda_->0$ and at $T<T_{lb}\lambda_-<0$. Finally, the expression for the lower-bound temperature T_{lb} becomes

$$T_{lb} = -\frac{\Delta E_{11}}{2\ln[(2\gamma/\Delta E_{11})|\langle 2|\hat{\mathbf{V}}_a|1\rangle\langle 2|\hat{\mathbf{V}}_b|1\rangle|]}. \tag{22}$$

So far only two of the eigenvalues of the matrix (15) have been evaluated. The other two eigenvalues are found to be strictly positive at and above the temperature T_{lb}. Therefore, the expression (22) defines the critical temperature for the partially transposed effective density matrix (15) and the lower bound temperature of the partially transposed density matrix (14).

Equation (22) can be generalized to an interaction term of the form $\Sigma\gamma_i\hat{\mathbf{V}}^i_a\otimes\hat{\mathbf{V}}^i_b$:

$$T_{lb} = -\frac{\Delta E_{11}}{2\ln[(2/\Delta E_{11})|\sum_i \gamma_i\langle 2|\hat{\mathbf{V}}^i_a|1\rangle\langle 2|\hat{\mathbf{V}}^i_b|1\rangle|]}, \tag{23}$$

provided $\Sigma_i\gamma_i\langle 2|\hat{\mathbf{V}}^i_a|1\rangle\langle 2|\hat{\mathbf{V}}^i_b|1\rangle\neq 0$. When this term vanishes there is no entanglement in the first order in the coupling strength γ.

For the system of two interacting spins the lower bound T_{lb} given by Eq. (22) coincides with the upper critical temperature T_{uc}; therefore in this case *the* critical temperature exists in the strict sense. Figure 2 shows results of the numerical calculation of the critical temperature as a function of coupling strength for a system of two interacting spins evolving from the initial product state of two thermal states. The Peres-Horodecki criterion was used and the partial transpose of the evolving density matrix was calculated numerically to determine entanglement. The shaded area in the parametric space of the logarithm of inverse coupling and the inverse initial temperature represents the values of the parameters where no entanglement develops. For coupling up to $\gamma=0.1$ T_{lb} given by Eq. (22) (the dashed line) corresponds well to the numerical values of T_{uc}. It is interesting to note that for large values of coupling the critical temperature asymptotically tends to a finite constant value of the same order of magnitude as the energy difference between the first excited and the ground state of the unperturbed composite system.

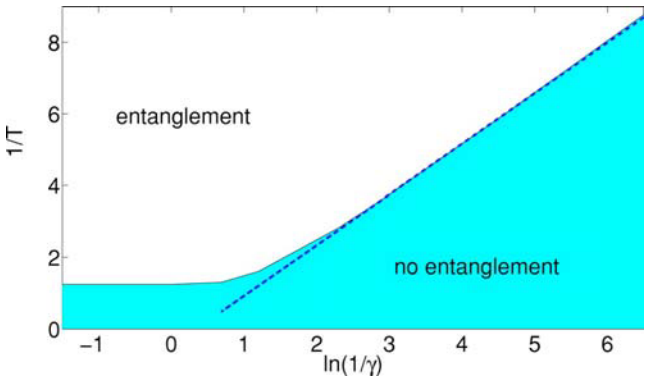

FIG. 2. (Color online) The shaded area in the parameter space of the inverse initial temperature T of two spins and the logarithm of the inverse coupling strength γ, represents values of T and γ, where entanglement does not develop in the course of the evolution. The composite system of two spins evolves from the initial product of thermal states under the Hamiltonian $\hat{\mathbf{H}}=(1/2)\omega[\hat{\boldsymbol{\sigma}}^a_z\otimes\hat{\mathbf{1}}+(\sqrt{2}-1)\hat{\mathbf{1}}\otimes\hat{\boldsymbol{\sigma}}^b_z]+\gamma(\hat{\boldsymbol{\sigma}}^a_x\otimes\hat{\boldsymbol{\sigma}}^b_x-\hat{\boldsymbol{\sigma}}^a_y\otimes\hat{\boldsymbol{\sigma}}^b_y)$. The evolution is calculated numerically for $\omega=1$. The border of the shaded area represents T_{uc} calculated numerically. The dashed line represents T_{lb} according to Eq. (22). Up to the coupling $\gamma=0.1$ T_{lb} approximates T_{lc} very well. Temperature is measured in units of ω.

At $T<T_{lb}$ the minimal eigenvalue of the partially transposed state (14) is negative. We want to show that above T_{lb} the negative eigenvalues of the matrix matrixform (14) are of higher order in γ and therefore are negligibly small when the coupling is weak.

Let us consider corrections to the eigenvalues $P_{i(j+1)}$ and $P_{(i+1)j}$ of the composite state (14). The order-of-magnitude estimate of the smallest one of the corrected eigenvalues is $\lambda^{ij}_-=\sqrt{P_{i(j+1)}P_{(i+1)j}}-\gamma P_{ij}/\Delta E_{ij}$, where $\Delta E_{ij}\equiv E^{i+1}_a-E^i_a+E^{j+1}_b-E^j_b$. For simplicity we assume $P_{i(j+1)}=P_{(i+1)j}$. Then $\lambda^{ij}_-=O(P_{i(j+1)}-\gamma P_{ij}/\Delta E_{ij})$. Below T_{lb} the minimal eigenvalue of the state (14) is $\lambda_-=O(-\gamma/\Delta E_{11})$. We shall estimate the ratio $r^{ij}\equiv\lambda^{ij}_-/\lambda_-$ and show that it is negligible when the coupling is weak. We shall assume without loss of generality that the ground-state energy is zero: $E^1_a+E^1_b=0$. Then the partition function Z of the composite system is larger than unity. It follows that

$$r^{ij} = \frac{\lambda_-^{ij}}{\lambda_-} = \frac{(\gamma/\Delta E_{ij})P_{ij} - P_{i(j+1)}}{\gamma/\Delta E_{11}} < \frac{(\gamma/\Delta E_{ij})ZP_{ij} - ZP_{i(j+1)}}{\gamma/\Delta E_{11}}$$
$$= \frac{(\gamma/\Delta E_{ij})e^{-E_{ij}/T} - e^{-E_{i(j+1)}/T}}{\gamma/\Delta E_{11}}. \quad (24)$$

We are looking for the maximal value of r^{ij} in the interval $0<T<T_c^{ij}$, corresponding to the condition $P_{i(j+1)} < \gamma P_{ij}/\Delta E_{ij}$, i.e., to the negative values of λ_-^{ij}. T_c^{ij} is determined by the condition $\lambda_-^{ij}=0$. The ratio r^{ij} is positive in the interval $0<T<T_c^{ij}$ and vanishes on its borders. Therefore r^{ij} has a maximum r_m^{ij} at $0<T_m^{ij}<T_c^{ij}$, which is found from the condition $\partial r^{ij}/\partial T|_{T_m^{ij}}=0$. The calculation gives

$$\exp[-\Delta E_{ij}/(2T_m^{ij})] = (\gamma/\Delta E_{ij})(E_{ij}/E_{i(j+1)}) < (\gamma/\Delta E_{ij})$$
$$= \exp[-\Delta E_{ij}/(2T_c^{ij})],$$

which proves that there is one maximum r_m^{ij} at $0<T_m^{ij}<T_c^{ij}$. We remark that T_c^{ij}, corresponding to the largest ΔE_{ij} over all i and j, T_{uc}^*, is of the order of the upper critical temperature, $T_{uc}^*=O(T_{uc})$. The maximal value of r^{ij} is given by

$$r_m^{ij} = \frac{\Delta E_{11}}{2E_{ij}+\Delta E_{ij}}\left(\frac{2E_{ij}}{2E_{ij}+\Delta E_{ij}}\right)^{2E_{ij}/\Delta E_{ij}}\left(\frac{\gamma}{\Delta E_{ij}}\right)^{2E_{ij}/\Delta E_{ij}}$$
$$< \frac{\Delta E_{11}}{2E_{ij}+\Delta E_{ij}}\left(\frac{\gamma}{\Delta E_{ij}}\right)^{2E_{ij}/\Delta E_{ij}}, \quad (25)$$

where the inequality follows from the fact that $1/e < [2E_{ij}/(2E_{ij}+\Delta E_{ij})]^{2E_{ij}/\Delta E_{ij}} < 1$ in general. As a next step we notice that $\Delta E_{11} \leqslant 2E_{ij}$; therefore

$$r^{ij} < r_m^{ij} < \frac{\Delta E_{11}}{2E_{ij}+\Delta E_{ij}}\left(\frac{\gamma}{\Delta E_{ij}}\right)^{2E_{ij}/\Delta E_{ij}}$$
$$\leqslant \frac{\Delta E_{11}}{\Delta E_{11}+\Delta E_{ij}}\left(\frac{\gamma}{\Delta E_{ij}}\right)^{\Delta E_{11}/\Delta E_{ij}}. \quad (26)$$

Introducing the definition $x_{ij} \equiv \Delta E_{ij}/\Delta E_{11}$ and taking $\Delta E_{11}=1$, which corresponds to a rescaling of the coupling strength γ, leads to

$$\frac{\lambda_-^{ij}}{\lambda_-} \equiv r^{ij} < \frac{1}{x_{ij}}\left(\frac{\gamma}{x_{ij}}\right)^{1/x_{ij}}. \quad (27)$$

Typically the spectrum becomes denser with increasing energy. In that case $x_{ij} \equiv \Delta E_{ij}/\Delta E_{11} \leqslant 1$. Values of λ_-^{ij} corresponding to $x_{ij} \ll 1$ need not be taken into account, because $T_c^{ij} < T_{lb}$ in this case and as a conseqence $\lambda_-^{ij} > 0$ at $T \geqslant T_{lb}$. At $x_{ij}=O(1)$ the upper bound for r scales as $O(\gamma)$ and therefore corresponding negative eigenvalues of Eq. (14) are negligible. In this case we expect that $T_{lb} \approx T_{uc}$.

In those cases when $x_{ij} \equiv \Delta E_{ij}/\Delta E_{11} \gg 1$ the upper bound for r scales as $O(1/x_{ij})$ and the corresponding negative eigenvalues of Eq. (14) can be neglected, too.

When x_{ij} is moderately larger than unity the upper bound Eq. (27) for r^{ij} has a local maximum. The position of the maximum weakly depends on γ: numerical calculations show $x_{ij} \approx 2$–10 in the range of $10^{-4} \leqslant \gamma \leqslant 10^{-1}$. The value of the minimum is a monotonically slowly increasing function of γ. In the range $10^{-4} \leqslant \gamma \leqslant 10^{-1}$ numerical estimation of Eq. (27) shows values 0.04–0.1 for the local maximum. It is clear that the upper bound Eq. (27) for r^{ij} is far from being tight. In fact, numerical calculations show that r^{ij} is generally much smaller. As a consequence, the corresponding negative eigenvalues of Eq. (14) can be neglected.

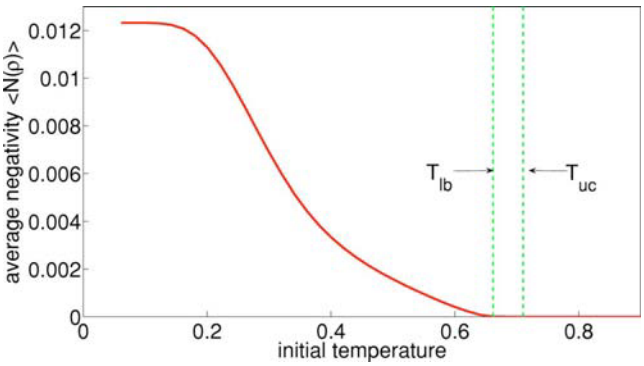

FIG. 3. (Color online) The time-averaged negativity as a function of initial temperature. The composite system is constructed from two interacting four-level subsystems. The initial state is a product of thermal states. The evolution is generated numerically by the Hamiltonian (2) (for details of the Hamiltonian see the text) with $\gamma=0.05$. The dashed lines correspond to the lower-bound temperature T_{lb}, Eq. (22), and to the upper critical temperature T_{uc}, found numerically. It can be seen that the entanglement is vanishingly small in the interval $T_{lb}<T<T_{uc}$. Temperature is measured in units of ω.}

It can be argued that although each one of the negative eigenvalues of Eq. (14) is negligible at $T \geqslant T_{lb}$ the (free) entanglement of the state cannot be neglected. In fact, the minimal negative eigenvalue of the partially transposed matrix is not a measure of entanglement. Various measures of entanglement have been defined [32]. In the present context we will employ a quantitative counterpart of the Peres-Horodecki criterion, the negativity [27]

$$N(\hat{\boldsymbol{\rho}}(t)) \equiv \frac{\|\hat{\boldsymbol{\rho}}(t)^{T_a}\| - 1}{2}, \quad (28)$$

where $\|\hat{\mathbf{X}}\| = \mathrm{Tr}\sqrt{\hat{\mathbf{X}}^\dagger \hat{\mathbf{X}}}$ is the trace norm of an operator $\hat{\mathbf{X}}$. The negativity of the state equals the absolute value of the sum of the negative eigenvalues of the partially transposed state. When the negativity of a composite bipartite state vanishes there is no free entanglement in the state. It can be shown by an order-of-magnitude analysis similar to the analysis above that values of the negativity of the composite state, corresponding to the partial transpose (14), are generally dominated by the minimal negative eigenvalue. As a consequence, the negativity of the state, evolving from the initial thermal product state at the temperature $T \geqslant T_{lb}$ is negligible under the weak-coupling assumption.

Figures 3 and 4 display results of numerical calculations of the time averaged negativity of the composite state (6) as a function of initial temperature for two different kinds of unperturbed spectra of the composite system $A \otimes B$. Both A and B are four-level systems. The composite system evolves

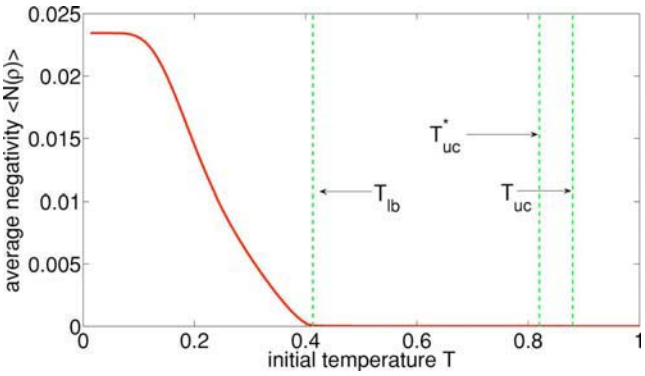

FIG. 4. (Color online) The time-averaged negativity as a function of initial temperature of the composite system. The composite system is constructed from two interacting four-level subsystems. The initial state is a product of thermal states. The evolution is generated numerically by the Hamiltonian (2) (for details of the Hamiltonian see the text) with $\gamma=0.05$. The dashed lines correspond to the lower-bound temperature T_{lb}, Eq. (22), to the numerical value of the upper critical temperature T_{uc} and to the value T_{uc}^{*}, corresponding to the largest spectrum spacing ΔE_{max}. We see that entanglement is vanishingly small at $T_{lb}<T<T_{uc}$, as expected, and T_{uc}^{*} is a good approximation to the upper critical temperature T_{uc}. Temperature is measured in units of ω.

from the initial product of thermal states of A and B under the Hamiltonian (2).

Figure 3 presents the results of calculations for the following choice of the unperturbed spectra of $\hat{\mathbf{H}}_a$ and $\hat{\mathbf{H}}_b$: $E_a^{\{1,2,3,4\}}=\{\omega,5\omega,8\omega,10\omega\}$ and $E_b^i=\sqrt{\omega E_a^i}$ (we set $\omega=1$). Care was taken to avoid resonances and the spectra were chosen to become denser with increasing energy. The interaction terms in the Hamiltonian were restricted to $(\hat{\mathbf{V}}_{a,b})_{ij}=\delta_{i,j\pm1}$ and the coupling strength $\gamma=0.05$. We see that $T_{uc}\approx T_{lb}$ and the time-averaged negativity $\langle N(\hat{\boldsymbol{\rho}}(t))\rangle$ is negligible in the interval $T_{lb}<T<T_{uc}$ as expected.

Figure 4 displays the time-averaged negativity $\langle N(\hat{\boldsymbol{\rho}}(t))\rangle$ as a function of initial temperature of the composite state of two interacting four-level subsystems A and B with the unperturbed energy spectra $E_a^{\{1,2,3,4\}}=\{\omega,3\omega,7\omega,13\omega\}$ and $E_b^i=\sqrt{\omega E_a^i}$. The composite state evolves from the initial product of two thermal states under the Hamiltonian (2), where $(\hat{\mathbf{V}}_{a,b})_{ij}=\delta_{i,j\pm1}$ and the coupling strength $\gamma=0.05$. In choosing the unperturbed spectra care was taken to avoid resonances and to ensure that the maximal value of $x_{ij}\equiv\Delta E_{ij}/\Delta E_{11}$ equals the position of the local maximum of the upper bound (27), corresponding to $\gamma=0.05$. Figure 3 shows that the time-averaged negativity $\langle N(\hat{\boldsymbol{\rho}}(t))\rangle$ is negligible in the interval $T_{lb}<T<T_{uc}$ as expected. The value of $T_c^{ij}\equiv T_{uc}^{*}$ [the definition of T_c^{ij} is given after Eq. (24)], corresponding to the maximal value $\Delta E_{max}\equiv\max_{ij}(\Delta E_{ij})$ is calculated. T_{uc}^{*} is in good correspondence with the value T_{uc}, calculated numerically.

In the following section the lower-bound temperature for the generation of entanglement in the case of indirect interaction will be calculated. It is expected on general perturbation theory grounds that the negativity is negligible in this case, too, at $T>T_{lb}$. A quantitative anlysis was not carried out due to the technical complexity of the indirect interaction case. Nevertheless, all the numerical tests confirm this view. The temperature dependence of the negativity for a given coupling strength in the case of indirect interaction is essentially equivalent to the temperature dependence in the direct-interaction case plotted in Figs. 3 and 4.

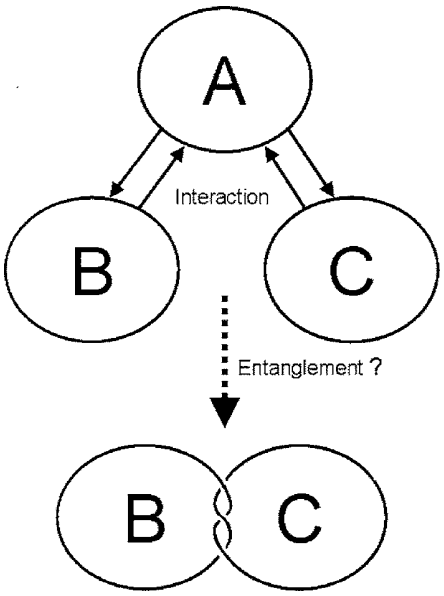

FIG. 5. Scheme of interaction for two noninteraction systems in contact with a common third party.

III. ENTANGLEMENT BETWEEN TWO NONINTERACTING SYSTEMS IN CONTACT WITH A COMMON THIRD PARTY

The dynamics studied is of the composite system $A\otimes B\otimes C$ where systems B and C do not interact directly (see. Fig. 5). The entanglement explored is of the reduced composite system $B\otimes C$.

The evolution is generated by the following Hamiltonian:

$$\hat{\mathbf{H}}_{total}=\hat{\mathbf{H}}+\gamma\hat{\mathbf{V}}, \tag{29}$$

where $\hat{\mathbf{H}}=\hat{\mathbf{H}}_a+\hat{\mathbf{H}}_b+\hat{\mathbf{H}}_c$ and $\hat{\mathbf{V}}=\gamma\hat{\mathbf{V}}_a\otimes(\hat{\mathbf{V}}_b\otimes\hat{\mathbf{1}}+\hat{\mathbf{1}}\otimes\hat{\mathbf{V}}_c)$. The analysis is carried out in the interaction picture. The initial state is taken to be $\hat{\boldsymbol{\rho}}(0)=\hat{\boldsymbol{\rho}}_a\otimes\hat{\boldsymbol{\rho}}_b\otimes\hat{\boldsymbol{\rho}}_c$, where $\hat{\boldsymbol{\rho}}_a$, $\hat{\boldsymbol{\rho}}_b$, and $\hat{\boldsymbol{\rho}}_c$ are thermal states. Since B and C are noninteracting entanglement will appear only in the second order in the coupling. Up to second order in γ the state of the composite system $A\otimes B\otimes C$ becomes

$$\hat{\boldsymbol{\rho}}(t)'=\hat{\boldsymbol{\rho}}(0)-i\gamma\int_0^t[\hat{\mathbf{V}}(t'),\hat{\boldsymbol{\rho}}(0)']dt'-\gamma^2\int_0^t\int_0^{t'}[\hat{\mathbf{V}}(t'),[\hat{\mathbf{V}}(t''),\hat{\boldsymbol{\rho}}(0)']]dt'dt'', \tag{30}$$

where

$$\hat{\boldsymbol{\rho}}'=e^{-i\hat{\mathbf{H}}t}\hat{\boldsymbol{\rho}}\,e^{i\hat{\mathbf{H}}t},$$

$$\hat{\mathbf{V}}(t) = e^{i\hat{\mathbf{H}}t}\hat{\mathbf{V}}e^{-i\hat{\mathbf{H}}t}. \tag{31}$$

In what follows the prime on the $\hat{\boldsymbol{\rho}}(t)$ is omitted.

Next the system is reduced to $B\otimes C$ by taking the partial trace of $\hat{\boldsymbol{\rho}}(t)$ over the system A degrees of freedom. The partial transposition of the reduced density operator with respect to the subsystem B gives:

$$\hat{\boldsymbol{\rho}}_{bc}^{T_b}(t) = \hat{\boldsymbol{\rho}}_{bc}^{T_b}(0) + \hat{\mathbf{M}}(t), \tag{32}$$

where $\hat{\boldsymbol{\rho}}_{bc}(t) \equiv \mathrm{Tr}_a\hat{\boldsymbol{\rho}}(t)$ and

$$\hat{\mathbf{M}} \equiv -i\gamma\int_0^t \mathrm{Tr}_a[\hat{\mathbf{V}}(t'),\hat{\boldsymbol{\rho}}(0)]^{T_b}dt' - \gamma^2\int_0^t\int_0^{t'} \mathrm{Tr}_a[\hat{\mathbf{V}}(t'),[\hat{\mathbf{V}}(t''),\hat{\boldsymbol{\rho}}(0)]]^{T_b}dt'dt''. \tag{33}$$

Let $|ik\rangle \equiv |i\rangle\otimes|k\rangle$ be the local orthonormal basis of the system $B\otimes C$ composed of the eigenstates of the Hamiltonian $\hat{\mathbf{H}}_b+\hat{\mathbf{H}}_c$:

$$\hat{\mathbf{H}}_{b,c}|i\rangle = E_{b,c}^i|i\rangle, \tag{34}$$

where $E_{b,c}^i$, $i=1,2,\ldots$, is the unperturbed energy spectrum of the Hamiltonian $\hat{\mathbf{H}}_{b,c}$. Since $\hat{\boldsymbol{\rho}}_{bc}(0)=\hat{\boldsymbol{\rho}}_b\otimes\hat{\boldsymbol{\rho}}_c$,

$$\hat{\boldsymbol{\rho}}_{bc}(0)^{T_b}|ik\rangle = \hat{\boldsymbol{\rho}}_{bc}(0)|ik\rangle = \hat{\boldsymbol{\rho}}_b\otimes\hat{\boldsymbol{\rho}}_c|ik\rangle = P_{ik}|ik\rangle, \tag{35}$$

where $P_{ik}\equiv p_{b,i}p_{c,k}$, and $p_{a,i}, p_{b,k}$ are defined by $p_{b,i}=\langle i|\hat{\boldsymbol{\rho}}_a|i\rangle$ and $p_{c,k}=\langle k|\hat{\boldsymbol{\rho}}_b|k\rangle$. The matrix elements of $\hat{\boldsymbol{\rho}}_{bc}(t)^{T_b}$ are given by

$$\langle ik|\hat{\boldsymbol{\rho}}_{bc}(t)^{T_b}|jl\rangle = P_{ik}\delta_{(ik),(jl)} + M_{ik,jl}, \tag{36}$$

where by definition $M_{ik,jl}=\langle ik|\hat{\mathbf{M}}|jl\rangle$.

From this point the calculations proceed along the same lines as in Sec. II following Eq. (11). The minimal eigenvalue of the partially transposed reduced state $\hat{\boldsymbol{\rho}}_{bc}(t)^{T_b}$ is shown to be negative at sufficiently low temperatures and the lower-bound temperature T_{lb} is calculated.

The negative eigenvalue of the partially transposed composite state Eq. (32) is calculated to the leading order in the coupling strength γ assuming $\langle n_i|\hat{\mathbf{V}}_i|m_i\rangle \propto \delta_{n_i m_i\pm 1}$. As in Sec. II the eigenvalue is found from the spectrum of the 2×2 matrix:

$$\begin{pmatrix} P_{12}+M_{12,12} & M_{12,21} \\ M_{12,21}^* & P_{21}+M_{21,21}\end{pmatrix}, \tag{37}$$

completely analogous to the matrix (16). The eigenvalues of Eq. (37) are

$$\lambda_\pm = \frac{P_{12}+M_{12,12}+P_{21}+M_{21,21}}{2} \pm \frac{\sqrt{(P_{12}+M_{12,12}+P_{21}+M_{21,21})^2 - 4[(P_{12}+M_{12,12})(P_{21}+M_{21,21}) - |M_{12,21}|^2]}}{2}, \tag{38}$$

and the eigenvalue λ_- becomes negative when $(P_{12}+M_{12,12})(P_{21}+M_{21,21}) < |M_{12,21}|^2$.

To calculate $M_{12,12}$, $M_{21,21}$, and $M_{12,21}$ we first note that the integrand in the first order term in Eq. (33) is

$$\begin{aligned}&\mathrm{Tr}_a[\hat{\mathbf{V}}(t'),\hat{\boldsymbol{\rho}}(0)]^{T_b}\\ &= \langle\hat{\mathbf{V}}_a\rangle[\hat{\mathbf{V}}_{bc}(t'),\hat{\boldsymbol{\rho}}_{bc}(0)]^{T_b}\\ &= \langle\hat{\mathbf{V}}_a\rangle\{[\hat{\mathbf{V}}_b(t'),\hat{\boldsymbol{\rho}}_b]^T\otimes\hat{\boldsymbol{\rho}}_c + \hat{\boldsymbol{\rho}}_b^T\otimes[\hat{\mathbf{V}}_c(t'),\hat{\boldsymbol{\rho}}_c]\}\\ &= -\langle\hat{\mathbf{V}}_a\rangle\{[\hat{\mathbf{V}}_b(t')^T,\hat{\boldsymbol{\rho}}_b]\otimes\hat{\boldsymbol{\rho}}_c - \hat{\boldsymbol{\rho}}_b\otimes[\hat{\mathbf{V}}_c(t'),\hat{\boldsymbol{\rho}}_c]\},\end{aligned} \tag{39}$$

where $\langle\hat{\mathbf{V}}_a\rangle$ means the thermal average of the operator $\hat{\mathbf{V}}_a$ and the notation $\hat{\mathbf{V}}_{bc}\equiv\hat{\mathbf{V}}_b\otimes\hat{\mathbf{1}}+\hat{\mathbf{1}}\otimes\hat{\mathbf{V}}_c$ is introduced. The initial condition $\hat{\boldsymbol{\rho}}_{bc}(0)=\hat{\boldsymbol{\rho}}_b\otimes\hat{\boldsymbol{\rho}}_c$ was used. Since $\hat{\boldsymbol{\rho}}_{b,c}|i\rangle=\delta_{i,1}|i\rangle$ the term Eq. (39) does not contribute to the eigenvalues of the matrix (37) in the first order.

To simplify the calculation of the second order corrections it is assumed that the thermal average of the system A coupling operator $\langle\hat{\mathbf{V}}_a\rangle$ vanishes. This assumption is not crucial for the qualitative picture of temperature dependence of the entanglement. Moreover, it is in line with common models of coupling, for example, the Caldeira-Leggett model [33], dipole interaction with the electromagnetic field [34], etc. The integrand in the second-order term in Eq. (33) is

$$\begin{aligned}&\mathrm{Tr}_a[\hat{\mathbf{V}}(t'),[\hat{\mathbf{V}}(t''),\hat{\boldsymbol{\rho}}(0)]]^{T_b}\\ &= \langle\hat{\mathbf{V}}_a(t')\hat{\mathbf{V}}_a(t'')\rangle[\hat{\mathbf{V}}_{bc}(t'),\hat{\mathbf{V}}_{bc}(t'')\hat{\boldsymbol{\rho}}_{bc}]^{T_b}\\ &- \langle\hat{\mathbf{V}}_a(t'')\hat{\mathbf{V}}_a(t')\rangle[\hat{\mathbf{V}}_{bc}(t'),\hat{\boldsymbol{\rho}}_{bc}\hat{\mathbf{V}}_{bc}(t'')]^{T_b}.\end{aligned} \tag{40}$$

Expanding the thermal averages in the orthonormal basis $|n\rangle$ of the Hamiltonian H_a leads to

$$\begin{aligned}&\mathrm{Tr}_a[\hat{\mathbf{V}}(t'),[\hat{\mathbf{V}}(t''),\hat{\boldsymbol{\rho}}(0)]]^{T_b}\\ &= \sum_{m,n} p_{a,n}|\langle m|\hat{\mathbf{V}}_a|n\rangle|^2(\cos[\omega_{mn}^a(t'-t'')]\\ &\times[\hat{\mathbf{V}}_{bc}(t'),[\hat{\mathbf{V}}_{bc}(t''),\hat{\boldsymbol{\rho}}_{bc}]] + i\sin[\omega_{mn}^a(t'-t'')]\\ &\times[\hat{\mathbf{V}}_{bc}(t'),\{\hat{\mathbf{V}}_{bc}(t''),\hat{\boldsymbol{\rho}}_{bc}\}])^{T_b},\end{aligned} \tag{41}$$

where ω_{mn}^a is the energy difference between the states $|n\rangle$ and $|m\rangle$ of the Hamiltonian H_a, the $\{\hat{\mathbf{X}},\hat{\mathbf{Y}}\}$ designates the anticommutator of operators $\hat{\mathbf{X}}$ and $\hat{\mathbf{Y}}$ and $p_{a,n}\equiv(\hat{\boldsymbol{\rho}}_a)_{nn}$.

For simplicity the notation $\hat{\mathbf{C}}(t',t'')$ is used for the operator (41). Expressing the operator $\hat{\mathbf{V}}_{bc}$ in terms of $\hat{\mathbf{V}}_b$ and $\hat{\mathbf{V}}_c$ we put the matrix elements of $\hat{\mathbf{C}}(t',t'')$ into the following form:

$$\langle 12|\hat{\mathbf{C}}(t',t'')|12\rangle = -2P_{11}\sum_{m,n} p_{a,n}|\langle m|\hat{\mathbf{V}}_a|n\rangle|^2|\langle 1|\hat{\mathbf{V}}_c|2\rangle|^2 \times\cos[(\omega^a_{mn}+\omega_c)(t'-t'')],$$

$$\langle 21|\hat{\mathbf{C}}(t',t'')|21\rangle = -2P_{11}\sum_{m,n} p_{a,n}|\langle m|\hat{\mathbf{V}}_a|n\rangle|^2|\langle 1|\hat{\mathbf{V}}_b|2\rangle|^2 \times\cos[(\omega^a_{mn}+\omega_b)(t'-t'')],$$

$$\langle 12|\hat{\mathbf{C}}(t',t'')|21\rangle = P_{11}\sum_{m,n} p_{a,n}|\langle m|\hat{\mathbf{V}}_a|n\rangle|^2\langle 2|\hat{\mathbf{V}}_b|1\rangle\langle 2|\hat{\mathbf{V}}_c|1\rangle \times e^{i\omega^a_{mn}(t'-t'')}(e^{-i(\omega_b t'+\omega_c t'')}+e^{-i(\omega_b t''+\omega_c t')}), \tag{42}$$

where $\omega_{b,c}$ stands for the energy difference between the first excited and the ground states of the unperturbed subsystem B (C). The matrix elements $M_{12,12}$, $M_{21,21}$, and $M_{12,21}$ are given by

$$M_{12,12} = -\gamma^2\int_0^t\int_0^{t'}\langle 12|C(t',t'')|12\rangle dt'dt'',$$

$$M_{21,21} = -\gamma^2\int_0^t\int_0^{t'}\langle 21|C(t',t'')|21\rangle dt'dt'',$$

$$M_{12,21} = -\gamma^2\int_0^t\int_0^{t'}\langle 12|C(t',t'')|21\rangle dt'dt''. \tag{43}$$

The integration is straightforward but the final expressions are cumbersome. Two cases are considered explicitly: (a) $\omega^a_{mn}\gg\omega_{b,c}$ and (b) $\omega_{b,c}\gg\omega^a_{mn}$. In both cases it is shown that at sufficiently low initial temperature of the system $B\otimes C$ one of the eigenvalues of the matrix (37) is negative and the lower-bound temperature T_{lb} is calculated.

A. Two slow systems interacting with a fast common third party

Performing the integrations in Eq. (43) and taking the leading terms in $\omega_{b,c}/\omega^a_{mn}$ brings us to

$$M_{12,12} = 4\gamma^2\sum_{m,n} p_{a,n}|\langle m|\hat{\mathbf{V}}_a|n\rangle|^2|\langle 1|\hat{\mathbf{V}}_c|2\rangle|^2\frac{\sin[(\omega^a_{mn}+\omega_c)t/2]^2}{(\omega^a_{mn})^2},$$

$$M_{21,21} = 4\gamma^2\sum_{m,n} p_{a,n}|\langle m|\hat{\mathbf{V}}_a|n\rangle|^2|\langle 1|\hat{\mathbf{V}}_b|2\rangle|^2\frac{\sin[(\omega^a_{mn}+\omega_b)t/2]^2}{(\omega^a_{mn})^2},$$

$$M_{12,21} = 2\gamma^2\sum_{m,n} p_{a,n}|\langle m|\hat{\mathbf{V}}_a|n\rangle|^2\langle 2|\hat{\mathbf{V}}_b|1\rangle \times\langle 2|\hat{\mathbf{V}}_c|1\rangle\frac{(1-e^{-i(\omega_b+\omega_c)t})}{\omega^a_{mn}(\omega_b+\omega_c)}. \tag{44}$$

At $T=0$ the minimal eigenvalue of Eq. (38) is given by $\lambda_- = -\sqrt{M_{12,12}M_{21,21}-|M_{12,21}|^2}$, which to the leading order in $\omega_{b,c}/\omega^a_{mn}$ gives $\lambda_- = -|M_{12,21}|^2$. This proves that the system $B\otimes C$ becomes entangled at sufficiently low temperature. We note that this result holds at any finite temperature of the system A. At infinite temperature of the system A $M_{12,21}\equiv 0$ and no free entanglement is generated in the system $B\otimes C$.

At finite initial temperature of $B\otimes C$ the condition $\lambda_- < 0$ translates to $P_{12}P_{21} < \gamma^4|M_{12,21}|^2P_{11}^2$ to the leading order in $\omega_{1,2}/\omega^a_{mn}$. The lower-bound temperature T_{lb} is found from the condition $P_{12}P_{21} = \gamma^4|M_{12,21}|^2P_{11}^2$. Since $|M_{12,21}|$ is an oscillating function of time the amplitude of $|M_{12,21}|$ must be substituted for $|M_{12,21}|$ in this equality, which leads to the following equation defining the lower bound temperature:

$$4\gamma^2\frac{|\langle 2|\hat{\mathbf{V}}_b|1\rangle\langle 2|\hat{\mathbf{V}}_c|1\rangle|}{\omega_b+\omega_c}\sum_{m,n}\frac{p_{a,n}|\langle m|\hat{\mathbf{V}}_a|n\rangle|^2}{\omega^a_{mn}} = \sqrt{\frac{P_2P_3}{P_1^2}} = \exp\left(-\frac{\omega_b+\omega_c}{2T_{lb}}\right), \tag{45}$$

finally leading to

$$T_{lb} = \frac{-(\omega_b+\omega_c)}{2\ln\left(4\gamma^2\frac{|\langle 2|\hat{\mathbf{V}}_b|1\rangle\langle 2|\hat{\mathbf{V}}_c|1\rangle|}{\omega_b+\omega_c}\sum_{m,n}\frac{p_{a,n}|\langle m|\hat{\mathbf{V}}_a|n\rangle|^2}{\omega^a_{mn}}\right)}. \tag{46}$$

A generalization of the formula to the case of interaction of the form $\Sigma\gamma_i\hat{\mathbf{V}}^i_a\otimes(\hat{\mathbf{V}}^i_b\otimes\hat{\mathbf{1}}+\hat{\mathbf{1}}\otimes\hat{\mathbf{V}}^i_c)$ can be carried out along the same lines.

The entanglement in the reduced system of two noninteracting slow spins interacting with the fast four-level bath was explored numerically and the results are plotted in Fig. 6. The shaded area in the parametric space of the logarithm of inverse coupling strength and the inverse initial temperature of the spins represents parametric values for which no entanglement develops in the course of the evolution. The border of the shaded area corresponds to the critical temperature for various coupling magnitudes. The Hamiltonian of the composite system is

$$\hat{\mathbf{H}} = \hat{\mathbf{H}}_a\otimes\hat{\mathbf{1}}_b\otimes\hat{\mathbf{1}}_c + \frac{1}{2}\omega[\hat{\mathbf{1}}_a\otimes(\hat{\boldsymbol{\sigma}}^b_z\otimes\hat{\mathbf{1}}_c+\sqrt{2}\hat{\mathbf{1}}_b\otimes\hat{\boldsymbol{\sigma}}^c_z)] + \gamma\hat{\mathbf{V}}_a\otimes(\hat{\boldsymbol{\sigma}}^b_x\otimes\hat{\mathbf{1}}_c+\hat{\mathbf{1}}_b\otimes\hat{\boldsymbol{\sigma}}^c_x), \tag{47}$$

where $(\hat{\mathbf{H}}_a)_{ij}=\delta_{ij}E^i_a$, $E^{\{1,2,3,4\}}_a=\{0,10\omega,20\omega,30\omega\}$ and $(\hat{\mathbf{V}}_a)_{ij}=\delta_{ij}$. The temperature of the thermal initial state of the bath is $T=5\omega$. The value of ω chosen for the numerical calculation is unity. The correspondence of Eq. (46) (the dashed line) to the numerical values is very good up to a coupling strength of the order of unity. We note that for large values of the coupling strength γ the critical temperature asymptotically tends to a finite constant value.

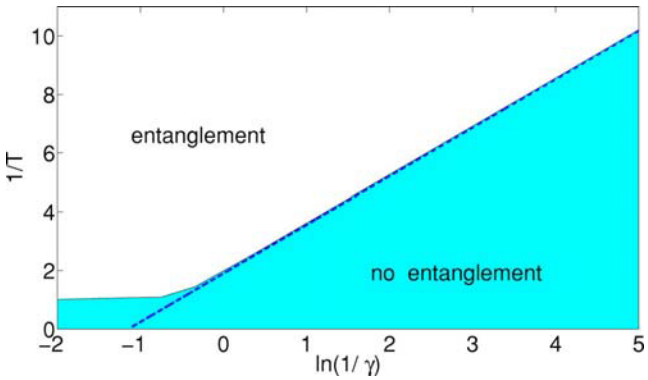

FIG. 6. (Color online) The shaded area in the parameter space of the inverse initial temperature T of the slow spin and the logarithm of the inverse coupling strength γ, represents values of T and γ where entanglement does not develop in the course of the evolution. The composite system of two slow spins interacting with a fast four-level system evolves from the initial product of thermal states under the Hamiltonian (47). The dashed line is the plot of T_{lb}, Eq. (46). Up to the coupling $\gamma=1$ its correspondence with the border of the shaded area is very good. Temperature is measured in units of ω.

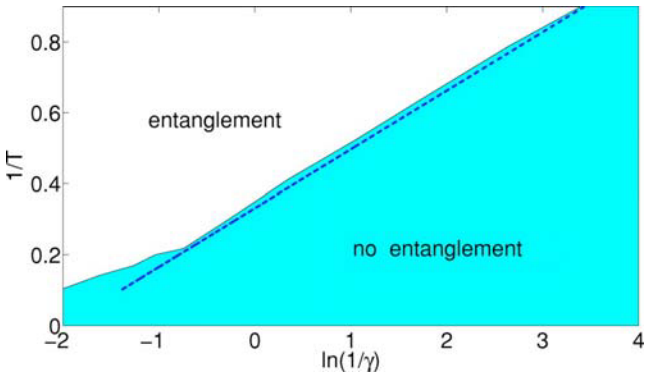

FIG. 7. (Color online) The shaded area in the parameter space of the inverse initial temperature T of the fast spins and the logarithm of the inverse coupling strength γ represents values of T and γ where entanglement does not develop in the course of the evolution. The composite system of two fast spins interacting with the slow four-level system evolves from the initial product of thermal states under the Hamiltonian (52). The dashed line is the plot of T_{lb}, Eq. (51). Up to the coupling $\gamma=1$ its correspondence with the border of the shaded area is good. Temperature is measured in units of ω.

B. Two fast systems interacting with a slow common third party

The case $\omega_{b,c} \gg \omega_{mn}^{a}$ is more complex. To demonstrate entanglement at zero temperature of the system $B \otimes C$ two simplifying assumptions were added. The first is that the temperature of the system A is also zero. The second is that the matrix elements of V_a couple only the neighboring states: $\langle n|\hat{\mathbf{V}}_a|m\rangle \propto \delta_{n,m\pm1}$. Under these two assumptions the expressions for $M_{12,12}$, $M_{21,21}$, and $M_{12,12}M_{M_{21,21}}-|M_{12,21}|^2$ become

$$M_{12,12} = P_{11}\left(\frac{2\gamma|\langle 2|\hat{\mathbf{V}}_a|1\rangle||\langle 1|\hat{\mathbf{V}}_c|2\rangle|\sin[(\omega_a+\omega_c)t/2]}{\omega_c}\right)^2,$$

$$M_{21,21} = P_{11}\left(\frac{2\gamma|\langle 2|\hat{\mathbf{V}}_a|1\rangle||\langle 1|\hat{\mathbf{V}}_b|2\rangle|\sin[(\omega_a+\omega_b)t/2]}{\omega_b}\right)^2,$$

$$M_{12,12}M_{M_{21,21}} - |M_{12,21}|^2 = P_{11}^2\left(\frac{2\gamma^2|\langle 2|\hat{\mathbf{V}}_a|1\rangle|^2|\langle 1|\hat{\mathbf{V}}_c|2\rangle||\langle 1|\hat{\mathbf{V}}_b|2\rangle|}{\omega_b\omega_c}\right)^2 S(t), \tag{48}$$

where

$$S(t) = \sin(\omega_a t)\{\sin(\omega_b t) + \sin(\omega_c t) - \sin[(\omega_a+\omega_b+\omega_c)t]\}. \tag{49}$$

To estimate $S(t)$ new variables $x=\sin(\omega_a t)$, $y=\sin(\omega_b t)$, and $z=\sin(\omega_c t)$ are introduced. Ignoring the zero-measure set of commensurable frequencies we can treat the function $S(t)$ as a function of three independent variables x,y, and z. The range of $S(t)$ in the cube, defined by $-1\leqslant x,y,z\leqslant 1$, can be explored numerically and is found to be $s\leqslant S(t)\leqslant 3$, where $s\approx -1.6834$. Therefore, from Eq. (48) $M_{12,12}M_{M_{21,21}} - |M_{12,21}|^2 < 0$, which proves that at zero temperature $\lambda_- < 0$ [see Eq. (38)] and the systems B and C are entangled by the interaction with the system A.

The lower-bound temperature is determined by the condition $\lambda_-=0$, which translates to $(P_{12}+M_{12,12})(P_{21}+M_{21,21}) = |M_{12,21}|^2$ [see Eq. (38)]. The latter condition can be put in the form $(M_{12,12}M_{21,21}-|M_{12,21}|^2)+P_{12}P_{21}+P_{12}M_{21,21} + P_{21}M_{12,12}=0$. Since $M_{12,21}$ and $M_{21,21}$ are nonnegative independent functions of time the minimum value of $(M_{12,12}M_{21,21}-|M_{12,21}|^2)+P_{12}P_{21}+P_{12}M_{21,21}+P_{21}M_{12,12}$ is obtained at $M_{21,21}=M_{12,12}=0$. Then the lower-bound temperature can be calculated from the condition that the amplitude of $M_{12,12}M_{21,21}-|M_{12,21}|^2$ equals $-P_{12}P_{21}$:

$$\frac{2\gamma^2\sqrt{|s|}|\langle 2|\hat{\mathbf{V}}_a|1\rangle|^2|\langle 1|\hat{\mathbf{V}}_c|2\rangle||\langle 1|\hat{\mathbf{V}}_b|2\rangle|}{\omega_b\omega_c} = \sqrt{\frac{P_{12}P_{21}}{P_{11}^2}}, \tag{50}$$

finally leading to

$$T_{lb} = \frac{-(\omega_b+\omega_c)}{2\ln\left(2\gamma^2\sqrt{|s|}\dfrac{|\langle 2|\hat{\mathbf{V}}_a|1\rangle|^2|\langle 1|\hat{\mathbf{V}}_c|2\rangle||\langle 1|\hat{\mathbf{V}}_b|2\rangle|}{\omega_b\omega_c}\right)}. \tag{51}$$

It is interesting to note that T_{lb} in this case does not depend on the time scales of the slow system.

The entanglement in the reduced system of two noninteracting fast spins interacting with the slow four-level bath was explored numerically and the results are plotted in Fig. 7. The shaded area in the parametric space of the logarithm of inverse coupling strength and the inverse initial temperature of the spins represents parametric values for which no entanglement develops in the course of the evolution. The border of the shaded area corresponds to the critical temperature

for various coupling magnitudes. The Hamiltonian is chosen to be similar to the previous example, [see Eq. (47)], but time scales of the subsystems are reversed:

$$\hat{\mathbf{H}} = \hat{\mathbf{H}}_a \otimes \hat{\mathbf{1}}_b \otimes \hat{\mathbf{1}}_c + 5\omega[\hat{\mathbf{1}}_a \otimes (\hat{\boldsymbol{\sigma}}_z^b \otimes \hat{\mathbf{1}}_c + \sqrt{2}\hat{\mathbf{1}}_b \otimes \hat{\boldsymbol{\sigma}}_z^c)] + \gamma\hat{\mathbf{V}}_a \otimes (\hat{\boldsymbol{\sigma}}_x^b \otimes \hat{\mathbf{1}}_c + \hat{\mathbf{1}}_b \otimes \hat{\boldsymbol{\sigma}}_x^c), \quad (52)$$

where $(\hat{\mathbf{H}}_a)_{ij} = \delta_{ij}E_a^i$, $E_a^{\{1,2,3,4\}} = \{0, \omega, 2\omega, 3\omega\}$, and $(\hat{\mathbf{V}}_a)_{ij} = \delta_{ij}$. The temperature of the thermal initial state of the bath was chosen as $T = 0.01\omega$, which is small compared to the energy scale of the bath chosen for the numerical calculation: $\omega = 1$. The dashed line in Fig. 7 is a plot of Eq. (51) and the correspondence with the border of the shaded area at coupling strength up to the order of unity is good.

IV. SUMMARY AND CONCLUSIONS

Entanglement is created by both direct and indirect weak interaction between two initially disentangled systems prepared in thermal states at sufficiently low temperatures. The study is restricted to the conditions where the ground states of both systems are not invariant under the interaction and the interaction is nonresonant. As a consequence, the present analysis left out some interesting models such as the Jaynes-Cummings model [35]. The generation of entanglement in cases of the weak *resonant* direct and undirect interactions will be considered elsewhere.

In the case of indirect interaction to show entanglement at $T = 0$ we have assumed that the thermal average of the third party coupling term in the initial state vanishes. The reason for the assumption was technical. It should be noted that many system-bath models of linear coupling satisfy this assumption [33]. The additional technical assumption was that the coupling terms of the noninteracting parties possess matrix elements only between the adjacent energy states. Here, too, the assumption is general for weak-coupling models. Two cases of time-scale separation were considered explicitly. The first is the case of two slow systems interacting via the fast third common party. The second is the case of two fast systems interacting via the slow third common party. In the first case the entanglement was shown to appear at sufficiently low initial temperature of the slow systems for any finite temperature of the third party. In the second case the entanglement develops at sufficiently low initial temperature of the fast systems. In this case we assumed that the third party was prepared at zero temperature and that the third-party coupling agent has nonvanishing matrix elements only between the adjacent energy states. This assumption is stronger than just assuming that its thermal average vanishes.

In these cases of indirect interaction and in the case of the direct interaction between the parts we have shown that if the initial temperature of the bipartite state is zero entanglement is generated by the interaction. From this result and the general theorem about the existence of a finite separable ball about the maximally mixed state [28–31] it follows that at least one crossover from the entanglement-generating to the separable evolution should exist at some finite initial temperature of the state. The same is true for the crossover from the NPPT (non-partial-positive transpose) to the PPT evolution. The lowest temperature corresponding to a crossover was termed the lower critical temperature T_{lc} and the highest was termed the upper critical temperature T_{uc}. Numerical experiments suggest that there is one such crossover for the interactions studied and therefore $T_{lb} = T_{uc}$. In both cases of a direct and an indirect interaction between the initially disentangled systems, prepared in thermal states, we calculated the lower bound T_{lb} for the lower critical temperature T_{lc}. When the initial temperature of both thermal states is below T_{lb} the interaction generates entanglement in the course of the evolution. For temperatures above the lower bound T_{lb} the negativity of the partially transposed composite state is zero in the leading order in the coupling strength and therefore negligible in the weak-coupling limit. It follows that T_{lb} may be considered as the *physical* critical temperature for the negativity of the composite state.

It was found that T_{lb} is a monotonically decreasing function of the coupling strength. As a consequence, the purity of the state evolving from the initial thermal state at $T = T_{lb}$ can be arbitrary high at weak enough coupling, but the entanglement generation is zero to the leading order in the coupling strength. This proves that far from the maximal separable (and the maximal PPT) ball [30,31] centered at the maximally mixed state there exist a quantum dynamics, which is effectively PPT.

In Ref. [26] it was proved that a PPT density operator of a sufficiently small rank is separable. We speculate that, aiming at a less stringent criterion for the *approximate* separability, one may be satisfied with showing that the PPT state is sufficiently pure.

A high-temperature limit is generally considered as bringing about classical features into the quantum evolution. A quantum system at high temperature can be efficiently simulated on the classical computer. The present analysis suggests that there exists a PPT (or perhaps, even separable) dynamics in a relatively cold quantum region, which hopefully can be simulated with a moderate scaling.

ACKNOWLEDGMENTS

We are grateful to Roi Baer, Jose Palao, and Lajos Diósi for critical comments. This work is supported by DIP and the Israel Science Foundation.

[1] R. Feynman, Int. J. Theor. Phys. **21**, 467 (1982).
[2] E. Schroedinger, Naturwiss. **23**, 807 (1935); **23**, 823 (1935); **23**, 844 (1935).
[3] A. Peres, *Quantum Theory: Concepts and Methods* (Kluwer Academic Publishers, Dordrecht, 1998).
[4] W. H. Zurek, Rev. Mod. Phys. **75**. 715 (2003).
[5] See *Decoherence and the Appearance of a Classical World in Quantum Theory*, 2nd ed., edited by D. Giulini, E. Joos, C. Kiefer, J. Kupsch, I. O. Stamatescu, and H. D. Zeh (Springer, Berlin, 2003).
[6] E. B. Davis, Rep. Math. Phys. **11**, 169 (1977).
[7] G. Lindblad, J. Phys. A **29**, 4197, (1996).
[8] J. Gemmer and G. Mahler, Eur. Phys. J. D **17**, 385 (2001).
[9] T. Durt, Z. Naturforsch., A: Phys. Sci. **50**, 425 (2004).
[10] D. Bruss, J. Math. Phys. **43**, 4237 (2002).
[11] R. F. Werner, Phys. Rev. A **40**, 4277 (1989).
[12] M. Horodecki, P. Horodecki, and R. Horodecki, Phys. Rev. Lett. **80**, 5239 (1998).
[13] J. Eisert and M. B. Plenio, Phys. Rev. Lett. **89**, 137902 (2002).
[14] K. Audenaert, J. Eisert, M. B. Plenio, and R. F. Werner, Phys. Rev. A **66**, 042327 (2002).
[15] D. Braun, Phys. Rev. Lett. **89**, 277901 (2002).
[16] S. Scheel, J. Eisert, P. L. Knight, and M. B. Plenio, J. Mod. Opt. **50**, 881 (2003).
[17] S. I. Doronin, Phys. Rev. A **68**, 052306 (2003).
[18] A. Hutton and S. Bose, e-print quant-ph/0408077.
[19] A. Hutton and S. Bose, Phys. Rev. A **69**, 042312 (2004).
[20] A. Sen (De), U. Sen, and M. Lewenstein, e-print quant-ph/0505006.
[21] D. Gelman, C. P. Koch, and R. Kosloff, J. Chem. Phys. **121**, 661 (2004).
[22] A. V. Dodonov, V. V. Dodonov, and S. S. Mizrahi, J. Phys. A **38** 683 (2005).
[23] A. Peres, Phys. Rev. Lett. **77**, 1413 (1996).
[24] M. Horodecki, P. Horodecki, and R. Horodecki, Phys. Lett. A **223**, 1 (1996).
[25] P. Horodecki, Phys. Lett. A **232**, 33 (1997).
[26] P. Horodecki, M. Lewenstein, G. Vidal, and I. Cirac, Phys. Rev. A **62**, 032310 (2000).
[27] G. Vidal and R. F. Werner, Phys. Rev. A **65**, 032314 (2002).
[28] K. Zyczkowski, P. Horodecki, A. Sanpera, and M. Lewenstein, Phys. Rev. A **58**, 883 (1998).
[29] G. Vidal and R. Tarrach, Phys. Rev. A **59**, 141 (1999).
[30] L. Gurvits and H. Barnum, Phys. Rev. A **66**, 062311 (2002).
[31] S. Bandyopadhyay and V. Roychowdhury, Phys. Rev. A **69**, 040302(R) (2004).
[32] M. Plenio and S. Virmani, e-print quant-ph/0504163.
[33] A. O. Caldeira and A. J. Leggett, Physica A **121**, 587 (1983).
[34] H. Carmichael, *An Open System Approach to Quantum Optics* (Springer-Verlag, Berlin, 1993).
[35] E. T. Jaynes and F. W. Cummings, Proc. IEEE **51**, 89 (1963). The Jaynes-Cummings model of an interacting two-level system and a quantized field mode was investigated in Ref. [16]. It was found that no free entanglement is generated in the course of the evolution of the composite system if the initial temperature of both the subsystems is sufficiently high.

Chapter 3

Quantum and classical correlations in an open-system evolution

3.1 Introduction

In Chapter 2 we discussed one generic pathway for quantum dynamics without entanglement - a unitary evolution of a sufficiently mixed initial state. The present Chapter explores another paradigm - the open-system dynamics. As pointed out in Section 1.2.4 of Chapter 1, an extensive theoretical and experimental evidence has been obtained in favor of the following intuitive formula: *local noise destroys entanglement.*

Coupling to a local environment is expected to destroy existing quantum correlation in a composite system and to restrict the generation of new quantum correlations by the interaction. As a consequence, one could expect to be able to simulate the corresponding open system evolution with higher efficiency. Investigation of various types of a local system-bath interaction in Section 3.2 reveals that *this formula is not universal.*

3.1.1 Gaussian noise

The common intuition is based on hypothesis of a large time-scales separation between the local dynamics of the open quantum system and the decoherence time scale. The latter can be understood as follows. Assume a large time-scale separation between the slow evolution of a certain hypothetic set of states - termed robust states - and the fast evolution of a generic superposition of robust states. Due to this property robust states can be considered as attractors for the open-system dynamics. As a consequence, the density operator of the

open-system assumes a quasidiagonal structure in the robust states basis. The dynamical (quasi) diagonalization is termed decoherence and is a basis-dependent phenomena by construction. If the robust states are local states, the evolving density matrix obtains quasidiagonal structure in the local basis, which implies that quantum correlations are restricted.

The quasidiagonal structure does not contradict generation of classical correlations between the subsystems. On the contrary, extensive classical correlations can develop in the open-system evolution (Section 3.2). Therefore, the effect of the local environments can be interpreted as a transformation of quantum correlations, generated by the interaction, to classical correlations.

This pattern has been found in the open dynamics of a composite system of interacting nonlinear oscillators (Section 3.2), when the local system-bath interaction corresponds to the Gaussian noise (Kubo, 1962; Gorini & Kossakowski, 1976). The Gaussian noise leads to the open system dynamics, which can be interpreted (Diosi, 2006) as a process of weak measurement of certain local observables.

A general mathematical framework for this pattern of open-system dynamics can be developed based on the concept of the generalized coherent states (GCS)(Zhang *et al.*, 1990; Perelomov, 1985), which turn out to be the robust states for particular system-bath interactions (Boixo *et al.*, 2007). The framework is introduced and developed in Chapter 4. Robust states seem to be an appropriate candidate for the computational basis of the simulation. For the reasons given in Section 4.1.1 of Chapter 4 the robust states must be GCS with respect to a particular subalgebra of observables in order to be an appropriate computational basis for efficient simulation. GCS are robust states with respect to a certain environment, but not vice versa (Boixo *et al.*, 2007). The robust states considered in Section 3.2 are eigenstates of particular local operators − local Hamiltonians − and are not GCS. Nonetheless, they are a subset of the GCS, associated with the subalgebra of all local operators, − the product states, which can be used as a computational basis.

3.1.2 Poissonian noise

The Poissonian noise models have been found to adequately describe dephasing dynamics driven by rare collisions in chemistry (Weiss *et al.*, 2006) and in solid state physics (Uskov *et al.*, 2000; Kammerer *et al.*, 2002; San-Jose *et al.*, 2002). In Section 3.2 it is shown that Poissonian type of local system-bath coupling does not exhibit the time-scale separation between the local dynamics and the decoherence. As a consequence, the generation of entanglement by the interaction

is not affected substantially by the Poissonian noise. Accordingly, the simulation of the corresponding open-system dynamics does not seem to be advantageous from the computational point of view.

3.1.3 Measures of correlations

The efficiency of a simulation will depend on the extent of quantum entanglement. Section 3.2 explores dynamics of quantum and classical correlations as a function of the effective Hilbert space dimension of the system in various open bipartite composite systems. A natural measure of the mixed state entanglement is the average entanglement of pure states in a convex decomposition of the density operator, minimized over all possible decompositions (Plenio & Virmani, 2007). The minimization is a difficult computational problem and this measure is unpractical in calculations.

A feasible measure of the mixed state entanglement is the negativity (Vidal & Werner, 2002). The disadvantage of the negativity is that generally it measures a lower bound on the mixed state entanglement, i.e., entangled states may still have vanishing negativity. In Section 3.3 we show that the negativity is an appropriate measure of the mixed state entanglement in a certain class of mixed states, where it measures the distance of the mixed state from the set of separable (i.e., classically correlated) states. The mixed states, generated by the open-system dynamics, considered in Section 3.2, are shown to belong to that class.

A measure of the classical (more accurately, of the total) correlations is developed in Section 3.2. The central idea (Zwolak & Vidal, 2004) is to view a density operator as a pseudo pure state (superket) in the Hilbert-Schmidt space of operators. Then a regular measure of the pure-state entanglement (Plenio & Virmani, 2007) can be applied to calculate the total correlations of the state.

3.2 Rise and Fall of Quantum and Classical Correlations in an Open System Dynamics

Rise and fall of quantum and classical correlations in open-system dynamics

Michael Khasin and Ronnie Kosloff
Fritz Haber Research Center for Molecular Dynamics, Hebrew University of Jerusalem, Jerusalem 91904, Israel
(Received 15 May 2006; revised manuscript received 13 February 2007; published 6 July 2007)

Interacting quantum systems evolving from an uncorrelated composite initial state generically develop quantum correlations—entanglement. As a consequence, a local description of interacting quantum systems is impossible as a rule. A unitarily evolving (isolated) quantum system generically develops *extensive* entanglement: the magnitude of the generated entanglement will increase without bounds with the effective Hilbert space dimension of the system. It is conceivable that coupling of the interacting subsystems to *local* dephasing environments will restrict the generation of entanglement to such extent that the evolving composite system may be considered as *approximately disentangled*. This conjecture is addressed in the context of some common models of a bipartite system with linear and nonlinear interactions and local coupling to dephasing environments. Analytical and numerical results obtained imply that the conjecture is generally false. Open dynamics of the quantum correlations is compared to the corresponding evolution of the classical correlations and a qualitative difference is found.

DOI: 10.1103/PhysRevA.76.012304 PACS number(s): 03.67.Mn, 03.65.Yz, 03.65.Ud

I. INTRODUCTION

The exploration of the nature and the extent of correlations generated by the many-body dynamics has both fundamental and practical applications. One of the fundamental issues in the investigation of many-body dynamics is finding an optimal set of coordinates [1,2]. This problem is solved in classical mechanics by introducing partition of a complex system into smaller subsystems, i.e., introducing degrees of freedom. The description of the composite system is furnished by local descriptions of the subsystems. The adequacy of a particular partition depends heavily on the nature and the extent of the correlations between the local degrees of freedom.

The role played by correlations in classical and quantum mechanics is substantially different. This is due to the presence of the quantum correlations, or entanglement, in a composite quantum state, having no analog in the classical world [3]. In contrast to classical correlations [4], extensive entanglement makes the partition of a quantum system meaningless, since local measurements do not provide information on the state of an entangled system [3].

The problem of the optimal partition is deeply connected to the foundation of many-body dynamical simulations. The complete description of the system composed of fully correlated subsystems should grow exponentially with the number of subsystems involved. The possibility of representing a state of a complex system as a mixture of independently evolving uncorrelated states (trajectories) solves in principle the problem of many-body simulations, permitting one to sample single trajectories for simulation and averaging the result subsequently [5,6]. This possibility is inherent in classical mechanics but is nongeneric in the quantum case, due to the fact that the typical interaction of a quantum system generates entanglement. If the growth of the total (i.e., quantum and classical) correlations becomes restricted, the quantum dynamics can be efficiently simulated [7–11]. Nonetheless, it is still an open question whether restrictions on quantum correlations alone are sufficient to provide for efficient simulations [12].

Addressing the problem of dynamical generation of correlations it is necessary to distinguish between the unitary evolution of an isolated system and the open evolution of a system coupled to an environment. While a given unitary evolution can generate extensive entanglement, coupling the system to an environment is generally expected to restrict entanglement generation. This expectation originates in the general philosophy, seeing in environmental-induced decoherence [13] the universal route of quantum-to-classical transition. It is consistent with some established results on open-systems entanglement dynamics.

Evolution of quantum correlations under the influence of the environment was investigated both in the context of quantum to classical transition [13] and in the context of quantum information processing [14]. Most studies have been concerned with dynamics of entanglement between *noninteracting* systems coupled to a bath. It was found that coupling to a common environment is able to entangle noninteracting systems [15,16]. On the other hand, coupling to certain local environments leads to total disentanglement of the systems in finite time [17–22]. The rates of disentanglement were calculated in bi- and multipartite systems of noninteracting qubits [19,23–26] and quidits [27,28], locally coupled to various environments. A number of studies addressed dynamical generation of correlations between *interacting* subsystems in the presence of the environment. Production of entanglement between qubits, modeling a system of ions, coupled to environment through their center of mass motion in ion traps, was investigated in Ref. [28]. It was found that the coupling to environment diminishes the maximally achievable entanglement, with the corresponding entanglement loss increasing with the number of ions. Reference [29] explored the dynamics of entanglement in the quantum Heisenberg *XY* chain, immersed in a global purely dephasing bath. The robustness of entanglement against the dephasing was related to the number of spins in the chain. The coupling of interacting subsystems to local environments was considered in Refs. [30,18]. Reference [30] investigated the generation and transfer of entanglement in harmonic chains. The creation of entanglement by suddenly

switching on the interaction in the chain was found to be robust against the decoherence induced by coupling of the oscillators to local harmonic baths. The model of two harmonically coupled quantum Brownian particles was treated in Ref. [18]. It was found that in the physically interesting range of parameters the interaction between the particles cannot prevent their eventual disentanglement, induced by coupling to local baths.

While the observed disentanglement of the noninteracting systems by coupling to local environments meets the common intuition about the quantum-to-classical transition, the picture of dynamics of entanglement in the presence of interaction is not so clear. Searching for an efficient and a universal environment-induced mechanism of restricting the extent of the generated entanglement, it seems necessary to focus on the following aspects of the dynamics of correlations.

First, the scaling of the generated correlations with the effective Hilbert space dimension of the interacting subsystems must be considered. This is in contrast to the context of the quantum information processing where the object of interest is usually the scaling of entanglement with the number of degrees of freedom (qubits). The expectation is that the environment-induced restriction on the generation of entanglement becomes most significant in the range of the large quantum numbers of the system, which is commonly associated with the quantum-to-classical transition. In fact, extensive entanglement in the large Hilbert space dimension seems impossible without creating the "cat-state" superpositions, which are expected to be destroyed by the decoherence.

Second, the dynamics of correlations must be followed on the short, interaction time scales. It is possible that the long-time dynamics of an open composite system, approaching equilibrium, is disentangled, but the entanglement generated on the interaction time scales is so large that the partition of the system has no meaning.

Moreover, since a *common* environment will generically entangle noninteracting systems, coupling to *local* environments seems necessary to provide for a generic route to a disentangled dynamics.

The present study focuses on the investigation of environment-induced constraints on the dynamics of quantum and classical correlations in the open bipartite composite system. The system consists of two nonlinearly interacting harmonic oscillators, coupled to local purely dephasing baths. The distinction between the dephasing and pure dephasing has first appeared in the context of NMR [31]. Pure dephasing corresponds to loss of coherence in the energy representation. The two prototypes of underlying stochastic processes leading to dephasing are the Gaussian and the Poissonian processes [32]. Kubo based his line-shape theory [33] on the Gaussian model. Kubo's model is the cornerstone of the condensed-matter spectroscopy. Recently, exceptions to the Gaussian paradigm have been found experimentally [34–36] in ultrafast vibrational spectroscopy. The Poissonian model was shown to describe the dynamics adequately. Quantum Poissonian stochastic models have first appeared in the gas collision theory. They are also employed in the condense phase physics. For example, the Poissonian noise has been considered as a source of decoherence in quantum dots [37–39]. Due to the fundamental and the experimental relevance of the Gaussian and the Poissonian stochastic processes they were chosen as the source of the dephasing in the present study.

The models aim to explore dynamics of correlations in a composite system of coupled multilevel subsystems at large effective Hilbert space dimension. Examples of such systems include multimode molecular vibrations [40], linear and nonlinear quantum optics [41], and cold trapped atomic ions [42]. The primary goal is to locate a generic mechanism by which the decoherence keeps an interacting composite system "approximately disentangled" all along the evolution. Dynamics of quantum and classical correlations and their scaling with the effective Hilbert space dimension of the system are compared.

The measures of quantum and total, i.e., quantum and classical, correlations are defined in Sec. II. Section III examines the issue of the generation of quantum correlations (entanglement) in the model problems. Section IV presents numerical results on the dynamics of both quantum and classical correlations and Sec. V summarizes the conclusions.

II. MEASURES OF CORRELATION

The state of a bipartite system is uncorrelated if it can be described by the form

$$\hat{\rho}_{ab} = \hat{\rho}_a \otimes \hat{\rho}_b. \tag{1}$$

A general correlated state can be Schmidt-decomposed [43] (cf. Appendix A) in the Hilbert-Schmidt space leading to

$$\hat{\rho}_{ab} = \sum_i^N c_i \hat{A}_a^i \otimes \hat{B}_b^i, \tag{2}$$

where the sets $\{\hat{A}\}$ and $\{\hat{B}\}$ of operators are orthonormal in the Hilbert-Schmidt spaces of systems a and b.

The number of nonvanishing coefficients c_i in the Schmidt decomposition of a vector in an abstract tensor-product Hilbert space is called the *Schmidt rank* of the vector. To avoid confusion in the following presentation the term HS-Schmidt rank (or just HS rank for brevity) is adopted for the Schmidt decomposition in the Hilbert-Schmidt (HS) space of operators, while retaining the term Schmidt rank for the Schmidt decomposition in the corresponding Hilbert (pure) state space. A HS rank is a natural measure of *total correlations* present in a mixed state $\hat{\rho}$ (cf. Appendix A).

A special subset of mixed states is the set of separable or classically correlated states [4]. The state is separable if it can be cast into the following form

$$\hat{\rho}_{ab} = \sum_i^N p_i \hat{\rho}_a^i \otimes \hat{\rho}_b^i, \tag{3}$$

where $0 \leqslant p_i \leqslant 1$, $\Sigma_i^N p_i = 1$, and $\hat{\rho}_a$ and $\hat{\rho}_b$ are density operators defined on the Hilbert spaces of the subsystems a and b, respectively. Separable states are mixtures of uncorrelated states, which can be completely characterized by local mea-

surements. Therefore, partition of a composite system into parts has a strong physical meaning. Such a partition is always possible for classical probability density distribution of a bipartite system [4,44].

States that do not comply with the form of Eq. (3) are called quantum-correlated or entangled. Pure correlated states are always entangled. The measure of a pure state entanglement can be defined by its Schmidt rank [45]. Estimating the measure of a mixed-state entanglement is a difficult conceptual and computational problem [45]. One can look for the decomposition of $\hat{\rho}_{ab}$ into a mixture of pure states that are least entangled on average. The average entanglement corresponding to such decomposition is a possible measure of the mixed state entanglement. Unfortunately, such measures are notoriously difficult to compute.

An alternative computable measure of the bipartite mixed state entanglement is the *negativity* [46] defined as follows:

$$\mathcal{N}(\hat{\rho}) \equiv \frac{\|\hat{\rho}^{T_a}\| - 1}{2}, \tag{4}$$

where $\|\hat{X}\| = \mathrm{Tr}\sqrt{\hat{X}^\dagger \hat{X}}$ is the trace norm of an operator $\hat{X}$ and T_a stands for the partial transposition with respect to the first subsystem. The partial transposition T_a, with respect to subsystem a of a bipartite state $\hat{\rho}_{ab}$ expanded in a local orthonormal basis as $\hat{\rho}_{ab} = \Sigma \rho_{ij,kl} |i\rangle\langle j| \otimes |k\rangle\langle l|$, is defined as

$$\rho_{ab}^{T_a} \equiv \sum \rho_{ij,kl} |j\rangle\langle i| \otimes |k\rangle\langle l|. \tag{5}$$

The spectrum of the partially transposed density matrix is independent of the choice of local basis or on the choice of the subsystem with respect to which the partial transposition is performed. The negativity of the state equals the absolute value of the sum of the negative eigenvalues of the partially transposed state. By the Peres-Horodecki criterion [47,48] the negativity vanishes in a separable state. On the other hand, vanishing of the negativity does not imply separability of the state in general [48].

Finite negativity is a necessary and sufficient condition for the presence of entanglement in a particular type of mixed states, the so-called Schmidt-correlated states [49–51]. In this case the negativity can be related to the structure of the density operator, which facilitates the evaluation of the entanglement.

The Schmidt-correlated states have the following form:

$$\hat{\rho} = \sum_{mn} \rho_{mn} |\phi_m\rangle\langle\phi_n| \otimes |\chi_m\rangle\langle\chi_n|, \tag{6}$$

where $\Xi_1 = \{|\phi_m\rangle\}_{m=1}^k$ and $\Xi_2 = \{|\chi_m\rangle\}_{m=1}^k$ are local orthonormal bases. Equation (6) implies that $\hat{\rho} = \Sigma_i p_i |\psi_i\rangle\langle\psi_i|$, where $|\psi_i\rangle = \Sigma_m c_m^i |\phi_m\rangle \otimes |\chi_m\rangle_2$ for every i, i.e., all pure states in the mixture share the same Schmidt bases (cf. Appendix A) Ξ_1 and Ξ_2. It has been proved [52] that for Schmidt-correlated states

$$\mathcal{N}(\hat{\rho}) = \sum_{m<n} |\rho_{mn}|, \tag{7}$$

i.e., the negativity equals half the sum of absolute values of the off-diagonal elements of the density operator, written in a $\Xi_1 \otimes \Xi_2$ local tensor product basis. It follows that the negativity of entangled Schmidt-correlated states is finite [52].

The negativity can be related to the structure of the density operator. Consider the density operator (6) having the following quasidiagonal structure:

$$\hat{\rho} = \sum_{|m-n| \leqslant \Delta} \rho_{mn} |\phi_m\rangle\langle\phi_n| \otimes |\chi_m\rangle\langle\chi_n|, \tag{8}$$

with $\Delta \ll k$. The sum of the absolute values of the off-diagonal elements can be estimated as follows:

$$\begin{aligned} \sum_{m \neq n} |\rho_{mn}| &= \sum_{mn} |\rho_{mn}| - 1 = \sum_m \sum_{n=m-\Delta}^{n=m+\Delta} |\rho_{mn}| - 1 \\ &< \sum_m \sum_{n=m-\Delta}^{n=m+\Delta} \sqrt{\rho_{mm}\rho_{nn}} \leqslant \sum_m \sum_{n=m-\Delta}^{n=m+\Delta} \frac{\rho_{mm} + \rho_{nn}}{2} \\ &= \frac{1}{2} \sum_m \sum_{n=m-\Delta}^{n=m+\Delta} \rho_{mm} + \frac{1}{2} \sum_m \sum_{n=m-\Delta}^{n=m+\Delta} \rho_{nn} < 2\Delta, \end{aligned} \tag{9}$$

where the first inequality follows from the positivity of the density operator and the second is the inequality of geometric and arithmetic means. Therefore,

$$\mathcal{N}(\hat{\rho}) < \Delta \tag{10}$$

in the state (8). Since the negativity of the maximally entangled state [corresponding to $|\rho_{mn}| = 1/k$ in Eq. (6)] equals $(k-1)/2$, as follows from Eq. (7), the negativity of the quasidiagonal density matrices is negligible compared to the maximally entangled state. It should be noted that the form (8) with $\Delta \ll k$ of the density matrix does not constrain the magnitude of the classical correlations present in the state. For example, a strictly diagonal matrix $\rho_{mn} = \delta_{mn}$ corresponds to a maximally (classically) correlated separable state.

Schmidt correlated states appear naturally in a composite bipartite dynamics admitting particular conservations laws [52]. The models of open-system dynamics considered in the following sections belong to that class. As a consequence, the presence and extent of entanglement in evolving composite systems can be related to the structure of the density matrix, which can be inferred on the basis of relatively general scaling considerations.

III. DENSITY OPERATOR OF A BIPARTITE SYSTEM UNDER LOCAL PURE DEPHASING

A. General considerations

The model of open system dynamics considered is described by

$$\frac{\partial}{\partial t}\hat{\rho} = (\mathcal{L}_1 + \mathcal{L}_2)\hat{\rho} + \mathcal{I}\hat{\rho}, \tag{11}$$

where the generators of local nonunitary evolution are $\mathcal{L}_j = -i[\hat{H}_j, \bullet] - \Gamma_j \mathcal{D}_j$, $j = 1,2$, and $\mathcal{I} = -i\gamma[\hat{H}_{12}, \bullet]$ stands for the interaction superoperator. The operators $\hat{H}_j$ are local system Hamiltonians, the operator $\hat{H}_{12}$ is the nonlocal (interaction) term in the composite system Hamiltonian, and $\mathcal{D}_j$ de-

notes the local bath-dependent superoperators. Coupling constants $\Gamma_{1,2}$ and γ measure, respectively, the strength of the coupling to the local environments and the strength of the interaction between the subsystems.

As a reference, the open evolution of noninteracting subsystems ($\gamma=0$) is considered first. In this case a local dephasing evolution of each separate system takes place,

$$\frac{\partial}{\partial t}\hat{\rho} = (\mathcal{L}_1 + \mathcal{L}_2)\hat{\rho}. \tag{12}$$

In many models of open evolution [13,53–55] it is found that the evolving state undergoes decoherence, characterized by the decay of the off-diagonal elements of the density operator represented in a particular basis of the *robust states*. Ideal robust states retain their purity notwithstanding the interaction with environment. Examples of such models include interaction with a purely dephasing environment, singling out energy states as the robust basis, quantum Brownian motion, and damped harmonic oscillator at zero temperature $T=0$, which select the robust basis of coherent states. While the robust state's basis is determined by the type of the bath and the system Hamiltonian, the time scales of the decoherence generally depend on the initial state as well.

Let us assume that the local superoperators $\mathcal{L}_1$ and $\mathcal{L}_2$ in Eq. (12) single out local robust state's bases Ξ_1 and Ξ_2. A composite noninteracting system evolving according to Eq. (12) from an arbitrary initial state is expected to decohere in the tensor product basis: $\Xi_1 \otimes \Xi_2$. That means that an arbitrary initial state density matrix will eventually diagonalize in this basis. Switching on the interaction between subsystems causes a competition between entanglement generation and decoherence induced by the local baths. For sufficiently weak interaction viewing the evolving density operator in the unperturbed tensor product basis $\Xi_1 \otimes \Xi_2$ of local robust states is a good starting point. If the interaction perturbs only slightly the evolution of an off-diagonal matrix element, it will decay on an almost unperturbed decoherence time scale.

To proceed with a more quantitative argument the concept of the effective Hilbert space $\mathcal{H}_{eff}$ is helpful. Since the energy of the evolving system is finite, the evolution can be effectively restricted to a Hilbert space with finite dimension. This Hilbert space is termed the effective Hilbert space of the system. Let λ be a spectral norm [56] of the interaction superoperator $\mathcal{I}$ restricted to the effective Hilbert-Schmidt space (i.e., the space of linear operators on $\mathcal{H}_{eff}$) and Λ be a spectral norm of the dissipator $\mathcal{D}=\mathcal{D}_1+\mathcal{D}_2$ restricted to this space. λ and Λ correspond to the shortest time scales of the evolution generated by the $\mathcal{I}$ and $\mathcal{D}$, respectively. When $\lambda \ll \Lambda$, the interaction time scale is slow compared to the shortest decoherence time scale. As a consequence, the evolution of certain matrix elements is only slightly perturbed by the interaction. In that case the perturbed dynamics of the matrix element will follow essentially the course of the decoherence. Therefore, a rough distinction can be made between the region of the density matrix dominated by the decoherence and the region dominated by the interaction. The border between the two regions is defined by the condition

$$\tau_{ij} = O(\lambda^{-1}), \tag{13}$$

where τ_{ij} is the unperturbed decoherence time scale of a matrix element ρ_{ij}, $i,j \in \Xi_1 \otimes \Xi_2$.

In the case where the decoherence-dominated regions of the density matrix are not populated initially, they will stay unpopulated in the course of the perturbed evolution. This property will shape the structure of the evolving density matrix. If the states are Schmidt-correlated states with local Schmidt-bases Ξ_1 and Ξ_2, being the local robust states bases, the relation can be established between the structure of the matrix and the entanglement of the state as indicated in the previous section. Qualitatively, the larger the decoherence-dominated region, the smaller the negativity of the state.

The relative extent of the decoherence- and the interaction-dominated regions in a given dynamics generally depends on the initial state and, in particular, on the effective Hilbert-space dimension k of the system. As a consequence, different scenarios may be expected at asymptotically large k. The growing contribution of the interaction-dominated regions will generally imply extensive entanglement generation. On the other hand, if the relative size of the interaction-dominated regions becomes negligible at large k the entanglement generated by the open system dynamics may be negligible or even asymptotically independent on k. This possibility appeals to one who believes in the environmental-induced decoherence as a universal instrument of quantum to classical transition. An interesting question is the fate of the classical correlations in this scenario. While decoherence-dominated dynamics can turn extensively entangled initial state into extensively classically correlated state, it is not clear that decoherence-dominated dynamics can generate extensive classical correlations when quantum entanglement is negligible all along the evolution. Negligible total correlations seem nongeneric and do not correspond to the intuitive picture of a "really interacting" system. Therefore, a scenario of negligible quantum and extensive classical correlations matches best to a generic mechanism of quantum to classical transition.

B. Model calculations

The model calculations are used to illustrate and verify the general considerations presented above. The evolution of a bipartite system is studied according to Eq. (11), $\frac{\partial}{\partial t}\hat{\rho}=(\mathcal{L}_1+\mathcal{L}_2)\hat{\rho}+\mathcal{I}\hat{\rho}$, where ($\mathcal{L}_j=-i[\hat{H}_j,\bullet]-\Gamma_j\mathcal{D}_j$, $j=1,2$, and $\mathcal{I}=-i\gamma[\hat{H}_{12},\bullet]$) with two types of dissipators, corresponding to the Gaussian [57,58] and the Poissonian [35] purely dephasing models

$$\mathcal{D}_j\hat{\rho} = \begin{cases} [\hat{H}_j,[\hat{H}_j,\hat{\rho}]] & \text{(Gaussian)}, \\ e^{-i\phi\hat{H}_j}\hat{\rho}e^{i\phi\hat{H}_j} - \hat{\rho} & \text{(Poissonian)}. \end{cases} \tag{14}$$

These dissipators have the Lindblad form [59] of a generators of quantum dynamical semigroups. The Gaussian and the Poissonian generators are the two examples explicitly mentioned in the seminal paper by Lindblad [59].

The model Hamiltonian is a simplified version of a nonlinearly interacting multimode system. The local Hamiltonians $\hat{H}_j$, $j=1,2$ are chosen to be Hamiltonians of harmonic oscillators $\hat{H}_j=\omega_j\hat{a}_j^\dagger\hat{a}_j$, where $\hat{a}_j^\dagger$ and $\hat{a}_j^\dagger$ are the creation and annihilation operators, respectively. Two general types of interaction are considered. The first ($\mathcal{I}_A$), termed *band-limited interaction*, is motivated by the stimulated Raman interaction between the translational modes of ions in cold traps [60–62] (for example, in Ref. [61] the effective interaction between the modes is reduced to the band-limited operator $\exp[\pm i\pi(\hat{a}_x^\dagger\hat{a}_y+\hat{a}_x\hat{a}_y^\dagger)]$). The second type of interaction ($\mathcal{I}_B$) is motivated by weakly nonlinear interacting modes emerging in molecular vibrations [40] and in nonlinear optics. The typical example in the nonlinear optics is the second harmonic generation modeled by the interaction Hamiltonian of the form $\hat{H}=\hbar g(\hat{a}^2\hat{b}^\dagger+\hat{a}^{\dagger 2}\hat{b})$ [41,60]. In addition, the dynamics of the cold ion traps can be operated in the regime, where the effective interaction is well approximated by a weakly nonlinear coupling [60–62].

The two types of interaction are generated by

$$\mathcal{I}=\begin{cases}-i\gamma[\hat{A}_1^\dagger\hat{A}_2+\hat{A}_2^\dagger\hat{A}_1,\bullet]\ (\equiv\mathcal{I}_A),\\ -i\gamma[(\hat{a}_1^\dagger)^s(\hat{a}_2)^r+(\hat{a}_2^\dagger)^s(\hat{a}_1)^r,\bullet],\quad s=1,2,\ldots;\ r=1,2,\ldots\ (\equiv\mathcal{I}_B),\end{cases}\tag{15}$$

where $\hat{A}_j$ is defined by its matrix elements in local energy basis $(\hat{A}_j)_{mn}=\delta_{m,n-1}$. The structure of $\hat{A}_j$ assures that $\mathcal{I}_A$ is band limited with the spectral norm $\lambda=O(\gamma)$.

The important property of the dynamics, Eq. (11), with local dephasing, Eq. (14), and interaction, Eq. (15), is conservation of a particular additive operator in each case. The first type of interaction, $\mathcal{I}_A$, preserves the number operator $\hat{N}=\hat{a}_1^\dagger\hat{a}_1+\hat{a}_2^\dagger\hat{a}_2$: $\mathcal{I}_A^\dagger(\hat{N})=0$, which is also preserved by the local generators $(\mathcal{L}_1^\dagger+\mathcal{L}_2^\dagger)(\hat{N})=0$. The second type of interaction, $\mathcal{I}_B$, preserves the generalized number operator $\hat{N}_{rs}\equiv r\hat{a}_1^\dagger\hat{a}_1+s\hat{a}_2^\dagger\hat{a}_2$: $\mathcal{I}_B^\dagger(\hat{N}_{rs})=0$, preserved by the local generators as well, $(\mathcal{L}_1^\dagger+\mathcal{L}_2^\dagger)(\hat{N}_{rs})=0$.

Assume a pure uncorrelated initial state $|\psi(0)\rangle=|k0\rangle$ (written in the local energies basis). The state $|\psi(0)\rangle$ is an eigenstate of $\hat{N}$ with the eigenvalue k. As a consequence, the first type of the interaction, $\mathcal{I}_A$, will drive the initial state into a mixture of eigenstates of $\hat{N}$ corresponding to the eigenvalue k, $\hat{\rho}(t)=\Sigma_{mn}c_{mn}|ml_m\rangle\langle nl_n|$ with $l_m=k-m$. Thus, k determines the effective Hilbert space dimension of the system in this case: $\dim(\mathcal{H}_{eff})=k$. Since $|\psi(0)\rangle$ is also an eigenstate of $\hat{N}_{rs}$ with the eigenvalue rk, the second type of interaction, $\mathcal{I}_B$, will take it into a mixture of eigenstates of $\hat{N}_{rs}$ corresponding to the same eigenvalue rk, $\hat{\rho}(t)=\Sigma_{mn}c_{mn}|ml_m\rangle\langle nl_n|$ with $l_m=\frac{r}{s}(k-m)$. The number of initial excitations k of the first oscillator determines the effective Hilbert space dimension of the system in this case: $\dim(\mathcal{H}_{eff})=k/s$. To summarize,

$$\hat{\rho}(t)=\sum_{mn}c_{mn}|ml_m\rangle\langle nl_n|\quad\text{where}\begin{cases}l_m=k-m & (\mathcal{I}_A)\\ l_m=\dfrac{r}{s}(k-m) & (\mathcal{I}_B)\end{cases}\tag{16}$$

In both cases, the resulting mixed state is a Schmidt-correlated state with a time-independent Schmidt bases. This property permits evaluation of the negativity of $\hat{\rho}$ in each case from its structure, as indicated in Sec. II.

1. Gaussian vs Poisson pure dephasing bath

The difference between the two types (14) of environments can be understood by comparing the local evolutions of a single oscillator coupled to the bath of each type,

$$\frac{\partial}{\partial t}\hat{\rho}=-i[\hat{H},\hat{\rho}]-\Gamma\mathcal{D}\hat{\rho}.\tag{17}$$

In the Gaussian case, Eq. (17) in the energy representation becomes

$$\dot{\rho}_{nm}=-i\omega_{mn}\rho_{nm}-\Gamma\omega_{mn}^2\rho_{nm},\tag{18}$$

with $\omega_{mn}\equiv\omega_m-\omega_n$, leading to the solution $\rho_{nm}(t)=\rho_{nm}(0)e^{-i\omega_{mn}t-\Gamma\omega_{mn}^2t}$. Thus the effect of the purely dephasing Gaussian bath is the "diagonalization" of the density matrix in the energy basis (the robust states basis for this model) on the time scale that varies for different matrix elements ρ_{nm} and increases with the distance $|m-n|$ of the element from the diagonal. The shortest decoherence time scale corresponds to the largest distance from the diagonal and decreases with the growing effective Hilbert space dimension of the system.

In the Poissonian case, Eq. (17) in the energy representation becomes

$$\dot{\rho}_{nm}=-i\omega_{mn}\rho_{nm}+\Gamma(e^{-i\omega_{mn}\phi}-1)\rho_{nm},\tag{19}$$

leading to the solution $\rho_{nm}(t)=\rho_{nm}(0)e^{-i\omega_{mn}t+\Gamma(e^{-i\omega_{mn}\phi}-1)t}$. Apparently, the robust states basis is once again the energy basis, but the decoherence rates of the matrix elements are limited by $|\Gamma(e^{-i\omega_{mn}\phi}-1)|=2\Gamma$, independently of the initial state.

This difference in properties of the Gaussian and the Poissonian environments will result in different dynamics of the correlations in the composite bipartite system dynamics, Eq. (11).

2. Local dephasing driven dynamics

To gain insight on the effect of dephasing on the correlations the simplest bath-driven dynamics is studied first, in which the composite system Hamiltonian vanishes altogether, meaning that no entanglement is generated during the evolution. The corresponding equation (11) transforms into

$$\frac{\partial}{\partial t}\hat{\rho} = -\sum_{j=1,2} \Gamma_j [\hat{H}_j,[\hat{H}_j,\hat{\rho}]] \quad \text{(Gaussian dephasing)}, \tag{20}$$

$$\frac{\partial}{\partial t}\hat{\rho} = -\sum_{j=1,2} \Gamma_j (e^{-i\phi\hat{H}_j}\hat{\rho}e^{i\phi\hat{H}_j} - \hat{\rho}) \quad \text{(Poissonian dephasing)}. \tag{21}$$

Since the dynamics preserve local energies the effective Hilbert space dimension of the evolving system is determined by the energy range of the initial state. The initial state of the form $|\psi\rangle = \frac{1}{\sqrt{k+1}}\Sigma_{n=0}^{k}|n\rangle|k-n\rangle$ ($|n\rangle$ is a local energy eigenstate) is a maximally entangled state. It corresponds to the effective Hilbert space spanned by the states $\{|n\rangle|k-n\rangle\}_{n=0}^{k}$.

The solution to Eq. (20), the Gaussian case, is found:

$$\hat{\rho}(t) = \frac{1}{k+1}\sum_{mn} e^{-(\Gamma_1\omega_{1,mn}^2+\Gamma_2\omega_{2,mn}^2)t}|n\rangle|k-n\rangle\langle m|\langle k-m|, \tag{22}$$

when the solution to Eq. (21), the Poissonian case, becomes

$$\hat{\rho}(t) = \frac{1}{k+1}\sum_{mn} e^{-(\Gamma_1[1-e^{-i\omega_{1,mn}\phi}]+\Gamma_2[1-e^{-i\omega_{1,mn}\phi}])t}|n\rangle|k-n\rangle \times\langle m|\langle k-m|. \tag{23}$$

Decoherence rates in the Gaussian case (22) are $\tau_{mn}^{-1} = \Gamma_1\omega_{1,mn}^2+\Gamma_2\omega_{2,mn}^2 \leqslant \Lambda_g \equiv \max_{m,n\leqslant k}\{\Gamma_1\omega_{1,mn}^2+\Gamma_2\omega_{2,mn}^2\}$ and generally increase without bounds with the effective Hilbert space dimension k. For example, taking $\hat{H}_j = \omega_j\hat{a}_j^\dagger\hat{a}_j$, $\tau_{mn}^{-1} = (\Gamma_1\omega_1^2+\Gamma_2\omega_2^2)(m-n)^2$ is obtained, with maximal rate $\Lambda_g = \tau_{0k}^{-1} = (\Gamma_1\omega_1^2+\Gamma_2\omega_2^2)k^2$. In the Poissonian case (23) the decoherence rates are bounded: $\tau_{mn}^{-1} = \mathrm{Re}\{\Gamma_1[1-e^{-i\omega_{1,mn}\phi}] + \Gamma_2[1-e^{-i\omega_{1,mn}\phi}]\} \leqslant \Lambda_p \equiv 2(\Gamma_1+\Gamma_2)$.

Note, that both solutions (22) and (23) are Schmidt-correlated states. Therefore, the corresponding negativities can be calculated from Eq. (7),

$$\mathcal{N}(\hat{\rho}(t)) = \frac{1}{k+1}\sum_{m<n} e^{-(\Gamma_1\omega_{1,mn}^2+\Gamma_2\omega_{2,mn}^2)t} \quad \text{(Gaussian dephasing)}, \tag{24}$$

$$\mathcal{N}(\hat{\rho}(t)) = \frac{1}{k+1}\sum_{m<n} e^{-(\Gamma_1[1-e^{-i\omega_{1,mn}\phi}]+\Gamma_2[1-e^{-i\omega_{1,mn}\phi}])t} \quad \text{(Poissonian dephasing)}. \tag{25}$$

From Eqs. (24) and (25) it follows that both types of the purely dephasing dynamics [Eqs. (20) and (21)] lead eventually to a complete decay of the quantum correlations (note that since the evolving state is Schmidt correlated, its negativity vanishes if and only if the state is disentangled [52]). But the dependence of the time scales of the decay on the effective Hilbert space dimension k is different in the two cases. In the Poissonian case the rate of the negativity (25) decay is bounded by $\Lambda_p = 2(\Gamma_1+\Gamma_2)$, independent of k, while in the Gaussian case (24), the bound is $\Lambda_g = \max_{m,n<k}\{\Gamma_1\omega_{1,mn}^2+\Gamma_2\omega_{2,mn}^2\}$, which generally grows with k.

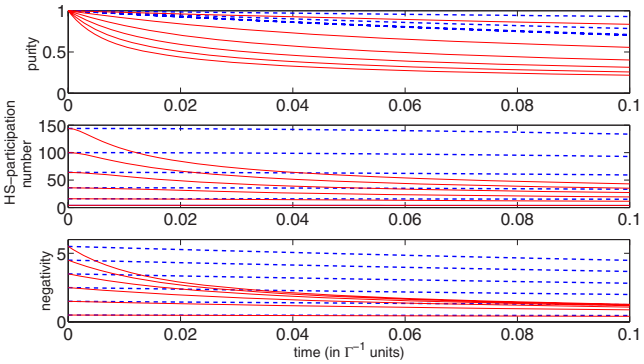

FIG. 1. (Color online) Purity, HS-participation number, and negativity of the density operator of two harmonic oscillators evolving under local purely dephasing Gaussian (solid lines) and Poissonian (dashed lines) environments [Eq. (14)]. The initial state is a pure maximally correlated state $|\psi\rangle = \frac{1}{\sqrt{k+1}}\Sigma_{n=0}^{k}|n\rangle|k-n\rangle$ for $k = 2,4,\ldots,12$. The coupling parameter to the bath $\Gamma = 1$ in both cases. The frequencies of the oscillators $\omega_1 = \omega_2 = 1$. While the decay rates in the Gaussian case depend on the initial state and increase with the effective Hilbert space dimension k, in the Poissonian case the rates are practically independent of k.

The total correlations (and, as a consequence, the classical correlations) follow a different course of evolution. The HS rank (and HS-participation number) of initial state is k^2 (see Appendix A for the calculation of HS rank of a pure state). The stationary solution corresponding to both Eqs. (22) and (23) is $\hat{\rho}_{st} = \frac{1}{k+1}\Sigma_m|m\rangle|k-m\rangle\langle m|\langle k-m|$ with HS rank (and HS participation number) equal to k. Therefore, although the total correlations decay in both models, the stationary solution contains extensive classical correlations, i.e., the correlations that grow without bounds with the effective Hilbert space dimension k.

Figure 1 displays the negativity, HS-participation number, and purity of the composite state evolving under Gaussian (20) and Poissonian (21) dephasing dynamics, corresponding to $\hat{H}_i = \omega\hat{a}_i^\dagger\hat{a}_i$, $\Gamma_1 = \Gamma_2$, and the initial state of the form $|\psi\rangle = \frac{1}{\sqrt{k+1}}\Sigma_{n=0}^{k}|n\rangle|k-n\rangle$. The effective Hilbert space dimension is varied, $k = 4,\ldots,12$. As anticipated from the difference of the two types of environments, the decay rates in the Gaussian case depend on the initial state and increases with the effective Hilbert space dimension, while in the Poissonian case the rates are effectively independent of the initial state.

3. Full dynamics

At this point the interaction between the oscillators are introduced, and the full dynamics according to Eq. (11) with

$\gamma \neq 0$ is followed. We shall consider a pure uncorrelated initial state of the composite system, $|\psi(0)\rangle = |k0\rangle$, i.e., the state corresponding to the excitation of the kth level of the first oscillator and the ground state of the second. In that case, as shown above, each type of the interaction (15) and the dephasing (14) considered admits a particular additive conserved quantity (a generalized number operator), which defines the effective Hilbert space of the composite system for each k and is responsible for the remarkable property of the evolving state: the density operator is a Schmidt-correlated state in a time-independent Schmidt bases: $\hat{\rho}(t) = \Sigma_{mn}\rho_{mn}(t)|m\rangle\langle n| \otimes |l_m\rangle\langle l_n|$ [Eq. (16)]. The Schmidt bases $\Xi_1 = \{|m\rangle\}$ and $\Xi_2 = \{|l_m\rangle\}$ are the robust (local energies) bases of the corresponding local open systems (17), with the correspondence $m \leftrightarrow l_m$, determined by the particular conservation law, depending on the type of interaction. This property allows us to relate the structure of the evolving density operator to its negativity, as indicated in Sec. II. The relevant structure of the evolving density operator is determined by the relative size of the decoherence- and the interaction-dominated regions of the corresponding density matrix. This structure is investigated for each type of interaction and dephasing and for different effective Hilbert space dimensions of the system.

The overview in the preceding section of the dynamics driven solely by the local dephasing reveals important differences between the two types of local environment with respect to the anticipated structure of the evolving density matrix. In the Poissonian case the decoherence rates are of the order of the system-bath coupling $\tau_{mn}^{-1} \leqslant 2(\Gamma_1 + \Gamma_2)$, as shown above. Therefore, evolution of the matrix elements is dominated either by the decoherence or by the interaction depending on the relative strength of the coupling constants and independently of the effective Hilbert space dimension. In models with weak system-bath coupling, $\Gamma_{1,2} \ll \lambda$, the structure of the evolving density operator will only slightly be affected by the coupling to the Poissonian bath on the interaction time scale $\gamma^{-1} \ll \tau_{mn}$. As a consequence, the quantum correlations will develop almost unperturbed on the interaction time scale.

A different dynamical pattern is anticipated in the case of the Gaussian purely dephasing bath. The decoherence rates in this case are

$$\tau_{mn}^{-1} = \Gamma_1\omega_1^2(m-n)^2 + \Gamma_2\omega_2^2(l_m - l_n)^2 \quad \text{where} \quad \begin{cases} l_m = k - m & (\mathcal{I}_A), \\ l_m = \dfrac{r}{s}(k-m) & (\mathcal{I}_B), \end{cases} \tag{26}$$

where $\mathcal{I}_A$ and $\mathcal{I}_B$ indicate the type of interaction: $\mathcal{I}_A \equiv -i\gamma[\hat{A}_1^\dagger\hat{A}_2 + \hat{A}_2^\dagger\hat{A}_1, \bullet]$, with $(\hat{A}_j)_{mn} = \delta_{m,n-1}$, and $\mathcal{I}_B \equiv -i\gamma[(\hat{a}_1^\dagger)^s(\hat{a}_2)^r + (\hat{a}_2^\dagger)^s(\hat{a}_1)^r, \bullet]$, with $(\hat{a}_j)_{mn} = \sqrt{m}\,\delta_{m,n-1}$ [see Eq. (15)]. In each case, the decoherence rate increases with the "distance" $|m-n|$ from the diagonal. As a consequence, the evolving density operator obtains a quasidiagonal structure in the local energies basis, with the width Δ of the interaction-dominated region about the diagonal depending on the type of interaction.

Let us assume for simplicity that $\Gamma_1\omega_1^2 = \Gamma_2\omega_2^2 = \Gamma$. In that case a matrix element ρ_{mn} decoheres on the time scale $\tau_{mn} = [2\Gamma(m-n)^2]^{-1}$. The spectral norm of $\mathcal{I}_A$ is $\lambda = O(\gamma)$. Therefore, the width about the diagonal of the evolving density matrix can be estimated from Eq. (13) as

$$\Delta = O(\sqrt{\gamma/\Gamma}), \tag{27}$$

where $\Gamma \ll \gamma$ is assumed. The spectral norm of $\mathcal{I}_B$ is $\lambda = O(k^{(r+s)/2})$, where k/s is the effective Hilbert space dimension of the system [see Eq. (16)]. As a consequence, from Eq. (13) Δ becomes

$$\Delta = O(\sqrt{\gamma/\Gamma}k^{(r+s)/4}). \tag{28}$$

In the band limited interaction case ($\mathcal{I}_A$) the quasidiagonal structure of the density operator emerges [Eq. (27)], while in the case of the nonlinear interaction ($\mathcal{I}_B$) a quasidiagonal structure is expected only if the nonlinearity is weak: $s+r < 4$ [Eq. (28)].

Perturbation theory supports the scaling considerations. For a normalized eigenoperator $\hat{O}_l$ of the local evolution generator $\mathcal{L}_1^\dagger + \mathcal{L}_2^\dagger$: $(\mathcal{L}_1^\dagger + \mathcal{L}_2^\dagger)\hat{O}_l = \lambda_l\hat{O}_l$. The interaction $\mathcal{I}$ perturbs the evolution. The action of the perturbed generator on $\hat{O}_l$ gives $(\mathcal{L}_1^\dagger + \mathcal{L}_2^\dagger + \mathcal{I}^\dagger)\hat{O}_l = \lambda_l(\hat{O}_l + \hat{\delta}_l)$. If the trace norm of $\hat{\delta}_l$ is small compared to unity: $\|\hat{\delta}_l\|_1 \ll \|\hat{O}_l\|_1 = 1$, the evolution of $\hat{O}_l$ is only slightly perturbed on the time scale of $(\lambda_l)^{-1}$. Therefore, if $\mathrm{Re}[\lambda_l] < 0$, the perturbed $\hat{O}_l$ will decay on a time scale of $|\mathrm{Re}[\lambda_l]|$ to the leading order in $\|\hat{\delta}_l\|_1$. To each density matrix element ρ_{mn} in the nonperturbed tensor-product basis of the local energy states (the robust states bases) there corresponds the normalized operator $\hat{O}_{mn} = |ml_m\rangle\langle nl_n|$ such that $\langle\hat{O}_{mn}\rangle = \mathrm{Tr}\{\hat{\rho}\hat{O}_{mn}\} = \rho_{mn}$. Defining $\hat{\delta}_{mn}$ by $(\mathcal{L}_1^\dagger + \mathcal{L}_2^\dagger + \mathcal{I}^\dagger)\hat{O}_{mn} = \lambda_{mn}(\hat{O}_{mn} + \hat{\delta}_{mn})$ with $\lambda_{mn} = i[\omega_1(m-n) + \omega_2(l_m - l_n)] - \Gamma[(m-n)^2 + (l_m - l_n)^2]$, we obtain for the trace norm of $\hat{\delta}_{mn}$ corresponding to the first type of interaction $\mathcal{I}_A$,

$$\|\hat{\delta}_{mn}\|_1 = O\left(\frac{\gamma}{\Gamma}\sqrt{\frac{1}{\left[\frac{\omega_1}{\Gamma}(m-n)\right]^2 + \left[\frac{\omega_2}{\Gamma}(l_m - l_n)\right]^2 + [(m-n)^2 + (l_m - l_n)^2]^2}}\right) < O\left(\frac{\gamma}{\Gamma}\frac{1}{(m-n)^2 + (l_m - l_n)^2}\right), \tag{29}$$

and for the trace norm of $\hat{\delta}_{mn}$ corresponding to the second type of interaction $\mathcal{I}_B$,

$$\|\hat{\delta}_{mn}\|_1 = O\left(\frac{\gamma}{\Gamma}\sqrt{\frac{n^r m^s + l_m^s l_n^r}{\left[\frac{\omega_1}{\Gamma}(m-n)\right]^2 + \left[\frac{\omega_2}{\Gamma}(l_m - l_n)\right]^2 + [(m-n)^2 + (l_m - l_n)^2]^2}}\right) < O\left(\frac{\gamma}{\Gamma}\frac{\sqrt{l_m^r m^s + n^s l_n^r}}{(m-n)^2 + (l_m - l_n)^2}\right). \quad (30)$$

The width Δ of the interaction-dominated region is estimated by solving

$$\frac{\gamma}{\Gamma}\frac{1}{(m-n)^2 + (l_m - l_n)^2} = 1 \quad (31)$$

for the interaction generated by $\mathcal{I}_A$ and

$$\frac{\gamma}{\Gamma}\frac{\sqrt{l_m^r m^s + n^s l_n^r}}{(m-n)^2 + (l_m - l_n)^2} = 1 \quad (32)$$

for the interaction generated by $\mathcal{I}_B$. Using Eq. (26), Eq. (31) is simplified to

$$\frac{\gamma}{2\Gamma}\frac{1}{(m-n)^2} = 1, \quad (33)$$

from which $\Delta = 2|m-n| = \sqrt{2\gamma/\Gamma}$ is found, in compliance with the estimate (27), and Eq. (32) is simplified to

$$\frac{\gamma}{2\Gamma}\left(\frac{r}{s}\right)^{r/2}\frac{\sqrt{[(k-m)^r m^s + n^s(k-n)^r]}}{2(m-n)^2} = 1. \quad (34)$$

In this case, the width about the diagonal $\Delta = 2|m-n|$ will depend on m. The upper bound on Δ was calculated from Eq. (34) in two cases. First, for the linear coupling $r=s=1$ gives $\Delta < 2^{3/4}\sqrt{\frac{\gamma k}{\Gamma}}$. Second, for the nonlinear coupling $r=1$, $s=2$ gives $\Delta < \sqrt{\frac{\gamma}{\Gamma}}k^{3/4}$. Both results comply with the estimation Eq. (28).

Figure 2 displays regions of the density matrix, dominated by the interaction, vs regions dominated by the decoherence, with the boundary between the regions determined by Eqs. (33) and (34) for $k=10$, 20, 40, 50, and $\gamma/\Gamma=3$. The figure represents the composite system density matrices $\hat{\rho} = \Sigma_{mn} c_{mn} |mk-m\rangle\langle nk-n|$ and $\hat{\rho} = \Sigma_{mn} c_{mn} |m_s^r(k-m)\rangle\langle n_s^r(k-n)|$, corresponding to Eqs. (33) and (34), with m indexing the columns and n indexing the rows. The contours of Eqs. (34) are plotted for the linear coupling ($r=s=1$) and the nonlinear coupling ($r=1$, $s=2$). The quasidiagonal structure of the density operator is apparent. Both in the case of linear and nonlinear coupling between the oscillators, the width grows with the effective Hilbert space dimension. This is in contrast to the case of the band-limited interaction ($\mathcal{I}_A$), where the width about the diagonal does not depend on the effective Hilbert space dimension k.

To conclude, in contrast to the Poissonian type dephasing, in the Gaussian case the interaction-dominated regions are located about the diagonal of the density operator represented in the local energies basis. Since the initial state $|\psi(0)\rangle = |k0\rangle$ corresponds to the density operator with an unpopulated decoherence-dominated region, this region will remain unpopulated all along the evolution. As a consequence, the evolving density operator will stay in the quasidiagonal form. According to Eq. (10) the value of negativity is bounded by Δ in each case: $\mathcal{N}(\hat{\rho}) < \Delta$. Asymptotically, i.e., as $k \gg 1$ for the band-limited interaction, $\sqrt{k} \gg 1$ for the linear interaction and $\sqrt[4]{k} \gg 1$ for the nonlinear case, the width about the diagonal becomes negligible compared to k. In this case, the generated entanglement is negligible compared to the maximal entanglement compatible with the effective Hilbert space dimension.

In the following section the results of the numerical calculations of the evolution of negativity, illustrating the foregoing discussion, are presented. The evolution of negativity is compared in each case with the dynamics of the total (i.e., quantum and classical) correlations, as measured by the effective HS rank and HS-participation number of the evolving density operator.

IV. NUMERICAL RESULTS

In the present section the results of numerical calculations of negativity $\mathcal{N}(\hat{\rho})$, HS-participation number $\tilde{\kappa}(\hat{\rho})$, and the effective HS-rank $\tilde{\chi}_{0.01}(\hat{\rho})$ (cf. Appendix A) are displayed and analyzed. The model is a bipartite composite state of two oscillators, evolving according to Eq. (11). The dynamics

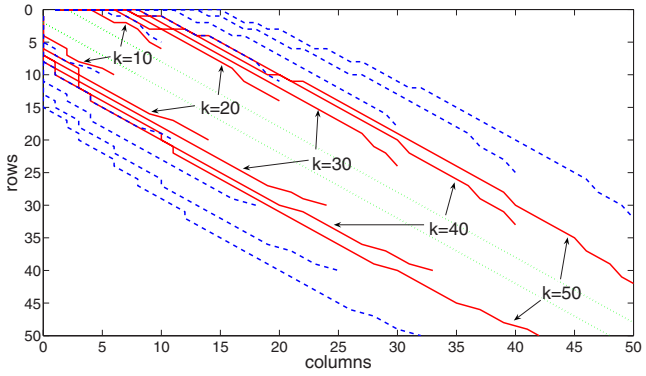

FIG. 2. (Color online) The density operator of the state, evolving according to Eqs. (11) for various interactions (15) and Gaussian type local baths (14) is represented in the product of local energies bases (Schmidt bases). Boundaries are indicated, in each case, separating the outer (off-diagonal) regions, dominated by the decoherence, from the inner (near diagonal) interaction-dominated regions. The interactions correspond to the band-limited case [case *A*, Eq. (15), dotted lines], linear coupling $r=s=1$ [case *B*, Eq. (15), solid lines], and the nonlinear coupling $r=1$, $s=2$ [case *B*, Eq. (15), dashed lines]. The density matrices in the band-limited case are of the form $\hat{\rho} = \Sigma_{mn} c_{mn} |mk-m\rangle\langle nk-n|$ and in the linear and nonlinear cases $\hat{\rho} = \Sigma_{mn} c_{mn} |m(r/s)(k-m)\rangle\langle n(r/s)(k-n)|$. The effective Hilbert space dimension corresponds to $k=10,20,30,40,50$ in each case. See explanations in the text.

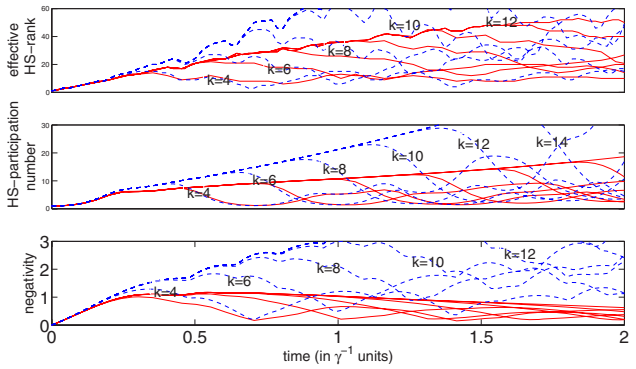

FIG. 3. (Color online) The negativity, the effective HS rank, and the HS-participation number of the evolving density operator: cases AG (solid lines) and A (dashed lines). In both cases $\omega_1=\omega_2=\omega$, $\Gamma_1=\Gamma_2=\Gamma$, with $\Gamma\omega^2=(1/3)\gamma=(1/15)\omega$ in case AG and $\Gamma=0$ in case A. Initial state $|\psi\rangle=|k0\rangle$, with $k=4,6,\ldots,14$.

simulated is classified according to the type of local bath, Eq. (14), and the type of interaction, Eq. (15):

(AG) The band-limited interaction $\mathcal{I}_A$. *Gaussian* pure dephasing (Figs. 3 and 4).

(AP) The band-limited interaction $\mathcal{I}_A$. *Poissonian* pure dephasing (Fig. 4).

(A) The band-limited interaction $\mathcal{I}_A$. Isolated reference case (Fig. 3).

(BG1) The linear ($r=s=1$) interaction $\mathcal{I}_B$. *Gaussian* pure dephasing (Figs. 5–7).

(BP1) The linear ($r=s=1$) interaction $\mathcal{I}_B$. *Poissonian* pure dephasing (Fig. 6).

(B1) The linear ($r=s=1$) interaction $\mathcal{I}_B$. Isolated reference case (Figs. 5 and 7).

(BG2) The nonlinear ($r=1$, $s=2$) interaction $\mathcal{I}_B$. *Gaussian* pure dephasing (Figs. 8–10).

(BP2) The nonlinear ($r=1$, $s=2$) interaction $\mathcal{I}_B$. *Poissonian* pure dephasing (Fig. 9).

(B2) The nonlinear ($r=1$, $s=2$) interaction $\mathcal{I}_B$. Isolated reference case (Figs. 8 and 10).

In each case the evolution of the composite system starts from a pure uncorrelated state $|\psi\rangle=|k0\rangle$, where k is the initial

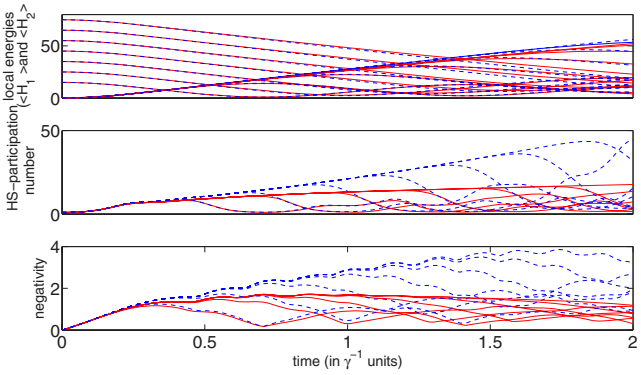

FIG. 4. (Color online) The negativity, the local energies and the HS-participation number of the density operator: cases AG and AP. Parameters: $\omega_1=\omega_2=\omega$, $\Gamma_1=\Gamma_2=\Gamma$ in both cases, $\Gamma\omega^2=0.125\gamma=0.025\omega$ in AG (solid lines), and $\Gamma=(1/15)\gamma=(1/75)\omega$, $\phi=2\pi/7$ in AP (dashed lines). Initial state $|\psi\rangle=|k0\rangle$, with $k=4,6,\ldots,14$.

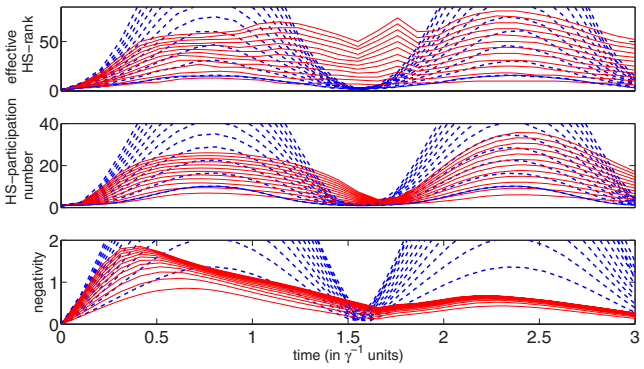

FIG. 5. (Color online) The negativity, the effective HS rank, and the HS-participation number of the evolving density operator: cases $BG1$ (solid lines) and $B1$ (dashed lines). In both cases $\omega_1=\omega_2=\omega$; in the $BG1$ case $\Gamma_1=\Gamma_2=\Gamma$, $\Gamma\omega^2=(1/3)\gamma=(1/15)\omega$; in the $B1$ case $\Gamma_1=\Gamma_2=0$. Initial state $|\psi\rangle=|k0\rangle$ for $k=4,6,\ldots,24$.

number of excitations of the first oscillator, which determines the effective Hilbert space dimension of the system.

Case AG (Figs. 3 and 4). In Fig. 3 the negativity, HS-participation number and effective HS rank of the evolving state in the presence of the bath is compared to the corresponding unitary evolution (case A). The amplitude of the negativity in the isolated case grows without bounds as the effective Hilbert space dimension k increases. Once the bath is introduced the amplitude of the negativity saturates to a value independent of k. On the other hand, both the HS-participation number and the effective HS rank of the evolving state show that the total correlations grow without bounds when the effective Hilbert space dimension of the system increases. It is interesting to note the qualitative difference, most obvious in the unitary evolution (dashed lines), between the dynamics of the HS-participation number and the effective HS rank on the shorter time scale, corresponding to the inverse frequency of the oscillators ω^{-1}. While the HS-participation number is smooth on that scale, the effective HS rank displays oscillations which follow closely after the corresponding dynamics of the negativity.

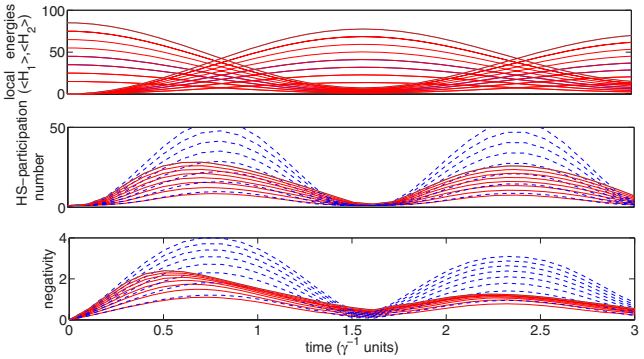

FIG. 6. (Color online) The negativity, the local energies, and the HS-participation number of the density operator: cases $BG1$ and $BP1$. Parameters: $\omega_1=\omega_2=\omega$, $\Gamma_1=\Gamma_2=\Gamma$ in both cases; $\Gamma\omega^2=(1/16)\gamma=(1/80)\omega$ in $BG1$ (solid lines); and $\Gamma=(1/10)\gamma=(1/50)\omega$, $\phi=2\pi/7$ in $BP1$ (dashed lines). Initial state $|\psi\rangle=|k0\rangle$, with $k=4,6,\ldots,18$.

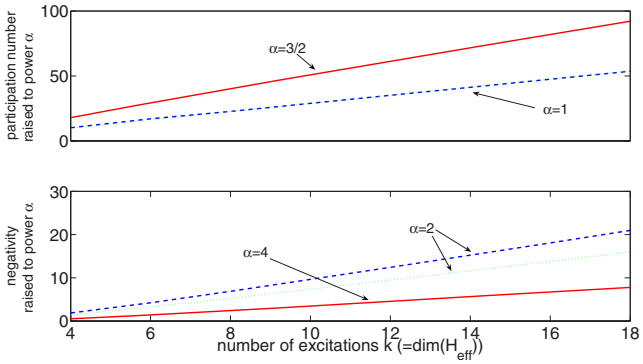

FIG. 7. (Color online) Negativity and HS-participation number (raised to various powers to fit linear dependence) measured at the first (in time) maximum in Fig. 5 for $BG1$ (solid line) and $B1$ (dashed lines) cases and in Fig. 6 for $BP1$ (dotted lines) case as a function of the number of excitations k [equal to $\dim(\mathcal{H}_{eff})$]. Negativity in the $BG1$ case is raised to power 4 and the negativity in both the $B1$ and $BP1$ cases is raised to power 2. The powers of the HS-participation number are 3/2 in the $BG1$ case and 1 in the $B1$ and $BP1$ cases.

Case AP. Figure 4 compares the dynamics of correlations in case AP to case AG. The relative strength of couplings to different types of environments is chosen to match the time scales of the local energies dephasing in both cases. It can be seen that in contrast to case AG both the negativity and the HS-participation number in case AP increase without bounds as the effective Hilbert space dimension grows similarly to the corresponding unitary evolution displayed in Fig. 3.

Case BG1 (Figs. 5–7). In Fig. 5 the negativity, HS-participation number, and effective HS rank of the evolving state in the presence of the bath is compared to the corresponding unitary evolution (case $B1$). The amplitude of the negativity in the isolated case grows without bounds as the effective Hilbert space dimension k increases. In the bath-on case the amplitude of the negativity is obviously restricted but the quantitive conclusions are better drawn from Figure 7 (see below). Both HS-participation number and effective HS-rank display the growth of the total correlations without

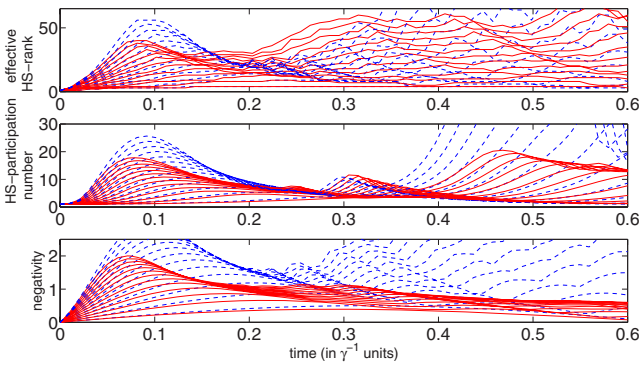

FIG. 8. (Color online) The negativity, the effective HS rank, and the HS-participation number of the evolving density operator: case $BG2$ (solid lines) and $B2$ (dashed lines). In both cases $2\omega_1=\omega_2=\omega$; in case $BG2$, $\Gamma_1\omega_1^2=\Gamma_2\omega_2^2=(1/3)\gamma=(1/30)\omega$; in case $B2$, $\Gamma_1=\Gamma_2=0$. Initial state $|\psi\rangle=|k0\rangle$ for $k=4,6,\ldots,28$.

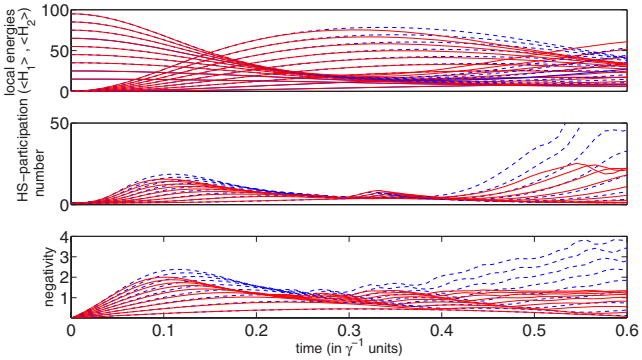

FIG. 9. (Color online) The negativity, the local energies, and the HS-participation number of the density operator: cases $BG2$ (solid lines) and $BP2$ (dashed lines). Parameters: $2\omega_1=\omega_2=\omega$ in both cases; $\Gamma_1\omega_1^2=\Gamma_2\omega_2^2=(1/8)\gamma=(1/80)\omega$ in $BG2$; $\Gamma_1=\Gamma_2=(1/4)\gamma=(1/40)\omega$, $\phi=2\pi/7$ in $BP2$. Initial state $|\psi\rangle=|k0\rangle$, with $k=4,6,\ldots,20$.

bounds with the effective Hilbert space dimension of the system. Note the qualitative difference in dynamics of the two measures.

Figure 7 displays the maximal values of the negativity and the HS-participation number obtained in cases $BG1$, $B1$, and $BP1$ as functions of the effective Hilbert space dimension k. It is seen that in the $B1$ case the squared negativity and the HS-participation number scale linearly with k in compliance with the calculation in Appendix B. The same scaling is found in case $BP1$. On the other hand, the negativity in the $BG1$ case scales as a fourth root of the effective Hilbert space dimension. The corresponding HS-participation number measuring the total correlations scales as $k^{2/3}$.

Case BP1. Figure 6 compares the dynamics of correlations in case $BP1$ to case $BG1$. The relative strength of couplings to different types of environments is chosen to match the local energies dephasing rates. From this figure and Fig. 7 it can be seen that in contrast to case $BG1$ both the negativity and the HS-participation number in case $BP1$ follow a dynamical pattern identical to the corresponding unitary evolution.

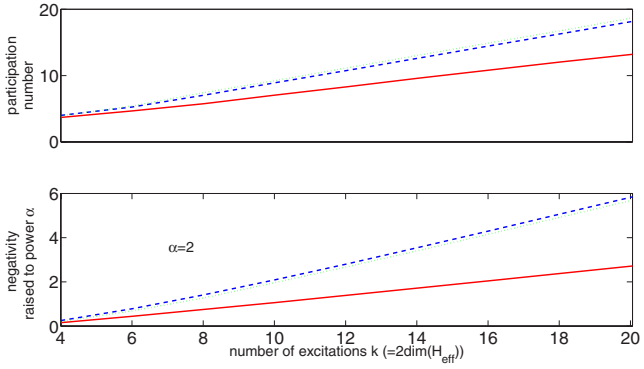

FIG. 10. (Color online) Negativity (squared to fit linear dependence) and HS-participation number measured at the first (in time) maximum in Fig. 8 for $BG2$ (solid line) and $B2$ (dashed lines) cases and in Fig. 9 for $BP2$ (dotted lines) case as a function of the number of excitations k [equal to $\dim(\mathcal{H}_{eff})$].

*Case BG*2 *(Figs. 8–10)*. In Fig. 8 the negativity, HS-participation number and effective HS rank of the evolving state in the presence of the bath is compared to the corresponding unitary evolution (case *B*2). For a nonlinear interaction both the amplitudes and time scales of the dynamics depend on the initial state. As a consequence, the pattern of behavior changes with the effective Hilbert space dimension. This makes it difficult to compare the evolutions corresponding to different k. Comparing the open to the closed unitary evolutions for a fixed k, it is seen that the global dynamics of the negativity is much stronger affected by the bath than the dynamics of the total correlations. For example, the total correlations may grow in the open dynamics similarly to the unitary case, while the negativity at this time is decaying in sharp contrast to the corresponding unitary behavior.

A possible way to compare values of the negativity and the total correlations at different k is to measure the values observed at the first maximum in the evolutions of these quantities. These measurement are displayed in Fig. 10. To understand the scaling, the negativity (squared to fit the linear dependence) and the HS-participation number obtained in cases *BG*2, *B*2, and *BP*2 are plotted as functions of the effective Hilbert space dimension k. It is found that the negativity scales with $\sqrt{k}$ while the HS-participation number scale linearly with k.

*Case BP*2. Figure 9 compares the dynamics of correlations in case *BP*2 to case *BG*2. The relative strength of couplings to different types of environments is chosen to match the local energies dephasing rates. The negativity and the HS-participation number in case *BP*2 follow a dynamical pattern identical to the corresponding unitary evolution displayed in Fig. 8. See also Fig. 10.

V. SUMMARY AND CONCLUSIONS

A variety of open interacting bipartite systems were investigated in order to characterize restrictions, imposed by coupling to local environments, on the generation of classical and quantum correlations.

The extent of the generated quantum correlations is determined by the interplay of two competing forces: the interaction, leading to development of entanglement, and the local decoherence, inducing a decay of entanglement. The relative magnitudes of the local decoherence rates and the cutoff frequency of the interaction in the effective Hilbert space of the composite system determines the relative size of decoherence- and interaction-dominated regions of the density operator in local robust states basis. The presence of the decoherence-dominated regions constrains the structure of the evolving composite density operator, restricting the extent of entanglement, generated by the interaction.

The character of restriction depends on the type of bath and the type of the interaction. The two different paradigms of the dephasing, the Poissonian and the Gaussian, lead to very different correlation dynamics. In models with band-limited decoherence such as the Poissonian pure dephasing model, either the decoherence or the interaction dominates the dynamics, depending on the relative strength of the coupling constants and irrespective of initial state. Numerical calculations performed on a bipartite system of two interacting harmonic oscillators, coupled to local Poissonian baths, support this conclusion.

Open systems with Gaussian pure dephasing belong to a different class of models. This class is characterized by unbounded growth of the decoherence time scales with the effective Hilbert space dimension of the system. As a consequence, constrains on the structure of evolving state and restriction on the extent of entanglement are generally expected. Still the precise character of the restriction depends on the type of interaction between the subsystems. Coupling local Gaussian environments to subsystems with band-limited interaction between them, imposes an upper bound on the extent of generated entanglement, which is independent of the effective Hilbert space dimension of the system. As a consequence, asymptotically, i.e., at sufficiently large effective dimension, the generated entanglement is negligible, compared to entanglement generated in the corresponding unitary dynamics. Interactions which are not band-limited generally produce extensive entanglement, notwithstanding the type of local environment. Nonetheless, in models with local Gaussian environments the scaling of entanglement with the effective dimension is limited by the local decoherence. The precise limit depends on the nonlinearity of the interaction. In the model of two nonlinearly interacting harmonic oscillators stronger nonlinearity implies weaker bounds on the generated entanglement. When the nonlinearity exceeds some maximal value no restriction on the extent of entanglement is expected. Numerical calculations support these predictions.

Estimation of bounds on negativity in the evolving state was based on analysis of the structure of the density matrix, in particular local robust states bases. Relating the negativity to the structure of the density operator was facilitated by the observation that the evolving states are Schmidt-correlated due to particular conservation laws observed by the interactions. The corresponding Schmidt bases are built of local robust states selected by local purely dephasing environments—the local energy bases. Since the presence of exact conservation laws is nongeneric in physical models, it should be noted that numerical evidence shows that the qualitative picture presented above is robust.

Dynamics of the total correlations was investigated numerically to compare with the corresponding dynamics of the entanglement. It was found that evolution of the total (and, as a consequence, classical) correlations display a different dynamical pattern. In the band-limited interaction model, the amplitude of the total correlations grows without bounds with the effective Hilbert space dimension, while the negativity tends to an asymptotic behavior independent of the effective dimension. In the linear interaction model, though the amplitudes of both the quantum and the total correlations grow without bounds with the effective Hilbert space dimension, the total correlations scale with a higher power of the dimension. In the nonlinear interaction, a comparison is impeded by the fact that the evolution of both the entanglement and the total correlations display a variety of time scales. Nonetheless, inspection of the numerical evidence shows that the total correlations always scale with a higher power of the effective Hilbert space dimension. These

findings can be informally interpreted as a trade off between the classical and quantum correlations: since the total correlations are (relatively) unaffected by the environment, restriction on the entanglement generation must be "compensated" by the growth of the classical correlations.

Considering the restriction on the generation of entanglement, a natural question arises: is the observed restriction substantial, i.e., is the given partition of the composite system meaningful? When can a composite systems be regarded as *approximately disentangled*? The answer depends on the definition of the relevant scale of a measure of entanglement in the evolving system. Is the scale unity or some power of the effective Hilbert space dimension or neither?

One possibility is to compare the entanglement, generated in the open evolution to the entanglement, generated in the corresponding unitary evolution. Numerical evidence obtained in the present study shows that entanglement is always relatively restricted in the open system dynamics. In some cases, such as the Gaussian pure dephasing, it can even be negligible in asymptotically large Hilbert space dimensions. This comparison elucidates the role of the decoherence in constraining the generation of the quantum correlations. Nevertheless, the magnitude of the entanglement generated in a particular open evolution may still be large in some absolute sense.

An alternative scale of entanglement is set by the maximal entanglement compatible with the effective Hilbert space dimension. The results of the present study show that in some models, such as the Gaussian pure dephasing and weakly nonlinear or band-limited interactions, coupling to local environments does the job, i.e., it restricts the generated entanglement to bounds, negligible compared to the maximal compatible entanglement. Still, in all cases apart from a band-limited type of the interaction, entanglement, generated on the interaction time scale in the open system evolution, grows without bounds with the effective Hilbert space dimension. As a consequence, this scale may become irrelevant in large effective Hilbert dimensions, due to a limited experimental resolution.

To conclude, common models of local decoherence do not provide a universal pathway to an approximately disentangled evolution of a bipartite composite system in the presence of interaction. It follows that, contrary to expectations, coupling to local environments does not generally validate partition of composite quantum systems.

ACKNOWLEDGMENTS

We are grateful to L. Diosi, D. Steinitz, and Y. Shimoni for useful comments. This work was supported by the Binational US-Israel Science Foundation (BSF). The Fritz Haber Center is supported by the Minerva Gesellschaft für die Forschung GmbH München, Germany.

APPENDIX A: THE SCHMIDT RANK AND THE HS-SCHMIDT RANK

The definition of the Schmidt rank of the bipartite composite state [3,43] is reviewed. Let $|\psi\rangle$ be a state in the composite Hilbert space $\mathcal{H}_{12}=\mathcal{H}_1\otimes\mathcal{H}_2$. There exist a following representation (a Schmidt decomposition) of the state: $|\psi\rangle=\Sigma_i c_i|i\rangle_1\otimes|i\rangle_2$, where $|i\rangle_{1,2}$ is an orthonormal basis in the Hilbert space $\mathcal{H}_{1,2}$. While a Schmidt decomposition is not unique, the set of nonvanishing coefficients c_i is invariant (modulo irrelevant phases) under the local unitary transformations and is characteristic of the state $|\psi\rangle$. This set is shown to be the square root of the spectrum of the reduced density operator of either subsystem. The number of nonvanishing coefficients c_i is called the Schmidt rank $\chi(\psi)$ of the state and equals the rank of the reduced density operator of either subsystem: $\chi(\psi)=\mathrm{rank}\{\mathrm{Tr}_1\{\hat{\rho}_{12}\}\}$. To calculate the Schmidt rank of a state expressed in an arbitrary tensor product basis $|\psi\rangle=\Sigma_{ij}c_{ij}|i\rangle_1|j\rangle_2$, one calculates the rank of the matrix $\rho_2=C^\dagger C$, where $C_{ij}=c_{ij}$: $\mathrm{Tr}_1\{\hat{\rho}_{12}\}=\Sigma_{\{n,i,j,k,l\}}c_{ij}c_{kl}^*\delta_{in}\delta_{kn}|j\rangle\langle l|=\Sigma_{\{i,j,l\}}c_{ij}c_{il}^*|j\rangle\langle l|=\Sigma_{\{j,l\}}(\rho_2)_{lj}|j\rangle\langle l|$.

The Schmidt rank characterizes the extent of correlations present in the state. The uncorrelated (product) state has $\chi=1$ but generally $\chi(\psi)\leqslant\min\{\dim(\mathcal{H}_1),\dim(\mathcal{H}_2)\}$. The maximally correlated state has $\chi(\psi)=\min\{\dim(\mathcal{H}_1),\dim(\mathcal{H}_2)\}$ and $c_i=c_j$, $\forall i,j$. Generally, some of the coefficients c_i are much smaller than others and as a consequence dropping the corresponding contributions to the Schmidt decomposition does not lead to an observable effect. This suggests a definition of the physically reasonable *effective Schmidt rank* [9] χ_ϵ: $\chi_\epsilon(\psi)\equiv\chi(\psi')$, with $|\psi'\rangle=\Sigma_{i\in I_\epsilon}c_i|i\rangle_1\otimes|i\rangle_2$, where I_ϵ is the smallest set of indices such that $\||\psi\rangle-|\psi'\rangle\|<\epsilon$. An alternative measure is a participation number [63] $\kappa(\psi)\equiv 1/\mathrm{Tr}\{\hat{\rho}_2^2\}$ with $\hat{\rho}_2=\mathrm{Tr}_1\{\hat{\rho}_{12}\}$. The participation number of a state, characterized by M equal substantial contributions to its Schmidt decomposition is seen to be M, which motivates the definition.

A mixed state displays both quantum (entanglement) and classical correlations. The extent of the *total* correlations can be characterized by the Schmidt rank of a density operator. With a slight abuse of terminology the term HS-Schmidt rank (HS indicating the Hilbert-Schmidt space) or just HS rank is adopted. The definition of the HS rank views the density operator of a composite system as a (unnormalized) pure state ("superket" [10]) in the Hilbert-Schmidt space of system operators. The Schmidt rank of the corresponding "superket" defines the HS rank [denoted $\tilde{\chi}(\hat{\rho})$] of the density operator. The notions of the effective Schmidt rank $\chi_\epsilon(\psi)$ and the participation number $\kappa(\psi)$ can be transferred to the HS rank of the density operator. For brevity, the corresponding measures of the total correlations are termed effective HS rank and HS-participation number and denoted by $\tilde{\chi}_\epsilon(\hat{\rho})$ and $\tilde{\kappa}(\hat{\rho})$, respectively.

The calculation of the HS rank proceeds as follows. Let $\hat{\rho}_{12}=\Sigma_{\{i,j,k,l\}}\rho_{ijkl}|ij\rangle\langle kl|$ be a density operator of the composite system. In the superket notation it has the form $|\hat{\rho}\rangle_{12}=\Sigma_{\{i,j,k,l\}}\rho_{ijkl}\||ij\rangle\langle kl|\rangle$. The corresponding density superoperator is $\mathcal{R}_{12}(\hat{\rho})=\Sigma_{\{i,j,k,l,i',j',k',l'\}}\rho_{ijkl}\rho_{i'j'k'}^*\||ij\rangle\langle kl|\rangle\langle|i'j'\rangle\times\langle k'l'|\|$ and the reduced density superoperator is

$$\begin{aligned}\mathcal{R}_2(\hat{\rho}) &= \mathrm{Tr}_1\{\mathcal{R}_{12}(\hat{\rho})\}\\ &= \sum\nolimits_{\{i,j,k,l,i',j',k',l',m,n\}}\rho_{ijkl}\rho_{i'j'k'l'}^*\\ &\quad\times\delta_{mi}\delta_{nk}\delta_{mi'}\delta_{nk'}\||j\rangle\langle l|\rangle\langle|j'\rangle\langle l'|\|\end{aligned}$$

$$= \sum_{\{j,l,j',l'\}} R_{jlj'l'} \|j\rangle\langle l|\rangle\langle j'|\rangle\langle l'\| $$

where $R_{jlj'l'} = \Sigma_{ik} \rho_{ijkl} \rho^*_{i'j'k'l'}$. The HS rank $\tilde{\chi}(\hat{\rho})$ of the density operator $\hat{\rho}$ is $\tilde{\chi}(\hat{\rho}) = \text{rank}\{\mathcal{R}_2(\hat{\rho})\}$. The effective HS rank and the HS-participation number are calculated similarly.

Finally, note that $\tilde{\chi}(|\psi\rangle\langle\psi|) = \chi(\psi)^2$. In fact,

$$\begin{aligned}
\chi_\psi^2 &= (\text{rank}\{\hat{\rho}_2\})^2 = \text{rank}\{\hat{\rho}_2 \otimes \hat{\rho}_2^T\} \\
&= \text{rank}\{\sum_{\{i,j,l,k,j',l'\}} a_{ij} a^*_{il} a_{kj'} a^*_{kl'} |j\rangle\langle l| \otimes |l'\rangle\langle j'|\} \\
&= \text{rank}\{\sum_{\{i,j,l,k,j',l'\}} \rho_{ijkl'} \rho^*_{ilkj'} |j\rangle\langle l| \otimes |l'\rangle\langle j'|\} \\
&= \text{rank}\{\sum_{\{j,l,j',l'\}} R_{jl'lj'} |j\rangle\langle l| \otimes |l'\rangle\langle j'|\} \\
&= \text{rank}\{\sum_{\{j,l,j',l'\}} R_{jlj'l'} |j\rangle\langle j'| \otimes |l\rangle\langle l'|\} \\
&= \text{rank}\{\sum_{\{j,l,j',l'\}} R_{jlj'l'} |jl\rangle\langle j'l'|\} = \tilde{\chi}(|\psi\rangle\langle\psi|)
\end{aligned}$$

.

APPENDIX B: CALCULATION OF THE EFFECTIVE SCHMIDT RANK OF THE COMPOSITE STATE OF TWO LINEARLY INTERACTING HARMONIC OSCILLATORS

A system of two linearly interacting harmonic oscillators is considered with the Hamiltonian $\hat{H} = \omega(\hat{a}_1^\dagger \hat{a}_1 + \hat{a}_2^\dagger \hat{a}_2) + \gamma(\hat{a}_1^\dagger \hat{a}_2 + \hat{a}_2^\dagger \hat{a}_1)$ The initial state is $|\psi(0)\rangle = |0k\rangle$ in the local energies basis. The state at $t > 0$ becomes $|\psi(t)\rangle = \Sigma_{n=0}^k c_n |k-nn\rangle$, where $c_n(t) = \sqrt{\frac{k!\cos(\gamma t)^{2n}\sin(\gamma t)^{2(k-n)}}{n!(k-n)!}} e^{-i\omega k t}$. The width Δ_k of the distribution of expansion coefficients $|c_n|^2$ is estimated at $t = \pi/4\gamma$ for $k \gg 1$. This width is a reasonable estimate for the amplitude of the effective Schmidt rank of the state, $\chi(\psi) \approx \Delta_k$.

The distribution of the coefficients $|c_n(\pi/4\gamma)|^2 = \frac{k!}{2^k n!(k-n)!}$ is peaked around $n = k/2$. To estimate Δ_k it is assumed that $\Delta_k \ll k$. Δ_k is defined by $\frac{\partial^2}{\partial n^2}|c_n(\pi/4\gamma)|^2|_{n=n^*} = 0$, where $n^* = k/2 - \Delta_k/2$. Performing the derivation under the Stirling approximation for the factorials (valid at $k \gg 1$) leads to $\frac{k}{n^*(k-n^*)} = \ln^2\left(\frac{k-n^*}{n^*}\right)$. For highly peaked distribution $\frac{k-n^*}{n^*} - 1 \ll 1$, therefore $\ln^2\left(\frac{k-n^*}{n^*}\right) \approx \left(\frac{k-2n^*}{n^*}\right)^2$. Also $\frac{k}{n^*(k-n^*)} \approx \frac{4}{k}$ to the leading order in $\frac{k-2n^*}{n^*}$. Finally $\frac{4}{k} \approx \left(\frac{k-2n^*}{n^*}\right)^2 \approx \left(\frac{k-2n^*}{k/2}\right)^2 = \left(\frac{\Delta_k}{k/2}\right)^2$ from which $\Delta_k = \sqrt{k}$ and $\chi(\psi) \approx \Delta_k = \sqrt{k}$. As follows from the relation $\tilde{\chi}(|\psi\rangle\langle\psi|) = \chi(\psi)^2$, proved in Appendix A, the amplitude of the effective HS rank scales as k.

The obtained result can be used to estimate the amplitude of the negativity in the pure state evolution. In fact $\mathcal{N}(|\psi(t)\rangle\langle\psi(t)|) = \frac{1}{2}(|\Sigma_n c_n|^2 - 1)$ by Ref. [46]. Taking $c_n = \frac{1}{\sqrt{\Delta_k}} = \frac{1}{\sqrt[4]{k}}$ for the purpose of scaling we obtain $\mathcal{N}[|\psi(\pi/4\gamma)\rangle \times \langle\psi(\pi/4\gamma)|] = \frac{1}{2}\sqrt{k}$ for the amplitude of the negativity.

[1] N. Moiseyev, Chem. Phys. Lett. **98**, 233 (1983).
[2] P. Jungwirth, M. Roeselova, and R. B. Gerber, J. Chem. Phys. **110**, 9833 (1999).
[3] A. Peres, *Quantum Theory: Concepts and Methods* (Kluwer, Boston, 1998).
[4] R. F. Werner, Phys. Rev. A **40**, 4277 (1989).
[5] W. H. Miller, J. Phys. Chem. B **106**, 8132 (2002).
[6] E. J. Heller, Acc. Chem. Res. **39**, 127 (2006).
[7] M. H. Beck, A. Jackle, G. A. Worth, and H. D. Meyer, Phys. Rep. **324**, 1 (2000).
[8] G. Vidal, Phys. Rev. Lett. **91**, 147902 (2003).
[9] G. Vidal, Phys. Rev. Lett. **93**, 040502 (2004).
[10] M. Zwolak and G. Vidal, Phys. Rev. Lett. **93**, 207205 (2004).
[11] Y. Y. Shi, L. M. Duan, and G. Vidal, Phys. Rev. A **74**, 022320 (2006).
[12] R. Jozsa and N. Linden, Proc. R. Soc. London, Ser. A **459**, 2011 (2003).
[13] *Decoherence and the Appearance of a Classical World in Quantum Theory*, edited by D. Giulini, E. Joos, C. Kiefer, J. Kupsch, I. O. Stamatescu, and H. D. Zeh (Springer, Berlin, 2003).
[14] M. A. Nielsen and I. L. Chuang, *Quantum Computation and Quantum Information* (Cambridge University Press, Cambridge, 2000).
[15] D. Braun, Phys. Rev. Lett. **89**, 277901 (2002).
[16] F. Benatti, R. Floreanini, and M. Piani, Phys. Rev. Lett. **91**, 070402 (2003).
[17] P. J. Dodd and J. J. Halliwell, Phys. Rev. A **69**, 052105 (2004).
[18] P. J. Dodd, Phys. Rev. A **69**, 052106 (2004).
[19] T. Yu and J. H. Eberly, Phys. Rev. B **68**, 165322 (2003).
[20] T. Yu and J. H. Eberly, Opt. Commun. **264**, 393 (2006).
[21] M. F. Santos, P. Milman, L. Davidovich and N. Zagury, Phys. Rev. A **73**, 040305(R) (2006).
[22] L. Diosi, in *Irreversible Quantum Dynamics*, edited by F. Benatti and R. Floreanini (Springer, Berlin, 2003).
[23] T. Yu and J. H. Eberly, Phys. Rev. B **66**, 193306 (2002).
[24] T. Yu and J. H. Eberly, Phys. Rev. Lett. **93**, 140404 (2004).
[25] A. R. R. Carvalho, F. Mintert, and A. Buchleitner, Phys. Rev. Lett. **93**, 230501 (2004).
[26] W. Dur and H. J. Briegel, Phys. Rev. Lett. **92**, 180403 (2004).
[27] A. R. R. Carvalho, F. Mintert, S. Palzer, and A. Buchleitner, e-print arXiv:quant-ph/0508114.
[28] F. Mintert, A. R. R. Carvalho, M. Kus, and A. Buchleitner, Phys. Rep. **415**, 207 (2005).
[29] S. B. Lee and J. B. Xu, Phys. Lett. A **311**, 313 (2003).
[30] J. M. B. Plenio and J. Eisert, New J. Phys. **6**, 36 (2004).
[31] A. Abragam, *The Principles of Nuclear Magnetism* (Clarendon Press, Oxford, 1961).
[32] C. W. Gardiner, *Handbook of Stochastic Methods* (Springer, Berlin, 1983).
[33] I. R. Kubo, *Fluctuations, Relaxation and Resonance in Magnetic Systems*, edited by D. ter Haar (Oliver and Boye, Edinburgh, 1962).
[34] T. Yamaguchi, J. Chem. Phys. **112**, 8530 (2000).
[35] E. Gershgoren, Z. Wang, S. Ruhman, J. Vala, and R. Kosloff, J. Chem. Phys. **118**, 3660 (2003).

[36] M. Demirplak and S. Rice, J. Chem. Phys. **125**, 194517 (2006).
[37] A. V. Uskov, A. P. Jauho, B. Tromborg, J. Mork, and R. Lang, Phys. Rev. Lett. **85**, 1516 (2000).
[38] C. Kammerer, C. Voisin, G. Cassabois, C. Delalande, Ph. Roussignol, F. Klopf, J. P. Reithmaier, A. Forchel, and J. M. Gerard, Phys. Rev. B **66**, 041306(R) (2002).
[39] P. San-Jose, G. Zarand, A. Shnirman, and G. Schon, Phys. Rev. Lett. **97**, 076803 (2002).
[40] F. Iachello and R. D. Levine, *Algebraic Theory of Molecules* (Oxford University Press, Oxford, 1995).
[41] J. Perina, *Quantum Statistics of Linear and Nonlinear Optical Phenomena* (Kluwer, London, 1991).
[42] D. J. Wineland, C. Monroe, W. M. Itano, D. Leibfried, B. E. King, and D. M. Meekhof, J. Res. Natl. Inst. Stand. Technol. **103**, 259 (1998).
[43] E. Schmidt, Math. Ann. **63**, 433 (1906).
[44] L. Diosi, *A Short Course in Quantum Information Theory* (Springer, Berlin, 2007).
[45] M. Plenio and S. Virmani, Quantum Inf. Comput. **7**, 1 (2007).
[46] G. Vidal and R. F. Werner, Phys. Rev. A **65**, 032314 (2002).
[47] A. Peres, Phys. Rev. Lett. **77**, 1413 (1996).
[48] M. Horodecki, P. Horodecki, and R. Horodecki, Phys. Lett. A **223**, 1 (1996).
[49] E. M. Rains, Phys. Rev. A **60**, 179 (1999).
[50] E. M. Rains, Phys. Rev. A **63**, 019902(E) (2001).
[51] S. Virmani, M. F. Sacchi, M. B. Plenio, and D. Markham, Phys. Lett. A **62**, 288 (2001).
[52] M. Khasin, R. Kosloff, and D. Steinitz, Phys. Rev. A **75**, 052325 (2007).
[53] W. H. Zurek, Phys. Rev. D **24**, 1516 (1981).
[54] L. Diosi and C. Kiefer, Phys. Rev. Lett. **85**, 3552 (2000).
[55] W. T. Strunz, in *Coherent Evolution in Noisy Environments*, edited by A. Buchleitner and K. Hornberger (Springer, Berlin, 2002).
[56] R. Horn and C. R. Johnson, *Matrix Analysis* (Cambridge University Press, Cambridge, 1990).
[57] V. Gorini and A. Kossakowski, J. Math. Phys. **17**, 1298 (1976).
[58] E. A. Weiss, G. Katz, R. H. Goldsmith, M. R. Wasielewski, M. A. Ratner, R. Kosloff, and A. Nitzan, J. Chem. Phys. **124**, 074501 (2006).
[59] G. Lindblad, Commun. Math. Phys. **48**, 119 (1976).
[60] G. S. Agarwal and J. Banerji, Phys. Rev. A **55**, R4007 (1997).
[61] D. J. Wineland, C. Monroe, W. M. Itano, B. E. King, D. Leibfried, C. Myatt, and C. Wood, Phys. Scr., T **76**, 147 (1998).
[62] M. Paternostro, M. S. Kim, and P. L. Knight, Phys. Rev. A **71**, 022311 (2005).
[63] R. Grobe, K. Rzazewski, and J. H. Eberly, J. Phys. B **27**, L503 (1994).

3.3 Negativity as a Distance from a Separable State

Negativity as a distance from a separable state

M. Khasin, R. Kosloff, and D. Steinitz
Fritz Haber Research Center for Molecular Dynamics, Hebrew University of Jerusalem, Jerusalem 91904, Israel
(Received 28 December 2006; published 21 May 2007)

The computable measure of the mixed-state entanglement, the negativity, is shown to admit a clear geometrical interpretation, when applied to Schmidt-correlated (SC) states: the negativity of a SC state equals a distance of the state from a pertinent separable state. As a consequence, the Peres-Horodecki criterion of separability is both necessary and sufficient for SC states. Another remarkable consequence is that the negativity of a SC can be estimated "at a glance" on the density matrix. These results are generalized to mixtures of SC states, which emerge in bipartite evolutions with additive integrals of motion.

DOI: 10.1103/PhysRevA.75.052325 PACS number(s): 03.67.Mn, 03.65.Ud, 03.65.Yz

Nonlocal quantum correlations are a key resource in quantum information processing [1]. The exclusive quantum part of this correlation has been termed entanglement. For a pure bipartite state the extent of entanglement is well defined by the Schmidt rank of the state [2,3], counting the number of nonvanishing terms in the product states decomposition [4]. For mixed quantum states the notion of entanglement is more involved and various measures have been suggested [4], each focusing on particular aspects of this phenomenon. In order to take advantage of the insights learned from different measures, it is advantageous to seek for classes of states where different entanglement measures agree [5]. Such a class is the bipartite Schmidt-correlated states class [6–8], where it has been shown that the distillable entanglement [9] and relative entropy of entanglement [10] both coincide and can be calculated by a simple formula [6,7,10,11]. The Schmidt-correlated (SC) states are defined as mixtures of pure states, sharing the same Schmidt bases [6–8]. Such states naturally appear in a bipartite system dynamics with additive integrals of motion (see below and Ref. [12]). Hence, these states form an important class of mixed states from a quantum dynamical perspective.

The present study establishes a remarkable property of the SC states: the handy, albeit obscure, negativity [13] measure of entanglement admits a clear geometrical interpretation. It is found that the negativity equals half the sum of the absolute values of the off-diagonal elements of the density matrix, which is a distance of the SC state from a pertinent separable state (see Fig. 1). As a consequence, unlike a general mixed state, a SC state is separable [16] if and only if its negativity vanishes, which implies that the Peres-Horodecki criterion [14,15] of separability is both necessary and sufficient for SC states. It should be noted, that the matrix norm used to define the distance, permits an estimation of the negativity "at a glance," which has a strong intuitive appeal. Quantum-dynamical considerations motivate a generalization of the results to particular mixtures of SC states. It is shown that the negativity of such a mixture is less or equal to the distance of the state from a pertinent separable state.

We start from a formal definition of a SC state.

Definition. A mixed bipartite state $\hat{\rho}=\Sigma_i p_i|\psi_i\rangle\langle\psi_i|$ is called Schmidt-correlated if $|\psi_i\rangle=\Sigma_m c_m^i|m\rangle_1\otimes|m\rangle_2$ for every i, i.e., all pure states in the mixture share the same Schmidt bases $\Gamma_1=\{|m\rangle_1\}_{m=1}^N$ and $\Gamma_2=\{|m\rangle_2\}_{m=1}^N$.

As a simple example of SC state consider the state $\hat{\rho}=\Sigma_{i=1,2}p_i|\psi_i\rangle\langle\psi_i|$ of a composite system of two qubits, where $|\psi_i\rangle=c_1^i|11\rangle+c_2^i|00\rangle$. On the other hand, a mixture of pure states $|\psi_1\rangle=c_1^1|11\rangle+c_2^1|00\rangle$ and $|\psi_2\rangle=c_1^2|10\rangle+c_2^2|01\rangle$ will not be SC, unless both states are maximally entangled, in which case a common Schmidt bases exist [8].

Theorem 1. Let a bipartite state $\hat{\rho}$ be a SC state with respect to Schmidt bases Γ_1 and Γ_2. Then the negativity of the state $\hat{\rho}$ equals a distance of $\hat{\rho}$ from a separable state $\hat{\rho}'$ diagonal in the tensor-product basis $\Gamma=\Gamma_1\otimes\Gamma_2$: $\mathcal{N}(\hat{\rho})=\frac{1}{2}d(\hat{\rho},\hat{\rho}')$, where $(\hat{\rho}')_{ij}=\delta_{ij}(\hat{\rho})_{ij}$, $i,j\in\Gamma$ and the distance $d(\hat{x},\hat{y})=\|\hat{x}-\hat{y}\|_\alpha$ is induced by the matrix norm $\|\hat{x}\|_\alpha=\Sigma_{i,j}|(\hat{x})_{i,j}|$ [17].

Remark. The separable state $\hat{\rho}'$, from which the distance induced by the norm $\|\bullet\|_\alpha$ is measured, is simply represented by the matrix of $\hat{\rho}$ with off-diagonal elements stripped off. If $\hat{\rho}$ is a pure state (which is trivially SC,) then $\hat{\rho}'$ is also the state that minimizes the relative entropy $S(\hat{\rho}\|\hat{\sigma})$ over all disentangled states $\hat{\sigma}$. In that case, the entanglement of relative entropy is $E_{\mathrm{RE}}(\hat{\rho})\equiv\min_{\text{separable }\hat{\sigma}}S(\hat{\rho}\|\hat{\sigma})=S(\hat{\rho}\|\hat{\rho}')$ [18,19].

Proof. Let $\hat{\rho}=\Sigma_i p_i|\psi_i\rangle\langle\psi_i|$, where $|\psi_i\rangle=\Sigma_{m=1}^N c_m^i|m\rangle_1\otimes|m\rangle_2$. Then $\hat{\rho}=\Sigma_i p_i\Sigma_{mn}c_n^i(c_m^i)^*|n\rangle\langle m|\otimes|n\rangle\langle m|=\Sigma_{mn}\rho_{mn}|n\rangle\langle m|\otimes|n\rangle\times\langle m|$, where $\rho_{mn}=\Sigma_i p_i c_n^i(c_m^i)^*$. By definition $d(\hat{\rho},\hat{\rho}')=\|\hat{\rho}-\hat{\rho}\|_\alpha=\Sigma_{mn}|\rho_{mn}|-1=2\Sigma_{m<n}|\rho_{mn}|$.

The negativity of a state is defined as the absolute value of the sum of the negative eigenvalues of the partially transposed density operator corresponding to the state [13]. In what follows we show that $\{-|\rho_{mn}|,m<n\}$ is the set of all the negative eigenvalues of the partially transposed $\hat{\rho}$. This completes the proof.

The partially transposed density matrix is given by

$$\hat{\rho}^{PT}=\sum_{mn}\rho_{mn}|n\rangle\langle m|\otimes(|n\rangle\langle m|)^T=\sum_{mn}\rho_{mn}|n\rangle\langle m|\otimes|m\rangle\langle n|. \tag{1}$$

Consider $N(N-1)$ vectors

$$|\psi_{kl}\rangle_\pm=-\rho_{lk}|k\rangle|l\rangle\pm|\rho_{kl}||l\rangle|k\rangle,\quad k<l,k=1,2,\ldots,N-1 \tag{2}$$

and N vectors

$$|\psi_{kk}\rangle=|k\rangle|k\rangle,\quad k=1,2,\ldots,N, \tag{3}$$

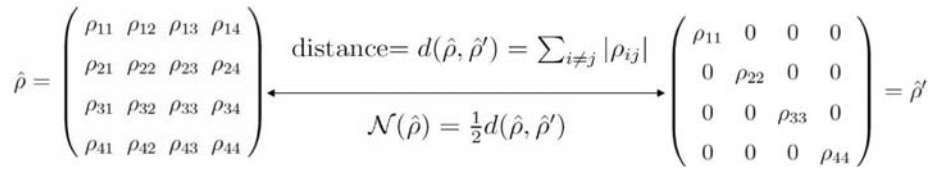

FIG. 1. The negativity of a SC state $\hat{\rho}$ equals half the sum of the absolute values of the off-diagonal elements of the density matrix, which is a distance of the state state from the separable state $\hat{\rho}'$.

$$\hat{\rho}^{PT}|\psi_{kl}\rangle_{\pm}=\sum_{mn}\rho_{mn}|n\rangle\langle m|\otimes|m\rangle\langle n|(-\rho_{lk}|k\rangle|l\rangle\pm|\rho_{kl}||l\rangle|k\rangle)=$$
$$-\sum_{mn}\rho_{mn}\rho_{lk}\delta_{mk}\delta_{nl}|n\rangle|m\rangle\pm\sum_{mn}\rho_{mn}|\rho_{kl}|\delta_{ml}\delta_{kn}|n\rangle|m\rangle$$
$$=-\rho_{kl}\rho_{lk}|l\rangle|k\rangle\pm\rho_{lk}|\rho_{kl}||k\rangle|l\rangle=-|\rho_{lk}|^2|l\rangle|k\rangle\pm\rho_{lk}|\rho_{kl}|$$
$$\times|k\rangle|l\rangle=\mp|\rho_{kl}|(-\rho_{lk}|k\rangle|l\rangle\pm|\rho_{kl}||l\rangle|k\rangle)=\mp|\rho_{kl}|$$
$$\times|\psi_{kl}\rangle_{\pm}. \quad (4)$$

Analogously we obtain

$$\hat{\rho}^{PT}|\psi_{kk}\rangle=|\rho_{kk}||\psi_{kk}\rangle. \quad (5)$$

Thus, the partially transposed matrix $\hat{\rho}^{PT}$ has been diagonalized and its $\frac{N(N-1)}{2}$ negative eigenvalues $-|\rho_{kl}|$, $k<l$ have been found, which completes the proof. ■

Corollary 1. Let a bipartite state $\hat{\rho}$ be SC. Then $\hat{\rho}$ is disentangled if and only if its negativity vanishes.

Proof. If $\hat{\rho}$ is disentangled its negativity $\mathcal{N}(\hat{\rho})$ vanishes by Peres-Horodeckii criterion [14,15]. If $\mathcal{N}(\hat{\rho})=0$ then by theorem 1 $\hat{\rho}$ is separable. ■

The following two corollaries of theorem 1 permit an estimation of entanglement of a SC state by simply "looking at" the occupied entries of the corresponding density matrix.

Corollary 2. The negativity of the SC (with respect to Schmidt bases $\Gamma_{1,2}$) state $\hat{\rho}$ equals half the sum of the off-diagonal elements of the corresponding density matrix in the Schmidt basis: $\mathcal{N}(\hat{\rho})=\frac{1}{2}\Sigma_{i\neq j}|\rho_{ij}|$, $i,j\in\Gamma_1\otimes\Gamma_2$.

Corollary 3. Let a SC state $\hat{\rho}$ be quasidiagonal, i.e., $\hat{\rho}=\Sigma_{mn}\rho_{mn}|n\rangle\langle m|\otimes|n\rangle\langle m|$, where $m,n=1,2,\ldots,N$ and $|m-n|=\Delta<N-1$. Then $\mathcal{N}(\hat{\rho})<\Delta$.

Proof. By corollary 2 it suffices to show that $\frac{1}{2}\Sigma_{m\neq n}|\rho_{mn}|<\Delta$. The sum of the absolute values of the off-diagonal elements can be estimated as follows:

$$\sum_{m\neq n}|\rho_{mn}|=\sum_{mn}|\rho_{mn}|-1=\sum_{m}\sum_{n=m-\Delta}^{n=m+\Delta}|\rho_{mn}|-1$$
$$<\sum_{m}\sum_{n=m-\Delta}^{n=m+\Delta}\sqrt{\rho_{mm}\rho_{nn}}\leqslant\sum_{m}\sum_{n=m-\Delta}^{n=m+\Delta}\frac{\rho_{mm}+\rho_{nn}}{2}$$
$$=\frac{1}{2}\sum_{m}\sum_{n=m-\Delta}^{n=m+\Delta}\rho_{mm}+\frac{1}{2}\sum_{m}\sum_{n=m-\Delta}^{n=m+\Delta}\rho_{nn}<2\Delta, \quad (6)$$

where the first inequality follows from the positivity of the density operator and the second is the inequality of geometric and arithmetic means. This concludes the proof. ■

The SC correlated states naturally emerge in certain quantum dynamical settings (see Ref. [12]). Assume a (generally non unitary) evolution of a bipartite composite system admitting an additive integral of motion $\hat{A}=\hat{A}_1\otimes\hat{I}_2+\hat{I}_1\otimes\hat{A}_2$, where $\hat{A}_{1,2}$ are local observables, i.e.,

$$\frac{\partial}{\partial t}\hat{\rho}=\mathcal{L}\hat{\rho} \quad (7)$$

and

$$\frac{d}{dt}\hat{A}=\mathcal{L}^{\dagger}\hat{A}=0. \quad (8)$$

Consider local bases of eigenstates of operators $\hat{A}_1$ and $\hat{A}_2$:

$$\Gamma_i=\{|m\rangle_i m=1,2,\ldots,N_i,\hat{A}_i|m\rangle_i=\lambda_m^i|m\rangle_i\},\quad i=1,2. \quad (9)$$

We denote as $\mathcal{H}^{\lambda}$ a subspace of the composite system Hilbert space $\mathcal{H}$ spanned by the eigenstates of $\hat{A}$, corresponding to an eigenvalue λ:

$$\mathcal{H}^{\lambda}=\mathrm{Sp}\{|m\rangle_1\otimes|n\rangle_2,\lambda_m^1+\lambda_n^2=\lambda\}. \quad (10)$$

Let us assume that the spectra of $\hat{A}_i$, $i=1,2$ are non degenerate, i.e., $\lambda_m^i=\lambda_n^i\Rightarrow m=n$. Then the equation $\lambda_m^1+\lambda_n^2=\lambda$ with fixed m and λ possesses a unique solution for n: $n=f^{\lambda}(m)$. Therefore the map $f^{\lambda}:\Gamma_1\to\Gamma_2$ provides a one-to-one correspondence between a state $|m\rangle_1\in\Gamma_1$ and a state $|n\rangle_2\in\Gamma_2$, i.e., it defines a unique common set of Schmidt bases for the Schmidt decomposition of all $|\psi^{\lambda}\rangle\in\mathcal{H}^{\lambda}$:

$$|\psi^{\lambda}\rangle=\sum_{\lambda_m^1+\lambda_n^2=\lambda}c_m|m\rangle_1|n\rangle_2. \quad (11)$$

Since all pure states $|\psi^{\lambda}\rangle\in\mathcal{H}^{\lambda}$ share the same Schmidt bases their mixture is a SC state.

If the initial state of the composite system is a mixture of eigenstates of $\hat{A}$, corresponding to the same eigenvalue λ, i.e., $\hat{\rho}(0)=\Sigma_i p_i|\psi_i^{\lambda}\rangle\langle\psi_i^{\lambda}|$ with $|\psi_i^{\lambda}\rangle\in\mathcal{H}^{\lambda}$ then the conservation of $\hat{A}$ would imply that $\hat{\rho}(t)=\Sigma_i p_i(t)|\psi_i(t)\rangle\langle\psi_i(t)|$, $|\psi(t)\rangle_i\in\mathcal{H}^{\lambda}$ at any $t>0$. Therefore, the evolving state $\hat{\rho}(t)$ remains SC and the negativity of the state can be calculated using theorem 1.

For illustration, the evolution of negativity of a composite state of a two noninteracting quantum systems coupled to a local purely dephasing baths is calculated. The composite system evolves according to the Liouville equation

$$\frac{\partial}{\partial t}\hat{\rho}=-[\hat{A}_1,[\hat{A}_1,\hat{\rho}]]-[\hat{A}_2,[\hat{A}_2,\hat{\rho}]]. \quad (12)$$

The local bases of eigenstates of operators $\hat{A}_1$ and $\hat{A}_2$ is $\Gamma_i=\{|m\rangle_i,m=1,2,\ldots,N_i,\hat{A}_i|m\rangle_i=\lambda_m^i|m\rangle_i\}$, $i=1,2$. The initial state of the composite system is a pure entangled state

$$|\psi(0)\rangle = \sum_m c_m |m\rangle_1 |m\rangle_2. \tag{13}$$

At $t>0$ the solution of Eq. (12) with initial state (13) is given by

$$\hat{\rho}(t) = \sum_{m,n} c_m c_n^* e^{-[(\lambda_m^1 - \lambda_n^1)^2 + (\lambda_m^2 - \lambda_n^2)^2]t} |m\rangle_1 |m\rangle_2 \langle n|_1 \langle n|_2. \tag{14}$$

Since $\hat{\rho}(t)$ is a SC state the theorem 1 applies and

$$\mathcal{N}(\hat{\rho}(t)) = \frac{1}{2} d(\hat{\rho}(t), \hat{\rho}'(t)) = \frac{1}{2}\left(\sum_{i,j \in \Gamma_1 \otimes \Gamma_2} |(\hat{\rho}^\lambda)_{i,j}| - 1 \right)$$

$$= \frac{1}{2}\left(\sum_{m,n} c_m c_n^* e^{-[(\lambda_m^1 - \lambda_n^1)^2 + (\lambda_m^2 - \lambda_n^2)^2]t} - 1 \right). \tag{15}$$

As a next step, the initial state for the evolution (7) is generalized from a state $\hat{\rho}(0) = \Sigma_i p_i |\psi_i^\lambda\rangle\langle\psi_i^\lambda|$ with $|\psi_i^\lambda\rangle \in \mathcal{H}^\lambda$ to a mixture of such states, corresponding to different eigenvalues λ of the conserved operator $\hat{A}$:

$$\hat{\rho}(0) = \sum_\lambda p_\lambda \hat{\rho}^\lambda, \tag{16}$$

where $\hat{\rho}^\lambda = \Sigma_i p_i^\lambda |\psi_i^\lambda\rangle\langle\psi_i^\lambda|$ with $|\psi_i^\lambda\rangle \in \mathcal{H}^\lambda$. By conservation of $\hat{A}$ we have $\hat{\rho}(t) = \Sigma_\lambda p_\lambda(t) \hat{\rho}^\lambda(t)$. An estimation of the negativity of $\hat{\rho}(t)$ is possible using a generalization of the theorem 1 (see theorem 2 below). The result is

$$\mathcal{N}(\hat{\rho}(t)) \leqslant \frac{1}{2} d(\hat{\rho}(t), \hat{\rho}'(t)), \tag{17}$$

where $(\hat{\rho}'(t))_{ij} = \delta_{ij}(\hat{\rho}(t))_{ij}$, $i,j \in \Gamma_1 \otimes \Gamma_2$ [see Eq. (9)] and the distance $d(\hat{x}, \hat{y}) = \|\hat{x} - \hat{y}\|_\alpha$ is induced by the norm $\|\hat{x}\|_\alpha = \Sigma_{i,j} |(\hat{x})_{i,j}|$.

Theorem 2 generalizes theorem 1 to particular *mixtures* of SC states. Consider a composite Hilbert space $\mathcal{H} = \mathcal{H}_1 \otimes \mathcal{H}_2$ of bipartite quantum system. Let $\Gamma_1 = \{|m\rangle_1, m = 1, 2, \ldots, N_1\}$ be an orthonormal basis of the local Hilbert space $\mathcal{H}_1$ and $\Gamma_2 = \{|m\rangle_2, m = 1, 2, \ldots, N_2\}$ be an orthonormal basis of the local Hilbert space $\mathcal{H}_2$. Consider a one-to-one correspondence f^λ between a subset $S_1^\lambda \subset \Gamma_1$ and a subset $S_2^\lambda \subset \Gamma_2$. The map f^λ defines a subspace $\mathcal{H}^\lambda \subset \mathcal{H}$ spanned by the states of the form $|m\rangle_1 \otimes |f^\lambda(m)\rangle_2$:

$$\mathcal{H}^\lambda = \mathrm{Sp}\{|m\rangle_1 \otimes |f^\lambda(m)\rangle_2, |m\rangle_1 \in S_1^\lambda\}. \tag{18}$$

All pure states $|\psi^\lambda\rangle \in \mathcal{H}^\lambda$ share the same Schmidt bases by construction. Therefore, a mixture $\hat{\rho}^\lambda = \Sigma_i p_i |\psi_i^\lambda\rangle\langle\psi_i^\lambda|$ is a SC state by definition and will be called λ-*SC state* for brevity in what follows.

Consider a family of such maps f^λ, indexed by λ, with the following property:

$$f^{\lambda_1}(|m\rangle_1) = f^{\lambda_2}(|m\rangle_1) \Leftrightarrow \lambda_1 = \lambda_2. \tag{19}$$

Then the following result can be proven.

Theorem 2. Let a bipartite state $\hat{\rho}$ be a mixture of λ-SC states: $\hat{\rho} = \Sigma_\lambda p_\lambda \hat{\rho}^\lambda$ with respect to local bases $\Gamma_{1,2}$ and a family of injective maps f^λ: $S_1^\lambda \subset \Gamma_1 \to \Gamma_2$ with the property (19). Then the negativity of the state $\hat{\rho}$ is less or equals a distance of $\hat{\rho}$ from a separable state $\hat{\rho}$ diagonal in the basis $\Gamma = \Gamma_1 \otimes \Gamma_2$: $\mathcal{N}(\hat{\rho}) \leqslant \frac{1}{2} d(\hat{\rho}, \hat{\rho})$, where $(\hat{\rho})_{ij} = \delta_{ij}(\hat{\rho})_{ij}$, $i,j \in \Gamma$ and the distance $d(\hat{x}, \hat{y}) = \|\hat{x} - \hat{y}\|_\alpha$, where $\|\hat{x}\|_\alpha = \Sigma_{i,j} |(\hat{x})_{i,j}|$.

Proof. Since the negativity is entanglement monotone [13] the following holds:

$$\mathcal{N}\left(\sum_\lambda p_\lambda \hat{\rho}^\lambda \right) \leqslant \sum_\lambda p_\lambda \mathcal{N}(\hat{\rho}^\lambda). \tag{20}$$

By theorem 1:

$$\sum_\lambda p_\lambda \mathcal{N}(\hat{\rho}^\lambda) = \sum_\lambda p_\lambda \frac{1}{2} d(\hat{\rho}^\lambda, \hat{\rho}'^\lambda) = \sum_\lambda p_\lambda \frac{1}{2} \|\hat{\rho}^\lambda - \hat{\rho}'^\lambda\|_\alpha$$

$$= \sum_\lambda p_\lambda \frac{1}{2} \sum_{i,j \in \Gamma} |(\hat{\rho}^\lambda - \hat{\rho}'^\lambda)_{i,j}|$$

$$= \sum_\lambda p_\lambda \frac{1}{2}\left(\sum_{i,j \in \Gamma} |(\hat{\rho}^\lambda)_{i,j}| - 1 \right)$$

$$= \frac{1}{2}\left(\sum_\lambda p_\lambda \sum_{i,j \in \Gamma} |(\hat{\rho}^\lambda)_{i,j}| - 1 \right). \tag{21}$$

From the property (19) it follows that

$$\sum_\lambda p_\lambda \sum_{i,j \in \Gamma} |(\hat{\rho}^\lambda)_{i,j}| = \sum_{i,j \in \Gamma} \left| \left(\sum_\lambda p_\lambda \hat{\rho}^\lambda \right)_{i,j} \right| = \sum_{i,j \in \Gamma} |(\hat{\rho})_{i,j}|. \tag{22}$$

Combining Eqs. (21) and (22) we get

$$\sum_\lambda p_\lambda \mathcal{N}(\hat{\rho}^\lambda) = \frac{1}{2}\left(\sum_\lambda p_\lambda \sum_{i,j \in \Gamma} |(\hat{\rho}^\lambda)_{i,j}| - 1 \right) = \frac{1}{2}\left(\sum_{i,j \in \Gamma} |(\hat{\rho})_{i,j}| - 1 \right)$$

$$= \frac{1}{2} d(\hat{\rho}, \hat{\rho}'). \tag{23}$$

From inequality (20) and Eq. (23) it follows that

$$\mathcal{N}(\hat{\rho}) \leqslant \frac{1}{2} d(\hat{\rho}, \hat{\rho}'). \tag{24}$$

■

Corollaries 1–3 of the theorem 1 can be generalized accordingly. As a simple example of a mixture of λ-SC states with respect to a family f^λ with the property (19), consider a mixture of pure states $|\psi_1\rangle = c_1^1 |11\rangle + c_2^1 |00\rangle$ and $|\psi_2\rangle = c_1^2 |10\rangle + c_2^2 |01\rangle$. The states $|\psi_1\rangle\langle\psi_1|$ and $|\psi_2\rangle\langle\psi_2|$ are λ-SC, $\lambda = 1, 2$, with respect to the family of maps $f^1 = \{|0\rangle \to |0\rangle, |1\rangle \to |1\rangle\}$ and $f^2 = \{|0\rangle \to |1\rangle, |1\rangle \to |0\rangle\}$. Note, that such mixture is generally not a SC state [8]. On the other hand, a mixture of pure states $|\psi_1\rangle = c_1^1 |11\rangle + c_2^1 |00\rangle$ and $|\psi_2\rangle = c_1^2 |++\rangle + c_2^2 |--\rangle$ (where $|\pm\rangle \equiv \frac{|0\rangle \pm |1\rangle}{\sqrt{2}}$) is generally neither SC nor a mixture of λ-SC states.

In conclusion, the negativity of a SC state can be interpreted geometrically as a distance in a particular metric d of the state from a separable state. An immediate consequence of this fact is that the negativity vanishes if and only if the SC state is separable, which implies that the Peres-Horodecki criterion of separability is both necessary and sufficient for SC states. The metric d that is induced by the α matrix norm,

is basis dependent, i.e., is not invariant under unitary transformations (and, in particular, is not invariant under local unitary transformations). Nevertheless, the basis in which the correspondence of this distance to the negativity is established is the Schmidt basis, which is a preferred basis for representing SC states [21].

In a SC state the negativity equals half the sum of the absolute values of the off-diagonal elements of the density matrix in the Schmidt bases. This finding suggests the "at a glance" estimation of the entanglement of SC states: the state is "substantially" entangled if and only if the off-diagonal entries in the corresponding density matrix are "substantially" populated. In particular, if the corresponding density matrix is quasidiagonal, i.e., the off-diagonal elements populate the strip about the diagonal of width Δ, the negativity is bounded by Δ.

We have considered Schmidt-correlated states and particular mixtures of Schmidt-correlated states. These states emerge in dynamical models with conservation laws. Dynamics where the conservation laws are relaxed generate mixed states that are not SC. Simulations of open-system dynamics, similar to those in Ref. [12], have suggested a generalization of the geometrical interpretation of negativity to arbitrary mixed states. It is conjectured that the negativity of an arbitrary mixed state is bounded by half the minimal distance d of the state to a corresponding separable state, where the distance is minimized over all possible local bases:

$$\mathcal{N}(\hat{\rho}) \leqslant \frac{1}{2} \min_{\Gamma_1 \otimes \Gamma_2} \left\{ d(\hat{\rho}, \hat{\rho}') \equiv \sum_{|i\rangle, |j\rangle \in \Gamma_1 \otimes \Gamma_2} |(\hat{\rho} - \hat{\rho}')_{ij}|, (\hat{\rho}')_{ij} = \delta_{ij} (\hat{\rho})_{ij} \right\}. \tag{25}$$

An interesting question is whether this minimal distance itself is an entanglement monotone [20]. Since $\Sigma_{ij} |(\hat{\rho} - \hat{\rho}')_{ij}| = 2\Sigma_{i<j} |\rho_{ij}|$ the conjecture (25) implies that the negativity of an arbitrary state is bounded by half the sum of the off-diagonal elements of the corresponding density matrix in *any local bases*, which gives an intuitive appraisal of the negativity (and entanglement) of an arbitrary mixed state.

This work was supported by the Binational U.S.-Israel Science Foundation (BSF).

[1] M. A. Nielsen and I. L. Chuang, *Quantum Computation and Quantum Information* (Cambridge University Press, Cambridge, 2000).
[2] E. Schmidt, Math. Ann. **63**, 433 (1906).
[3] A. Peres, *Quantum Theory: Concepts and Methods* (Kluwer, Boston, 1998).
[4] M. Plenio and S. Virmani, Quantum Inf. Comput. **7**, 1 (2007).
[5] K. G. H. Vollbrecht and R. F. Werner, Phys. Rev. A **64**, 062307 (2001).
[6] E. M. Rains, Phys. Rev. A **60**, 179 (1999).
[7] E. M. Rains, Phys. Rev. A **63**, 019902(E) (2000).
[8] S. Virmani, M. F. Sacchi, M. B. Plenio, and D. Markham, Phys. Lett. A **288**, 62 (2001).
[9] C. H. Bennett, D. P. DiVincenzo, J. A. Smolin, and W. K. Wootters, Phys. Rev. A **54**, 3824 (1996).
[10] V. Vedral, M. B. Plenio, M. A. Rippin, and P. L. Knight, Phys. Rev. Lett. **78**, 2275 (1997).
[11] T. Hiroshima and M. Hayashi, Phys. Rev. A **70**, 030302(R) (2004).
[12] M. Khasin and R. Kosloff, e-print arXiv:quant-ph/0605140.
[13] G. Vidal and R. F. Werner, Phys. Rev. A **65**, 032314 (2002).
[14] A. Peres, Phys. Rev. Lett. **77**, 1413 (1996).
[15] M. Horodecki, P. Horodecki, and R. Horodecki, Phys. Lett. A **223**, 1 (1996).
[16] R. F. Werner, Phys. Rev. A **40**, 4277 (1989).
[17] R. Bellman, *Introduction to Matrix Analysis*, 2d ed. (McGraw-Hill, New York, 1970).
[18] V. Vedral and M. B. Plenio, Phys. Rev. A **57**, 1619 (1998).
[19] L. Henderson and V. Vedral, Phys. Rev. Lett. **84**, 2263 (2000).
[20] M. Khasin, R. Kosloff, and D. Steinitz (unpublished).
[21] It should be noted that finding common Schmidt bases of SC states is a difficult problem in itself, which has been addressed in Ref. [8] in the case of a mixture of two pure states.

Chapter 4

Efficient simulation of strongly quantum-correlated dynamics

4.1 Introduction

In Chapters 2 and 3 we discussed two routes to a quantum system dynamics with vanishing or restricted quantum correlations: i) taking sufficiently mixed (hot) initial states (Chapter 2); ii) coupling a composite system to local environments (Chapter 3).

The present Chapter follows the route of Chapter 3 but in a more general mathematical framework. This framework is the theory of the generalized coherent states (GCS) (Zhang *et al.*, 1990; Perelomov, 1985), associated with a Lie-algebra of observables of a quantum system. In the general framework we obtain conditions on the Lie-algebra of observables, its Hilbert space representation and on the Hamiltonian of the system, necessary for efficient simulation of the observable quantum dynamics (Section 4.2). Moreover, the time-dependent basis of the GCS is shown to be a distinguished computational basis for simulation of the corresponding Lie-algebra of observables (Section 4.4).

4.1.1 The generalized coherent states as a computational tool

The concept of entanglement can be put into a general Lie-algebraic framework (Barnum *et al.*, 2003; Klyachko, quant-ph/0206012) as pointed out in Chapter 1. The starting point of the generalization is an understanding that entanglement is an observable-oriented concept. The same state of a quantum system is characterized by different magnitudes of entanglement with respect to different partitions. The second important observation is that unentangled pure states

of a composite system look pure from the restricted perspective of the local operators. The generalization of the concept of entanglement to the Lie-algebraic framework proceeds by defining the (generalized) unentangled states as states having maximal purity from the standpoint of a given Lie-algebra of observables.

This relative purity is termed the *generalized purity* of the state with respect to the given subalgebra of observables (Barnum *et al.*, 2003). It measures the generalized entanglement of the state and is shown to be intimately related to computational complexity of quantum dynamics (Sections 4.2−4.4).

In the case of compact semisimple Lie-algebras (Gilmore, 1974) of observables, which is important in finite-dimensional Hilbert spaces, the generalized unentangled states turn out (Barnum *et al.*, 2003) to be the GCS, associated with the Lie-algebra (see Section 4.2 for the detailed definition of the GCS). GCS with respect to the subalgebra of local operators are product states. Their exclusive role in simulating dynamics of local observables of composite quantum systems (Beck *et al.*, 2000) implies that GCS may be a distinguished computational basis in the general Lie-algebraic framework.

The status of GCS as a preferred computational basis for simulation of the corresponding Lie-algebra of observables can be established by a direct argument. In Section 4.4 it is shown that

- The spectrum-generating algebra (SGA)(Bohm *et al.*, 1988) of observables is a distinguished subset of observables for the purpose of efficient simulation of quantum dynamics.

- The associated GCS comprise preferred computational basis for the simulation of the SGA observables.

The dynamics of the SGA observables can be simulated efficiently only if the size of the GCS computational basis is sufficiently small. Generic Hamiltonian (nonlinear in the elements of the SGA) leads to an evolution, characterized by extensive generalized entanglement with respect to the SGA of the system. An extensive generalized entanglement corresponds to a large GCS basis, necessary to represent the evolving state. Therefore, new ideas must be introduced to simulate a generic quantum dynamics of a many-body system.

4.1.2 The idea of the method

The following idea is proposed to solve the problem of efficient simulation of a strongly generalized-entangled quantum evolution (Section 4.2). Since the original Hamiltonian generates extensive (generalized) entanglement by assumption, the original dynamics cannot be simulated efficiently. A different (surrogate) dynamics must be simulated. Three conditions must be satisfied:

- The surrogate dynamics can be simulated efficiently.

- The surrogate dynamics is equivalent to the original one modulo the expectation values of the distinguished subset of observables, i.e., the elements of the SGA.

- The initial state of the system can be simulated efficiently.

The results of Chapter 3 suggest the following choice of the surrogate dynamics. The surrogate dynamics is the open-system dynamics, resulting from the coupling of the system of interest to a special bath. The bath has the effect of weak measurement of the elements of the SGA.

In Section 4.2 it is shown that in a rigorously defined classical limit the open-system dynamics displays widely separated time-scales. The first time-scale is an observable time-scale on which the dynamics of the elements of the SGA are affected by the measurement. The other time-scale is the decoherence time-scale, on which the evolving state undergoes coarse-graining in the phase-space, associated with the SGA. The classical limit is the limit of a strong inequality (termed the *classicality condition* in Section 4.2) imposed on the SGA and its Hilbert space representation. The classicality condition is satisfied only in higher dimensional Hilbert space representations of the SGA, but the converse is generally not true. For example, the dynamics of the algebra of local operators does not have a classical limit (Section 4.2). As a consequence, the proposed method does not apply to simulation of local observables.

Due to the time-scales separation the SGA of observables can be negligibly effected on the physically relevant time-scale of their unitary evolution, while the coarse-graining in the phase-space is substantial. The evolving state of the open-system can be represented as a statistical mixture of pure-state quantum trajectories (unravelings), driven by the stochastic Nonlinear Schroedinger equation (sNLSE)(Gisin, 1984; Diosi, 1988b; Gisin & Percival, 1992). In the sNLSE picture the coarse-graining corresponds to localization of the pure-state solution in the phase-space (Section 4.3). The localization is measured by the generalized purity of the state with respect to the SGA. In Section 4.3 we prove that an arbitrary stochastic quantum trajectory, driven by the weak measurement of a compact semisimple algebra of observables, ends up in a GCS, associated with the algebra.

In the case of a compact semisimple SGA , it can be proved [1] that the generalized purity of a single pure-state unraveling of the open system tends to the generalized purity of a GCS in the classical limit. Therefore, the pure-state solutions of the sNLSE tend to GCS in the classical limit. As a consequence, the pure-state solution can be represented efficiently in the GCS basis, which is a necessary condition for efficient simulation.

For efficient dynamical simulation the initial state of the system must be simulated efficiently. As pointed out in Chapter 1 the initial state of a system in a pump-probe experiment is generally a thermal state. A thermal state can be viewed as a result of imaginary-time propagation of identity operator. Identity operator is a proper mixture of the GCS with respect to the SGA observables (Zhang *et al.*, 1990). Therefore, a thermal initial state can be simulated using our method. The argument can be generalized to an arbitrary initial state, which is canonical with respect to an appropriate Hamiltonian, i.e., which can be viewed as the result of the imaginary-time propagation, generated by an appropriate Hamiltonian. A detailed definition of an appropriate Hamiltonian for the application of our method is given in Section 4.4.2. It should be noted that a GCS is canonical with respect to the corresponding SGA of observables[2].

The expectation values of observables are obtained by averaging over the stochastic realizations of the sNLSE. The averaging introduces classical correlations into the dynamics. Quantum correlations are bounded by the generalized entanglement of the pure-state unraveling, which tends to zero in the classical limit. It follows that in the classical limit (generalized) classical correlations can simulate (generalized) quantum correlations modulo the expectation values of the SGA operators.

---

[1] The following proof is based on the results and uses the definitions of Section 4.2. Let P_0 and P denote the generalized purity of a GCS and of a pure-state solution ψ of the sNLSE, respectively. Let $\Delta_0 = C - P_0$ and $\Delta = C - P$ stand for the generalized uncertainty in a GCS and in the state ψ, respectively (C is the eigenvalue of the Casimir operator in the (irreducible) Hilbert space representation). P can be estimated from the condition that the decoherence time-scale and the time-scale of the generalized purity decay in the corresponding unitary evolution are equal. If $\Delta \gg \Delta_0$ $\gamma\Delta$ is the decoherence rate in the state ψ. The generalized purity decays on the time-scale of the SGA observables in the unitary evolution. Let the sNLSE correspond to the strength of measurement γ such that the evolution of the SGA observables is negligibly affected. Then $\gamma\Delta = O(\omega)$, where ω is the inverse time-scale of the unitary evolution of the SGA observables, which is independent on the Hilbert space representation (if the Hamiltonian is moderately nonlinear which is assumed). $\gamma\Delta \geq \gamma\Delta_0$. In the classical limit $\gamma\Delta_0 \to \infty \Rightarrow \gamma\Delta \to \infty$. Contradiction. Therefore, $\Delta = O(\Delta_0)$, i.e., $P = P_0 + O(\Delta_0)$. In the classical limit $C/\Delta_0 \to \infty \Rightarrow (P_0 + \Delta_0)/\Delta_0 \to \infty \Rightarrow P_0/\Delta_0 \to \infty \Rightarrow P/P_0 = (P_0 + O(\Delta_0))/P_0 \to 1$ □

[2] A GCS can be viewed as a ground state of a Hamiltonian linear in the elements of the SGA (Zhang *et al.*, 1990; Barnum *et al.*, 2003)

4.2 Efficient Simulation of Quantum Evolution using Dynamical Coarse-Graining

Efficient simulation of quantum evolution using dynamical coarse graining

M. Khasin and R. Kosloff
Fritz Haber Research Center for Molecular Dynamics, Hebrew University of Jerusalem, Jerusalem 91904, Israel
(Received 8 April 2008; published 11 July 2008)

A scheme to simulate the evolution of a restricted set of observables of a quantum system is proposed. The set comprises the spectrum-generating algebra of the Hamiltonian. Focusing on the simulation of the restricted set allows to drastically reduce the cost of the simulation. This reduction is the result of replacing the original unitary dynamics by a special open-system evolution. This open-system evolution can be interpreted as a process of weak measurement of the distinguished observables performed on the evolving system of interest. Under the condition that the observables are "classical" and the Hamiltonian is moderately nonlinear, the open-system dynamics displays a large time-scale separation between the relaxation of the observables and the decoherence of a generic state. This time-scale separation allows the unitary dynamics of the observables to be efficiently simulated by the open-system dynamics on the intermediate time scale. The simulation employs unraveling of the corresponding master equations into pure-state evolutions, governed by the stochastic nonlinear Schrödinger equation. The stochastic pure-state evolution can be simulated efficiently using a representation of the state in the time-dependent basis of the generalized coherent states, associated with the spectrum-generating algebra.

DOI: 10.1103/PhysRevA.78.012321 PACS number(s): 03.67.Lx, 03.67.Mn, 03.65.Ud

I. INTRODUCTION

The number of independent observables of a quantum system with the Hilbert space dimension N is N^2-1. In many-body systems, when N increases exponentially with the number of degrees of freedom, that large number of observables can be neither measured nor calculated. Only a limited number of dynamical variables is accessible to an experimentalist, while all the uncontrollable parameters are averaged out. This means that generically, an observed quantum system is characterized by a small number of the expectation values of accessible observables. To theoretically characterize the dynamics of a quantum system it is desirable (i) to find equations of motion for this reduced set of expectation values, (ii) to be able to solve the associated equations of motion efficiently.

In the context of the computational complexity theory the term "'efficient"' is reserved for a computation involving memory and CPU resources, scaling polynomially with the size of the problem. The term "efficient" is used in a different sense in the present paper. A computational cost of a direct quantum simulation scales as $O(N^{\delta})$, $\delta>1$ [1], with the Hilbert space dimension N. A simulation is defined as efficient for the purpose of the present discussion if its computational cost is substantially lower than that.

We explore the possibility of such efficient simulation of a restricted set of observables, using a paradigm for the simulation. Assuming that the set of experimentally accessible observables is small, it is plausible that there exist a number of microscopic theories, leading to the same observed dynamics. If a microscopic theory can be found, which leads to equations of motion that can be solved efficiently, the dynamics of the restricted set of observables can be efficiently simulated. More specifically, we propose to simulate the unitary dynamics of a quantum system by embedding it in a particular open-system dynamics. In this dynamics the coupling to the bath is constructed to have a negligible impact on the evolution of the selected set of observables on the characteristic time scale of their unitary evolution. The key point is that the resulting open-system dynamics can be simulated with much higher efficiency. The reduction of the computational complexity of the evolution, imposed by the bath, is attributed to dynamical coarse graining, collapsing the system to a preselected representation which is used as the basis for the dynamical description. Since the bath has no observable effect by construction it should be considered solely as a computational tool. For that reason a term fictitious bath is used in the paper to refer to it.

The quantum systems considered in the present work have finite Hilbert space dimension. The dynamics is generated by the Lie-algebraic Hamiltonians

$$\hat{\mathrm{H}} = \sum_i a_i \hat{\mathrm{X}}_i + \sum_{ij} b_{ij} \hat{\mathrm{X}}_i \hat{\mathrm{X}}_j + \cdots, \tag{1}$$

where the set $\{\hat{\mathrm{X}}_i\}$ of observables is closed under the commutation relations

$$[\hat{\mathrm{X}}_i, \hat{\mathrm{X}}_j] = i \sum_{k=1}^{K} f_{ijk} \hat{\mathrm{X}}_k, \tag{2}$$

i.e., it forms the spectrum-generating [2] Lie algebra [3] of the system. This algebra is labeled by the letter $\mathfrak{g}$ in what follows. Lie-algebraic Hamiltonians (1) are abundant in molecular [4,5], nuclear [2,5], and condensed matter physics [2]. The basis of the algebra $\{\hat{\mathrm{X}}_i\}$ is chosen as a distinguished set of observables, which are to be simulated efficiently. Lie algebras considered in the present work are compact semisimple algebras [3] and the basis $\{\hat{\mathrm{X}}_i\}$ is assumed to be orthonormal with respect to the Killing form [3].

The corresponding open-system dynamics, which is alleged to simulate the unitary dynamics of the elements of $\mathfrak{g}$, is governed by the following Liouville–von Neumann equation of motion:

$$\frac{\partial}{\partial t}\hat{\rho} = \mathcal{L}\hat{\rho} = -i[\hat{\mathrm{H}},\hat{\rho}] - \gamma\sum_{j=1}^{K}[\hat{\mathrm{X}}_j,[\hat{\mathrm{X}}_j,\hat{\rho}]], \tag{3}$$

which has the Lindblad form [6,7], i.e., it describes a Markovian completely positive [7] nonunitary evolution of the quantum system. The physical interpretation of the evolution, governed by Eq. (3) is the process of weak measurements [8] of the algebra of observables $\mathfrak{g}$, performed on the quantum system, evolving under the Hamiltonian (1).

The foundation of the method is the observation that coupling to the bath induces a decoherence of the evolving density operator in a particular basis known as generalized coherent states (GCS), associated with the algebra (Sec. II). It is shown that if the Hamiltonian is linear in $\hat{\mathrm{X}}_i$ and a certain "classicality condition" is satisfied by the Hilbert space representation of the algebra, the decoherence time scale is much shorter than the time scale on which the effect of the bath on the elements of $\mathfrak{g}$ is measurable, i.e., the relaxation time scale. It is argued that this strong time-scale separation will also hold for moderately nonlinear Hamiltonians (Sec. III). The claim is supported by an order of magnitude analysis.

We propose to take advantage of this property of the open-system dynamics for efficient simulation of the unitary evolution of $\{\hat{\mathrm{X}}_i\}$, using stochastic unraveling of the evolution [9–11] and representing the evolving stochastic pure state in the time-depending basis of the GCS [12,13] (Sec. IV). The effect of the decoherence translates into localization of evolving stochastic pure state in the GCS basis, which enables efficient representation and simulation of the stochastic evolution. Averaging over the unraveling recovers the *unitary* dynamics of the algebra generators. The effect of coupling to the fictitious bath is illustrated by the dynamics of a Bose-Einstein condensate (BEC) in a double-well trap [14,15] modeled by the two-mode Bose-Hubbard Hamiltonian (Sec. V). It is demonstrated that the bath induces drastic localization on the level of a stochastic pure-state evolution, while having no observed effect on the dynamics of the elements of the spectrum-generating algebra of the system.

II. EVOLUTION OF STATES

A central theme in this section is the intimate relation between the evolution of the subalgebra of observables and the dynamics of the generalized coherent states (GCS) associated with this subalgebra. The GCS minimize the total uncertainty with respect to the basis elements of the subalgebra and in addition are maximally robust to interaction with the bath, modeled by Eq. (3).

A. Generalized coherent states and the total uncertainty

Let us assume that the subalgebra $\mathfrak{g}$ is represented irreducibly on the system's Hilbert space $\mathcal{H}$. Then an arbitrary state $\psi \in \mathcal{H}$ can be represented as a superposition of the GCS [12,13] $|\Omega,\psi_0\rangle$ with respect to the corresponding dynamical group G and an arbitrary state ψ_0,

$$|\psi\rangle = \int d\mu(\Omega)|\Omega,\psi_0\rangle\langle\Omega,\psi_0|\psi\rangle, \tag{4}$$

where $\mu(\Omega)$ is the group-invariant measure on the coset space G/H [3], $\Omega \in G/H$, $H \subset G$ is the maximal stability subgroup of the reference state ψ_0,

$$h|\psi_0\rangle = e^{i\phi(h)}|\psi_0\rangle, \quad h \in H \tag{5}$$

and the GCS $|\Omega,\psi_0\rangle$ are defined as follows:

$$\hat{\mathrm{U}}(g)|\psi_0\rangle = \hat{\mathrm{U}}(\Omega h)|\psi_0\rangle = e^{i\phi(h)}\hat{\mathrm{U}}(\Omega)|\psi_0\rangle \equiv e^{i\phi(h)}|\Omega,\psi_0\rangle,$$

$$g \in G,\ h \in H,\ \Omega \in G/H, \tag{6}$$

where $\hat{\mathrm{U}}(g)$ is a unitary transformation generated by a group element $g \in G$.

The group-invariant total uncertainty of a state with respect to a compact semisimple algebra $\mathfrak{g}$ is defined as [12,16]

$$\Delta(\psi) \equiv \sum_{j=1}^{K}\langle\Delta\hat{\mathrm{X}}_j^2\rangle_\psi = \sum_{j=1}^{K}\langle\hat{\mathrm{X}}_j^2\rangle_\psi - \sum_{j=1}^{K}\langle\hat{\mathrm{X}}_j\rangle_\psi^2. \tag{7}$$

The first term on the right-hand-side of Eq. (7) is the eigenvalue of the Casimir operator of $\mathfrak{g}$ in the Hilbert space representation,

$$\hat{\mathrm{C}} = \sum_{j=1}^{K}\hat{\mathrm{X}}_j^2 \tag{8}$$

and the second term is termed the generalized purity [17] of the state with respect to $\mathfrak{g}$,

$$P_{\mathfrak{g}}[\psi] \equiv \sum_{j=1}^{K}\langle\hat{\mathrm{X}}_j\rangle_\psi^2. \tag{9}$$

We define $\Delta_{\min}$ as a minimal total uncertainty of a quantum state and $c_{\mathcal{H}}$ as the eigenvalue of the Casimir operator of $\mathfrak{g}$ in the system Hilbert space. Then

$$\Delta_{\min} \le \Delta(\psi) \le c_{\mathcal{H}}. \tag{10}$$

The total uncertainty (7) is invariant under an arbitrary unitary transformation generated by $\mathfrak{g}$. Therefore, all the GCS, associated with the subalgebra $\mathfrak{g}$ and a reference state ψ_0 have a fixed value of the total invariance. It has been proved in Ref. [16] that the minimal total uncertainty $\Delta_{\min}$ is obtained if and only if ψ_0 is a highest (or lowest) weight state of the representation (the Hilbert space). The value of $\Delta_{\min}$ is given by [16,18]

$$\Delta_{\min} \equiv (\Lambda,\mu) \le \Delta(\psi) \le (\Lambda,\Lambda+\mu) = c_{\mathcal{H}}, \tag{11}$$

where $\Lambda \in \mathbb{R}^r$ is the highest weight of the representation, $\mu \in \mathbb{R}^r$ is the sum of the positive roots of $\mathfrak{g}$, r is the rank of $\mathfrak{g}$ [3] and $(\cdots,\cdots)$ is the Euclidean scalar product in $\mathbb{R}^r$. The corresponding CGS were termed the generalized unentangled states with respect to the subalgebra $\mathfrak{g}$ [17,18]. The maximal value of the uncertainty is obtained in states termed maximally or completely entangled [17,18] with respect to $\mathfrak{g}$. The maximum value equals $c_{\mathcal{H}}$ in the states having $\langle\psi|\hat{\mathrm{X}}_j|\psi\rangle^2=0$ for all i. Such states exist in a generic irreduc-

ible representation of an arbitrary compact simple algebra of observables [18]. Generic superpositions of the GCS have larger uncertainty and are termed generalized entangled states with respect to $\mathfrak{g}$ [17,18]. In what follows, it is assumed that the reference state ψ_0 for the GCS minimize the total invariance (7).

B. Decoherence time scales

The rate of purity loss in an arbitrary pure state $\hat{\rho}=|\psi\rangle\langle\psi|$ can be calculated using Eq. (3) as follows [19]:

$$\begin{aligned}\frac{d}{dt}\mathrm{Tr}\{\hat{\rho}^2\}=\mathrm{Tr}\{2\dot{\hat{\rho}}\hat{\rho}\}&=2\ \mathrm{Tr}\left\{i[\hat{\mathrm{H}},\hat{\rho}]\hat{\rho}-\gamma\sum_{j=1}^{K}[\hat{\mathrm{X}}_j,[\hat{\mathrm{X}}_j,\hat{\rho}]]\hat{\rho}\right\}\\&=-2\gamma\,\mathrm{Tr}\left\{\sum_{j=1}^{K}[\hat{\mathrm{X}}_j,[\hat{\mathrm{X}}_j,\hat{\rho}]]\hat{\rho}\right\}\\&=-4\gamma\sum_{j=1}^{K}(\langle\psi|\hat{\mathrm{X}}_j^2|\psi\rangle-\langle\psi|\hat{\mathrm{X}}_j|\psi\rangle^2)\\&=-4\gamma\sum_{j=1}^{K}\langle\Delta\hat{\mathrm{X}}_j^2\rangle_\psi,\end{aligned}\tag{12}$$

i.e., the rate is proportional to the group-invariant uncertainty (7). From Eqs. (12) and (10) it follows that the time scale of the purity loss in a generic state is $(\gamma c_{\mathcal{H}})^{-1}$, where $c_{\mathcal{H}}$ is the eigenvalue of the Casimir, Eq. (8). On the contrary, the rate of purity loss of a GCS is determined by $\Delta_{\min}$, Eq. (11), which implies that GCS are robust against the influence of the bath [19].

Assume that

$$\Delta_{\min}\ll c_{\mathcal{H}}.\tag{13}$$

The strong inequality (13) can be interpreted as follows. Under the action of the bath, modeled by Eq. (3), a generic superposition of the GCS, Eq. (4), decoheres on the fast time scale $(\gamma c_{\mathcal{H}})^{-1}$ into a proper mixture of the GCS, which then follows the slow evolution on a time scale fixed by $\Delta_{\min}$. As a consequence, the effect of the bath is to "diagonalize" the evolving density operator into a time-dependent statistical mixture of the GCS.

Accordingly, $(\gamma c_{\mathcal{H}})^{-1}$ determines the decoherence time scale of the density operator in the basis of the GCS.

Condition (13) does not depend on the strength of coupling to the bath and therefore is a property of the subalgebra of observables and its Hilbert space representation. Condition (13) will be termed the *classicality condition* on the algebra of observables (see Appendix B for some examples).

III. EVOLUTION OF THE OBSERVABLES

Following the evolution of observables in the Heisenberg picture we can show that the classicality condition (13) implies a large time-scale separation between the decoherence of the state and the relaxation of the observables comprising the spectrum-generating algebra of the system. The relaxation rate is calculated for the case when the Hamiltonian (1) is linear in the algebra elements and the time-scale separation is demonstrated. An order of magnitude considerations imply that the time-scale separation still persists for moderately nonlinear Hamiltonians. It follows, that the unitary evolution of the observables in the intermediate time scale can be simulated by the open-system dynamics. Then, the decoherence can be employed to increase the simulation efficiency.

Consider a Hamiltonian linear in the elements of the algebra $\mathfrak{g}$, i.e., all $b_{ij}=0$ in Eq. (1). The corresponding Heisenberg equations for the observables in $\mathfrak{g}$ becomes

$$\begin{aligned}\frac{\partial}{\partial t}\hat{\mathrm{X}}_i&=-i[\hat{\mathrm{H}},\hat{\mathrm{X}}_i]-\gamma\sum_{j=1}^{K}[\hat{\mathrm{X}}_j,[\hat{\mathrm{X}}_j,\hat{\mathrm{X}}_i]]\\&=-i\sum_{k=1}^{K}(ia_{ik})\hat{\mathrm{X}}_k-\gamma\sum_{j,l=1}^{K}(if_{jik})(if_{jkl})\hat{\mathrm{X}}_l\\&=-i\sum_{k=1}^{K}(ia_{ik})\hat{\mathrm{X}}_k-\gamma\sum_{j,l=1}^{K}(T^j)_{il}^2\hat{\mathrm{X}}_l,\end{aligned}\tag{14}$$

where $T_{jk}^i=if_{ijk}$ is a matrix element of the adjoint representation [3] of $\hat{\mathrm{X}}_i$. It is assumed without loss of generality that $\mathfrak{g}$ is a compact simple subalgebra of observables [in the general case of a semisimple algebra, the system of Eq. (14) decouples into systems of equations for the simple components of the algebra]. The coefficients on the right-hand side of (14) obey

$$\sum_{j=1}^{K}(T^j)^2=C_2,\tag{15}$$

where C_2 is the quadratic Casimir of $\mathfrak{g}$ in the adjoint representation. Therefore,

$$\left(\sum_{j=1}^{K}(T^j)^2\right)_{il}=(C_2)_{il}=c_{\mathrm{adj}}\delta_{il}\tag{16}$$

leading to

$$\frac{\partial}{\partial t}\hat{\mathrm{X}}_i=-i\sum_{k=1}^{K}(ia_{ik})\hat{\mathrm{X}}_k-\gamma c_{\mathrm{adj}}\hat{\mathrm{X}}_i,\tag{17}$$

which in a matrix notation reads as

$$\frac{\partial}{\partial t}\hat{\mathrm{X}}=-i(A-\gamma c_{\mathrm{adj}})\hat{\mathrm{X}},\tag{18}$$

where $A=A^\dagger$ is defined by $A_{kl}=ia_{kl}$ and $\hat{\mathrm{X}}\equiv\{\hat{\mathrm{X}}_1,\hat{\mathrm{X}}_2,\ldots,\hat{\mathrm{X}}_k\}$. We define $\hat{\mathrm{Y}}\equiv\{\hat{\mathrm{Y}}_1,\hat{\mathrm{Y}}_2,\ldots,\hat{\mathrm{Y}}_k\}$ by

$$\frac{\partial}{\partial t}\hat{\mathrm{Y}}_i=-iA\hat{\mathrm{Y}}_i=-i\omega_i\hat{\mathrm{Y}}_i,\tag{19}$$

where ω_i are real since A is Hermitian. Then $\hat{\mathrm{Y}}$ diagonalize also Eq. (18),

$$\frac{\partial}{\partial t}\hat{\mathrm{Y}}_i=(-iA-\gamma c_{\mathrm{adj}})\hat{\mathrm{Y}}_i=(-i\omega_i-\gamma c_{\mathrm{adj}})\hat{\mathrm{Y}}_i,\tag{20}$$

leading to the solution of Eq. (18),

$$\hat{\mathrm{Y}}_i(t) = \hat{\mathrm{Y}}_i(0)e^{-(i\omega_i+\gamma c_{\mathrm{adj}})t} \tag{21}$$

and

$$\hat{\mathrm{X}}_i(t) = \sum_j c_{ij}\hat{\mathrm{Y}}_i(t). \tag{22}$$

The solution (21) is obtained for an arbitrary compact simple subalgebra of the system observables $\mathfrak{g} \cong \mathrm{su}(K) \subseteq \mathrm{su}(N)$ for a quantum system in a N-dimensional Hilbert space. It can be generalized to a semisimple subalgebra of observables, i.e., a direct sum of simple subalgebras, $\mathfrak{g} = \oplus_{i=1}^{n} \mathrm{su}(K_i) \subseteq \mathrm{su}(N)$, corresponding to a tensor-product partition of the system Hilbert space $\mathcal{H} = \otimes_{i=1}^{n} \mathcal{H}_i$. In this case, Eq. (21) corresponds to local observables of any given subsystem.

The dynamics displayed by Eq. (21) shows that the expectation values of observables in $\mathfrak{g}$ oscillate on the time scales ω_i and decay on the time scale γc_{adj}. Consider an observable $\hat{\mathrm{Y}}_i$ such that $\omega_i \gg \gamma c_{\mathrm{adj}}$. When the measurement of $\hat{\mathrm{Y}}_i$ in a time interval

$$(\omega_i)^{-1} \ll \tau \ll (\gamma c_{\mathrm{adj}})^{-1} \tag{23}$$

is performed, the nonunitary character of the evolution cannot be discovered. Therefore, given the time interval τ any γ with the property $\tau \ll (\gamma c_{\mathrm{adj}})^{-1}$ will lead to apparently unitary dynamics of $\hat{\mathrm{Y}}_i$ on the time interval τ.

Next we note that since $(\Lambda, \mu) \neq 0$ in Eq. (11) (a positive root has strictly positive scalar product with the maximal weight vector) strong inequality (13) implies $|\Lambda| \gg |\mu|$, which leads to the following strong inequality:

$$\sqrt{c_{\mathcal{H}}} \gg \sqrt{c_{\mathrm{adj}}}. \tag{24}$$

Therefore, a time interval τ exists such that

$$(\gamma c_{\mathcal{H}})^{-1} \ll \omega_i^{-1} \ll \tau \ll (\gamma c_{\mathrm{adj}})^{-1} \tag{25}$$

for some i corresponding to an observable $\hat{\mathrm{Y}}_i$ in Eq. (21). The term $(\gamma c_{\mathcal{H}})^{-1}$ on the left-hand side of the inequality (25) is the decoherence rate of a generic superposition of the GCS, associated with the algebra $\mathfrak{g}$ and the term $(\gamma c_{\mathrm{adj}})^{-1}$ on the right-hand side is the relaxation rate of the observable $\hat{\mathrm{Y}}_i$. This system of strong inequalities implies two important properties of the open-system dynamics, Eq. (14): (i) A generic superposition of the GCS collapses into a mixture of the GCS on a time scale much shorter than a physically interesting time scale of the unitary evolution of the observable; (ii) the time scale of the unitary evolution of the observable is much shorter than its relaxation time scale.

If the Hamiltonian is nonlinear in the spectrum-generating algebra elements this simple analysis can no longer be made. Nonetheless, it is argued that that if the Hamiltonian is only moderately nonlinear, the time-scale separation between the decoherence and the relaxation still holds. The order of magnitude argument is based on considering a nonlinear Hamiltonian of the following form:

$$\hat{\mathrm{H}} = \sum_{i_1} a_{i_1}^{(1)}\hat{\mathrm{X}}_{i_1} + \sum_{i_1 i_2} a_{i_1 i_2}^{(2)}\hat{\mathrm{X}}_{i_1}\hat{\mathrm{X}}_{i_2} + \cdots + \sum_{i_1 \ldots i_m} a_{i_1 \cdots i_m}^{(m)}\hat{\mathrm{X}}_{i_1}\cdots\overset{\cdots}{\mathrm{X}}_{i_m}, \tag{26}$$

i.e., a polynomial of order m in the algebra of elements, where m is independent on the Hilbert space representation of the algebra. The Hamiltonian is defined to be *moderately nonlinear* if $|a_{i_1 \cdots i_k}^{(k)}| = \omega O(1/|\Lambda|^{k-1})$, $1 \leq k \leq m$, where $|\Lambda|$ is the norm of the maximal weight of the representation, and ω^{-1} is an arbitrary reference time scale. The moderate nonlinearity implies that the dynamical time scales ω_i^{-1} of an element of the algebra are of the order of unity with respect to $|\Lambda|$. In fact,

$$\begin{aligned}\omega_i &= |\Lambda|^{-1} O\left(\left\langle \frac{\partial}{\partial t}\hat{\mathrm{X}}_i \right\rangle\right) \\ &= |\Lambda|^{-1} O(-i\langle[\hat{\mathrm{H}}, \hat{\mathrm{X}}_i]\rangle) \\ &= |\Lambda|^{-1} O\left(\sum_{k=1}^{m} \sum_{i_1 \cdots i_k} k b_{i_1 \cdots i_k}^{(k)} \langle \hat{\mathrm{X}}_{i_1} \cdots \hat{\mathrm{X}}_{i_k} \rangle\right),\end{aligned} \tag{27}$$

where $|b_{i_1 \ldots i_k}^{(k)}| = \omega O(1/|\Lambda|^{k-1})$ and $|\langle \overset{\cdots}{\mathrm{X}}_{i_1} \cdots \hat{\mathrm{X}}_{i_k} \rangle| = O(\Lambda^k)$. Therefore,

$$\omega_i = |\Lambda|^{-1} O\left(\sum_{k=1}^{m} \sum_{i_1 \ldots i_k} k b_{i_1 \ldots i_k}^{(k)} |\Lambda|^k\right) = \omega O(1), \tag{28}$$

since m is assumed to be independent on the representation, i.e., $m = O(1)$. The time scales $\omega_i'^{-1}$ of the element of the algebra in the open-system evolution follows from the calculations leading to Eq. (17) and the fact that $c_{\mathrm{adj}} = O(1)$, satisfy

$$\omega_i' = \omega O(1) + \gamma O(1) = \omega O(1) \tag{29}$$

as well, for $\gamma \lesssim \omega$.

Let us assume that ω_i' is analytic in γ. Then to the first order in γ,

$$\omega_i' = \omega_i + \omega_i^{(1)}\gamma. \tag{30}$$

Since Eq. (29) holds for any fixed $\gamma \lesssim \omega$, it follows that $\omega_i^{(1)} = \omega O(1)$. The rate $\gamma\omega_i^{(1)} = \gamma O(1)$ is the relaxation rate of the algebra element $\hat{\mathrm{X}}_i$. The decoherence rate of the state is $\gamma c_{\mathcal{H}} = \gamma O(|\Lambda|^2)$. Therefore, for sufficiently large $|\Lambda|$ or, equivalently, for sufficiently strong "classicality" (13), a time interval τ exists such that

$$O((\gamma|\Lambda|^2)^{-1}) = (\gamma c_{\mathcal{H}})^{-1} \ll \omega_i^{-1} \ll \tau \ll (\gamma\omega_i^{(1)})^{-1} = O(\gamma^{-1}), \tag{31}$$

i.e., the decoherence is substantial on the physically interesting time interval $\omega_i^{-1} \ll \tau$, while the relaxation of the observable is negligible. In the analysis above we did not keep track of the order m of the polynomial (26) since $m = O(1)$ by assumption. Equation (28) implies that the relaxation rates of observables increase with the growing order, therefore, a stronger "classicality" (larger $|\Lambda|$) is needed to satisfy the inequalities (31).

IV. EFFICIENT SIMULATION OF THE EVOLUTION OF THE SPECTRUM-GENERATING ALGEBRA OF OBSERVABLES

Efficient simulation is defined as a simulation based on a numerical solution of the first-order differential equations for a number of dynamical variables which is much smaller than the Hilbert space dimension of the system. As pointed out in the introduction, the term "efficient" does not imply a change in the complexity class, i.e., reduction to a computational problem belonging to a polynomial rather than exponential complexity class. "Efficient" in the present context means that the computation can be performed with a substantial speed-up over a "brute-force" simulation which scales as some power of the size of the Hilbert space.

The number of dynamical variables m cannot be smaller than the number of observables to be simulated, which equals the dimension K of the spectrum-generating algebra $\mathfrak{g}$. If there is a large gap between the dimension of the algebra and the Hilbert space dimension $K=\dim\{\mathfrak{g}\}\ll\dim\{\mathcal{H}\}=N$ the simulation based on the number of variables $K\lesssim m\ll N$ is considered efficient.

The proposed method of efficient simulation of the observables, forming the spectrum-generating algebra $\mathfrak{g}$ of the Hamiltonian (1) is based upon the following.

(i) Simulating the unitary evolution of the observables by the fictitious open-system dynamics, governed by the Liouville–von Neumann equation (3).

(ii) Unraveling the Liouville–von Neumann equation (3) into pure-state evolutions, governed by the stochastic nonlinear Schrödinger equation (sNLSE) (see below).

(iii) Efficient simulation of the stochastic nonlinear pure-state dynamics, using expansion of the state in a time-dependent basis of the GCS, associated with the spectrum-generating algebra $\mathfrak{g}$.

In the preceding section we have discussed the first of the listed items. The other two items focus on the principles of efficient simulation of the open-system evolution.

Solving directly the Liouville–von Neumann master equation (3) is more difficult than the original problem. A reduction in complexity is based on the equivalence between the Liouville–von Neumann equation and the sNLSE [9–11],

$$d|\psi\rangle=\{-i\hat{\mathrm{H}}dt-\gamma\sum_{i=1}^{K}(\hat{\mathrm{X}}_i-\langle\hat{\mathrm{X}}_i\rangle_\psi)^2dt+\sum_{i=1}^{K}(\hat{\mathrm{X}}_i-\langle\hat{\mathrm{X}}_i\rangle_\psi)d\xi_i\}|\psi\rangle, \tag{32}$$

where the Wiener fluctuation terms $d\xi_i$ satisfy

$$\langle d\xi_i\rangle=0,\quad d\xi_i d\xi_j=2\gamma dt. \tag{33}$$

To demonstrate the equivalence, Eq. (32) can be cast into the evolution of the projector $\hat{\mathrm{P}}_\psi=|\psi\rangle\langle\psi|$,

$$d\hat{\mathrm{P}}_\psi=\left(-i[\hat{\mathrm{H}},\hat{\mathrm{P}}_\psi]-\gamma\sum_{j=1}^{K}[\hat{\mathrm{X}}_j,[\hat{\mathrm{X}}_j,\hat{\mathrm{P}}_\psi]]\right)dt+\sum_i\{(\hat{\mathrm{X}}_i-\langle\hat{\mathrm{X}}_i\rangle_\psi)d\xi_i,\hat{\mathrm{P}}_\psi\}. \tag{34}$$

Averaging Eq. (34) over the noise recovers the original Liouville–von Neumann equation (3). Therefore, the problem of efficient simulation of the Liouville–von Neumann dynamics is transformed to the problem of efficient simulation of the nonlinear stochastic dynamics, governed by sNLSE (32).

The simulation of the pure-state evolution according to the sNLSE (32) is based on an expansion of the evolving state in the time-dependent basis of the GCS, Eq. (4). In the case of a finite Hilbert space an arbitrary state can be represented as a superposition of $M\leq N$ GCS,

$$|\psi\rangle=\sum_{i=1}^{M}c_i|\Omega_i,\Lambda\rangle, \tag{35}$$

where Ω_i is an element of the coset space G/H, G is the dynamical group of the system generated by $\mathfrak{g}$, H is the maximal stability subgroup, corresponding to the reference state $|\Lambda\rangle$, and Λ is the highest weight of the Hilbert space representation of the algebra. The coset space G/H has natural symplectic structure [13] and can be considered as a phase space of the quantum system, corresponding to $\mathfrak{g}$. Accordingly, Ω_i is a point in the phase space. The total number of variables defining (up to an overall phase) the state ψ (35) equals M times the dimension of the phase space G/H plus the number M of amplitudes c_i. The dimension of G/H depends on the properties of the Hilbert space representation of the algebra, but is always strictly less then the dimension of the algebra K [13]. Therefore, the number m of real parameters, characterizing the state ψ (35) satisfies the following inequality:

$$m<M(K+2). \tag{36}$$

It follows that the necessary condition for efficient simulation of the dynamics is that $1\lesssim M\ll N$ in the physically relevant time interval.

It is assumed that initial state of the system is a GCS, corresponding to $M=1$ in the expansion (35). If we omit the nonlinear and stochastic terms in Eq. (32), it becomes an ordinary Schrödinger equation, governing the unitary evolution of the state. Under the action of a Hamiltonian linear in the elements of $\mathfrak{g}$, the initial GCS evolves into a GCS by the definition, Eq. (6). Restoring the nonlinear and stochastic terms to Eq. (32) breaks the unitarity of the evolution but a GCS still evolves into a GCS under the full equation, Ref. [20]. Therefore, a GCS solves the sNLSE (32), driven by a linear Hamiltonian. In Ref. [20] it is proved that a CGS is a globally stable solution in that case, i.e., an arbitrary initial state evolves asymptotically into a GCS.

Adding bilinear terms to the Hamiltonian (1) breaks the invariance of the subalgebra $\mathfrak{g}$ under the action of the Hamiltonian and, as a consequence, an initial GCS evolves into a superposition of a number $M>1$ of the GCS (35) in the

corresponding unitary evolution. If the number of terms M becomes large, $M=O(N)$, the unitary evolution can no longer be simulated efficiently. The nonlinear and stochastic terms (representing the effect of the fictitious bath) in Eq. (32) is expected to decrease the effective number M of terms in the expansion (35) of the evolving state. This effect will be termed localization. The natural measure of the localization is the total uncertainty of the evolving state with respect the spectrum-generating algebra $\mathfrak{g}$ or, equivalently, the generalized purity of the state with respect to $\mathfrak{g}$ [21].

The localizing effect of the bath is proved and discussed in Ref. [20]. Heuristically, it can be summarized as follows. If each sum in the sNLSE (32) is replaced by a single contribution of a given operator $\hat{\mathrm{X}}$ the uncertainty of the evolving state with respect to $\hat{\mathrm{X}}$ is strictly decreasing under the action of the bath, unless the state is an eigenstate of $\hat{\mathrm{X}}$, in which case it vanishes [9–11]. Therefore, the effect of the bath is to bring an arbitrary state into an eigenstate of $\hat{\mathrm{X}}$. In our case, the observables $\hat{\mathrm{X}}_i$ are noncommuting and cannot be diagonalized simultaneously. Therefore, it is expected that the effect of the bath in this case will be to take an arbitrary state to a state which minimizes the total uncertainty with respect to the elements of the algebra, i.e., to a GCS.

The characteristic time scale of the localization is the decoherence time scale $(\gamma c_{\mathcal{H}})^{-1}$. If the classicality condition (13) holds and the nonlinearity of the Hamiltonian is moderate (cf. the end of Sec. III), the localization is effective on a time interval much shorter than the relaxation of the observables in $\mathfrak{g}$. As a consequence, the unitary dynamics of these observables can be obtained by (i) simulating the nonlinear stochastic evolution of the localized pure states, (ii) calculating the expectation values of the observables in each stochastic unraveling, and (iii) averaging over the stochastic realizations.

Calculating the expectation values and averaging [steps (ii) and (iii) above] are not part of the definition of efficient simulation, and therefore should be considered separately. Even if the step (i) can be performed efficiently according to the definition, it is left to show that the computational cost of steps (ii) and (iii), measured, for example, by a number of elementary computer operations, does not undermine the efficiency of the total scheme.

To calculate the expectation value of an observable in a state represented by the GCS expansion (35) one must calculate $M(M+1)/2$ matrix elements of the operator between the GCS. Each matrix element for an operator $\hat{\mathrm{X}}_i \in \mathfrak{g}$ can be calculated group theoretically [13,22], i.e., independently on the Hilbert space representation. Therefore, if $M \ll N$ the computation of the expectation values of the elements of $\mathfrak{g}$ can be performed efficiently.

The computational cost of the step (iii) is measured by the number of stochastic realizations necessary to obtain the expectation values of the observables to a prescribed accuracy. From statistics, this number n equals the ratio of the dispersion of the observable D and the squared absolute error ϵ, $n=D/\epsilon^2$, i.e., the inverse relative error squared. If the relative error is the quantity of interest, the number of the realizations does not depend on the properties of the dynamics and, in particular, on the size of the problem. If the stochastic evolution simulation provides only a moderate speed-up over its "brute-force" unitary counterpart, as will happen in simulations of small quantum systems, the averaging may turn out to be the bottleneck of the proposed scheme. On the other hand, for large systems, the efficiency gained by the stochastic simulation will be the main factor of the efficient implementation of the algorithm. In addition, it is important to emphasize that it is not necessary to converge the averaging process in order to obtain a meaningful information: even a single "trajectory" bears important information. The absolute error of the estimation depends on the dispersion of the observable and the corresponding number of stochastic realizations may grow with the Hilbert space dimension of the system. In Appendix C it is shown that the number $n_{st}(\epsilon)$ of stochastic realizations, necessary to obtain the expectation value of each observable $\hat{\mathrm{X}}_i \in \mathfrak{g}$ to an absolute accuracy ϵ is comparable to the number of experimental runs, necessary to obtain the same absolute accuracy. More precisely,

$$n_{st}(\epsilon) \leq n_{ex}(\epsilon)\dim\{\mathfrak{g}\}. \tag{37}$$

The dimension of the subalgebra of observables $\dim\{\mathfrak{g}\}$ is assumed to be a small number. Therefore, $n_{st}(\epsilon)$ is smaller or of the order of $n_{ex}(\epsilon)$.

Finally we focus on step (i) of simulating the nonlinear stochastic evolution of the localized pure states. The localization means that the number of GCS terms M in the expansion (35) is much smaller than the Hilbert space dimension N and, by virtue of the inequality (36), the number m of parameters that characterize the evolving state is much smaller than N.

The details of the derivation of equations of motion for the parameters will be given elsewhere [23]. Here we point out the main ingredients of the derivation. We set the sNLSE (32) in the equivalent exponential form

$$\begin{aligned}|\psi\rangle + |d\psi\rangle &= \exp\left\{-i\hat{\mathrm{H}}dt - 2\gamma\sum_{i=1}^{K}(\hat{\mathrm{X}}_i - \langle\hat{\mathrm{X}}_i\rangle_\psi)^2 dt \right.\\ &\left. + \sum_i (\hat{\mathrm{X}}_i - \langle\hat{\mathrm{X}}_i\rangle_\psi)d\xi_i\right\}|\psi\rangle\\ &= \exp\left\{-2\gamma\sum_{i=1}^{K}(\hat{\mathrm{X}}_i - \langle\hat{\mathrm{X}}_i\rangle_\psi)^2 dt \right.\\ &\left. + \sum_i (\hat{\mathrm{X}}_i - \langle\hat{\mathrm{X}}_i\rangle_\psi)d\xi_i\right\}e^{-i\hat{\mathrm{H}}dt}|\psi\rangle,\end{aligned} \tag{38}$$

using the fact that the infinitesimal transformations commute to the leading order.

The transformation

$$|\psi'\rangle = e^{-i\hat{\mathrm{H}}dt}|\psi\rangle \tag{39}$$

is a unitary evolution, corresponding to the Schrödinger equation. The first-order differential equation of motions of parameters of the representation (35) under this unitary evolution can be derived variationally [24], using (35) as a variational ansatz. Therefore, the unitary evolution can be simu-

lated efficiently, provided the number of terms in the expansion (35) is small.

Consider the second, nonunitary transformation

$$
\begin{aligned}
|\psi'\rangle &= \exp\left\{-2\gamma\sum_{i=1}^{K}(\hat{\mathrm{X}}_i-\langle\hat{\mathrm{X}}_i\rangle_\psi)^2dt+\sum_{i=1}^{K}(\hat{\mathrm{X}}_i-\langle\hat{\mathrm{X}}_i\rangle_\psi)d\xi_i\right\}|\psi'\rangle \\
&\overset{*}{=} e^{\phi(t)}\exp\left\{\sum_{i=1}^{K}\hat{\mathrm{X}}_i(4\gamma\langle\hat{\mathrm{X}}_i\rangle_\psi dt+d\xi_i)\right\}|\psi'\rangle \\
&= e^{\phi(t)}\sum_{i=1}^{M}c_i'\exp\left\{\sum_{i=1}^{K}\hat{\mathrm{X}}_i(4\gamma\langle\hat{\mathrm{H}}_i\rangle_\psi dt+d\xi_i)\right\}|\Omega_i',\Lambda\rangle \\
&\overset{**}{=} e^{\phi(t)}\sum_{i=1}^{M}c_i'e^{\phi_i}|\Omega_i'',\Lambda\rangle \\
&= \sum_{i=1}^{M}c_i''|\Omega_i'',\Lambda\rangle, \qquad (40)
\end{aligned}
$$

where the starred equality follows from the fact that the Casimir operator $\Sigma_{i=1}^{K}\hat{\mathrm{X}}_i^2$ act as identity on an arbitrary state ψ', and the double-starred equality follows from the fact that a not necessarily unitary transformation generated by an element of the algebra maps a GCS to a GCS modulo a complex phase [13]. This transformation can be performed group theoretically [13], i.e., efficiently.

The unitary evolution, Eq. (39), generated by the nonlinear Hamiltonian (1), will lead to delocalization of the evolving state. The nonunitary evolution, Eq. (40), will lead to localization. At sufficiently strong localization the number of terms M necessary to converge the solution of the sNLSE (32) on a fixed time interval will be much smaller, than in the corresponding unitary evolution, and a substantial gain in the computational efficiency will be achieved.

The next section takes up an example of a two-mode Bose-Hubbard model of a Bose-Einstein condensate in a double-well trap to illustrate the localizing properties of the fictitious bath.

V. EXAMPLE: TWO-MODE BOSE-HUBBARD MODEL

A common model for an ultracold gas of bosonic atoms in a one-dimensional periodic optical lattice is described by the Bose-Hubbard Hamiltonian [25],

$$
\hat{\mathrm{H}} = -\Delta\sum_i(\hat{\mathrm{a}}_{i+1}^\dagger\hat{\mathrm{a}}_i+\hat{\mathrm{a}}_i^\dagger\hat{\mathrm{a}}_{i+1})+\frac{U}{2}\sum_i(\hat{\mathrm{a}}_i^\dagger\hat{\mathrm{a}}_i)^2, \qquad (41)
$$

where Δ is the nearest-neighbors hopping rate and U is the strength of the on-site interactions between particles. In the simplest case of a two-sites lattice model, which has been realized experimentally by confining a condensate in a double-well trap [14,15], the Hamiltonian (41) reduces to

$$
\hat{\mathrm{H}} = -\Delta(\hat{\mathrm{a}}_1^\dagger\hat{\mathrm{a}}_2+\hat{\mathrm{a}}_2^\dagger\hat{\mathrm{a}}_1)+\frac{U}{2}[(\hat{\mathrm{a}}_1^\dagger\hat{\mathrm{a}}_1)^2+(\hat{\mathrm{a}}_2^\dagger\hat{\mathrm{a}}_2)^2], \qquad (42)
$$

where Δ is the tunneling rate. Equation (42) can be transformed [26] to the su(2) set of operators

$$
\begin{aligned}
\hat{\mathrm{J}}_x &= \tfrac{1}{2}(\hat{\mathrm{a}}_1^\dagger\hat{\mathrm{a}}_2+\hat{\mathrm{a}}_2^\dagger\hat{\mathrm{a}}_1), \\
\hat{\mathrm{J}}_y &= \frac{1}{2i}(\hat{\mathrm{a}}_1^\dagger\hat{\mathrm{a}}_2-\hat{\mathrm{a}}_2^\dagger\hat{\mathrm{a}}_1), \\
\hat{\mathrm{J}}_z &= \tfrac{1}{2}(\hat{\mathrm{a}}_1^\dagger\hat{\mathrm{a}}_1-\hat{\mathrm{a}}_2^\dagger\hat{\mathrm{a}}_2), \qquad (43)
\end{aligned}
$$

leading to the following Lie-algebraic form:

$$
\hat{\mathrm{H}} = -\omega\hat{\mathrm{J}}_x+U\hat{\mathrm{J}}_z^2, \qquad (44)
$$

where $\omega=2\Delta$. The Hilbert space of the system of N bosons in this model corresponds to the $j=N/2$ irreducible representation of the su(2) algebra. We seek to simulate the evolution of the operators (43), driven by the Hamiltonian (44), where the initial state of the system is a GCS with respect to the su(2), the spin-coherent state [13,27,28]. More specifically, the initial state is chosen as

$$
|\psi(0)\rangle = |-j\rangle, \qquad (45)
$$

which corresponds to the state of the condensate, localized in a single well.

The dynamics driven by the weak measurement of the operators (43) on the evolving condensate is described by the Liouville–von Neumann equation of the form (3):

$$
\frac{\partial}{\partial t}\hat{\rho} = -i[\hat{\mathrm{H}},\hat{\rho}]-\gamma\sum_{i=0}^{2}[\hat{\mathrm{J}}_i,[\hat{\mathrm{J}}_i,\hat{\rho}]]. \qquad (46)
$$

The classicality condition (13) for the $2j+1=N+1$-dimensional representation of the su(2), corresponding to N atoms in the trap, translates into the $N\gg 1$ condition (Appendix B). Therefore, for sufficiently large numbers of atoms in the trap the classicality condition is satisfied and a sufficiently weak measurement of the operators $\hat{\mathrm{J}}_x$, $\hat{\mathrm{J}}_y$, and $\hat{\mathrm{J}}_z$ is expected to induce strong decoherence in the spin-coherent state basis, but leaving the dynamics of the operators practically unperturbed. As a consequence, the generalized purity of a stochastic unraveling of Eq. (46), $P_{\mathrm{su}(2)}[\psi]=\Sigma_i\langle\hat{\mathrm{J}}_i/j\rangle^2$, is expected to remain close to unity, which enables efficient simulation of the corresponding dynamics.

Figure 1 displays the evolution of the expectation values of the operators $\hat{\mathrm{J}}_x/j$, $\hat{\mathrm{J}}_y/j$, and $\hat{\mathrm{J}}_z/j$ in the unitary evolution $\gamma=0$ and in the nonunitary case $\gamma=\omega/(300j)$ for $N=2j=128$ particles in the condensate. The hopping rate ω and the strength of the on-site interaction are related by $U=\omega/2j$. It can be seen that the evolution is negligibly perturbed by the bath for the chosen strength of the coupling γ. We also plot the generalized purity of the unitarily evolving state and of a random stochastic unraveling of the nonunitary evolution. The generalized purity in the unitary case decreases to the value of about 0.06, which corresponds (Appendix A) to the number of configurations $M=0.75(2j+1)\approx 100=O(N)$ in the GCS expansion of the solution. On the other hand, the generalized purity in the stochastic unraveling is about 0.9–0.95 which corresponds to a drastic reduction of the number of configurations to $M=0.04(2j+1)\approx 5\ll N$.

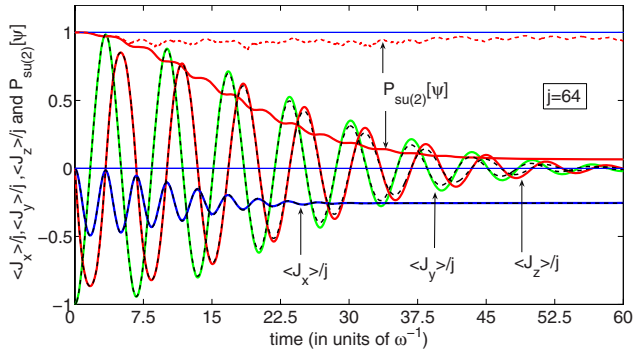

FIG. 1. (Color online) The purity and expectation values of observables as a function of time. An initial GCS, Eq. (45), undergoes (i) unitary, $\gamma=0$ (solid lines); (ii) nonunitary, $\gamma=\omega/(300j)$ (dashed lines), evolution according to the Liouville equation (46). The strength of the on-site interaction chosen for the numerical solution is $U=\omega/2j$. The observed dynamics of the expectation values of $\hat{J}_x/j$, $\hat{J}_y/j$, and $\hat{J}_z/j$ is negligibly affected by the bath while the generalized purity $P_{\mathrm{su}(2)}[\psi]$ of the stochastic unraveling of the nonunitary evolution is larger by the factor of 15 than the minimal purity of the unitarily evolving state.

An interesting feature of the stochastic evolution displayed in Fig. 1 (and observed in other numerical simulations, see Fig. 2) is that apparently, the generalized purity approaches a constant value on average. Since the generalized purity is a measure of localization of the state on the corresponding phase space [which is the Bloch sphere for the su(2) algebra [13,27,28]] such behavior is suggestive of a solitonlike solution of the sNLSE (32). Investigation of existence and properties of these solitonlike solutions seems to be an interesting topic for future research. For the time being let us assume that the stationary (on average) value P of the generalized purity as displayed in Fig. 1 is an analytical function of $1/j$ (see Fig. 2 for some evidence). Then

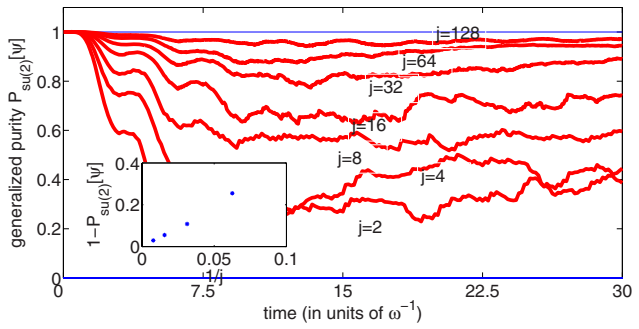

FIG. 2. (Color online) Generalized purity averaged over a small number (2–10) of stochastic unraveling of the Liouville–von Neumann equation (46). Initial state and parameters of the equation are as in Fig. 1. Purity is plotted for $j=2,4,8,16,32,64,128$. The inset shows the generalized purity as a function of $1/j$. At larger j the value of the averaged purity is apparently consistent with the estimate $1-\frac{1}{j}f(\omega^a U^b \gamma^c)$, with $f(\omega^a U^b \gamma^c)=3$, corresponding to $M=3$ number of the GCS terms in the expansion of the solution.

$$P = 1 - \frac{1}{j} f(\omega^a U^b \gamma^c), \tag{47}$$

to the lowest order in $1/j$, where f is an unknown function of the dimensionless argument $\omega^a U^b \gamma^c$ and $a+b+c=0$. Using the estimate (Appendix A) for the number of configurations we obtain

$$M = (2j+1)(1-\sqrt{P}) = f(\omega^a U^b \gamma^c), \tag{48}$$

i.e., the number of configurations in the expansion of the stochastic unraveling does not depend on j. Numerical evidence implies that generally $f(\omega^a U^b \gamma^c) \neq 1$. For example, the value of $f(\omega^a U^b \gamma^c)$ is 3, deduced from Fig. 2. This implies, that asymptotically, as $j \to \infty$, the dynamics of the single-particle observables of the two-modes Bose-Hubbard model can be reproduced not by an averaging over stochastic GCS evolutions (stochastic mean-field solutions), but rather by an averaging over the stochastic evolutions of superpositions of a constant small number $M>1$ of GCS.

Similar behavior has been observed in different parametric regimes of the Bose-Hubbard model and in the study of other su(2) Hamiltonians, including the Lipkin–Meshkov–Glick model [29] of a system of interacting fermions. It should be noted that drawing inferences from these models requires certain caution since both the two-mode Bose-Hubbard and Lipkin–Meshkov–Glick are exactly solvable models [30]. The proposed method does not rely on the quantum integrability of the system. Nonetheless, its efficiency may depend on the integrability. Investigation of this important question seems to be a meaningful objective for future research.

VI. DISCUSSION AND OPEN QUESTIONS

A strategy for efficient simulation of a unitary evolution of a restricted set of observables has been proposed (cf. Fig. 3). The present strategy can lead to a dramatic speed-up compared to a brute-force computation. The price paid for the speed-up is that the dynamics of only a restricted set of observables can be simulated. The simulation focuses on the set of the observables which comprises the spectrum-generating Lie algebra of the system. This set of observables is interesting theoretically and often accessible experimentally [2]. The main idea of the proposed method is that the unitary evolution of the distinguished observables is simulated by a particular open-system dynamics, corresponding to the process of weak measurement of the observables, performed on the evolving quantum system.

A successful implementation of the scheme is based on the assumption that a large time-scale separation exists between the decoherence of the evolving state in the basis of the GCS, associated with the algebra, and the relaxation of the expectation values of the elements of the algebra. The necessary condition for the existence of the time-scale separation is the classicality condition (13) on the spectrum-generating algebra and its Hilbert space representation. This necessary condition excludes efficient simulation of certain subalgebras of observables (Appendix B). For example, the unitary dynamics of local observables of a composite system

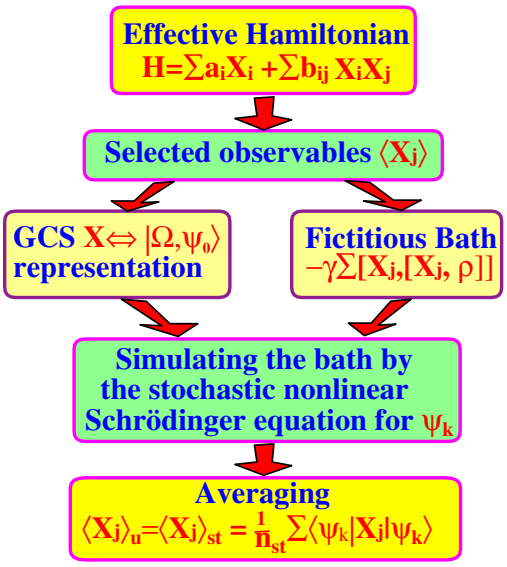

FIG. 3. (Color online) A schematic flow chart of the proposed approach to simulate dynamics of the operators $\hat{X}_i$ of the spectrum-generating algebra of the system. The unitary evolution of the observables is simulated by the open-system evolution, modeling weak measurement of the evolving observables. The open-system dynamics is unraveled into stochastic pure-state evolutions, efficiently simulated using expansion of the pure state in the GCS. Averaging over n_{st} realizations obtains the expectation values, corresponding to the unitary evolution $\langle \hat{X}_j \rangle_u = \langle \hat{X}_j \rangle_{st}$.

of qubits cannot be simulated with higher efficiency by the open-system evolution. It is expected that the classicality condition is also sufficient for the time-scale separation, provided the nonlinearity is moderate. An order of magnitude argument is presented to support a claim that if the Hamiltonian is a polynomial in the algebra elements, the time-scale separation exists, provided the classicality condition is satisfied sufficiently well. Higher orders of the polynomial require a stronger "classicality" condition to ensure the time-scale separation. Numerical investigation of the su(2) case with Hamiltonians bilinear in the algebra elements has shown that time-scale separation is strong already in Hilbert space representations of dimension <100.

The proposed numerical algorithm allows for an empirical check of convergence by repeating the calculation with a reduced coupling to the fictitious bath. If a simulation is found to converge the results are valid and a theoretical justification for time-scale separation is no longer required. If the time-scale separation is small or nonexistent, in order to obtain convergent results one must take the coupling to the bath so weak that the localization, generated by the bath will not be sufficient to provide any substantial speed-up. Once the results are converged in the strength of the coupling and in the number of the generalized coherent states in the computational basis, the results can be relied on irrespectively on the magnitude of the time-scale separation.

The fast decoherence reduces the computational complexity of the evolution, while the slow relaxation leaves the dynamics of the restricted set of observables practically unaffected on physically interesting time scales. The effect of a fictitious coupling to a bath can be viewed as a dynamically induced coarse graining of the evolving state in the phase space, associated with the spectrum-generating Lie algebra. The fine structure of the evolving state, irrelevant for the expectation values of the "smooth" observables, is rubbed out by the decoherence, thereby reducing the computational complexity of the evolution. This coarse graining can be seen as a generalization of the process of conversion of quantum correlations (entanglement) to classical correlations under the action of local dephasing environments [31]. The reduction of the computational complexity is realized by simulating the sNLSE, governing the stochastic unraveling of the nonunitary evolution. The GCS are globally stable solutions of the sNLSE, corresponding to a Hamiltonian, linear in the algebra elements [20]. Numerical evidence obtained in the su(2) case suggests that Hamiltonians bilinear in the generators asymptotically lead to solitonlike stable localized solutions of the corresponding sNLSE. Averaging over the stochastic realizations of the open-system evolution recovers the unitary dynamics of the restricted set of observables.

The fictitious bath is fine-tuned—it corresponds to a process of weak measurement of the orthonormal basis set of the operators, performed with equal rates and strengths. This fine-tuned bath is constructed as a computational tool. On the other hand, if the fine-tuning condition is dropped, the resulting open-system dynamics can represent a real physical situation, where the linear part of the Hamiltonian is perturbed by the time-dependent δ-correlated noise [32]. In that case the density operator of the system will follow an open evolution, corresponding to a process of weak measurement of the algebra elements, performed with generally different rates [32]. It is expected, that if the noise is sufficiently weak, the constant part of the Hamiltonian will induce fast (on the relaxation time scale) rotation in the Hilbert-Schmidt operator space, which effectively will average out the difference between the contributions of various measurements. Therefore, this real bath is expected to induce the same type of localization as the fine-tuned fictitious bath. Numerical evidence obtained in the su(2) case supports this conjecture [23]. Restricting the measurements to the algebra elements, the experimentalist will not observe the effect of the bath if the noise is sufficiently small, while measuring the higher-order correlations will reveal the nonunitary character of the evolution. Generally, it is expected that the open-system dynamics can be simulated with higher efficiency than the corresponding unitary dynamics, provided the classicality condition holds.

The main directions for future research are the following:

(i) Investigation of the effect of nonlinear terms in the Hamiltonian (1) on the relaxation time scales of the observables in the spectrum-generating algebra in the corresponding fictitious open-system dynamics, Eq. (3).

(ii) Development of an efficient and convergent algorithm for simulating the evolution of a state in the GCS basis representation.

(iii) Investigation of the extent of localization as a function of the "classicality," and in particular, proving the conjecture that the localization is independent of the Hilbert space representation of the spectrum-generating algebra if the "classicality" is sufficiently strong.

(iv) Comparison of the efficiency of the proposed method in applications to quantum integrable vs nonintegrable models.

ACKNOWLEDGMENTS

We are grateful to H. Barnum, L. Diosi, Y. Khodorkovsky, D. Steinitz, and A. Vardi for discussions. This work is supported by DIP and the Israel Science Foundation (ISF). The Fritz Haber Center is supported by the Minerva Gesellschaft für die Forschung GmbH München, Germany.

APPENDIX A: RELATION OF THE GENERALIZED PURITY TO THE NUMBER OF CONFIGURATIONS IN THE GCS EXPANSION OF THE STATE: su(2) CASE

The phase space of a quantum system, associated with the su(2) spectrum-generating algebra is a two-dimensional sphere [13,27,28], usually called a Bloch sphere. The localization of a state ψ of the system in the phase space means localization of its P distribution [13,28] about a point in the phase space. Without loss of generality it can be assumed that the state is localized about the origin. In fact, an appropriate unitary transformation, generated by the su(2), maps a state localized about an arbitrary point to the state, localized about the origin, leaving both the generalized purity and the number of the GCS in the expansion invariant. For definiteness let us assume that the P distribution has a finite support area $\mathcal{S}$ of radius α about an origin on the phase space. Using the expression for the resolution of identity in terms of the GCS [13,28] $|\tau\rangle$,

$$\hat{\mathrm{I}} = \frac{2j+1}{\pi}\int \frac{d^2\tau}{(1+|\tau|^2)^2}|\tau\rangle\langle\tau|, \tag{A1}$$

the number of the GCS in the expansion of the state can be estimated as follows:

$$\begin{aligned} M[\psi] &= \frac{2j+1}{\pi}\int_{\mathcal{S}} \frac{d^2\tau}{(1+|\tau|^2)^2} \\ &= (2j+1)\int_0^{|\alpha|^2} \frac{d|\tau|^2}{(1+|\tau|^2)^2} \\ &= (2j+1)\frac{|\alpha|^2}{1+|\alpha|^2}. \end{aligned} \tag{A2}$$

To calculate the generalized purity we must calculate the expectation values of $\hat{\mathrm{J}}_x$, $\hat{\mathrm{J}}_y$, and $\hat{\mathrm{J}}_z$. Given the P representation of the state, the expectation value of an observable $\hat{\mathrm{X}}$ can be calculated using its Q representation,

$$\langle\hat{\mathrm{X}}\rangle = \frac{2j+1}{\pi}\int \frac{d^2\tau}{(1+|\tau|^2)^2}P(\tau)Q_{\hat{\mathrm{X}}}(\tau), \tag{A3}$$

where $Q_{\hat{\mathrm{X}}}(\tau)=\langle\tau|\hat{\mathrm{X}}|\tau\rangle$. We have [13,28]

$$\begin{aligned} Q_{\hat{\mathrm{J}}_x} &= j\frac{\tau+\tau^*}{1+|\tau|^2}, \\ Q_{\hat{\mathrm{J}}_y} &= j\frac{\tau-\tau^*}{i(1+|\tau|^2)}, \\ Q_{\hat{\mathrm{J}}_z} &= j\frac{|\tau|^2-1}{1+|\tau|^2}. \end{aligned} \tag{A4}$$

Assuming that $P(\tau)$ is symmetric about the origin ($\tau=0$), we see that the expectation values of $\hat{\mathrm{J}}_x$ and $\hat{\mathrm{J}}_y$ vanish and

$$\langle\hat{\mathrm{J}}_z\rangle = \frac{2j+1}{\pi}\int \frac{d^2\tau}{(1+|\tau|^2)^2}P(\tau)j\frac{|\tau|^2-1}{1+|\tau|^2}. \tag{A5}$$

We assume that

$$P(\tau) = \begin{cases} p, & |\tau| \le |\alpha|, \\ 0, & |\tau| > |\alpha|. \end{cases} \tag{A6}$$

The distribution (A6) as it stands does not correspond to a pure state. Nonetheless, it can be understood as a coarse-grained version of a localized pure state, useful for calculation of the expectations of $\hat{\mathrm{J}}_x$, $\hat{\mathrm{J}}_y$, and $\hat{\mathrm{J}}_z$ and the generalized purity $P_{\mathrm{su}(2)}[\psi]$, Eq. (A10). In fact, Eq. (A4) gives the characteristic scale of unity for the change of the Q representation in the integral (A3). On the other hand, the resolution of identity (A1) implies the characteristic scale of the fine structure of the P distribution (the width of the overlap of two coherent states) of the order of $(1+|\tau|^2)/\sqrt{j}$. Therefore, as long as $(1+|\alpha|^2)/\sqrt{j} \ll 1$ in Eq. (A6) the coarse-grained distribution can be used for calculation of the generalized purity. As can be seen below, Eq. (A10), for $j \gg 1$ the coarse-grained description is valid for calculation of the generalized purity asymptotically as $1/j$.

For a particular form of the distribution (A6), Eq. (A5) simplifies to

$$\begin{aligned} \langle\hat{\mathrm{J}}_z\rangle &= pj(2j+1)\int_0^{|\alpha|^2} \frac{d|\tau|^2}{(1+|\tau|^2)^2}\frac{|\tau|^2-1}{1+|\tau|^2} \\ &= j - pj(2j+1)\int_0^{|\alpha|^2} \frac{2d|\tau|^2}{(1+|\tau|^2)^3} \\ &= j - pj(2j+1)\left(1-\frac{1}{(1+|\alpha|^2)^2}\right). \end{aligned} \tag{A7}$$

The number p in Eq. (A6) can be found from the normalization condition

$$\begin{aligned} 1 = \langle\hat{\mathrm{I}}\rangle &= \frac{2j+1}{\pi}\int \frac{d^2\tau}{(1+|\tau|^2)^2}P(\tau) \\ &= p(2j+1)\int_0^{|\alpha|^2} \frac{d|\tau|^2}{(1+|\tau|^2)^2} \\ &= p(2j+1)\frac{|\alpha|^2}{1+|\alpha|^2}, \end{aligned} \tag{A8}$$

from which $p=(1+|\alpha|^2)/[|\alpha|^2(2j+1)]$. Inserting this expression into Eq. (A7), we obtain

$$\langle \hat{J}_z \rangle = j - pj(2j+1)\left(1 - \frac{1}{(1+|\alpha|^2)^2}\right)$$
$$= j - \frac{1+|\alpha|^2}{|\alpha|^2} j\left(1 - \frac{1}{(1+|\alpha|^2)^2}\right)$$
$$= -\frac{j}{1+|\alpha|^2}. \tag{A9}$$

Therefore,

$$P_{\mathrm{su}(2)}[\psi] = \frac{1}{j^2}\sum_i \langle \hat{J}_i \rangle^2 = \frac{1}{j^2}\langle \hat{J}_z \rangle^2 = \left(\frac{1}{1+|\alpha|^2}\right)^2 \tag{A10}$$

and

$$|\alpha|^2 = \frac{1}{\sqrt{P_{\mathrm{su}(2)}[\psi]}} - 1. \tag{A11}$$

Inserting the latter expression into Eq. (A2), we obtain for the number of GCS in the expansion

$$M[\psi] = (2j+1)(1 - \sqrt{P_{\mathrm{su}(2)}[\psi]}). \tag{A12}$$

As argued after Eq. (A6) expressions (A10) and (A12) are valid for $P_{\mathrm{su}(2)}[\psi] \gg 1/j$.

APPENDIX B: CLASSICALITY CONDITION: (i) SUBALGEBRA su(n) OF SINGLE PARTICLES OBSERVABLES OF THE n-MODES BEC IN AN OPTICAL LATTICE; (ii) SUBALGEBRA OF LOCAL OBSERVABLES OF A SYSTEM OF n d-LEVEL SYSTEM

1. BEC

The spectrum-generating algebra of the Bose-Hubbard model for the n-modes BEC in optical lattice is su(n) subalgebra of the single particles observables [33,34]. It is shown that the classicality condition (13) is satisfied in this case, provided the number of atoms N in the condensate complies with

$$N \gg n. \tag{B1}$$

The Hilbert space of the condensate is a totally symmetric irreducible representation of the su(n) [N] [5] and the value of the Casimir in this representation is [5]

$$c_{\mathcal{H}} = \frac{n-1}{2n} N(N+n). \tag{B2}$$

The total uncertainty in the GCS is [16,18]

$$\Delta_{\min} = c_{\mathcal{H}} - \langle \Lambda_N | \Lambda_N \rangle = c_{\mathcal{H}} - \frac{n-1}{2n} N^2 = \frac{1}{2} N(n-1), \tag{B3}$$

where we have used the known expression [5] for the norm of the maximal weight vector [3] Λ_N in the totally symmetric irreducible representation of the su(n) [N]. The value of the Casimir in the adjoint representation is [5]

$$c_{\mathrm{adj}} = n. \tag{B4}$$

Thus Eq. (13) holds if and only if Eq. (B1) holds. Moreover,

$$\sqrt{\frac{c_{\mathcal{H}}}{c_{\mathrm{adj}}}} = \sqrt{\frac{n-1}{2n^2} N(N+n)}, \tag{B5}$$

which implies Eq. (23), provided Eq. (B1) holds.

Therefore, using the sNLSE (32), propagation can be advantageous for calculation of the single particles observables, provided the on-site interaction preserves the time-scale separation in Eq. (23).

2. Local observables

Let $\mathfrak{g}$ be a subalgebra of local observables on the composite Hilbert space. For simplicity, let us consider n d-level systems in the Hilbert space $\mathcal{H} = \otimes_{i=1}^n \mathcal{H}_i$ and a subalgebra of local observables $\mathfrak{g} = \oplus_{i=1}^n \mathrm{su}(L) \subseteq \oplus_{i=1}^n \mathrm{su}(d) \subseteq \mathrm{su}(d^n)$. Since the minimum of the total uncertainty (7) for a local subalgebra is obtained in a product state $\psi_{\mathrm{prod}} = \otimes_{i=1}^n \psi_i$, where each ψ_i is a GCS with respect to the local subalgebra su(L) it follows that

$$\Delta_{\min} = \Delta[\psi_{\mathrm{prod}}] = c_{\mathcal{H}} - P_{\mathfrak{g}}[\psi_{\mathrm{prod}}] = \sum_{i=1}^n (c_{\mathcal{H}_i} - P_{\mathrm{su}(L)}[\psi_i])$$
$$= n(c_{\mathcal{H}_d} - P_{\mathrm{su}(L)}[\mathrm{GCS}]) = n\Delta_{d,\min}, \tag{B6}$$

where $\mathcal{H}_d$ is the Hilbert space of a d-level subsystem and $\Delta_{d,\min}$ is the minimal total uncertainty of a state of any subsystem with respect to the subsystem subalgebra su(L). Therefore, the condition (13) is equivalent to

$$\frac{\Delta_{\min}}{c_{\mathcal{H}}} = \frac{\Delta_{d,\min}}{c_{\mathcal{H}_d}} \ll 1, \tag{B7}$$

i.e., holds if and only if the local subalgebras su(L) of the subsystems operators comply with the classicality condition. For example, in the composite system of a two-level system the only subalgebra of local observables is the local subalgebra $\mathfrak{g} = \oplus_{i=1}^n \mathrm{su}(2)$. The eigenvalue of the local Casimir equals $(1/2)(1/2+1) = 3/4$ and the generalized purity with respect to a su(2) algebra of each two-level system is 1/4. Therefore, the minimal total uncertainty with respect to a su(2) algebra of each two-level system equals $3/4 - 1/4 = 1/2$ and the ratio of the uncertainty to the Casimir equals $(1/2)/(3/4) = 2/3$. Therefore, the strong inequality (B7) is not satisfied. More generally, it can be shown using Eq. (B6) that the local algebra $\mathfrak{g} = \oplus_{i=1}^n \mathrm{su}(d) \subseteq \mathrm{su}(d^n)$ gives

$$\frac{\Delta_{\min}}{c_{\mathcal{H}}} = \frac{d}{d+1}, \tag{B8}$$

therefore the classicality condition (13) does not hold.

APPENDIX C: ESTIMATION OF THE NUMBER OF STOCASTIC REALIZATIONS, NECESSARY TO CONVERGE THE EXPECTATION VALUES OF THE OBSERVABLES IN $\mathfrak{g}$ TO A PRESCRIBED ABSOLUTE ACCURACY ϵ

Given a random variable $\hat{X}$ with dispersion $D_X \equiv \langle \hat{X}^2 \rangle - \langle \hat{X} \rangle^2$ the number of samplings $n(\epsilon)$, necessary to estimate

the expectation value $\langle \hat{X} \rangle$ to the absolute accuracy ϵ equals

$$n(\epsilon)_X = \frac{D_X}{\epsilon^2}. \tag{C1}$$

Let us assume that each observable $\hat{X}_i \in \mathfrak{g}$ is measured in an experiment to a prescribed accuracy ϵ. The corresponding number of experimental runs is $n(\epsilon)_{X_i}$. Then

$$\sum_{i=1}^{\dim\{\mathfrak{g}\}} n(\epsilon)_{X_i} = \frac{\sum_{i=1}^{\dim\{\mathfrak{g}\}} D_{X_i}}{\epsilon^2} = \frac{\sum_{i=1}^{\dim\{\mathfrak{g}\}} (\langle \hat{X}_i^2 \rangle - \langle \hat{X}_i \rangle^2)}{\epsilon^2} = \frac{C_{\mathcal{H}} - \sum_{i=1}^{\dim\{\mathfrak{g}\}} \langle \hat{X}_i \rangle^2}{\epsilon^2}. \tag{C2}$$

Now consider the computation of expectation values of observables $\hat{X}_i \in \mathfrak{g}$ in a state $\hat{\rho}(t)$, evolving according to Eq. (3), by averaging over stochastic unraveling (32). By Eq. (C1) the number of unraveling necessary to compute the expectation value of $\hat{X}_i$ to the accuracy ϵ is $n(\epsilon)'_{X_i} = D'_{X_i}/\epsilon^2$, where D'_{X_i} is the dispersion of the observable in the state $\hat{\rho}(t)$. Then

$$\sum_{i=1}^{\dim\{\mathfrak{g}\}} n(\epsilon)'_{X_i} = \frac{\sum_{i=1}^{\dim\{\mathfrak{g}\}} D'_{X_i}}{\epsilon^2} = \frac{\sum_{i=1}^{\dim\{\mathfrak{g}\}} (\langle \hat{X}_i^2 \rangle' - \langle \hat{X}_i \rangle'^2)}{\epsilon^2} = \frac{C_{\mathcal{H}} - \sum_{i=1}^{\dim\{\mathfrak{g}\}} \langle \hat{X}_i \rangle'^2}{\epsilon^2}, \tag{C3}$$

where $\langle \hat{X} \rangle'$ means statistical average over the unraveling of the quantum expectation values obtained in each unraveling [which is the random variable for the purpose of Eq. (C1)]. But on the time interval of the simulation (Sec. III)

$$\langle \hat{X}_i \rangle' = \langle \hat{X}_i \rangle, \tag{C4}$$

therefore Eqs. (C2)–(C4) imply

$$\sum_{i=1}^{\dim\{\mathfrak{g}\}} n(\epsilon)'_{X_i} = \sum_{i=1}^{\dim\{\mathfrak{g}\}} n(\epsilon)_{X_i}. \tag{C5}$$

It follows that

$$n(\epsilon)_{st} \equiv \max_i \{n(\epsilon)'_{X_i}\} \leq \sum_{i=1}^{\dim\{\mathfrak{g}\}} n(\epsilon)'_{X_i} = \sum_{i=1}^{\dim\{\mathfrak{g}\}} n(\epsilon)_{X_i} \leq \dim\{\mathfrak{g}\} \max_i \{n(\epsilon)_{X_i}\} \equiv \dim\{\mathfrak{g}\} n(\epsilon)_{ex}, \tag{C6}$$

where $n_{st}(\epsilon)$ is the number of stochastic realizations, necessary to obtain the expectation value of each observable $\hat{X}_i \in \mathfrak{g}$ to an absolute accuracy ϵ, $n_{ex}(\epsilon)$ is the number of experimental runs, necessary to obtain the expectation value of each $\hat{X}_i$ to the absolute accuracy ϵ.

[1] Ronnie Kosloff, J. Phys. Chem. **92**, 2087 (1988).
[2] A. Bohm, Y. Neeman, and A. O. Barut, *Dynamical Groups and Spectrum Generating Algebras* (World Scientific, Singapore, 1988).
[3] R. Gilmore, *Lie Groups, Lie Algebras and Some of Their Applications* (Wiley, New York, 1974).
[4] F. Iachello and R. Levine, *Algebraic Theory of Molecules* (Oxford University Press, Oxford, 1995).
[5] F. Iachello, *Lie Algebras and Applications* (Springer, Berlin, 2006).
[6] G. Lindblad, Commun. Math. Phys. **48**, 119 (1976).
[7] H.-P. Breuer and F. Petruccione, *Open Quantum Systems* (Oxford University Press, Oxford, 2002).
[8] L. Diosi, "Weak measurements in quantum mechanics," in *Encyclopedia of Mathematical Physics*, edited by J.-P. Fransoise, G. L. Naber, and S. T. Tsou (Elsevier, Oxford, 2006), Vol. 4, pp. 276–282.
[9] N. Gisin, Phys. Rev. Lett. **52**, 1657 (1984).
[10] L. Diosi, Phys. Lett. A **129**, 419 (1988).
[11] N. Gisin and I. C. Percival, J. Phys. A **25**, 5677 (1992).
[12] A. Perelomov, *Generalized Coherent States and Their Applications* (Springer, Berlin, 1985).
[13] W. Zhang, D. H. Feng, and R. Gilmore, Rev. Mod. Phys. **62**, 867 (1990).
[14] T. Schumm, S. Hofferberth, L. M. Andersson, S. Wildermuth, S. Groth, I. Bar-Joseph, J. Schmiedmayer, and P. Kruger, Nat. Phys. **1**, 57 (2005).
[15] R. Gati, B. Hemmerling, J. Folling, M. Albiez, and M. K. Oberthaler, Phys. Rev. Lett. **96**, 130404 (2006).
[16] R. Delbourgo and J. R. Fox, J. Phys. A **10**, L233 (1977).
[17] H. Barnum, E. Knill, G. Ortiz, and L. Viola, Phys. Rev. A **68**, 032308 (2003).
[18] A. A. Klyachko, e-print arXiv:quant-ph/0206012.
[19] S. Boixo, L. Viola, and G. Ortiz, EPL **79**, 40003 (2007).
[20] M. Khasin and R. Kosloff, e-print arXiv:0804.1103v1.
[21] L. Viola and W. G. Brown, J. Phys. A **40**, 8109 (2007).
[22] R. Somma, H. Barnum, G. Ortiz, and E. Knill, Phys. Rev. Lett. **97**, 190501 (2006).
[23] M. Khasin and R. Kosloff (unpublished).
[24] P. Kramer and M. Saraceno, *Geometry of the Time-Dependent Variational Principle in Quantum Mechanics* (Springer-Verlag, Berlin, 1981).
[25] D. Gerald, *Mahan, Many-Particle Physics* (Kluwer Academic, Plenum, New York, 2000).
[26] A. Vardi and J. R. Anglin, Phys. Rev. Lett. **86**, 568 (2001).
[27] F. T. Arecchi, E. Courtens, R. Gilmore, and H. Thomas, Phys.

Rev. A **6**, 2211 (1972).
[28] V. R. Vieira and P. D. Sacramento, Ann. Phys. **242**, 188 (1995).
[29] H. J. Lipkin, N. Meshkov, and A. J. Glick, Nucl. Phys. **62**, 188 (1965).
[30] G. Ortiz, R. Somma, J. Dukelsky, and S. Rombouts, Nucl. Phys. B **707**, 421 (2005).
[31] M. Khasin and R. Kosloff, Phys. Rev. A **76**, 012304 (2007).
[32] V. Gorini and A. Kossakowski, J. Math. Phys. **17**, 1298 (1976).
[33] I. Tikhonenkov, J. R. Anglin, and A. Vardi, Phys. Rev. A **75**, 013613 (2007).
[34] F. Trimborn, D. Witthaut, and H. J. Korsch, Phys. Rev. A **77**, 043631 (2008).

4.3 The Globally Stable Solution of a Stochastic Nonlinear Schrodinger Equation

IOP PUBLISHING JOURNAL OF PHYSICS A: MATHEMATICAL AND THEORETICAL

J. Phys. A: Math. Theor. **41** (2008) 365203 (10pp) doi:10.1088/1751-8113/41/36/365203

The globally stable solution of a stochastic nonlinear Schrödinger equation

M Khasin and R Kosloff

Fritz Haber Research Center for Molecular Dynamics, Hebrew University of Jerusalem, Jerusalem 91904, Israel

E-mail: misha@fh.huji.ac.il and ronnie@fh.huji.ac.il

Received 30 May 2008, in final form 8 July 2008
Published 30 July 2008
Online at stacks.iop.org/JPhysA/41/365203

Abstract

Weak measurement of a subset of noncommuting observables of a quantum system can be modeled by the open-system evolution, governed by the master equation in the Lindblad form. The open-system density operator can be represented as a statistical mixture over non-unitarily evolving pure states, driven by the stochastic nonlinear Schrödinger equation (sNLSE). The globally stable solution of the sNLSE is obtained in the case where the measured subset of observables comprises the spectrum-generating algebra of the system. This solution is a generalized coherent state (GCS), associated with the algebra. The result is based on proving that the GCS minimizes the trace-norm of the covariance matrix, associated with the spectrum-generating algebra.

PACS numbers: 03.65.Ta, 03.65.Yz, 02.50 Ey

1. Introduction

The number of solvable quantum dynamics models is quite limited. The importance of such models is that they form a source of insight into quantum phenomena. In addition, the solvable models are the starting point of approximate theories. An important class of solvable models is based on a Lie-algebraic Hamiltonian of the following form:

$$\hat{H} = \sum_j a_j \hat{X}_j \tag{1}$$

where the set $\{\hat{X}_j\}$ of observables is closed under the commutation relations:

$$[\hat{X}_i, \hat{X}_j] = \mathrm{i} \sum_{k=1}^{K} f_{ijk} \hat{X}_k, \tag{2}$$

i.e., it forms Lie algebra (Gilmore 1974) of the system operators, known as the spectrum-generating algebra (Bohm *et al* 1988) of the system.

The solvable nature of the dynamics generated by equation (1) motivates the search of transformation of complex many-body problems to an algebraic description. The next level of complexity is to add the binary term

$$\hat{H} = \sum_j a_j \hat{X}_j, + \sum_{kl} b_{kl} \hat{X}_k \hat{X}_l, \tag{3}$$

where $a_j = a_j^*$ and $b_{kl} = b_{lk}^*$. Such Lie-algebraic Hamiltonians are encountered in various fields of the many-body physics, such as molecular (Iachello and Levine 1995, Iachello 2006), nuclear (Bohm *et al* 1988, Iachello 2006) and condensed matter physics (Bohm *et al* 1988).

A useful property of the Lie-algebraic setting is a set of states which can be thought of as the most classical states with respect to measurement performed on the elements of the algebra. These states are termed generalized coherent states (GCS) with respect to the algebra (Perelomov 1985, Zhang *et al* 1990). An important property of the GCS is their invariance under the action of the unperturbed Hamiltonian, linear in the algebra elements, equation (1). This means that a GCS evolves into a GCS under the action of the Hamiltonian (1). In the perturbed case (3) GCS are generally no longer invariant but the GCS ansatz can be used for a mean-field approximation of the many-body dynamics (Kramer and Saraceno 1981, Zhang *et al* 1990).

Any realistic physical system is open, i.e., the interaction with the dissipating environment cannot be neglected. It is therefore of necessity to include the effect of an environment on the dynamics. Particularly interesting is the open-system evolution modeling the process of weak measurement (Diosi 2006). The open-system dynamics studied in the present work is generated by the Lindblad semi-group (Lindblad 1976, Breuer and Petruccione 2002):

$$\frac{\partial}{\partial t}\hat{\rho} = \mathcal{L}\hat{\rho} = -\mathrm{i}[\hat{H}, \hat{\rho}] - \sum_{j=1}^{K} \gamma_j [\hat{X}_j, [\hat{X}_j, \hat{\rho}]], \tag{4}$$

where the Hamiltonian has the algebraic form (1). The spectrum-generating algebra of the system spanned by $\{\hat{X}_i\}$ is assumed to be a compact semisimple algebra (Gilmore 1974) and the basis $\{\hat{X}_i\}$ is chosen to be orthonormal with respect to the Killing form (Gilmore 1974). The second term on the rhs of the Lindblad master equation (4) (the *dissipation term* in what follows) is responsible for the non-unitary character of the open-system evolution and is due to the system–bath interaction. This interaction can be interpreted as a process of weak measurement (Diosi 2006) of operators $\{\hat{X}_i\}_{i=1}^K$, performed on a quantum system, driven by the Hamiltonian (3), and the coupling constant γ_j reflects the strength of the measurement of the observable $\hat{X}_j$. It will be assumed that all the coupling constants are equal, $\gamma_j = \gamma$. This form of the dissipation term in equation (4) is chosen to ensure invariance under the group of unitary transformations, generated by spectrum-generating algebra, which is assumed to be the symmetry of the system–bath interaction. As a paradigm for such open-system dynamics (4) one may consider dynamics of a spin, immersed into an isotropic dissipating environment:

$$\frac{\partial}{\partial t}\hat{\rho} = -\mathrm{i}\omega[\hat{J}_1, \hat{\rho}] - \gamma \sum_{j=1}^{3} [\hat{J}_j, [\hat{J}_j, \hat{\rho}]], \tag{5}$$

where J_i satisfy the commutation relations of the $\mathfrak{su}(2)$: $[\hat{J}_i, \hat{J}_j] = \mathrm{i}\epsilon_{ijk}\hat{J}_k$. Here, the $SU(2)$ group invariance of the dissipation term results from the isotropy of the system–bath interaction.

The solution of the master equation (4) can be represented as a statistical mixture of pure states, evolving according to the stochastic nonlinear Schrödinger equation (sNLSE) (Gisin 1984, Diosi 1988a, Gisin and Percival 1992):

$$d|\psi\rangle = \left\{-\mathrm{i}\hat{H} - \sum_{i=1}^{K}\gamma_j(\hat{X}_i - \langle\hat{X}_i\rangle_\psi)^2\right\}\mathrm{d}t|\psi\rangle + \sum_{i=1}^{K}(\hat{X}_i - \langle\hat{X}_i\rangle_\psi)\,\mathrm{d}\xi_i|\psi\rangle, \tag{6}$$

where the Wiener fluctuation terms $\mathrm{d}\xi_i$ satisfy

$$\langle\mathrm{d}\xi_i\rangle = 0, \qquad \mathrm{d}\xi_i\,\mathrm{d}\xi_j = 2\delta_{ij}\gamma_j\,\mathrm{d}t. \tag{7}$$

The purpose of the present work is to study the asymptotical properties of solutions of the sNLSE (6). We will show that the GCS associated with the spectrum-generating algebra of the system, driven by the Lindblad equation (4), are the globally stable solutions of the associated sNLSE (6). This property means that a group-invariant coupling to a dissipating environment will result in dynamics which can be represented as a statistical mixture of stable trajectories of the GCS, associated with the corresponding algebra.

2. Generalized coherent states and the total uncertainty

Let us assume that the algebra $\mathfrak{g}$ is represented irreducibly on the system's Hilbert space $\mathcal{H}$. Then an arbitrary state $\psi \in \mathcal{H}$ can be represented as a superposition of the *generalized coherent states (GCS)* (Perelomov 1985, Zhang *et al* 1990) $|\Omega, \psi_0\rangle$ with respect to the corresponding dynamical group G and an arbitrary state ψ_0:

$$|\psi\rangle = \int \mathrm{d}\mu(\Omega)|\Omega, \psi_0\rangle\langle\Omega, \psi_0|\psi\rangle, \tag{8}$$

where $\mu(\Omega)$ is the group-invariant measure on the coset space G/H (Gilmore 1974), $\Omega \in G/H$, $H \subset G$ is the maximal stability subgroup of the reference state ψ_0:

$$h|\psi_0\rangle = \mathrm{e}^{\mathrm{i}\phi(h)}|\psi_0\rangle, \qquad h \in H \tag{9}$$

and the GCS $|\Omega, \psi_0\rangle$ are defined as follows:

$$\begin{aligned}\hat{U}(g)|\psi_0\rangle &= \hat{U}(\Omega h)|\psi_0\rangle = \mathrm{e}^{\mathrm{i}\phi(h)}\hat{U}(\Omega)|\psi_0\rangle \\ &\equiv \mathrm{e}^{\mathrm{i}\phi(h)}|\Omega, \psi_0\rangle, \quad g \in G, \quad h \in H, \quad \Omega \in G/H,\end{aligned} \tag{10}$$

where $\hat{U}(g)$ is a unitary transformation generated by a group element $g \in G$.

The group-invariant *total uncertainty* of a state with respect to a compact semisimple algebra $\mathfrak{g}$ is defined as (Delbourgo and Fox 1977, Perelomov 1985)

$$\Delta[\psi] \equiv \langle\hat{\Delta}_\psi\rangle_\psi = \sum_{j=1}^{K}\langle\hat{X}_j^2\rangle_\psi - \sum_{j=1}^{K}\langle\hat{X}_j\rangle_\psi^2, \tag{11}$$

where we have used the notation $\hat{\Delta}_\psi \equiv \sum_i(\hat{X}_i - \langle\hat{X}_i\rangle_\psi)^2$. The first term on the rhs of equation (11) is the eigenvalue of the the Casimir operator of $\mathfrak{g}$ in the (irreducible) Hilbert space representation:

$$\hat{C} = \sum_{j=1}^{K}\hat{X}_j^2 \tag{12}$$

and the second term is the generalized purity (Barnum *et al* 2003) of the state with respect to $\mathfrak{g}$:

$$P_\mathfrak{g}[\psi] \equiv \sum_{j=1}^{K}\langle\hat{X}_j\rangle_\psi^2. \tag{13}$$

Let us define $\Delta_{\min}$ as a minimal total uncertainty of a quantum state and $c_{\mathcal{H}}$ as the eigenvalue of the Casimir operator of $\mathfrak{g}$ in the system Hilbert space. Then

$$\Delta_{\min} \leqslant \Delta[\psi] \leqslant c_{\mathcal{H}}, \tag{14}$$

The total uncertainty (11) is invariant under an arbitrary unitary transformation generated by $\mathfrak{g}$. Therefore, all the GCS with respect to the algebra $\mathfrak{g}$ and a reference state ψ_0 have a fixed value of the total invariance. It has been proved (Delbourgo and Fox 1977) that the minimal total uncertainty $\Delta_{\min}$ is obtained if and only if ψ_0 is the highest (or lowest) weight state of the representation. The value of $\Delta_{\min}$ is given by (Delbourgo and Fox 1977, Klyachko 2002)

$$\Delta_{\min} \equiv (\Lambda, \mu) \leqslant \Delta[\psi] \leqslant (\Lambda, \Lambda + \mu) = c_{\mathcal{H}}, \tag{15}$$

where $\Lambda \in \mathbb{R}^r$ is the highest weight of the representation, $\mu \in \mathbb{R}^r$ is the sum of the positive roots of $\mathfrak{g}$, r is the rank of $\mathfrak{g}$ (Gilmore 1974) and $(\ldots, \ldots)$ is the Euclidean scalar product in $\mathbb{R}^r$. The corresponding GCS were termed the generalized unentangled states with respect to the algebra $\mathfrak{g}$ (Barnum *et al* 2003, Klyachko 2002). The maximal value of the uncertainty is obtained in states termed maximally or completely entangled (Barnum *et al* 2003, Klyachko 2002) with respect to $\mathfrak{g}$. The maximum value equals $c_{\mathcal{H}}$ in the states having $\langle\psi|\hat{X}_j|\psi\rangle^2 = 0$ for all i. Such states exist in a generic irreducible representation (*irrep* in what follows) of an arbitrary compact simple algebra of observables (Klyachko 2002). Generic superpositions of the GCS have larger uncertainty and are termed generalized entangled states with respect to $\mathfrak{g}$ (Barnum *et al* 2003, Klyachko 2002). In what follows, it is assumed that the reference state ψ_0 for the GCS minimizes the total invariance (11).

3. The main result: global stability of the generalized coherent states

3.1. The time evolution of the total uncertainty

The time evolution of the total uncertainty (11) of a pure state evolving according to the sNLSE (6) can be calculated as follows:

$$\begin{aligned} \mathrm{d}\Delta[\psi(t)] &= \mathrm{d}\sum_i \left(\langle\hat{X}_i^2\rangle_\psi - \langle\hat{X}_i\rangle_\psi^2\right) = -\mathrm{d}\sum_i \langle\hat{X}_i\rangle_\psi^2 \\ &= -\sum_i (2\,\mathrm{d}\langle\hat{X}_i\rangle_\psi \langle\hat{X}_i\rangle_\psi + \mathrm{d}\langle\hat{X}_i\rangle_\psi\,\mathrm{d}\langle\hat{X}_i\rangle_\psi), \end{aligned} \tag{16}$$

where we have used prescription of the Ito calculus: $\mathrm{d}(xy) = \mathrm{d}x\,y + x\,\mathrm{d}y + \mathrm{d}x\,\mathrm{d}y$ and the fact that $\mathrm{d}\sum_i \langle\hat{X}_i^2\rangle_\psi = 0$ by the invariance of the Casimir operator (12) under dynamics in an irreducible representation. To calculate $\mathrm{d}\hat{X}_i$ we derive the Heisenberg equations of motion, corresponding to the sNLSE (6).

Equation (6) is equivalent to the following equation for the corresponding projector $\hat{P}_\psi = |\psi\rangle\langle\psi|$:

$$\mathrm{d}\hat{P}_\psi = \left(-\mathrm{i}[\hat{H}, \hat{P}_\psi] - \gamma \sum_{j=1}^{K} [\hat{X}_j, [\hat{X}_j, \hat{P}_\psi]]\right)\mathrm{d}t + \sum_i \{(\hat{X}_i - \langle\hat{X}_i\rangle_\psi)\,\mathrm{d}\xi_i, \hat{P}_\psi\}. \tag{17}$$

Equation (17) implies that the following stochastic Heisenberg equation can be used to calculate the increment $\mathrm{d}\langle\hat{X}_i\rangle$ for an arbitrary operator $\hat{X}_i$:

$$\begin{aligned} \mathrm{d}\hat{X}_i &= \left(\mathrm{i}[\hat{H}, \hat{X}_i] - \gamma \sum_{j=1}^{K} [\hat{X}_j, [\hat{X}_j, \hat{X}_i]]\right)\mathrm{d}t + \sum_j \{(\hat{X}_j - \langle\hat{X}_j\rangle_\psi)\,\mathrm{d}\xi_j, \hat{X}_i\} \\ &= (\mathrm{i}[\hat{H}, \hat{X}_i] - \gamma c_{\mathtt{adj}}\hat{X}_i)\,\mathrm{d}t + \sum_j \{(\hat{X}_j - \langle\hat{X}_j\rangle_\psi)\,\mathrm{d}\xi_j, \hat{X}_i\}, \end{aligned} \tag{18}$$

where $c_{\mathtt{adj}}$ is the quadratic Casimir in the adjoint representation (see equation (12)). Multiplying equation (18) by $\langle \hat{X}_i \rangle_\psi$, summing up over all the observables and computing the expectation value we obtain

$$\begin{aligned}\sum_{i=1}^{K} \langle \hat{X}_i \rangle_\psi \, \mathrm{d}\langle \hat{X}_i \rangle &= \left(\mathrm{i} \sum_{i=1}^{K} \langle \hat{X}_i \rangle_\psi \langle [\hat{H}, \hat{X}_i] \rangle_\psi - \gamma c_{\mathtt{adj}} \sum_{i=1}^{K} \langle \hat{X}_i \rangle_\psi^2 \right) \mathrm{d}t \\ &\quad + \sum_{j,i} \langle \hat{X}_i \rangle_\psi \langle \{ (\hat{X}_j - \langle \hat{X}_j \rangle_\psi) \, \mathrm{d}\xi_j, \hat{X}_i \} \rangle_\psi \\ &= -\gamma c_{\mathtt{adj}} \sum_{i=1}^{K} \langle \hat{X}_i \rangle_\psi^2 \, \mathrm{d}t \\ &\quad + \sum_{i,j=1}^{K} \langle \hat{X}_i \rangle_\psi (\langle \{ \hat{X}_j, \hat{X}_i \} \rangle_\psi - 2 \langle \hat{X}_j \rangle_\psi \langle \hat{X}_i \rangle_\psi) \, \mathrm{d}\xi_j, \end{aligned} \tag{19}$$

where the contribution of the Hamiltonian term has vanished due to the antisymmetry of the structure constants f_{jik} of $\mathfrak{g}$:

$$\begin{aligned}\mathrm{i} \sum_{i,j=1}^{K} a_j \langle \hat{X}_i \rangle_\psi \langle [\hat{X}_j, \hat{X}_i] \rangle_\psi &= \mathrm{i} \sum_{i,j,k=1}^{K} a_j \langle \hat{X}_i \rangle_\psi \langle \mathrm{i} f_{jik} \hat{X}_k \rangle_\psi \\ &= -\sum_{j=1}^{K} a_j \sum_{i,k=1}^{K} f_{jik} \langle \hat{X}_i \rangle_\psi \langle \hat{X}_k \rangle_\psi = 0. \end{aligned} \tag{20}$$

From equation (18) we get

$$\begin{aligned}\mathrm{d}\langle \hat{X}_i \rangle_\psi d\langle \hat{X}_i \rangle_\psi &= \sum_{k,l} \mathrm{d}\xi_k \, \mathrm{d}\xi_l \langle \{ (\hat{X}_k - \langle \hat{X}_k \rangle_\psi), \hat{X}_i \} \rangle_\psi \langle \{ (\hat{X}_l - \langle \hat{X}_l \rangle_\psi), \hat{X}_i \} \rangle_\psi \\ &= 2\gamma \, \mathrm{d}t \sum_{k} \langle \{ (\hat{X}_k - \langle \hat{X}_k \rangle_\psi), \hat{X}_i \} \rangle_\psi^2 \\ &= 2\gamma \, \mathrm{d}t \sum_{k} (\langle \{ \hat{X}_k, \hat{X}_i \} \rangle_\psi - 2 \langle \hat{X}_k \rangle_\psi \langle \hat{X}_i \rangle_\psi)^2. \end{aligned} \tag{21}$$

Inserting equations (21) and (20) into equation (16) we obtain

$$\begin{aligned}\mathrm{d}\langle \hat{\Delta} \rangle_\psi &= -\sum_{i} (2 \, \mathrm{d}\langle \hat{X}_i \rangle_\psi \langle \hat{X}_i \rangle_\psi + \mathrm{d}\langle \hat{X}_i \rangle_\psi \, \mathrm{d}\langle \hat{X}_i \rangle_\psi) \\ &= 2\gamma \left(c_{\mathtt{adj}} \sum_{i=1}^{K} \langle \hat{X}_i \rangle_\psi^2 - \sum_{k,i} (\langle \{ \hat{X}_k, \hat{X}_i \} \rangle_\psi - 2 \langle \hat{X}_k \rangle_\psi \langle \hat{X}_i \rangle_\psi)^2 \right) \mathrm{d}t \\ &\quad - 2 \sum_{j,i} \langle \hat{X}_i \rangle_\psi (\langle \{ \hat{X}_j, \hat{X}_i \} \rangle_\psi - 2 \langle \hat{X}_j \rangle_\psi \langle \hat{X}_i \rangle_\psi) \, \mathrm{d}\xi_j. \end{aligned} \tag{22}$$

The remaining terms in equation (22) describe the effect of the bath (weak measurement) on the total uncertainty of a pure state evolving according to the sNLSE. It can be shown by direct calculation that these terms vanish in a GCS. But a simpler way to show this is to note that the infinitesimal evolution of the state, corresponding to the sNLSE (6) dropping the

Hamiltonian term, is given by

$$|\psi\rangle + |d\psi\rangle = \exp\left\{-2\gamma\hat{\Delta}_\psi\,\mathrm{d}t + \sum_i(\hat{X}_i - \langle\hat{X}_i\rangle_\psi)\,\mathrm{d}\xi_i\right\}|\psi\rangle$$
$$= \exp\left\{\sum_i(\hat{X}_i - \langle\hat{X}_i\rangle_\psi)\,\mathrm{d}\xi_i\right\}\exp\{-2\gamma\hat{\Delta}_\psi\,\mathrm{d}t\}|\psi\rangle$$
$$= \exp\{\phi(t)\}\exp\left\{\sum_i(\hat{X}_i - \langle\hat{X}_i\rangle_\psi)\,\mathrm{d}\xi_i\right\}|\psi\rangle, \tag{23}$$

where we have used the fact (Delbourgo and Fox 1977) that a GCS is an eigenstate of the operator $\hat{\Delta}_\psi$, defined after equation (11). From equation (23) we see that the infinitesimal transformation of the state is driven by the operator *linear* in the generators of the algebra. Therefore, a GCS transforms into a GCS under the infinitesimal evolution[1] and the total uncertainty of the evolving state remains constant (and minimal).

The first term in equation (22), considered as a functional on the Hilbert space, has global maximum in the GCS (Subsection C). Therefore, on average, the rate of uncertainty loss (termed *localization* rate) is minimal in a GCS. In a GCS the second (stochastic) term vanishes. Since the rate of localization is zero in a GCS, as proved above, it follows that the average rate of localization obtains minimum at zero. Therefore, an arbitrary state localizes on average. Since the uncertainty is minimal in a GCS, the localization on average implies that almost every solution of the sNLSE (6) approaches asymptotically a GCS.

3.2. An illustration. $\mathfrak{su}(2)$*-case*

For the purpose of illustration let us consider a quantum system, driven by a $\mathfrak{su}(2)$-algebraic Hamiltonian $\hat{H} = \omega\hat{J}_1$, i.e., a spin. The GCS, associated with the $\mathfrak{su}(2)$ algebra, are the so-called spin-coherent states (Arecchi *et al* 1972) which are characterized by the maximal projection of the spin. A spin-coherent state of the system in the irreducible $(2j+1)$-dimensional Hilbert space representation has the group-invariant uncertainty (11) equal to j, the spin quantum number of the representation. A superposition of GCS has larger uncertainty. For example, a superposition $(|-j\rangle + |j\rangle)/\sqrt{2}$ has uncertainty equal to the maximal possible value $j(j+1)$, i.e., the eigenvalue of the Casimir operator. This follows from the fact that the projection of the spin in this state in any direction vanishes and, as a consequence, its generalized purity (13) is zero.

The Lindblad master equation, corresponding to the weak measurement of the projections of the spin $\hat{J}_i$, is equation (5). Taking $(|-j\rangle+|j\rangle)/\sqrt{2}$ for the initial state, we expect to observe stochastic evolution of a pure-state unraveling of equation (5) according to the corresponding sNLSE (6), approaching asymptotically a spin-coherent state. The spin coherent state will have minimal uncertainty and maximal amplitude of the spin projection.

Figure 1 shows the evolution of the normalized expectation values of the spin projections $\langle\hat{J}_i\rangle/j, i = 1, 2, 3$, for the pure state $\psi(t)$ evolving according to the sNLSE (6), associated with the master equation (5). Initial state of the system is $(|-j\rangle + |j\rangle)/\sqrt{2}$ and the total spin quantum number is $j = 16$. In addition, the normalized total uncertainty $\Delta[\psi]/j^2$ is

[1] This fact does not follow directly from the definition of the GCS, since the evolution in equation (23) is not unitary. Nonetheless, by an application of the Baker–Campbell–Hausdorff disentangling formula (Zhang *et al* 1990) it can be shown that $\forall\,\zeta_i \in \mathbb{C}$ and $\hat{X}_i \in \mathfrak{g}\exp(\sum_i \zeta_i\hat{X}_i)|\Omega,\Lambda\rangle \propto \exp(\sum_\alpha \eta_\alpha\hat{E}_{-\alpha})|\Omega,\Lambda\rangle$ ($\hat{E}_{-\alpha}$ is the lowering operator of the algebra, corresponding to the positive root α), which is a GCS up to a normalization [see Kramer and Saraceno (1981), pp 31–2 for details].

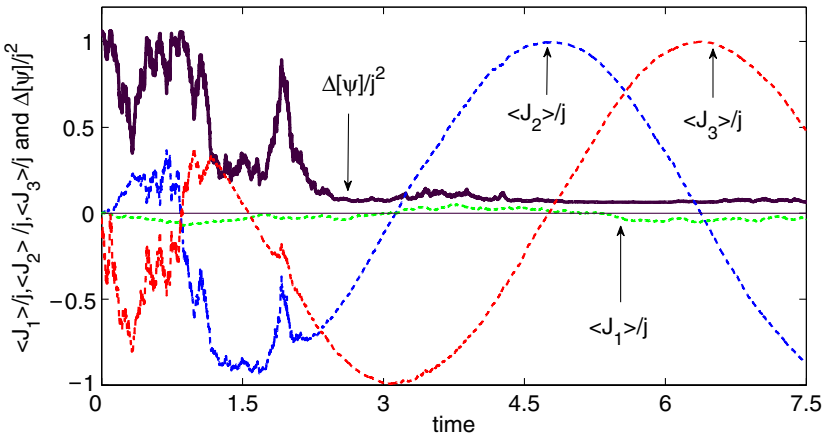

Figure 1. The normalized expectation values of the spin projections $\langle \hat{J}_i \rangle / j, i = 1, 2, 3$ (dashed lines), and the normalized total uncertainty $\Delta[\psi]/j^2$ (solid line) as a function of time. The pure state $\psi(t)$ evolves according to the sNLSE (6), corresponding to the master equation (5). Time is measured in units of ω^{-1} and the spin–bath coupling is $\gamma = \omega/160$. Initial state of the system is $(|-j\rangle + |j\rangle)/\sqrt{2}$ and the total spin quantum number is $j = 16$. The asymptotic solution has minimal (normalized) uncertainty of $1/16$, i.e., it is a spin-coherent state.

plotted as a function of time. The stochastic evolution asymptotically leads to a state having constant value of the (normalized) uncertainty equal to $1/16$, i.e., the minimal value in the representation. It follows therefore that the asymptotic solution is a spin-coherent state.

3.3. The proof of the main result

Next we prove that the first term in equation (22), considered as a functional on the Hilbert space, has global maximum in the GCS. The first sum in this term is just the generalized purity of the state (13), which has a global maximum in a GCS (Barnum *et al* 2003, Klyachko 2008), while the second sum is the trace-norm of the covariance matrix, which obtains global minimum in a GCS.

Theorem. *The trace-norm of the covariance matrix* $M_{ij} = \langle \{\hat{X}_i, \hat{X}_j\} \rangle_\psi - 2\langle \hat{X}_i \rangle_\psi \langle \hat{X}_j \rangle_\psi$ *is minimal in a maximal (minimal) weight state of the irrep, i.e., in a GCS.*

Proof. The trace-norm is invariant under unitary transformations, generated by the algebra $\mathfrak{g}$. Therefore, any orthonormal basis $\hat{X}_i$ can be used for the calculation of the trace-norm. Consider a particular choice of the basis $\hat{X}_i$ such that the projection of the density operator $\hat{\rho} = |\psi\rangle\langle\psi|$ on $\mathfrak{g}$ is contained in the Cartan subalgebra $\mathfrak{h} \subset \mathfrak{g}$. Let us use index i, j for the elements of $\mathfrak{h}$ and α, β for the elements of the root subspace. Then,

$$\mathrm{Tr}\{M^2\} = \sum_{i,j} M_{i,j}^2 + \sum_{i,\alpha} M_{i,\alpha}^2 + \sum_{i,\alpha} M_{\alpha,i}^2 + \sum_{|\alpha|\neq|\beta|} M_{\alpha,\beta}^2 + \sum_{|\alpha|=|\beta|} M_{\alpha,\beta}^2. \tag{24}$$

Let us focus on the last term in equation (24). Since the projection of the state on $\mathfrak{g}$ is contained in the Cartan subalgebra, it vanishes on the root subspace, i.e., $\langle \hat{X}_\alpha \rangle = 0$, for every α. Then

$$\sum_{|\alpha|=|\beta|} M_{\alpha,\beta}^2 = \sum_{|\alpha|=|\beta|} \langle \{\hat{X}_\alpha, \hat{X}_\beta\} \rangle_\psi^2. \tag{25}$$

Using notation $E_{\pm\alpha}$ for the raising and the lowering operators of the algebra, corresponding to the positive root α we obtain

$$\begin{aligned}\sum_{|\alpha|=|\beta|} M_{\alpha,\beta}^2 &= \sum_{|\alpha|=|\beta|} \langle\{\hat{X}_\alpha, \hat{X}_\beta\}\rangle_\psi^2 = -\frac{1}{2}\sum_{\alpha>0}\langle(\hat{E}_\alpha + \hat{E}_{-\alpha})(\hat{E}_\alpha - \hat{E}_{-\alpha})\\ &\quad + (\hat{E}_\alpha - \hat{E}_{-\alpha})(\hat{E}_\alpha + \hat{E}_{-\alpha}))^2 + \sum_{\alpha>0}\langle(\hat{E}_\alpha + \hat{E}_{-\alpha})^2\rangle^2 + \sum_{\alpha>0}\langle(\hat{E}_\alpha - \hat{E}_{-\alpha})^2\rangle^2\\ &= -2\sum_{\alpha>0}\left\langle\hat{E}_\alpha^2 - \hat{E}_{-\alpha}^2\right\rangle^2 + \sum_{\alpha>0}\left\langle\hat{E}_\alpha^2 + \hat{E}_{-\alpha}^2 + \hat{E}_\alpha\hat{E}_{-\alpha} + \hat{E}_{-\alpha}\hat{E}_\alpha\right\rangle^2\\ &\quad + \sum_{\alpha>0}\left\langle\hat{E}_\alpha^2 + \hat{E}_{-\alpha}^2 - \hat{E}_\alpha\hat{E}_{-\alpha} - \hat{E}_{-\alpha}\hat{E}_\alpha\right\rangle^2\\ &= -2\sum_{\alpha>0}\left\langle\hat{E}_\alpha^2 - \hat{E}_{-\alpha}^2\right\rangle^2 + 2\sum_{\alpha>0}\left\langle\hat{E}_\alpha^2 + \hat{E}_{-\alpha}^2\right\rangle^2 + 2\sum_{\alpha>0}\langle\hat{E}_\alpha\hat{E}_{-\alpha} + \hat{E}_{-\alpha}\hat{E}_\alpha\rangle^2\\ &= 8\sum_{\alpha>0}\left\langle\hat{E}_\alpha^2\right\rangle\langle\hat{E}_{-\alpha}^2\rangle + 2\sum_{\alpha>0}\langle\hat{E}_\alpha\hat{E}_{-\alpha} + \hat{E}_{-\alpha}\hat{E}_\alpha\rangle^2. \end{aligned} \tag{26}$$

The density operator $\hat{\rho} = |\psi\rangle\langle\psi|$ can be expressed in the basis of the eigenstates $|\mu\rangle$ of the Cartan operators $\hat{X}_i \in \mathfrak{h}$, $\hat{X}_i|\mu\rangle = \mu_i|\mu\rangle$

$$\hat{\rho} = \sum_{\mu,\mu'} c_\mu c_{\mu'}^* |\mu\rangle\langle\mu'|. \tag{27}$$

Then the last term in equation (26) obtains

$$\begin{aligned}2\sum_{\alpha>0}\langle\hat{E}_\alpha\hat{E}_{-\alpha} + \hat{E}_{-\alpha}\hat{E}_\alpha\rangle^2 &= 2\sum_{\alpha>0}\left(\sum_{\mu,\mu'} c_\mu c_{\mu'}^*\langle\mu'|\hat{E}_\alpha\hat{E}_{-\alpha} + \hat{E}_{-\alpha}\hat{E}_\alpha|\mu\rangle\right)^2\\ &= 2\sum_{\alpha>0}\left(\sum_{\mu}|c_\mu|^2\langle\mu|\hat{E}_\alpha\hat{E}_{-\alpha} + \hat{E}_{-\alpha}\hat{E}_\alpha|\mu\rangle\right)^2. \end{aligned} \tag{28}$$

States $|\mu + k\alpha\rangle$ form an irreducible representation of the $\mathfrak{su}(2)$, spanned by

$$E^\pm \equiv E_{\pm\alpha}/|\alpha| \qquad E_3 \equiv \alpha\cdot\hat{H}/|\alpha|^2, \qquad \hat{H}_i \equiv \hat{X}_i \in \mathfrak{h} \tag{29}$$

obeying $\mathfrak{su}(2)$ commutation relations (Georgi 1982)

$$[E_3, E^\pm] = \pm E^\pm; \qquad [E^+, E^-] = E_3. \tag{30}$$

Therefore, the state $|\mu\rangle$ can be labeled as $|m_\alpha, j_\alpha\rangle$, where j_α is the maximal weight of the corresponding irrep of the $\mathfrak{su}(2)$ and m_α is the weight, corresponding to the state $|\mu\rangle$ in the irrep. Then,

$$\begin{aligned}\langle\hat{E}_{-\alpha}\hat{E}_\alpha + \hat{E}_\alpha\hat{E}_{-\alpha}\rangle_\psi^2 &= |\alpha|^4\langle 2\hat{E}^-\hat{E}^+ + \hat{E}_3\rangle_\psi^2 = |\alpha|^4\langle m_\alpha, j_\alpha|2\hat{E}^-\hat{E}^+ + \hat{E}_3|m_\alpha, j_\alpha\rangle^2\\ &= |\alpha|^4(j_\alpha + j_\alpha^2 - m_\alpha^2)^2. \end{aligned} \tag{31}$$

The term (31) obtains minimum in the maximal (minimal) weight state of the j_α irrep, corresponding to $m_\alpha = j_\alpha (m_\alpha = -j_\alpha)$. Therefore, $|m_\alpha, j_\alpha\rangle$ is annihilated by the $E^+(E^-)$, and, by equations (29), the state $|\mu\rangle$ is annihilated by $E_\alpha(E_{-\alpha})$. The minimum of the sum (29) is obtained in the state, annihilated by $E_\alpha(E_{-\alpha})$ for all positive roots α, i.e., in the maximal (minimal) weight state $\hat{\rho} = |\Lambda\rangle\langle\Lambda|$. The first term in equation (26) is nonnegative and vanishes at $|\psi\rangle = |\Lambda\rangle$, therefore it obtains minimum at $|\Lambda\rangle$. Therefore, the term (26) in the sum (24) obtains minimum at $|\Lambda\rangle$. Since $|\Lambda\rangle$ is an eigenstate of every Cartan operator $\hat{X}_i$, the first term

in equation (24) vanishes at $|\Lambda\rangle$. For the same reason and the fact that the projection of $\hat{\rho}$ on the root subspace vanishes both the second and the third terms in equation (24) also vanish at $|\Lambda\rangle$. The fourth term in equation (24) vanishes at $|\Lambda\rangle$ since $\langle\Lambda|\hat{E}_\alpha\hat{E}_\beta|\Lambda\rangle = 0, \forall|\alpha| \neq |\beta|$. Since all these terms are nonnegative, they obtain minimum at the maximal (minimal) weight state $\hat{\rho} = |\Lambda\rangle\langle\Lambda|$. Therefore, the whole expression (24) for the trace-norm of the covariance matrix obtains minimum at $\hat{\rho} = |\Lambda\rangle\langle\Lambda|$. □

4. Conclusions

The globally stable solutions of quantum dynamics modeled by the stochastic nonlinear Schrödinger equation (6) are the generalized coherent states, associated with the spectrum-generating algebra of the system. Stable solutions of the sNLSE in the case of Heiseberg–Weyl algebra have been obtained before (Diosi 1988b, Halliwell and Zoupas 1995, Schack *et al* 1995). Our result refers to a compact semisimple spectrum-generating algebra. The description by the stochastic nonlinear Schrödinger equation is equivalent to Lindblad semi-group modeling of the process of group-invariant weak measurement of the elements of the algebra. The Hamiltonian of the system is linear in the algebra elements, i.e., possesses dynamical symmetry. It is conjectured that breaking the symmetry by adding nonlinearity to the Hamiltonian results in the asymptotically stable localized solutions of the corresponding sNLSE (see (Khasin and Kosloff 2008) for some numerical evidence). The proof of stability is based on proving that the trace-norm of the covariance matrix, associated with the algebra, becomes minimal in a generalized coherent state.

Acknowledgments

This work is supported by DIP and the Israel Science Foundation (ISF). The Fritz Haber Center is supported by the Minerva Gesellschaft für die Forschung GmbH München, Germany.

References

Arecchi F, Courtens E, Gilmore R and Thomas H 1972 *Phys. Rev.* A **6** 2211
Barnum H, Knill E, Ortiz G and Viola L 2003 *Phys. Rev.* A **68** 032308
Bohm A, Neeman Y and Barut A O 1988 *Dynamical Groups and Spectrum Generating Algebras* (Singapore: World Scientific)
Breuer H P and Petruccione F 2002 *Open Quantum Systems* (Oxford: Oxford University Press)
Delbourgo R and Fox J R 1977 *J. Phys A: Math. Gen.* **10** L233
Diosi L 1988a *Phys. Lett.* A **129** 419
Diosi L 1988b *Phys. Lett.* A **132** 233
Diosi L 2006 *Encyclopedia of Mathematical Physics* (Weak Measurements in Quantum Mechanics vol 4) ed J-P Francoise, G L Naber and S T Tsou (Oxford: Elsevier) pp 276–82
Georgi H 1982 *Lie Algebras in Particle Physics: From Isospin to Unified Theories* (Reading, MA: Benjamin)
Gilmore R 1974 *Lie Groups, Lie Algebras and Some of Their Applications* (New York: Wiley)
Gisin N 1984 *Phys. Rev. Lett.* **52** 1657
Gisin N and Percival I C 1992 *J. Phys A: Math. Gen.* **25** 56775
Halliwell J and Zoupas A 1995 *Phys. Rev.* D **52** 7294
Iachello F 2006 *Lie Algebras and Applications* (Berlin: Springer)
Iachello F and Levine R 1995 *Algebraic Theory of Molecules* (Oxford: Oxford University Press)
Khasin M and Kosloff R 2008 *Phys. Rev.* A **78** 012321
Klyachko A 2008 *Preprint* arXiv:0802.4008
Klyachko A A 2002 *Preprint* quant-ph/0206012

Kramer P and Saraceno M 1981 *Geometry of the Time-Dependent Variational Principle in Quantum Mechanics* (Berlin: Springer)
Lindblad G 1976 *Commun. Math. Phys.* **48** 119
Perelomov A 1985 *Generalized Coherent States and their Applications* (Berlin: Springer)
Schack A, Brun T A and Percival I C 1995 *J. Phys A: Math. Gen.* **28** 5401
Zhang W, Feng D H and Gilmore R 1990 *Rev. Mod. Phys.* **62** 867

4.4 An Algorithm for Simulation of a Many-Body Dynamics using Dynamical Coarse-Graining.

4.4.1 Introduction

Simulation of quantum many-body dynamics is a challenging task (Kohn, 1999). The computational resources of a direct solution scale with the size of the Hilbert space. The effective Hilbert space dimension of a typical many-body system is huge, practically eliminating any direct approach to simulation of the dynamics. Typical approximate solutions rely on limiting the extent of quantum many-body correlations, i.e., mean-field approaches. An alternative is to restrict the scope of the simulation to a subset of observables. In the present Section we describe a method of simulation which is restricted to a subset of dynamical observables. This restriction allows to develop an efficient and converged algorithm for the dynamics of this restricted set.

To demonstrate the approach we apply the algorithm to the simulation of the dynamics of $N = 2*10^4$ cold atoms in a double-well trap. The system is modeled by the two-site Bose-Hubbard model (Mahan, 2000) with the Hamiltonian:

$$\hat{\mathrm{H}} = -\Delta \sum_{i=1,2} (\hat{\mathrm{a}}_{i+1}^{\dagger}\hat{\mathrm{a}}_i + \hat{\mathrm{a}}_i^{\dagger}\hat{\mathrm{a}}_{i+1}) + \frac{U}{2N}\sum_{i=1,2}(\hat{\mathrm{a}}_i^{\dagger}\hat{\mathrm{a}}_i)^2, \tag{4.1}$$

where $\hat{\mathrm{a}}_i$ ($\hat{\mathrm{a}}_i^{\dagger}$) is the creation (annihilation) operator of a particle in the i-th well. Δ describes the hopping rate and U scales the two-body interaction. The transformation to the operators

$$\begin{aligned} \hat{\mathrm{J}}_x &= \frac{1}{2}(\hat{\mathrm{a}}_1^{\dagger}\hat{\mathrm{a}}_2 + \hat{\mathrm{a}}_2^{\dagger}\hat{\mathrm{a}}_1) \\ \hat{\mathrm{J}}_y &= \frac{1}{2i}(\hat{\mathrm{a}}_1^{\dagger}\hat{\mathrm{a}}_2 - \hat{\mathrm{a}}_2^{\dagger}\hat{\mathrm{a}}_1) \\ \hat{\mathrm{J}}_z &= \frac{1}{2}(\hat{\mathrm{a}}_1^{\dagger}\hat{\mathrm{a}}_1 - \hat{\mathrm{a}}_2^{\dagger}\hat{\mathrm{a}}_2) \end{aligned} \tag{4.2}$$

leads to the following Lie-algebraic form of the Hamiltonian

$$\hat{\mathrm{H}} = -\omega\hat{\mathrm{J}}_x + \frac{U}{N}\hat{\mathrm{J}}_z^2, \tag{4.3}$$

where $\omega = 2\Delta$. The set of single-particle operators $\{\hat{\mathrm{J}}_x, \hat{\mathrm{J}}_y, \hat{\mathrm{J}}_z\}$ is closed under the commutation relation and spans the $\mathfrak{su}(2)$ spectrum-generating algebra (Bohm *et al.*, 1988) of the system. The observables: $\hat{\mathrm{J}}_x, \hat{\mathrm{J}}_y, \hat{\mathrm{J}}_z$ are the target of the dynamical simulation, representing coherence, current and population difference between the wells.

The Hilbert space of the system of N atoms carries the $N+1$ dimensional irreducible representation (Zhang *et al.*, 1990) of the the spectrum-generating $\mathfrak{su}(2)$ algebra, corresponding to the pseudo-spin quantum number $j = N/2$. A direct numerical propagation of the corresponding Schrödinger equation requires multiplication of the $N+1$-dimensional state vector of the system by the $(2N+1) \times (2N+1)$ matrix of the Hamiltonian. In order to propagate to a time scale of ω^{-1} $O(N)$ such multiplications are needed. As a result, the propagation of the state vector requires $O(N^3)$ elementary operations from which any expectation value can be calculated (Kosloff, 1988). The memory resources for the storage of the $(2N+1) \times (2N+1)$ matrices with the double precision is $O(10N^2)$ bytes. Taking $N = 2 * 10^4$ brings the memory requirements to the edge of the $2Gb$ RAM capacity of a regular modern computer. Having $N = 10^5$ will make it prohibitive to store the Hamiltonian matrix in the RAM. The challenge of an efficient simulation is that the computational resources become independent of the Hilbert space dimension.

The basic idea of the current algorithm relies on the close connection between the algebra of observables and the generalized coherent states which minimize the generalized uncertainty with respect to these observables. These states serve as dynamical basis functions for expanding the state of the system. The second ingredient is to replace the original unitary dynamics generated by Eq. (4.3) by by a certain surrogate dynamics. The surrogate dynamics is an open-system dynamics, corresponding to a weak measurement performed on the original system. This substitution is realized by averaging the dynamics generated by the *stochastic nonlinear Schrödinger equation*(sNLSE)(Gisin, 1984; Diosi, 1988b; Gisin & Percival, 1992)over the stochastic realizations. The sNLSE corresponds to a single realization of the the process of weak measurement of the elements of the spectrum generating algebra (4.2) performed on the system, evolving under the Hamiltonian (4.3). If the measurement is sufficiently strong, the computational complexity of the sNLSE is dramatically smaller than complexity of solving the corresponding Schrödinger equation. As a consequence, the numerical solution of the sNLSE becomes practical.

The expectation values of observables are obtained by averaging over the stochastic realizations. The number of realizations for a prescribed relative error is independent of N, therefore asymptotically the complexity of the simulation is determined by the cost of solving the sNLSE. The parameter of the sNLSE, corresponding to the strength of the measurement, is lowered until the open dynamics of the single-particle observables (4.2) converges to the original *unitary* dynamics, driven by the Hamiltonian (4.3). It is shown that a convergent solution is obtained at the values of the measurement strength sufficient for a drastic reduc-

tion of the computational complexity of the sNLSE, compared to the Schrödinger equation.

The reduction of the computational complexity is achieved by virtue of the localization of the solution of the sNLSE of the system in the corresponding phase space under the action of the measurement as explained in Sections 4.2 and 4.3. On the level of the density matrix the localization leads to a coarse-graining of the phase-space representation of the state, destructing the fine structure but leaving unaffected the dynamics of smooth observables, such as the single-particle observables.

The localization of the sNLSE solution is equivalent to compression of the effective Hilbert space of the system. The multiplication of $N \times 1$ state vector by a $N \times N$ matrix necessary for the propagation of the Schrödinger equation, is replaced by multiplication of $M \times 1$ state vector by a $M \times M$ matrix, where the number $M \ll N$ is asymptotically independent on N. In the application, considered in Section 4.4.3, $M \approx 3 * 10^{-3} N$. This spectacular compression of the computational basis results in dramatic speed-up of the computation by the order of 10^3 and reduction of the involved RAM resources by the factor of 10^5.

Section 4.4.2 outlines the basic ideas in the foundation of the algorithm. It summarizes the main results of Sections 4.2 and 4.3 and applies them to construction of an algorithm for simulation of quantum dynamics, driven by the $\mathfrak{su}(2)$-Hamiltonians.

Section 4.4.3 focuses on the application of the algorithm to the Bose-Hubbard model. Discussion and conclusions are presented in Section 4.4.4.

4.4.2 The algorithm

Generalal considerations

The algorithm for simulation of a many-body quantum dynamics, is based on the following sequence of steps (Section 4.2):

1. The choice of the time-dependent computational basis, built of the generalized coherent states (GCS), associated with the spectrum-generating algebra (SGA) of the system.

2. The choice of the elements of the SGA of the system as the distinguished set of observables for the simulation.

3. Numerical solution of the stochastic Nonlinear Schrödinger Equation (sNLSE), corresponding to the weak measurement of the elements of the SGA, performed on the evolving system.

4. Averaging of the expectation values of the SGA observables over many different stochastic realizations.

5. Decreasing the strength of measurement until convergence is obtained to the unitary evolution of the SGA observables.

The choice of the time-dependent basis The motivation for the algorithm is the following definition of the efficient simulation of a quantum many-body dynamics:

Definition: *The simulation of dynamics of a Lie algebra of observables of the system is efficient if and only if the necessary memory and the CPU resources for the computation do not depend on the Hilbert space (irreducible) representation of the algebra.*

An example of efficient simulation is the solution of the Heisenberg equations of motion for the algebra elements, when the Hamiltonian is itself an element of the algebra. Another example is a mean field solution of the quantum dynamics, i.e., solution of the variational equations of motion for the ansatz, parametrized by the expectation values of the operators, belonging to the algebra (Kramer & Saraceno, 1981).

The starting point for the algorithm is the assumption that a reduction of the computational complexity is achieved by using a time-dependent basis of a small number of states. It is further assumed that the many-body Hamiltonian is given in terms of the spectrum-generating algebra $SGA = span\left\{\hat{\mathrm{X}}_i\right\}$ of the system as in Eq.(4.3).

A necessary ingredient of a simulation scheme is a calculation of the matrix elements of the Hamiltonian in the time-dependent basis. Let $\psi_i(t)$ be the time-dependent computational basis. Let the Hilbert space dimension be n. Then the state vector of the system becomes

$$|\Psi(t)\rangle = \sum_{i=1}^{M} c_i(t)\,|\psi_i(t)\rangle = \sum_{i=1}^{M} c_i(t)\hat{\mathrm{U}}_i(t)\,|\psi_i(0)\rangle\,, \tag{4.4}$$

where $M \leq n$ and $\hat{\mathrm{U}}_i(t)$ is a nonunique time-dependent unitary transformation of the reference state $\psi_i(0)$. An efficient computation of the matrix elements of the Hamiltonian in the time-dependent basis $\left\langle \psi(t)_i \left| \hat{\mathrm{H}} \right| \psi(t)_j \right\rangle$ implies that the following transformation is performed efficiently:

$$\hat{\mathrm{H}} \rightarrow \hat{\mathrm{U}}_i(t)\hat{\mathrm{H}}\hat{\mathrm{U}}_j(t) \tag{4.5}$$

and, in particular, the unitary transformation

$$\hat{\mathrm{H}} \rightarrow \hat{\mathrm{U}}_i(t)\hat{\mathrm{H}}\hat{\mathrm{U}}_i(t). \tag{4.6}$$

is performed efficiently. By the assumption, the Hamiltonian is given as a function of the SGA operators $\hat{\mathrm{X}}_i$. Efficient transformation (4.6) implies that the transformation of $\hat{\mathrm{X}}_i$ under the action of $\hat{\mathrm{U}}_j(t)$ is performed efficiently. It follows that $\hat{\mathrm{U}}_j(t)$ is generated by the SGA itself. Each $\psi_i(t)$ is an orbit of the reference state $\psi_i(0)$ under the action of the SGA. According to the definition (Perelomov, 1985; Zhang *et al.*, 1990) the $\psi_i(t)$ is a *generalized coherent state* (GCS), associated with the SGA and the reference state $\psi_i(0)$. Therefore, the time-dependent computational basis is a basis of the GCS, associated with the SGA of the system.

The choice of the reference states $\psi_i(0)$ affects the computational complexity of the simulation. The matrix elements $\left\langle \psi_i(0) \left| \hat{\mathrm{H}} \right| \psi_j(0) \right\rangle$ and, therefore, the matrix elements $\left\langle \psi_i(0) \left| \hat{\mathrm{X}}_k \right| \psi_j(0) \right\rangle$ must be computed efficiently. Generally, complexity of the computation of $\left\langle \psi_i(0) \left| \hat{\mathrm{X}}_k \right| \psi_j(0) \right\rangle$ will depend on the Hilbert space representation of the SGA. Nonetheless, if the reference state $\psi_i(0)$ is chosen as the maximal (minimal) weight state of the representation, the computation can be performed group-theoretically (Zhang *et al.*, 1990), i.e., efficiently. These considerations lead to the choice of the basis of the GCS, associated with the SGA of the system and the maximal(minimal) weight state of the representation, as the time-dependent computational basis.

The choice of the SGA observables for the simulation Given the ansatz (4.4) computation of the expectation value of an observables $\hat{\mathrm{X}}$ demands computing of $\left\langle \hat{\mathrm{X}} \right\rangle = \left\langle \psi(t)_i \left| \hat{\mathrm{X}} \right| \psi(t)_j \right\rangle$, i.e., performing the transformation

$$\hat{\mathrm{X}} \rightarrow \hat{\mathrm{U}}_i(t) \hat{\mathrm{X}} \hat{\mathrm{U}}_j(t). \tag{4.7}$$

In the previous subsection we found that $\hat{\mathrm{U}}_i(t)$ is generated by the SGA. For efficient computation of $\left\langle \hat{\mathrm{X}} \right\rangle$ it is necessary that the transformation (4.7) is independent on the Hilbert space representation of the SGA. It follows that $\hat{\mathrm{X}}$ must be of the form:

$$\hat{\mathrm{X}} = \sum_{i=1}^{K} a_i \hat{\mathrm{X}}_i + \sum_{ij} b_{ij} \hat{\mathrm{X}}_i \hat{\mathrm{X}}_j + \ldots \sum_{i_1, i_2, \ldots i_L} c_{i_1, i_2, \ldots i_L} \prod_{j=1}^{L} \hat{\mathrm{X}}_{i_j}, \tag{4.8}$$

where each $1 \leq i_j \leq K = \mathtt{dim}\{SGA\}$ and L is a fixed number, independent on the representation of the SGA. In particular, the Hamiltonian of the system must have this form in order that an efficient simulation be possible. The elements $\hat{\mathrm{X}}_i$ of the SGA is the simplest choice of observables of the form (4.8).

Solving the stochastic Nonlinear Schrödinger Equation For efficient simulation it is necessary that M in Eq.(4.4) be independent of the Hilbert space

representation of the SGA. This implies in particular that $M \ll n$ as $n \to \infty$. Generic Hamiltonian, nonlinear in the SGA elements, is expected to take an initial state of a many-body system to a state Eq.(4.4), corresponding to $M = O(n)$. Therefore, a generic unitary dynamics cannot be simulated efficiently.

A possible solution has been proposed in Section 4.2: a pertinent open-system dynamics can be found, approximating the unitary dynamics modulo the expectation values of the restricted set of observables − the elements of the SGA. The open-system dynamics corresponds to the process of weak measurement of the elements of the SGA, performed on the system of interest, evolving under the action of the original Hamiltonian.

The open-system evolution can be simulated using stochastic unraveling of the evolving density operator into pure-state evolutions (quantum trajectories), governed by the stochastic Nonlinear Schrödinger equation (sNLSE)(Gisin, 1984; Diosi, 1988b; Gisin & Percival, 1992). The pure state, evolving along a quantum trajectory, can be expressed in the form Eq.(4.4), corresponding to $M \ll n$, provided the measurement is sufficiently strong.

Averaging The expectation values of the SGA observables are calculated along the quantum trajectory for each stochastic realization of the sNLSE. Averaging over the stochastic realizations recovers the open-system dynamics of the observables. The number of realizations necessary for convergence of the averaged values to a given relative error is independent of the Hilbert space representation of the SGA. Therefore, the averaging can be performed efficiently.

Convergence to the unitary evolution As the strength of the measurement decreases the open-system dynamics of the SGA observables converges to their original unitary dynamics. If the classicality condition (Section 4.2) is satisfied, the open system follows the evolution on widely separated time-scales. Due to this time-scales separation the open-system dynamics of the SGA observables converges to the unitary evolution at the value of the measurement strength which is sufficient to ensure that $M \ll n$ in the expansion (4.4) of the pure-state solution of the corresponding sNLSE. Therefore, the unitary evolution of the SGA observables can be simulated at comparatively low computational cost. The question when and whether this reduction of the computational complexity amounts to an efficient simulation is left for Section 4.4.4.

A linear implementation

The algorithm outlined in the previous subsection can be implemented in a variety of ways. This is in part due to the non uniqueness of the transformations $\hat{\mathrm{U}}_i(t)$ in

Eq.(4.4) of the computational basis elements. In the present implementation we adopt the choice $\hat{\mathrm{U}}_i(t) = \hat{\mathrm{U}}_j(t) = \hat{\mathrm{U}}(t)$, leading to the term *linear implementation*. In the linear implementation the pure-state solution of the sNLSE is represented by

$$|\Psi(t)\rangle = \sum_{i=1}^{M} c_i(t)\hat{\mathrm{U}}(t)\,|\psi_i(0)\rangle\,, \tag{4.9}$$

where $\psi_i(0)$ is a fixed set of the GCS, associated with the SGA and a maximal(minimal) weight state of the Hilbert space representation of the algebra.

The advantage of this choice is that the numerical effort is reduced to solving a system of linear equations. This explains the term. The disadvantage is that the number of the elementary computer operations will necessarily depend on the Hilbert space dimension for reasons discussed in Section 4.4.4. Therefore, the linear implementation cannot in principle lead to an efficient simulation in the strict sense of our definition. Still, as will be demonstrated in Section 4.4.3, the reduction of the computational complexity can be so dramatic, that the simulation of the many-body dynamics becomes feasible in the case where solving the Schrödinger equation is unpractical.

An infinitesimal time step of the simulation is represented as a superposition of a linear transformation $\hat{\mathrm{T}}_1$ of the state represented in the fixed instantaneous basis, i.e., the transformation of the vector c_i in Eq.(4.9) and a subsequent unitary transformation $\hat{\mathrm{T}}_2$ of the basis itself. The transformation $\hat{\mathrm{T}}_1$ corresponds to the physical (measurable) evolution of the state, driven by the sNLSE. The transformation $\hat{\mathrm{T}}_2$ serves to set the origin of the linear transformation $\hat{\mathrm{T}}_1$ at the subsequent time step. $\hat{\mathrm{T}}_2$ ensures that the evolving state remains localized in the Hilbert subspace spanned by the instantaneous basis. Connection of the infinitesimal unitary transformation $\hat{\mathrm{T}}_2$ to $\hat{\mathrm{U}}(t)$ in Eq.(4.9) is established by the following relation:

$$T_2 = \hat{1} - \hat{\mathrm{U}}(t)'dt. \tag{4.10}$$

The time-dependent basis is chosen from the GCS, associated with the SGA as argued above. It is interesting that the updating of the basis can be viewed as an analog of the Schmidt decomposition (Peres, 1998) in the generalized entanglement setting (Barnum *et al.*, 2003).

Application to the $\mathfrak{su}(2)$ spectrum-generating algebra

The algorithm presented above can be given an intuitive geometric meaning in the special case of the SGA spanned by the operators $\hat{\mathrm{J}}_x$, $\hat{\mathrm{J}}_y$ and $\hat{\mathrm{J}}_z$ satisfying the

commutation relations

$$\left[\hat{\mathrm{J}}_i, \hat{\mathrm{J}}_j\right] = i\epsilon_{ijk}\hat{\mathrm{J}}_k, \tag{4.11}$$

of the $\mathfrak{su}(2)$ algebra. Examples of a many-body quantum system with the $\mathfrak{su}(2)$ SGA include the Lipkin-Meshkov-Glick model of interacting fermions (Lipkin *et al.*, 1965) and cold bosonic atoms in the double-well trap (Vardi & Anglin, 2000; Trimborn *et al.*, 2008) among others (Bohm *et al.*, 1988).

The GCS of the $\mathfrak{su}(2)$ are represented by points in the phase space, associated with the algebra (Arecchi *et al.*, 1972). The phase-space globally is a two-dimensional sphere and the GCS are parametrized by spherical coordinates, for example by the azimuthal and the polar angles. The $2j+1$ dimensional Hilbert space, carrying an irreducible representation of the algebra, is spanned by a linearly independent basis of GCS, represented by $2j+1$ points on the sphere. A localized state can be expanded in a small fraction of the total basis, represented by points inside a relatively small portion of the phase-space.

The corresponding sNLSE has the following structure:

$$\begin{aligned} d\left|\psi\right\rangle &= \left\{-i\hat{\mathrm{H}} - \gamma\sum_{i=1}^{3}\left(\hat{\mathrm{J}}_i - \left\langle\hat{\mathrm{J}}_i\right\rangle_\psi\right)^2\right\} dt\left|\psi\right\rangle \\ &+ \sum_{i=1}^{3}\left(\hat{\mathrm{J}}_i - \left\langle\hat{\mathrm{J}}_i\right\rangle_\psi\right) d\xi_i\left|\psi\right\rangle, \end{aligned} \tag{4.12}$$

where $\hat{\mathrm{H}}$ is the Hamiltonian of the system and where the Wiener fluctuation terms $d\xi_i$ satisfy

$$< d\xi_i >= 0, \quad d\xi_i d\xi_j = 2\gamma\delta_{ij}dt. \tag{4.13}$$

The parameter γ is the strength of the measurement of elements $\hat{\mathrm{J}}_x$, $\hat{\mathrm{J}}_y$ and $\hat{\mathrm{J}}_z$ of the spectrum-generating $\mathfrak{su}(2)$ algebra of the system.

A Hamiltonian nonlinear in $\hat{\mathrm{J}}_x$, $\hat{\mathrm{J}}_y$ and $\hat{\mathrm{J}}_z$ leads to delocalization an initially localized state. The non unitary stochastic contribution of the evolution due to the measurement, leads to a localization(Section 4.3). Therefore, a single stochastic realization of the open system evolution can be viewed as a small spot on the sphere, involving each instant a small fraction of the GCS, moving stochastically in the phase space.

The infinitesimal linear transformation $\hat{\mathrm{T}}_1$ includes two parts: the original Hamiltonian part and the non unitary part, which contains a stochastic and a deterministic element. Both elements depend on the instantaneous state of the system. Therefore, while the infinitesimal transformation $\hat{\mathrm{T}}_1$ is a linear transformation, the superposition of these transformations is described by the nonlinear

Eq.(4.12). The infinitesimal linear transformation $\hat{\mathrm{T}}_1$ is performed on the instantaneous state of the system represented by a superposition of the states of the instantaneous fixed basis of the GCS.

The GCS basis must be updated at each time step. Practically a different but physically equivalent transformation has been found to be more convenient. Instead of updating the basis to match the evolving state we update the state to match the fixed basis. Therefore, the unitary transformation $\hat{\mathrm{T}}_2$ is performed on the state itself and the inverse transformation $\hat{\mathrm{T}}_2^{-1}$ – on the Hamiltonian and other observables. The unitary transformation $\hat{\mathrm{T}}_2$ is generated by the $\mathfrak{su}(2)$ elements $\hat{\mathrm{J}}_x$, $\hat{\mathrm{J}}_y$ and $\hat{\mathrm{J}}_z$ and rotates the state to the position localized in the fixed basis of the GCS.

Without loss of generality an initial state can be assumed to be localized about a south pole of the phase space having zero expectation values of the operators $\hat{\mathrm{J}}_x$ and $\hat{\mathrm{J}}_z$. An infinitesimal transformation $\hat{\mathrm{T}}_1$ takes the state into a new position having finite expectation values of $\hat{\mathrm{J}}_x$ and $\hat{\mathrm{J}}_z$. The purpose of the unitary transformation $\hat{\mathrm{T}}_2$ is to rotate the state back to the position with vanishing expectation values of $\hat{\mathrm{J}}_x$ and $\hat{\mathrm{J}}_z$. This rotation is performed by the $SU(2)$ group transformation and is equivalent to rotating of the density operator in the Hilbert-Schmidt space to ensure that the projection of the density operator on the algebra is spanned by the $\hat{\mathrm{J}}_z$ operator. This procedure is analogous to the Schmidt-decomposition of the state in the generalized entanglement setting (Barnum *et al.*, 2003) as pointed out above.

The back-rotation of the operators by the inverse transformation $\hat{\mathrm{T}}_2^{-1}$ can be performed analytically, knowing how the $\mathfrak{su}(2)$ algebra elements transform under the $SU(2)$ group itself.

The superposition of the two transformations $\hat{\mathrm{T}}_2 \circ \hat{\mathrm{T}}_1$ of the state results in a new state, still localized about the south pole. The convergence of the computation to the exact *open-system-dynamics* solution is obtained by increasing the size of the GCS basis until the evolution of the single-particle observables has ceased to change. The convergence of computation to the exact *unitary* evolution of the single-particle observables is obtained by decreasing the strength of the measurement until the evolution of the single-particle observables has ceased to be affected.

4.4.3 Application to the two-site Bose-Hubbard model

Introduction

The gas of cold atoms (bosons) in a double-well trap (Schumm *et al.*, 2005; Gati *et al.*, 2006) is described by the two-site Bose-Hubbard model. The Hamiltonian

(4.1) contains two terms: the one-body (linear) term responsible for the hopping of the atoms from one well to another and the two-body (nonlinear) or interaction term responsible for the on-site attraction or repulsion of the atoms. In the present application we consider repulsive interaction, measured by the coupling strength $2U/N$, where N is the total number of particles in the trap. The hopping rate is fixed by the coefficient Δ of the one-body part.

The spectrum-generating algebra of the system is the $\mathfrak{su}(2)$ algebra of the single-particle operators (4.2). The system of N particles correspond to the $N+1$-dimensional irreducible representation of the algebra with the principle pseudo-spin quantum number $j = N/2$. Condensed state of the system is a generalized coherent state (Tikhonenkov *et al.*, 2007; Trimborn *et al.*, 2008), associated with the algebra, termed spin-coherent states in the literature (Arecchi *et al.*, 1972; Zhang *et al.*, 1990; Viera & Sacramento, 1995).

The character of dynamics at fixed N depends essentially on a single parameter: $U/2\omega$ (Vardi & Anglin, 2000), where $\omega = 2\Delta$. The weak interaction regime $U/2\omega \ll 1$, corresponds to dynamics preserving coherence of the atomic condensate for times much larger than the the oscillation period of the population between the two wells. High coherence corresponds to a weak delocalization, i.e., an initial spin-coherent state remains localized for a very long time. The corresponding dynamics is well described by solution of the mean-field variational equations of motion, assuming a spin-coherent state as the variational ansatz (Kramer & Saraceno, 1981) (Fig.1).

Solving mean-field equations is no challenge for numerical computation. Therefore our focus will be on the second, strong interaction regime. The dynamics at $U/2\omega = 1$ corresponds to the oscillations of the condensate which is overdamped by the on-site interaction, i.e., a substantial depletion of the condensate occurs on the time-scale of a single oscillation. At $U/2\omega = 1$ the dynamics is strongly delocalizing, characterized by the exponential loss of coherence (Khodorkovsky *et al.*, 2008) as measured by the purity of the single-particle density operator.

The loss of coherence can also be measured by the generalized purity (Barnum *et al.*, 2003) of the state with respect to the $\mathfrak{su}(2)$ algebra of the single-particle observables. The generalized purity of the state ψ is defined by

$$P_{\mathfrak{su}(2)}[\psi] \equiv \sum_{i=x,y,z} \left\langle \hat{\mathrm{J}}_i \right\rangle^2 . \tag{4.14}$$

$P_{\mathfrak{su}(2)}[\psi] \leq 1$ and equals to unity if and only if ψ is a spin-coherent state. A mean-field solution is a generalized pure state by the definition. The mean-field approximation breaks down as the generalized purity decreases substantially.

Figs.1 and 2 show dynamics of the system of $N = 128, 256, 512$ particles in the weak and strong interaction regime respectively, obtained by a direct solution

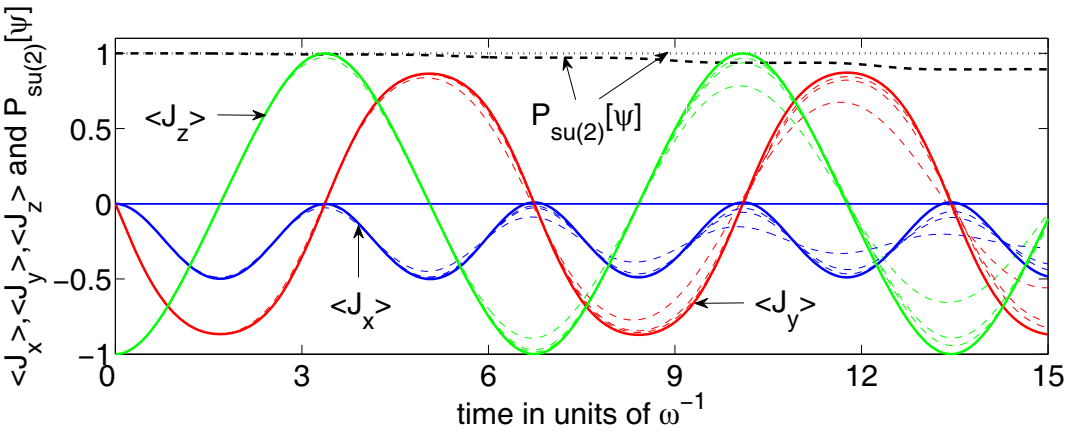

Figure 4.1: (Color online) The mean-field solution for the expectation values of the single-particle observables $\hat{\mathrm{J}}_x$ (blue, solid), $\hat{\mathrm{J}}_y$ (red, solid) and $\hat{\mathrm{J}}_z$ (green,solid), Eq.(4.2), and the generalized purity (dotted), Eq.(4.14), as a function of time vs. the exact solution of the Schrödinger equation (dashed lines) for $N = 128, 256, 512$ (expectation values) and $N = 512$ (generalized purity). The system of N atoms resides initially in a spin-coherent state corresponding to the condensate prepared in the left well of the trap. The value of the on-site interaction is chosen $U/2\omega = 1/2$, corresponding to the weak interaction regime. Time is measured in units of $\omega^{-1} = 0.5\Delta^{-1}$. The expectation values are normalized by the factor $j = N/2$. As the number of particles grows the exact solution approaches the mean-field solution on the characteristic time-scale of the oscillations.

of the Schrödinger equation using the Chebyshev method (H. Tal Ezer and R. Kosloff, 1984). Initial state of the system is chosen to be the condensed state of the atoms located in the left well. This is a spin-coherent eigenstate of the $\hat{\mathrm{J}}_z$ single-particle operator, measuring the difference of the right- and left-well populations of the atoms. Apparently the mean-field solution works well for the weak interaction regime, where the generalized purity of the evolving remains close to unity. In the strong interaction region the purity decreases on the time-scale of a single oscillation of the condensate and the mean-field solution fails to reproduce correctly the character of the dynamics.

Application to a system of $N = 2 * 10^4$ cold atoms

Equations of motion The numerical solution of the sNLSE (4.12) proceeds as a sequence of infinitesimal linear transformations:

$$|\psi\rangle \rightarrow \hat{\mathrm{T}}_1 |\psi\rangle \tag{4.15}$$

$$|\psi\rangle \rightarrow \hat{\mathrm{T}}_2 |\psi\rangle \,, \tag{4.16}$$

$$\hat{\mathrm{X}} \rightarrow \hat{\mathrm{T}}_2 \hat{\mathrm{X}} \hat{\mathrm{T}}_2^{\dagger}, \tag{4.17}$$

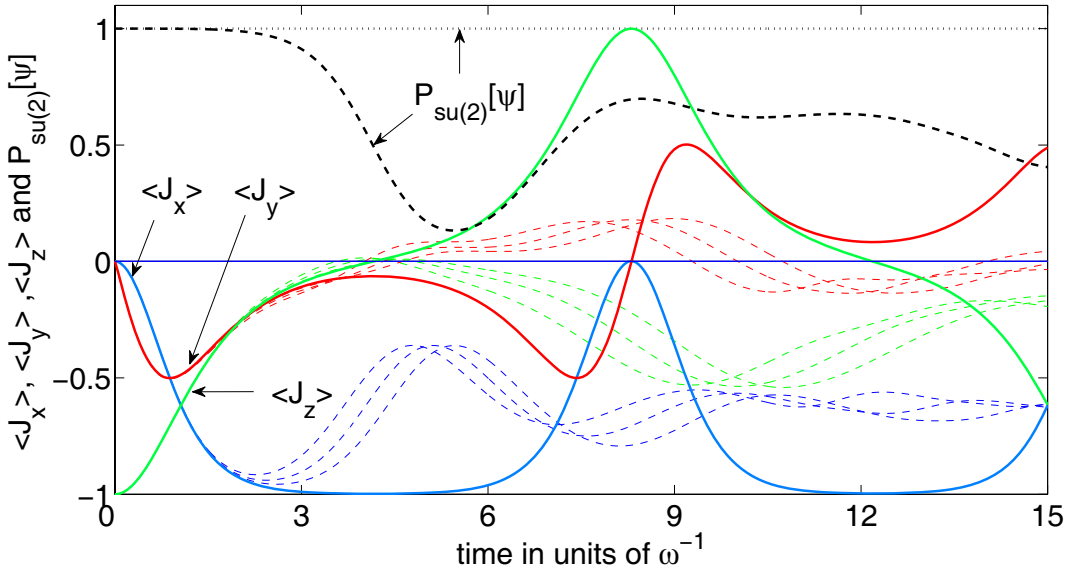

Figure 4.2: (Color online) The mean-field solution for the expectation values of the single-particle observables $\hat{\mathrm{J}}_x$ (blue, solid), $\hat{\mathrm{J}}_y$ (red, solid) and $\hat{\mathrm{J}}_z$ (green,solid), Eq.(4.2), and the generalized purity (dotted), Eq.(4.14), for $N = 512$ as a function of time vs. the exact solution of the Schrödinger equation (dashed lines) for $N = 128, 256, 512$ (expectation values) and $N = 512$ (generalized purity). The system of N atoms resides initially in a spin-coherent state corresponding to the condensate prepared in the left well of the trap. The value of the on-site interaction is chosen $U/2\omega = 1$, corresponding to the strong interaction regime. Time is measured in units of $\omega^{-1} = 0.5\Delta^{-1}$. The expectation values are normalized by the factor $j = N/2$. The mean-field approximation breaks down on the time-scale of a single oscillation.

where $\hat{\mathrm{X}}$ stand for all relevant operators, i.e., the Hamiltonian and the single-particle observables, the linear transformation $\hat{\mathrm{T}}_1$ drives the physical evolution of the state in the fixed computational basis of spin-coherent states and the unitary transformation $\hat{\mathrm{T}}_2$ keeps the state localized in the basis. The state ψ in Eqs.(4.15) and (4.16) is given by

$$|\Psi(t)\rangle = \sum_{i=1}^{M} c_i(t)\,|\psi_i(0)\rangle\,, \tag{4.18}$$

where $\psi_i(0)$ is the *fixed* computational basis of spin-coherent states. From Eq.(4.12)

$$\hat{\mathrm{T}}_1 = \hat{\mathrm{I}} + \left\{ -i\hat{\mathrm{H}}dt - \gamma \sum_{i=1}^{3} \left(\hat{\mathrm{J}}_i - \left\langle \hat{\mathrm{J}}_i \right\rangle_\psi \right)^2 dt + \sum_{i=1}^{3} \left(\hat{\mathrm{J}}_i - \left\langle \hat{\mathrm{J}}_i \right\rangle_\psi \right) d\xi_i \right\}, \tag{4.19}$$

where $\left\langle \hat{\mathrm{J}}_i \right\rangle$ are the instantaneous expectation values of the single-particle operators. From Eqs.(4.15), (4.19) and (4.4) we obtain

$$\sum_{k=1}^{M} C_{jk} \quad dc_k \tag{4.20}$$
$$= \sum_{k=1}^{M} \left\{ -i(\hat{\mathrm{H}})_{jk} dt - \gamma \sum_{i=1}^{3} \left((\hat{\mathrm{J}}_i)_{jk} - \left\langle \hat{\mathrm{J}}_i \right\rangle_{\psi} \right)^2 dt + \sum_{i=1}^{3} \left((\hat{\mathrm{J}}_i)_{jk} - \left\langle \hat{\mathrm{J}}_i \right\rangle_{\psi} \right) d\xi_i \right\} c_k,$$

where $(\hat{\mathrm{X}})_{jk} \equiv \left\langle \psi_j(0) \left| \hat{\mathrm{X}} \right| \psi_k(0) \right\rangle$ and

$$C_{jk} \equiv \langle \psi_j(0) | \psi_k(0) \rangle \tag{4.21}$$

is the overlap matrix. It should be noted that the overlap matrix is time-independent.

The unitary transformation $\hat{\mathrm{T}}_2$ is not unique and serves to rotate the state in such a manner that the rotated state is localized in the fixed basis. In the simulation we use an initial spin-coherent state $|-j\rangle$, i.e., a point at the southern pole of the phase-space. Accordingly, the fixed basis of M states is localized about the south pole. Therefore, the unitary transformation $\hat{\mathrm{T}}_2$ has to ensure that the expectation values of $\hat{\mathrm{J}}_x$ and $\hat{\mathrm{J}}_y$ in the rotated state vanish. As pointed out in Section 4.4.2, in the Hilbert-Schmidt picture this rotation corresponds to rotation of the density operator in such a way that its projection on the SGA of the single-particles observables be proportional to $\hat{\mathrm{J}}_z$. $\hat{\mathrm{T}}_2$ is not unique. In our simulations $\hat{\mathrm{T}}_2$ is chosen to be a unitary transformation, generated by $\hat{\mathrm{J}}_x$ and $\hat{\mathrm{J}}_y$. Since $\hat{\mathrm{T}}_2$ is generated by the $\mathfrak{su}(2)$ SGA itself, the transformation (4.17) of the single-particle observables and the Hamiltonian is performed analytically at each time-step.

The choice of numerical values A converged solution should be independent of the numerical parameters in the Eq.(4.20). They include the parameters of the basis, its size M, the strength of the measurement γ and the size of the time-step dt. The convergence is obtained by increasing M and dt and decreasing γ.

Choice of basis The choice of the basis is practically determined by its size M. In fact, a solution of the sNLSE is localized in the phase-space under the action of the noise (Sections 4.2 and 4.3). Therefore, a localized basis of states is sufficient to represent the solution. A set of $N+1$ spin-coherent states comprises the full basis of the Hilbert space. A spin-coherent state is represented by a point of the phase-space sphere. A natural choice is a uniform distribution of the points on the sphere. A state, localized in an area A on the sphere can be represented

by $M = (N+1)A/4\pi$ points uniformly distributed on the area A. In practice, a more dense sampling has proved to be better for numerical stability of solution.

The value of M in the convergent solution depends on the strength of the measurement γ. An estimate based on the theory presented in Section 4.2 shows that for $U/2\omega = O(1)$

$$M \lesssim \frac{2\omega}{\gamma N} \tag{4.22}$$

provided $M \gg 1$. As γ goes to zero M approaches the Hilbert space dimension in the strong interaction regime where the generalized purity of the exact state of the system becomes low. For the purpose of the simulation we are interested at the maximal value of γ for which the open-system dynamics of the single-particle observables is indistinguishable from the exact unitary one. Therefore, an estimate for this maximal value will also give an estimate for M.

Choice of a time-step From the Eq.(4.20) the size of the time-step should be chosen to ensure that $|(\hat{\mathrm{H}})_{jk}|dt \ll 1$, where $|(\hat{\mathrm{H}})_{jk}|$ stands for the spectral norm of the Hamiltonian matrix in the computational basis. A good estimate for the spectral norm is the inverse of the characteristic time scale of the dynamics, which for $U/2\omega = O(1)$ is of the order of ω. As N goes to infinity the area in the phase space, corresponding to the localized basis for any fixed M decreases as $1/N$, i.e., its linear dimension decreases as $1/\sqrt{N}$. On the time interval dt the localized state is expected to move the distance of $dt\omega$ on the sphere. For the infinitesimal transformation the state must remain localized in the basis. Therefore, we demand that

$$dt\omega \ll O(1/\sqrt{N}). \tag{4.23}$$

It follows that the simulation on the time interval of ω^{-1} must take no less than $O(\sqrt{N})$ time-steps.

The expectation of the term $\gamma \sum_{i=1}^{3} \left(\hat{\mathrm{J}}_i - \left\langle \hat{\mathrm{J}}_i \right\rangle_\psi\right)^2$ in Eq.(4.20) in a localized state is of the order of $O(\gamma NM)$ (Section 4.2). Since $O(\gamma NM) = O(\omega)$, as follows from Eq.(4.22), this term is sufficiently small at $dt = O(1/\sqrt{N})$.

The last stochastic term $\sum_{i=1}^{3} \left((\hat{\mathrm{J}}_i)_{jk} - \left\langle \hat{\mathrm{J}}_i \right\rangle_\psi\right)$ has spectral norm of the order of N. Therefore, we must have $d\xi_i N \ll 1$. Using Eqs.(4.13) and (4.22) we obtain $dt\gamma \ll O(1/N^2)$ and, finally

$$dt\omega \ll O(1/N), \tag{4.24}$$

which leads to the number of time-steps on the time interval of ω^{-1} of the order of $O(N)$. It follows that the algorithm is not efficient in the sense of the definition in Section 4.4.2.

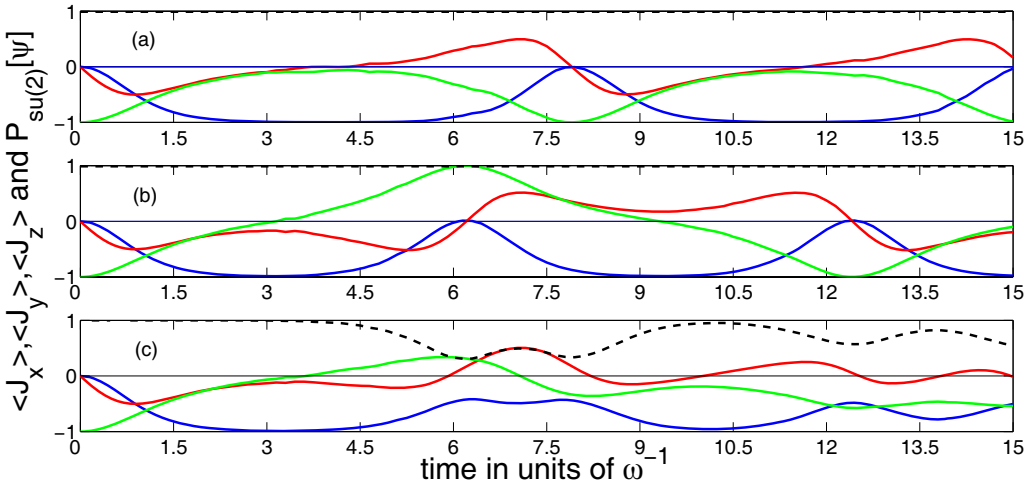

Figure 4.3: (Color online). Panels (a) and (b) display the (normalized by the factor $j = N/2$) expectation values of the single-particle observables $\hat{\mathrm{J}}_x$ (blue, solid), $\hat{\mathrm{J}}_y$ (red, solid) and $\hat{\mathrm{J}}_z$ (green,solid), Eq.(4.2), and the generalized purity (black,dashed), Eq.(4.14) as a function of time. The expectation values are calculated in pure-states solutions of the sNLSE (4.12) for two different realizations of noise. The system of N atoms resides initially in a spin-coherent state corresponding to the condensate prepared in the left well of the trap. The value of the on-site interaction is chosen $U/2\omega = 1$, corresponding to the strong interaction regime. Time is measured in units of $\omega^{-1} = 0.5\Delta^{-1}$. Panel (c) is the average of realizations in panel (a) and (b).

Choice of γ If the time-scales of the open-system dynamics, corresponding to the sNLSE (4.12) are analytical in γ, the effect of the measurement on the dynamics of the single-particles observables must be asymptotically (i.e. as $N \to \infty$) negligible on a fixed time interval at $\gamma \ll \omega$ (Section 4.2). Surprisingly, for the parametric choice $U/2\omega = 1$, convergent solution obtains at $\gamma \ll \omega/N$! This implies some singular dependence of the dynamical time-scales on the measurement strength. The problem is further discussed in Section 4.4.4.

Numerical results Convergence in the size of the basis can be checked on the level of a single stochastic realization of the sNLSE (4.12). Figure (4.3) (a) and (b) displays dynamics of the single-particle observables for two different realizations of noise in Eq.(4.12). The size of the basis is $M = 40$ and the value of γ is $0.5/N$. The strong localization results in the values of the generalized purity indistinguishable from unity as in a single spin-coherent state. The two trajectories coincide on a short time interval, corresponding to high generalized purity of the exact solution (Fig(4.4)). On this short time interval the mean-field

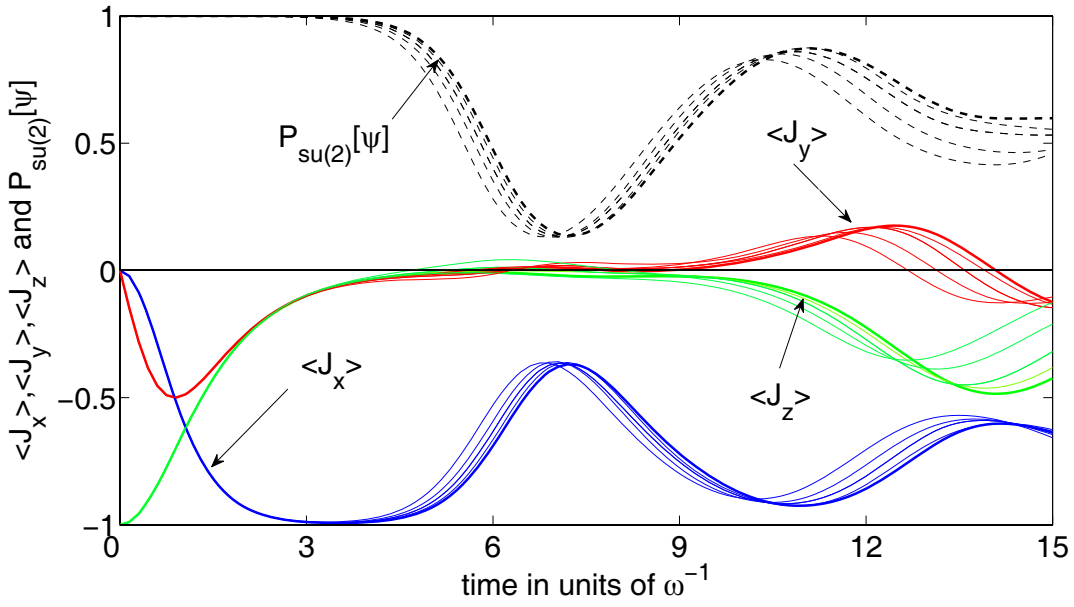

Figure 4.4: (Color online). The (normalized by the factor $j = N/2$) expectation values of the single-particle observables $\hat{\mathrm{J}}_x$ (blue, solid), $\hat{\mathrm{J}}_y$ (red, solid) and $\hat{\mathrm{J}}_z$ (green,solid), Eq.(4.2), and the generalized purity (black,dashed), Eq.(4.14) as a function of time. The system of $N = 2 * 10^4$ atoms resides initially in a spin-coherent state corresponding to the condensate prepared in the left well of the trap. The value of the on-site interaction in the Hamiltonian (4.3) is chosen $U/2\omega = 1$, corresponding to the strong interaction regime. Time is measured in units of ω^{-1}. The plots for five values of the measurement strength are presented: $\gamma = 8/N, 4/N, 2/N, 1/N$(thin lines),$0.5/N$ (thick line). The expectation values are averages of 2000 stochastic pure-states solutions of the sNLSE (4.12) for each value of γ.

solution (Cf.Fig(4.2)) is a perfect approximation. Starting at $t \approx 2\omega^{-1}$ the two trajectories start to diverge abruptly, remaining very smooth function of time. Each simulation takes a couple of minutes on a PC.

Figure (4.3) (c) shows the dynamics of the single-particle observables averaged over the two realizations and the corresponding generalized purity . The main feature is an apparent decrease of the generalized purity, already resembling the dynamics of the exact solution. This implies that some features of a many-body dynamics are attainable from a small number of realizations.

Averaging over 2000 stochastic trajectories leads to a relative error of 2.5% for the expectation values of the observables. Figure (4.4) presents the averaged results. The averaging has been performed for solutions of the sNLSE, corresponding to $\gamma = 8/N, 4/N, 2/N, 1/N$ and, finally, to $\gamma = 0.5/N$ at which the

convergence to the unitary evolution becomes apparent. The evolution on the time interval $0 < t < 2\omega^{-1}$ corresponds to the mean-field behaviour and is not visibly perturbed by the measurement. The size of the basis for the convergent solution is $M_{sNLSE} = 60$.

The size of the basis necessary to span the pure-state evolution, governed by the original Schrödinger equation can be estimated from Figure (4.4). The minimal purity obtains at $t \approx 7.5\omega^{-1}$. Its (normalized) value at this point is $P_{\mathfrak{su}(2)}[\psi] \approx 0.13$ which corresponds to

$$M_{SE} = (N+1)\left(1 - \sqrt{P_{\mathfrak{su}(2)}[\psi]}\right) \approx 0.64N. \tag{4.25}$$

according to the formula derived in Section 4.2.

Therefore, the size of the time-dependent basis is compressed by the factor of $M_{SE}/M_{sNLSE} \approx 2 \cdot 10^2$! As a result, the memory cost is reduced by the factor of $4 * 10^4$. The number of the time-steps for the propagation is $2 * 10^6$, which results in reduction of the CPU resources by the factor of 10^3.

4.4.4 Conclusions and Discussion

An algorithm for simulation of a many-body dynamics, generated by a $\mathfrak{su}(2)$-Hamiltonian has been described, analyzed and applied to simulation of the dynamics of cold atoms in the double-well trap. The dynamics reflects a competition between the hopping rate of the atoms from well to well and the two-body repulsive interaction between the particles. The single-particle observables of the system were simulated in the strong interaction regime and the convergence of the simulation was checked.

The simulation is based on numerical solution of the stochastic Nonlinear Schrödinger Equation, corresponding to weak measurement of the elements of the spectrum-generating $\mathfrak{su}(2)$ algebra of the single-particle observables. Dynamics of the smooth SGA observables is negligibly affected by sufficiently weak measurement, which is nonetheless strong enough to localize solutions of the sNLSE in the corresponding phase-space.

The localization leads to substantial reduction of the computational complexity of the many-body dynamics. The algorithm is applied to simulation of the single-particle observables of a system of $N = 2 * 10^4$ cold atoms in a double-well trap. The localization allows to describe the pure-state solution of sNLSE by a superposition of only 60 spin-coherent states, which is smaller by the factor of $2 \cdot 10^2$ than the size of the spin-coherent basis necessary to span the solution of the original Schrödinger equation on the corresponding time interval. This "compression" of the time-dependent basis results in dramatic reduction of the computational complexity of the simulation.

Two important questions are left for future investigations:

- What is the maximal strength of the measurement, at which the evolution of the SGA operators is negligibly affected on the time-scale of their unitary evolution?
- Does the method provide an efficient simulation of the SGA observables in the sense of definition in Section 4.4.2?

The first question is raised by the numerical results of the simulation presented in Section 4.4.3. The value of the measurement strength at which the open-system evolution of the single-particles observables of cold atoms converged to their unitary evolution is smaller by the factor of N than its theoretical estimate (Section 4.4.3). The theoretical estimate is based on assumption that the time-scale of the open evolution of the SGA observables is analytic in the measurement strength (Section 4.2). The finding seems to imply the radius of convergence of the inverse time-scale is of the order of ω/N, where ω stands for the inverse time-scale of the unitary evolution. This singular behavior is probably related to the singular choice of the parameter $U/2\omega = 1$ for the simulation, corresponding to the crossover from the weakly interacting dynamical regime to the regime of strong interaction (Vardi & Anglin, 2000). This choice of the parameter corresponds to maximal delocalization of the phase-space unitary dynamics and therefore poses the real challenge for the simulation.

The second question is raised by the estimation performed in Section 4.4.3, according to which the number of time-steps of the simulation scales linearly with the number of particles (the Hilbert space dimension) N on a fixed time interval. This implies that the algorithm is not efficient in the strict sense of our definition, according to which the computational resources of an efficient simulation do not depend on the Hilbert space representation of the Lie-algebra of observables. The estimation has been performed for the linear implementation of the method, which relies on solving linear equations of motion. The estimation has been performed in the special case of the $\mathfrak{su}(2)$ SGA but can be generalized to an arbitrary compact semisimple algebra of observables with a similar result. It is possible that the scaling with N is a drawback of the linear implementation of the method. An algorithm based of solving nonlinear equations of motion, corresponding to the situation where each element of the time-dependent basis follows its own unitary evolution, may have a different scaling.

Chapter 5

Conclusions and open question

5.1 Conclusions

We define a quantum system by a Lie-algebra of observables and its irreducible Hilbert space representation. It is assumed that the Hamiltonian is a function of the elements of the algebra. As a consequence, the distinguished algebra can be appropriately termed a *spectrum-generating algebra*(SGA) (Dothan, 1970; Bohm *et al.*, 1988). We propose the following definition of efficient simulation of the evolution of a subset of observables:

Definition: *The simulation of a subset of observables is defined as efficient if the memory and the CPU time resources necessary to compute the evolution of the distinguished observables do not depend on the (Hilbert space) representation of the SGA.*

Stated differently, the simulation is efficient if it can be performed group-theoretically. The main conclusions of the presented work can be summarized in the following scheme (Fig 5.1).

Necessary conditions on the subset of observables which can be simulated efficiently are:

- The set consists of operators weakly nonlinear in the elements of the spectrum generating algebra (SGA) of the system
- The Hamiltonian is weakly nonlinear in the elements of the SGA of the system

Weakly nonlinear is defined as being a polynomial (in the elements of the SGA) of a fixed order, independent on the Hilbert space representation of the SGA. If the necessary conditions hold and

- The evolving state can be represented as superposition of a small number of the generalized coherent states (GCS), associated with the SGA

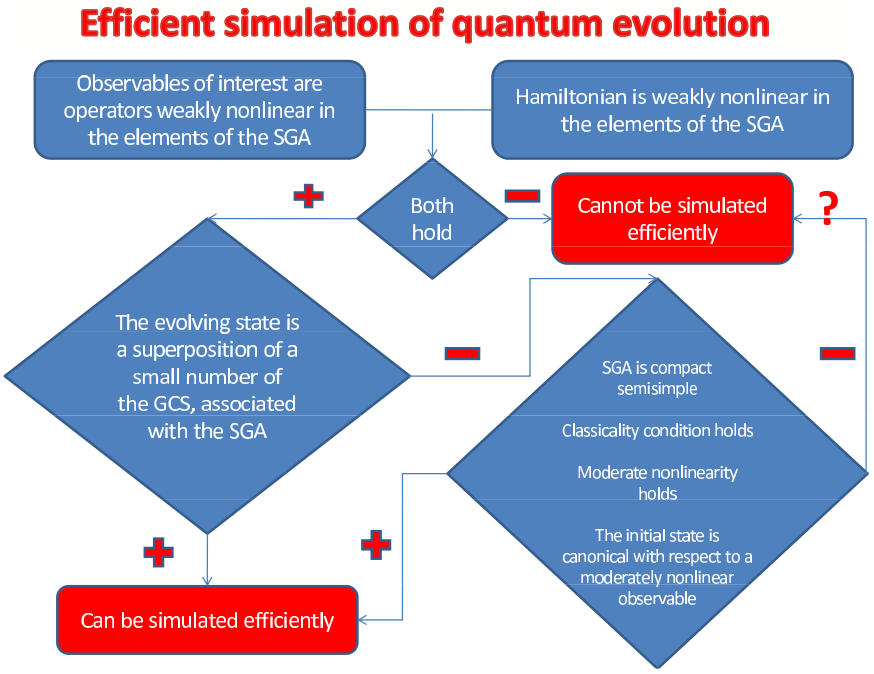

Figure 5.1: The block scheme of relations between various conditions on the SGA of observables, its Hilbert space representation and the efficiency of dynamical simulation of a subset of observables.

the evolution can be simulated efficiently. *Small number* is defined as a number independent on the Hilbert space representation of the SGA.

If the necessary conditions hold and the evolving state *cannot* be represented as superposition of a small number of the GCS but

- The SGA is a compact semisimple Lie-algebra of operators
- The SGA and its Hilbert space representation comply with the well-defined classicality condition
- The Hamiltonian is moderately nonlinear[1] in the elements of the SGA
- The initial state of the system is canonical with respect to an operator moderately nonlinear in the elements of the SGA

a radical gain in efficiency can be obtained using a method proposed in Chapter 4[2]. This method employs simulation of the unitary dynamics of interest by a

[1]Moderate nonlinearity is defined in Section 4.2 and is not equivalent to the weak nonlinerity defined above.

[2]Recently a preprint appeared in the arXiv (Sidles *et al.*, arXiv:0805.1844v1), containing very similar ideas

pertinent open-system dynamics. The open-system dynamics corresponds to a nonunitary evolution of the original system under the weak measurement of the SGA elements. It is simulated using unraveling of the evolving density operator into pure-states stochastic trajectories. The pure-state evolution can be simulated at low cost due to localization of the states in the corresponding phase-space under the action of the measurement.

The method has been implemented in an algorithm for simulation of many-body dynamics, driven by a $\mathfrak{su}(2)$-algebraic Hamiltonian. The algorithm has been applied to simulation of the single-particle observables of a system of $2 * 10^4$ cold atoms in a double-well trap. A dramatic reduction of the computational complexity has been demonstrated. The algorithm is not efficient in the strict sense of our definition since the CPU time scales linearly with the Hilbert space dimension. It is conjectured that this is a drawback of the particular implementation of the method relying on solving a system of linear equations of motion.

Adding weak measurement to the unitary dynamics serves as a computational tool in the proposed method. A by-product of the method is a tool of simulating a real open-system dynamics. The open-system dynamics does not need to have the particular form assumed in the present work. It is sufficient that the bath has a strong localizing effect on the dynamics. On the other hand, it seems necessary that the open-system dynamics be Markovian. Otherwise, the reduced dynamics of the system will involve polynomials of arbitrary orders in the SGA of the system and the simulation cannot be performed efficiently.

5.2 Open questions

5.2.1 Can the sNLSE be solved efficiently?

The algorithm presented in Section 4.4 is not efficient in the strict sense of the definition given above, since the CPU time scales linearly with the Hilbert space dimension of the system (Section 4.4.3). The order-of-magnitude analysis similar to the argument presented in Section 4.4.3 shows that this feature is independent of the SGA and characterizes the linear implementation of the algorithm (Section 4.4.2) in general. It is an open question whether this feature is inherent in the sNLSE or is a drawback of the linear implementation.

5.2.2 What is the optimal unraveling of the open-system dynamics?

Unraveling of an open-system evolution into quantum stochastic trajectories is not unique. Particular unraveling may have stronger localization properties and, as a consequence, be more advantageous from the computational point of view. For example, the open system evolution corresponding to a weak measurement of operators in the SGA of the system can be unraveled into statistic mixtures of pure-states trajectories, driven by the real noise (Chapter 4), which leads to strong localization. A different unraveling corresponds to imaginary noise. In the latter case the pure-state stochastic trajectory is driven by the original Hamiltonian, perturbed by the operator *linear* in the elements of the SGA, coupled to the δ-correlated noise (Gorini & Kossakowski, 1976). Since the perturbation is linear in the SGA it does not change the generalized purity of the state with respect to the SGA and, as a consequence, has no localization effect at all.

Optimal unraveling from the computational point of view is unraveling having the strongest localization property. This unraveling is a dynamical equivalent of the optimization procedure for finding the measure of the mixed state (generalized) entanglement. The mixed state entanglement can be defined as an averaged entanglement of the pure states in the mixture, minimized over all the possible decompositions of the density operator into a mixture of pure states (Plenio & Virmani, 2007; Barnum *et al.*, 2003). The dynamical equivalent of this decomposition is an unraveling. Maximizing the localization corresponds to minimizing the generalized entanglement.

Finding the optimal unraveling seems to be at least as complex a problem as calculating the mixed state entanglement, which is notoriously difficult(Plenio & Virmani, 2007). Therefore, a physical insight is needed to guide the choice of unraveling in the applications. This is left as an important open problem.

5.2.3 Is quantum integrability of the dynamics relevant?

Given a SGA of observables (or any other subalgebra of observables), the irreducible Hilbert space representation of the algebra and an appropriate reference state of the system, one can construct the corresponding phase space of the quantum system (Onofri, 1975; Simon, 2000). GCS of the system with respect to the reference states can be represented by a point in the phase-space (Zhang *et al.*, 1990) and an arbitrary evolution generated by the SGA can be represented as a trajectory in the phase-space. The corresponding equations of motion are classical Hamiltonian equations (Kramer & Saraceno, 1981). Moreover, they are linear equations of motion, corresponding to a system of harmonic oscillators in

appropriate canonical coordinates.

When the Hamiltonian is nonlinear in the SGA elements (excluding the case where the nonlinearity enters through a combination of Casimirs) an initial GCS does not evolve into a GCS and trajectories are no longer an adequate description of the dynamics. Still one can assume a GCS ansatz (the mean-field ansatz) for the evolving state. The variational equations of motion are still classical Hamiltonian equations of motion, but they are no longer linear and are generally non integrable (Kramer & Saraceno, 1981; Zhang & Feng, 1995). Quantum integrability is the property of the mean field dynamics of the quantum system in the phase space.

Our method is based on representing evolving density operator as a statistical mixture of pure states, evolving according to a nonlinear Schroedinger equation. Each state is a superposition of a small number of the GCS and is localized in the phase space. The limit of extreme localization corresponds to the mean-field dynamics perturbed by the nonlinear and stochastic contributions from the measurements. As is well known from the classical mechanics, the effect of the perturbation on the dynamics depends strongly on the integrability of the unperturbed dynamics. While integrable dynamics is stable under the action of sufficiently small perturbation (Arnold, 1989), non integrable system are generally not. It is conceivable that strongly localized solutions bear some characteristics of the mean-field solutions, at least in the regular zones of the phase space. Therefore, it is expected that the effect of the measurement (the fictitious bath) depends strongly on the quantum-integrability.

5.2.4 What is the physical meaning of the classical limit?

The classical limit is the limit of a certain strong inequality imposed on the SGA and its Hilbert space representation (Section (4.2)). In the case of the $\mathfrak{su}(2)$ SGA this limit corresponds to taking the dimension of the representation to infinity.

The same SGA can describe very different systems. For example the $\mathfrak{su}(2)$ is the SGA of both the system of cold atoms in a double-well trap (Vardi & Anglin, 2000) and of a vibrational degree of freedom of a diatomic molecule (Iachello & Levine, 1995). In the latter case, the classical limit is usually associated with a semiclassical limit of high vibrational numbers. In the former case, the classical limit is associated with the thermodynamical limit of a large number of particles.

We ask the following speculative question: is the classical world a semiclassical or a thermodynamical limit of quantum degrees of freedom, of both , of neither?

References

Aharonov, D., & Ben-Or, M. quant-ph/9611029. . e-print.

Arecchi, F.T., Courtens, E., Gilmore, R., & Thomas, H. 1972. *Phys. rev. a*, **6**, 2211.

Arnold, V. I. 1989. *Mathematical methods of classical mechanics*. 2nd edition, New York: Springer.

Barnum, H., Knill, E., Ortiz, G., & Viola, L. 2003. *Phys. rev. a*, **68**, 032308.

Beck, M. H., Jackle, A., Worth, G.A., & Meyer, H.D. 2000. *Phys. rep.*, **324**, 1.

Bohm, A., Neeman, Y., & Barut, A. O. 1988. *Dynamical groups and spectrum generating algebras*. Singapur: World Scientific.

Boixo, S., Viola, L., & Ortiz, G. 2007. *Epl*, **79**, 40003.

Brassard, G., & Bratley, P. 2000. *Algorithmics: Theory and Practice*. Engelwood Cliffs: Prentice-Hall.

Cohen-Tannoudji, C., Dlu, B., & Laloe, F. 1977. *Quantum Mechanics*. New York: Wiley.

Diosi, L. 1988a. *Physics letters a*, **132**, 233.

Diosi, L. 1988b. *Physics letters a*, **129**, 419.

Diosi, L. 2006. *Weak measurements in quantum mechanics* . v 4, p276-282 in: Encyclopedia of Mathematical Physics, eds.: J.-P. Fransoise, G.L. Naber, and S.T. Tsou , Elsevier, Oxford.

Diosi, L. 2007. *A Short Course in Quantum Information Theory.* Berlin: Springer.

Dothan, Y. 1970. *Phys. rev. d*, **2**, 2944.

Filippo, S. De. 2000. *Phys. rev. a*, **62**, 052307.

Gardiner, C.W. 1983. *Handbook of Stochastic Methods*. Berlin: Springer.

Gati, R., Hemmerling, B., Folling, J., Albiez, M., & Oberthaler, M. K. 2006. *Phys. rev. lett.*, **96**, 130404.

Gershgoren, E., Vala, J., Kosloff, R., & Ruhman, S. 2001. *J. phys. chem. a*, **105**, 5081.

Gilmore, R. 1974. *Lie groups, Lie Algebras and Some of Their Applications*. New York: John Wiley and Sons.

Gisin, N. 1984. *Phys. rev. lett.*, **52**, 1657.

Gisin, N., & Percival, I. C. 1992. *J. phys a: Math.gen.*, **25**, 5677.

Gisin, N., & Percival, I.C. 1993. *J. phys a: Math.gen.*, **26**, 2233.

Gorini, V., & Kossakowski, A. 1976. *J. math. phys.*, **17**, 1298.

Gurvitz, L., & Barnum, H. 2003. *Phys. rev. a*, **68**, 042312.

Halliwell, J.J., & Zoupas, A. 1995. *Phys. rev. d*, **52**, 7294.

Hoover, W.G. 1999. *Time Reversibility Computer Simulation and Chaos*. Singapore: World Scientific.

Iachello, F., & Levine, R.D. 1995. *Algebraic Theory of Molecules*. Oxford: Oxford University Press.

Jozsa, R., & Linden, N. 2003. *Proc. r. soc. lond. a*, **459**, 2011.

Kammerer, C., Voisin, C., Cassabois, G., Delalande, C., Roussignol, Ph., Klopf, F., Reithmaier, J. P., Forchel, A., & Gerard, J. M. 2002. *Phys. rev. b*, **66**, 041306(R).

Khodorkovsky, Y., Kurizki, G., & Vardi, A. 2008. *Phys. rev. lett.*, **100**, 220403.

Klyachko, A. A. quant-ph/0206012. . e-print.

Kohn, W. 1999. *Nobel Lecture*. January 28.

Kosloff, R. 1988. *J. phys. chem.*, **92**, 2087.

Kramer, P., & Saraceno, M. 1981. *Geometry of the Time-Dependent Variational Principle in Quantum Mechanics*. Berlin: Springer-Verlag.

Kubo, R. 1962. *Fluctuations, Relaxation and Resonance in Magnetic Systems*. Edinburgh: edited by D. ter Haar, Oliver and Boye.

Lipkin, H. J., Meshkov, N., & Glick, A.J. 1965. *Nucl. phys.*, **62**, 188.

Mahan, Gerald D. 2000. *Many-particle physics* . New York: Kluwer Academic/Plenum Publishers.

Miller, W. H. 2005. *Proc. natl. acad. sci. u s a*, **102**.

Nielsen, M. A., & Chuang, I. L. 2000. *Quantum computation and quantum information*. Cambridge University Press.

Onofri, E. 1975. *J. math. phys.*, **16**, 1087.

Perelomov, A. 1985. *Generalized Coherent States and their Applications*. Berlin: Springer.

Peres, A. 1998. *Quantum Theory: Concepts and Methods*. Kluwer, Boston.

Plenio, M., & Virmani, S. 2007. *Quant. inf. comp.*, **7**, 1.

San-Jose, P., Zarand, G., Shnirman, A., & Schon, G. 2002. *Phys. rev. lett.*, **97**, 076803.

Schumm, T., Hofferberth, S., Andersson, L.M., Wildermuth, S., Groth, S., Bar-Joseph, I., Schmiedmayer, J., & Kruger, P. 2005. *Nature physics.*, **1**, 57.

Sidles, J. A., Garbini, J. L., Harrell, L. E., Hero, A. O., Jacky, J. P., Malcomb, J. R., Norman, A. G., & Williamson, A. M. arXiv:0805.1844v1.

Simon, R. 2000. *Phys. rev. lett.*, **84**, 2726.

Tal-Ezer, H., & Kosloff, R. 1984. *J. chem. phys.*, **81**, 3967–3970.

Tikhonenkov, I., Anglin, J. R., & Vardi, A. 2007. *Phys. rev. a*, **75**, 013613.

Trimborn, F., Witthaut, D., & Korsch, H. J. 2008. *Phys. rev. a*, **77**, 043631.

Uskov, A. V., Jauho, A. P., Tromborg, B., Mork, J., & Lang, R. 2000. *Phys. rev. lett.*, **85**, 1516.

Vardi, A., & Anglin, J. R. 2000. *Phys. rev. lett.*, **86**, 568.

Vidal, G. 2003. *Phys. rev. lett.*, **91**, 147902.

Vidal, G., & Werner, R. F. 2002. *Phys. rev. a*, **65**, 032314.

Viera, V.R., & Sacramento, P.D. 1995. *Ann. phys.*, **242**, 188.

Viola, L., Knill, E., & Laflamme, R. 2001. *J. phys a: Math.gen.*, **34**, 7067.

Weiss, E. A., Katz, G., Goldsmith, R. H., Wasielewski, M. R., Ratner, M. A., & R. Kosloff, A. Nitzan. 2006. *J. chem. phys.*, **124**, 074501.

Werner, R. F. 1989. *Phys. rev. a*, **40**, 4277.

Zanardi, P. 2001. *Phys. rev. lett.*, **87**, 077901.

Zhang, W., & Feng, D. H. 1995. *Phys. rep.*, **252**, 1.

Zhang, W., Feng, D. H., & Gilmore, R. 1990. *Rev. mod. phys.*, **62**, 867.

Zwolak, M., & Vidal, G. 2004. *Phys. rev. lett.*, **93**, 207205.